

Enzymes for Enhanced Oil Recovery (EOR)

Hamidreza Nasiri

**Dissertation for the degree of
Philosophiae Doctor (PhD)**



University of Bergen, Norway

2011

Hamidreza Nasiri
Centre for Integrated Petroleum Research
Department of Chemistry
University of Bergen
Allégaten 41
N-5007 Bergen
Norway

Thesis submitted for the degree of Philosophiae Doctor

University of Bergen

April 2011

To my intelligent, gorgeous and lovely wife,

Maryam

Preface

The dissertation is submitted to the University of Bergen in partial fulfillment of the requirements for the degree of Doctor of Philosophy. The research work has been carried out at the Center for Integrated Petroleum Research (CIPR), University of Bergen in the period 2007-2010. This work is a part of the PETROMAKS program which is initiated in 2004 and sponsored by the Norwegian Research Council. Dr. Kristine Spildo and Professor Arne Skauge have been the main supervisors for this PhD project. Professor Anne Marit Blokkhus has been the co-advisor for this work.

The main motivation for this research study initiates in the development of a new enhanced oil recovery method and improve understanding of underlying processes. The study addresses using enzyme-proteins and their combination by surfactants to improve oil recovery.

The dissertation divided in 12 chapters which includes theoretical and experimental investigation. In experimental part dynamic and static experiments were conducted. Dynamic experiments include core flooding experiments using sandstone and carbonate rocks to study the effect of enzyme-proteins in the core material; and glass micromodel experiments to observe their effect on changing residual oil saturation. Static experiments include different approaches such as interfacial tension, contact angle, adsorption and electrophoretic mobility measurements to find out enzyme-proteins influence on oil/water and oil/water/solid interfaces.

Acknowledgment

I am very grateful for having been given the opportunity to participate in the PhD program at the University of Bergen, CIPR and I owe a great debt of thanks to all the individuals who made this experience possible. First and foremost, I must mention my supervisors, Dr. Kristine Spildo and Professor Arne Skauge who have been an inspirational role model to me and words can not express my sincere appreciation for their guidance, encouragement and support. I would also like to thank my co-supervisor Professor Anne Marit Blokkhus at the Chemistry Department at the University of Bergen.

I would like to acknowledge Professors Harald Høiland and Tania Barth and Associate Professor Tore Skodvin at the Chemistry Department at the University of Bergen for their suggestions and supports. Special thanks to Per Arne Ormehaug for his immense help in the lab during my work at CIPR. I would also like to express my gratitude to senior researcher Sverre Hetland at CIPR for his advises in laboratory works; PhD student Ina Hvidsten who helped me to perform some of the experimental works at the Chemistry Department and master students Anders Nymark and Asle Sandven who had collaboration in this work.

Grateful acknowledge is also made to the Research Council of Norway for financial support obtained during PhD period through the PETROMAKS program. I also thank Novozyme, Denmark for providing some of the enzyme samples.

I am also thankful to my fellow students and colleges at CIPR especially administration staff who made CIPR a friendly and cheerful working atmosphere.

My deep notes of appreciation are directed towards my parents, Gholamali Nasiri and Atlas Malaki and siblings in Iran. Without their support, guidance and love, it is inconceivable for me to ponder to move towards the goal of my life. A deep note of gratitude also goes to my parents in law, Hatam Nasseri and Mahvash Shahali. My father in law always supported me by following up my progress and cheered me up by asking this question (with his special accent): “when are you going to be a doctor?”

Finally and most importantly, I must express my profound gratitude to my dear wife, Maryam Nasseri for her support, suggestions, love and passion. Without her supports and love I would not have been able to accomplish this work.

Abstract

Primary oil recovery by reservoir pressure depletion and secondary oil recovery by waterflooding usually result in poor displacement efficiency. As a consequence there is always some trapped oil remaining in oil reservoirs. Oil entrapment is a result of complex interactions between viscous, gravity and capillary forces. Improving recovery from hydrocarbon fields typically involves altering the relative importance of the viscous and capillary forces. The potential of many EOR methods depends on their influence on fluid/rock interactions related to wettability and fluid/fluid interactions reflected in IFT (Green and Willhite, 1998). If the method has the potential to change the interactions favorably, it may be considered for further investigation, i.e. core flooding experiment, pilot and reservoir implementation.

Enzyme-proteins can be introduced as an enhanced oil recovery method to improve waterflood performance by affecting interactions at the oil-water-rock interfaces. An important part of this thesis was to investigate how selected enzymes may influence wettability and capillary forces in a crude oil-brine-rock system, and thus possibly contribute to enhanced oil recovery.

To investigate further by which mechanisms selected enzyme-proteins may contribute to enhance oil recovery, groups of enzymes with different properties and catalytic functions, known to be interfacially active, were chosen to cover a wide range of possible effects. These groups include (1) Greenzyme (GZ) which is a commercial EOR enzyme and consists of enzymes and stabilizers (surfactants), (2) The Zonase group consists of two types of pure enzyme, Zonase1 and Zonase2 which are protease enzymes and whose catalytic functions are to hydrolyze (breakdown) peptide bonds, (3) The Novozyme (NZ) group consists of three types of pure enzyme, NZ2, NZ3 and NZ6 which are esterase enzymes and whose catalytic

functions are to hydrolyze ester bonds, and (4) Alpha-Lactalbumin (α -La) which is an important whey protein.

The effect of enzymes on interactions in the oil/brine/solid system was studied. It was found that enzymes can change the adhesion behavior of the crude oil on glass surfaces from adhesion to non-adhesion when they are added to the brine solution. This was confirmed by contact angle measurements, which showed that contact angles became more water-wet (i.e. decreased) after exposure to enzyme solutions. Possible mechanisms giving rise to these observations, including catalysis of ester hydrolysis and enzyme adsorption, were discussed and tested.

An experimental study of changes in oil-water interfacial properties by addition of enzymes and proteins, including measurements of interfacial tension and electrophoretic mobility, has been performed. It was found that the effect of enzymes on oil-water properties is minor compared to their effect on oil-water-solid properties. Their contribution to change interfacial tension between oil and water is not significant while they affect the electrophoretic mobility of emulsified oil in enzyme-brine solution to some extent. Attempts were also made to study changes in both oil and water phase composition after equilibration with enzymes. However, since the chemical composition of crude oil is highly complex, a model oil was used in some of the experiments. The model oil was chosen to be a water insoluble ester (ethyl decanoate) solved in mineral oil in an effort to verify the possible role of catalysis of ester hydrolysis.

Dynamic core displacements using sandstone and carbonate rocks were conducted to show the potential of improved oil recovery by enzyme- and combined enzyme-surfactant flooding. Most of the core flooding experiments commenced with water flooding from initial water saturation, S_{wi} , (established with synthetic sea water) which will be referred to as secondary mode displacements. Accordingly, tertiary oil recovery processes were used to describe injection of enzyme and/or enzyme-surfactant solutions from residual oil saturation, S_{or} , established by the secondary displacements. The core floodings were conducted on various cores of the same type to check the reproducibility of the experiments. Flooding carbonates and aged Berea sandstone cores, waterflooded to residual oil saturation, with Greenzyme added to the water phase gave an additional recovery of between 3 and 11 % OOIP. One experiment on aged sandstone core and two on carbonate cores performed with one of the

esterase enzymes also showed a reduction in residual oil in the same ranges as that observed for Greenzyme.

From a capillary desaturation point of view, the reduction in interfacial tension obtained by adding Greenzyme is not sufficient to induce mobilization of residual oil. Further, a reduction in residual oil saturation was found after flooding with one of the esterase enzymes, which did not affect the oil-water interfacial tension. Based on these observations, we expect wettability changes to be the main factor contributing to mobilization of oil remaining after regular waterflood. To explore this hypothesis further, micromodel experiments were undertaken.

Micromodel experiments showed change in amount of residual oil saturation by enzyme-brine flooding when 1wt% Greenzyme and NZ2 were added to the brine solution. The amount of change in residual oil saturation was consistent with the incremental oil recovery produced in the core flooding experiments. Micromodel experiments also showed that the pattern of residual oil saturation change significantly to more distributed oil patches by injecting enzyme-brine solutions although the additional oil production was relatively low. This change in pattern of residual oil saturation is likely related to wettability alteration toward more water-wet state induced by enzyme-brine solution. The evidences of wettability alteration made by micromodel experiments could validate our proposal, wettability alteration, as the main mechanism contributing to increasing oil recovery.

Contents

Preface	III
Acknowledgment	V
Abstract	VII
List of Figures	XV
List of Tables	XIX
Symbols and abbreviations	XXI
Chapter 1 Introduction	2
Chapter 2 Enhanced oil recovery mechanisms	5
2.1 Displacement efficiency	5
2.1.1 Volumetric sweep efficiency	6
2.2 Microscopic displacement efficiency	7
2.2.1 Capillary forces	7
2.2.2 Viscous forces	8
2.2.3 Capillary number	8
2.2.4 Trapping of oil at the pore scale	8
2.2.5 Capillary desaturation curve (CDC)	10
2.3 Classification of enhanced oil recovery methods	11
Chapter 3 Enzymes	13
3.1 Enzyme structure and function	13
3.2 Mechanism of enzyme action	14
3.2.1 Lock and Key Theory	16

3.2.2	Induced Fit Theory	17
3.3	Classification of enzymes.....	17
3.4	Different enzymes and their uses	18
3.5	Enzyme applications in relation to oil and gas production	19
3.5.1	Permeability modification	20
3.5.2	Removal of formation damage.....	20
3.5.3	Pre-treatment of biopolymers.....	20
3.5.4	Breaker	21
3.5.4	Improved oil recovery	21
3.6	Surfactant-enzyme interactions	21
3.7	Potential enzymes to use for enhanced oil recovery	22
Chapter 4 Surfactants for EOR		25
4.1	Surfactant structures, types and properties.....	25
4.2	Increased oil recovery by surfactant flooding.....	27
4.3	Phase behavior.....	28
4.3.1	The role of alcohol	30
4.4	IFT and phase behavior	31
Chapter 5 Wettability		33
5.1	Types of Wettability.....	34
5.1.1	Homogeneous wettability.....	34
5.1.2	Heterogeneous wettability.....	34
5.2	Factors affecting wettability.....	35
5.3	Methods of wettability measurement	36
5.3.1	Flat surfaces.....	37
5.3.2	Porous media.....	37
5.3.2.1	The Amott Method:.....	37
5.4	Wettability and oil recovery.....	40
5.5	Effect of wettability on Capillary Desaturation Curve (CDC).....	43
Chapter 6 Interactions at interfaces		47
6.1	DLVO theory and the electrical double layer	47
6.1.1	The electrical double layer	47
6.2	Disjoining pressure and water film stability	49
6.3	The crude oil-water interface	49
6.5	Adsorption at the liquid-liquid interface	51
6.5.1	Adsorption of enzymes and proteins at the oil/water interface.....	51
6.6	The solid-liquid interface	52
6.6.1	The solid/water interface.....	52
6.6.2	Adsorption at the solid/liquid interface.....	53
6.6.3	Adsorption of enzymes and proteins at solid/liquid interface.....	54
6.7	The crude oil-water-solid interface	56
Chapter 7 Experimental study of oil-water-solid interfaces		59

7.1	Adhesion tests	59
7.1.1	Effect of enzymes on adhesion.....	63
7.2	Contact angle measurements involving different enzymes.....	64
7.2.1	Greenzyme	64
7.2.1.1	Crude oil A.....	64
7.2.1.2	Crude oil B.....	67
7.2.2	Zonase enzymes	70
7.2.3	Esterase enzymes.....	71
7.2.4	Alpha-Lactalbumin.....	73
7.2.5	Effect of enzyme exposure time on measured contact angle	74
7.3	Visual observations of the enzyme effect	75
7.4	Proposed mechanism for wettability alteration by enzyme-proteins	78
7.5	Adsorption measurements.....	79
Chapter 8 Experimental study of oil-water interface		83
8.1	Interfacial tension (IFT) measurement.....	83
8.1.1	Effect of enzymes and proteins on crude oil-brine interfacial tension.....	84
8.1.2	Effect of enzyme on crude oil-brine interfacial tension at high and low pH ...	86
8.1.3	Effect of enzyme and proteins on model oil-brine interfacial tension	89
8.1.4	Effect of surfactants on crude oil-brine interfacial tension	91
8.1.5	Combined effect of surfactants and enzymes on crude oil-brine IFT	92
8.2	Electrophoretic mobility measurements.....	93
8.2.1	Effect of salinity on Electrophoretic mobility:.....	95
8.3	Detection of changes in oil and water phase composition by enzyme action	96
8.3.1	Gas chromatography	97
8.3.2	Isotachophorese (ITP) measurements	98
Chapter 9 Core displacement experiments.....		99
9.1	Effect of enzymes on oil recovery.....	99
9.1.1	Sandstone cores	100
9.1.1.1	Brine Flooding Followed by Greenzyme-Brine Flooding, Cores B1 and B2 100	
9.1.1.2	Spontaneous Imbibition and Flooding Scenario, Cores B3 and B4.....	103
9.1.1.3	Brine Flooding Followed by Enzyme-Brine Flooding, Cores LB1 and LB3 106	
9.1.2	Carbonate cores	108
9.1.2.1	Brine Flooding Followed by GZ-Brine Flooding, Core S-889	108
9.1.2.2	Brine Flooding Followed by Enzyme-Brine Flooding, Cores Th1-Th4....	109
9.1.3	Proposed mechanism for enhanced oil recovery by enzymes.....	110
9.2	Combined enzyme-surfactant injection.....	112
9.2.1	Enzyme-Surfactant-Brine Flooding, Core LB1 and LB3.....	114
9.2.2	Surfactant-Brine Flooding, Core LB2.....	115
9.3	Capillary number analysis.....	117
9.4	Wettability and water end point permeability	118
Chapter 10 Micromodel experiments.....		121
10.1	Glass micromodels	121

10.2	Study of enzyme-brine injection by glass micromodel.....	122
10.2.1	Waterflooding.....	123
10.2.2	Enzyme-brine flooding.....	126
10.2.3	Evidence of wettability change in the micromodel.....	129
Chapter 11 Summary of the main results		133
11.1	Scope of this study	133
11.3	“Evidence” of wettability alteration by enzymes.....	134
11.4	Enzymes and the potential for oil mobilization	137
11.5	Validation of results obtained from static and dynamic experiments	141
Chapter 12 Concluding remarks		145
Appendix A Material.....		147
A.1	Solid	147
A.2	Oil.....	148
A.3	Brine.....	149
A.4	Enzyme-Protein.....	149
A.5	Surfactant	150
Appendix B Method and procedure.....		151
B.1	Core displacement experiments	151
B.2	Experiments on the glass plate.....	155
B.3	Adsorption measurement.....	158
B.4	Interfacial tension (IFT) measurement.....	161
B.5	Electrophoretic mobility.....	164
B.6	Gas chromatography	166
B.7	Isotachophoresis.....	167
B.8	Micromodel experiments.....	169
Appendix C SCA paper.....		175
Bibliography		189

List of Figures

Figure 2.1: Schematic of the bypassing mechanism in imbibition for water-wet (a) and oil-wet (b) conditions. In water-wet system oil-water interface moving faster in small pore than in large pore and in oil-wet system is vice versa (Redrawn from Chatzis et al., 1983).	9
Figure 2.2: Schematic of the snap-off mechanism in imbibition (Sorbie and Van Dijke, 2005).	9
Figure 2.3: The Capillary Desaturation Curves for the non-wetting phase, for different types of porous media. The curves are reconstructions of those presented by Lake (1984).	10
Figure 2.4: Main EOR methods classification (chemical, miscible and thermal) upon macroscopic and microscopic sweep efficiency. The table is reconstruction of that presented by Marle (1991).....	11
Figure 3.1: Left: General amino acid structure. Right: An example of three-dimensional structure of an enzyme.	14
Figure 3.2: General mechanism of enzymes to catalyze chemical reactions.	16
Figure 3.3: Mechanisms which describe the binding of enzymes and substrates.	17
Figure 4.1: Surfactant structure.	27
Figure 4.2: Micelles with different structures. (a) Spherical micelle (b) Cylindrical micelle.	27
Figure 4.3: Schematic definition of the critical micelle concentration (Lake, 1984).....	27
Figure 4.4: Schematic representation of phase behavior generated upon mixing oil, brine and surfactant. (a) Type II(-). (b) Type II(+). (c) Type III. The figures are reconstructions of those presented by Lake (1984).	30
Figure 4.5: interfacial tension (IFT), solubilization parameter and phase behavior of microemulsion systems versus salinity (Healy and Reed, 1974).	31
Figure 5.1: Contact angle in an oil-water-solid system.....	33
Figure 5.2: Pore size distributions showing the fraction of oil wet pores (a) and their distribution for (a) a fractionally-wet (FW) system; (b) a mixed-wet system where the large pores are oil wet (MWL); and (c) a mixed-wet system where the small pores are oil wet (MWS).....	35

Figure 5.3: Imbibition and drainage capillary pressure curve required determining the Amott-Harvey and USBM wettability indices.....	39
Figure 5.4: Residual oil saturation vs. I_{a-h} for Berea sandstone (Anderson, 2006).	42
Figure 5.5: Residual oil saturation vs. I_{a-h} for several other sandstones (Anderson, 2006).	42
Figure 5.6: Residual oil saturation vs. I_{a-h} for several carbonates (Anderson, 2006).....	43
Figure 5.7: Effect of wettability on CDCs for Berea Sandstone (Mohanty and Salter, 1983). Figure regenerated by Anderson (2006).....	44
Figure 5.8: Effect of wettability on CDCs for carbonates (Kamath et al., 2001). Figure regenerated by Anderson (2006).....	45
Figure 6.1: A typical schematic of electrostatic double layer structure for a positively charged surface in an electrolyte and corresponding electrostatic potential profile, where decays from a maximum value at the surface through zero in the bulk solution.	48
Figure 6.2: Mechanisms of interaction between crude oil components and solid surfaces (Buckley et al., 1998).	57
Figure 7.1: Photo of an oil droplet that adherer to the clean glass surface.	61
Figure 7.2: The conventional sessile drop contact angle technique.	64
Figure 7.3: $\Delta\theta/\theta_{Ref}$ vs. GZ concentration when ordinary glass without aging was used as the solid surface and crude oil A as the oleic phase.....	65
Figure 7.4: $\Delta\theta/\theta_{Ref}$ vs. GZ concentration when aged glass in crude oil A (aged at 80° C) was used as the solid surface and crude oil A as the oleic phase.	66
Figure 7.5: $\Delta\theta/\theta_{Ref}$ vs. different wetting state when identical concentration (0.1 and 0.5 wt%) of GZ was used as the aqueous phase, crude oil A as the oleic phase and aged glass (aged at 80° C) as the solid surface.	67
Figure 7.6: $\Delta\theta/\theta_{Ref}$ vs. GZ concentration when ordinary glass without aging was used as the solid surface and crude oil B as the oleic phase.....	69
Figure 7.7: $\Delta\theta/\theta_{Ref}$ vs. GZ concentration when aged glass in crude oil B (aged at 80° C) was used as the solid surface and crude oil B as the oleic phase.	70
Figure 7.8: $\Delta\theta/\theta_{Ref}$ vs. Zonase 1 & 2 concentration when aged glass in crude oil A (aged at 80° C) was used as the solid surface and crude oil A as the oleic phase.....	71
Figure 7.9: $\Delta\theta/\theta_{Ref}$ vs. NZ2, NZ3 & NZ6 concentration when aged glass in crude oil B (at 80° C) was used as the solid surface and crude oil B as the oleic phase.	73
Figure 7.10: $\Delta\theta/\theta_{Ref}$ vs. α -La concentration when aged glass in crude oil B (at 80° C) was used as the solid surface and crude oil B as the oleic phase.....	74
Figure 7.11: Contact angle change by introduction of enzyme to the system.	74
Figure 7.12: Contact angle measurements as a function of time corresponding to washing effect of enzymes.	75
Figure 7.13: Breaking down of ester bonds by NZ group enzymes and alter the wetting behavior of the slid surface.	79
Figure 8.1: IFT for different concentration of different enzyme-brine solutions and crude oil B after 2 and 4 weeks equilibration.	85
Figure 8.2: IFT between different concentrations of GZ solution and crude oil B.....	86

Figure 8.3: IFT between crude oil B and brine with varying pH and NaCl concentration with and without enzyme.	87
Figure 8.4: Photo of the samples immediately after the equilibrating in the rotator (number in accordance with sample numbers in Table 8.1.	88
Figure 8.5: IFT between identical concentration (1wt%) of different enzyme-brine solutions and model oil, with and without ester.	90
Figure 8.6: Electrophoretic mobility for emulsion of crude oil A, B and model oil in different enzyme-brine solution.	94
Figure 8.7: Electrophoretic as a function of dilution times of SSW.	96
Figure 8.8: Relative amount of the ester to the reference case without adding any enzyme for model oil after equilibration with different enzyme-brine solutions.....	98
Figure 9.1: Oil production, differential pressure profiles and WBT time for water flooding core B1.	101
Figure 9.2: Oil production during different injection rates for 1wt% GZ flooding core B1..	102
Figure 9.3: Oil production, differential pressure profiles and WBT time for water flooding core B2.	102
Figure 9.4: Oil production during different injection rates for 1wt% GZ flooding core B2..	103
Figure 9.5: Oil production by imbibition vs dimensionless time cores B3 and B4.	104
Figure 9.6: Production profile for GZ-brine flooding cores B3 and B4.	105
Figure 9.7: Oil production, differential pressure profiles and WBT time for water flooding core LB1.	106
Figure 9.8: Oil production, differential pressure profiles and WBT time for water flooding core LB3.	106
Figure 9.9: Oil production, differential pressure profiles and WBT time for water flooding core S-889.	109
Figure 9.10: Enzymes that moves forward along the pore channels and change the oil-wet sections to water-wet (Feng et al., 2007).	112
Figure 9.11: Oil production, differential pressure profiles and WBT time for water flooding core LB2.	116
Figure 9.12: Capillary desaturation curve (CDC) cores LB1, LB2 and LB3.	118
Figure 10.1: Micromodel (a) @ S_{wi} and (b) @ S_{or} after waterflooding No.1.	123
Figure 10.2: Micromodel @ S_{or} after waterflooding (a) experiment No.2 (b) experiment No. 3 (c) experiment No.4 (d) experiment No. 5.	124
Figure 10.3: Micromodel (experiment No.1) @ S_{or} after different stages of flooding (a) waterflooding (b) 1 day enzyme-brine, (c) 2 days enzyme-brine and (d) 3 days enzyme-brine.	128
Figure 10.4: Micromodel (experiment No.4) @ S_{or} after different stages of flooding (a) after waterflooding, (b) after 1 day NZ2-brine flooding and (c) after 2 days NZ2-brine flooding.	129
Figure 10.5: (a) S_{or} after water flooding No.2 (b) Focused area in different time steps of enzyme-brine flooding.	130

Figure 10.6: Examples of snap-off event by injection of enzyme-brine in experiment No.3. Time interval between images is about one minute.	131
Figure 10.7: Example of effect of wettability change on residual oil saturation in micromodel experiments after enzyme-brine flooding (experiment NO.3). (a) after waterflooding (b) after about one day enzyme-brine flooding.	131
Figure 11.1: Breaking down of ester bonds by NZ group enzymes and alter the wetting behavior of the solid.	136
Figure 11.2: Oil recovery in different flooding scenario for all cores.	138
Figure 11.3: An example of micromodel @ S_{or} after different stages of flooding (a) after waterflooding and (b) after enzyme-brine flooding.	142
Figure 11.4: Examples of snap-off event by injection of enzyme-brine in experiment No.3. Time interval between images is about one minute.	143
Figure 11.5: Example of effect of wettability change on residual oil saturation in micromodel experiments after enzyme-brine flooding (experiment NO.3). (a) after waterflooding (b) after about one day enzyme-brine flooding.	144

List of Tables

Table 3.1: Classes of enzymes (Baker and Chaykin, 1962).....	18
Table 7.1: Adhesion map for crude oil A with clean glass.	60
Table 7.2: Adhesion map for crude oil B with clean glass.	61
Table 7.3: Adhesion map for crude oil B with aged glass.	63
Table 7.4: Adhesion behavior of crude oil B at pH 3 and 0.5M NaCl concentration by NZ2 enzyme introduction.	63
Table 7.5: Contact angle measurements for crude oil A-Brine+GZ-Glass.	65
Table 7.6: Contact angle measurements for crude oil A-Brine+GZ-Aged Glass (aged at 80°C).	66
Table 7.7: Contact angle measurements for crude oil A-Brine+GZ-Aged Glass (aged at 80°C), identical concentration of GZ in the solution.	67
Table 7.8: Contact angle measurements for crude oil B-Brine+GZ- Glass.	68
Table 7.9: Contact angle measurements for crude oil B-Brine+GZ-Aged Glass (aged at 80°C).	69
Table 7.10: Contact angle measurements for crude oil A-Brine+Zonase 1 & 2-Aged Glass (aged at 80°C).	70
Table 7.11: Contact angle measurements for crude oil B-Brine+NZ2, NZ3 & NZ6-Aged Glass (aged at 80°C).	72
Table 7.12: Contact angle measurements for crude oil A-Brine+ α -La -Aged Glass (aged at 80°C).	73
Table 7.13: Photos show the washing effect of enzymes for different time intervals. Glass slides are pre-aged in crude oil B, and are not washed prior to immersion in the enzyme-brine solutions.	77
Table 7.14: Adsorption measurements of NZ2 enzyme by silica and kaolin.	81
Table 8.1: Overview of the samples, the pH change and measured interfacial tension.	87
Table 8.2: IFT measurements with different types and concentrations of surfactants and co-solvent.	92
Table 8.3: IFT measurements for surfactant (1 wt% O342-c) -enzyme solutions.	93
Table 8.4: pH values for brine and enzyme-brine solutions.	95

Table 8.5: Amount of different components in the model oil after equilibrated with the enzymes.	97
Table 9.1: Dynamic displacement scenarios for sandstone cores.	100
Table 9.2: Summary of production data for cores B1 and B2.....	103
Table 9.3: Summary of production data for cores B3 and B4.....	105
Table 9.4: Summary of production data for cores LB1 and LB3.....	107
Table 9.5: Dynamic displacement scenarios for carbonate cores.	108
Table 9.6: Summary of production data for core S-889.....	109
Table 9.7: Summary of production data for cores Th1-Th4.	110
Table 9.8: Dynamic displacement scenarios for sandstone cores, LB1, LB2 and LB3.	113
Table 9.9: Summary of production data for cores LB1 and LB3.....	115
Table 9.10: Summary of production data for cores LB2.....	116
Table 9.11: Calculated capillary numbers (for injection rate of 1 cc/min) and corresponding S_{or} (fraction OOIP) for aged Berea cores, LB1, LB2 and LB3.....	117
Table 9.12: End point permeabilities and S_{or} for different stages of the sandstone cores.	119
Table 10.1: Dynamic displacement scenarios for micromodel experiments.	123
Table 10.2: Residual oil saturation at different stage of flooding for different experiments.	127

Symbols and abbreviations

A and B	Crude oil
AN	Acid number
B1,2,3 and 4	Short Berea sandstone cores
BN	Base number
C	Empirical constant
CDC	Capillary desaturation curves
CMC	Critical micelle concentration
COBR	Crude oil/brine/rock
DLVO	Derjaguin-Landau-Verwey-Overbeek
E	Total displacement efficiency
EnF	Enzyme flood
E_D	Microscopic displacement efficiency
E_V	Volumetric displacement efficiency
EOR	Enhanced oil recovery
F_a	Van der Waals force
F_r	Repulsive double layer forces
FID	Flame ionization detector
FW	Fractionally wet system
G	Gravitational constant
GC	Gas chromatography
GZ	Greenzyme
HCl	Hydrochloric acid
HLB	Hydrophile-lipophile balance
$[HA]_{o,tot.}$	Total concentration of the component (moles/liter) in the bulk oleic phase
$[HA]_{w,tot.}$	Total concentration of the component (moles/liter) in the bulk aqueous phase

IAA	Isoamyl alcohol
IFT	Interfacial tension
I_{a-h}	Amott-Harvey wettability index
I_O	Wettability indexes to oil
I_W	Wettability indexes to water
I_{USBM}	USBM wettability index
ITP	Isotachophoresis
J	Mean surface curvature
K	Permeability
K_r	Relative permeability
K_{ro}	Relative permeability to oil
K_{rw}	Relative permeability to water
k_w	Effective permeability to water
$k_o(S_{wi})$	Oil permeability at initial water saturation
L	Length of the porous medium
L_c	Characteristic length
LB1, 2 and 3	Long Berea sandstone cores
LDV	Laser Doppler Velocimetry
M	Mobility ratio
Marcol 152	Mineral oil
MWL	Mixed-wet system where the large pores are oil wet
MWS	Mixed-wet system where the small pores are oil wet
NaCl	Sodium chloride
N_c	Capillary number
N_{cc}	Critical capillary number
NMR	Nuclear magnetic resonance
NSO	Compounds containing nitrogen (N), sulfur (S) and oxygen (O)
NZ	Novozyme
OOIP	Original oil in place
O332, O342-c, O342-h and O342-I	Anionic surfactants (internal olefine sulfonate)
P	Partition ratio
P_c	Capillary pressure
P_O	Pressure in the oil phase
P_{nw}	Pressure in non-wetting phase

P_w	Pressure in wetting phase
P_W	Pressure in the water phase
pH	$-\log[H^+]$
PV	Pore volume
pzc	Point of zero charge
QCM	Quartz crystal microbalance
R	Ratio
R_1 and R_2	principal radii of curvature at any point on the oil-water interface
S	Saturation
S-889	Carbonate core
S_o	Oil saturation
S_{oi}	Initial oil saturation
$S_{or(SW)}$	Residual oil saturation after sea water flood
S_{or}	Residual oil saturation
S_{or1}	Residual oil saturation after brine flood
S_{or2} and 3	Residual oil saturation after enzyme-brine flood
SP*	Solubilization parameter at optimum
SP_0	Solubilization parameter for oil, i.e. volume oil per volume surfactant in microemulsion
SP_w	Solubilization parameter for water, i.e. volume water per volume surfactant in microemulsion
SP Imb	Spontaneous imbibition
SSW	Synthetic sea water
S_w	Water saturation
S_{wi}	Initial water saturation
t	Imbibition time
t_D	Dimensionless time
T	Temperature
Th1,2,3 and 4	Carbonate cores
USBM	The US Bureau of Mines
u	Darcy velocity
u	Injection rate
UV	Ultra violet
V_{spo}	Oil volume displaced by spontaneous water imbibition

V_{spw}	Water volume displaced by spontaneous oil imbibition alone
V_{to}	Total oil volume displaced by imbibition and centrifugal (forced) displacement
V_{tw}	Total displaced by oil imbibition and forced displacement
v	Velocity of fluid in the pores of the porous medium
V	Volume
WBT	Water breakthrough
Winsor I	Lower phase microemulsion
Winsor II	Upper phase microemulsion
Winsor III	Middle phase microemulsion
WOR	Water-oil ratio
wt%	Weight percent
θ	Contact angle
θ_{REF}	Reference contact angle
ΔP	Differential pressure
α -La	Alpha-Lactalbumin
β	Shape factor
γ	Shear rate
γ_0	Initial interfacial tension before addition of surfactant
γ	Final interfacial tension
π	Expanding (interfacial) pressure
σ	Interfacial tension
σ_{ow}	Interfacial energy between oil and water
σ_{ws}	Interfacial energy between water and solid
σ_{os}	Interfacial energy between oil and solid
Π	Disjoining pressure
ϕ	Porosity of the porous medium
μ	Viscosity
μ_o	Viscosity of oil
μ_w	Viscosity of water
λ_d	Mobility of displaced phase
λ_D	Mobility of displacing phase
ρ	Density
τ	Shear stress

ω Velocity of rotation

Chapter 1 Introduction

As oil resources are depleted around the world, finding easy targets for primary oil recovery becomes more difficult. On the other hand, the demand for energy and crude oil increases rapidly. This calls for more efficient production of existing oil resources by conducting enhanced oil recovery methods. During the past 40 years, a variety of enhanced oil recovery (EOR) methods have been developed and applied to mature and mostly depleted oil reservoirs. These methods improve the efficiency of oil recovery compared with primary (pressure depletion) and secondary (water-flooding) oil recovery methods. At the microscopic scale, capillary forces cause oil to be left behind in the waterflooded zones of an oil reservoir. For a typical waterflood the average oil recovery, is usually on the order of one-third (Green and Willhite 1998). This implies that after the completion of a waterflood significant amount of oil remains in the reserve.

One way of recovering capillary trapped oil after water flooding is by chemical flooding. Examples of classic chemical flooding processes are: surfactant flooding and alkali/surfactant/polymer flooding. Three important factors to consider in relation to enhanced oil recovery processes are, viscosity of the displaced and displacing fluids and relation between those (mobility ratio); interfacial tension between displaced and displacing fluids; and wettability of the porous media.

Wettability is an important factor in controlling the location, flow, and distribution of fluids in a reservoir (Anderson 1986-a) and several publications have discussed the influence of wettability on oil recovery. Wettability is a significant issue in multiphase flow problems ranging from oil migration from source rocks to enhanced recovery processes (Morrow, 1990). Several researchers have attempted to alter the wettability favorably in oil reservoirs in order to improve spontaneous imbibition of water and waterflood performance to enhance oil recovery. Austad et al. (1998) and Xu et al. (2005) reported different production profiles using

surface active agents to enhance spontaneous imbibition into chalk cores and ascribed this difference in behavior to the change of wettability by surface active agents. Several authors (e.g. Morrow et al., 1998; Zhang et al., 2006; Yu et al., 2008) have reported effects of brine composition on wettability change and Alagic (2010) demonstrated the use of low salinity water plus surfactant to change wettability and improve oil recovery.

It has been suggested that enzymes-proteins can be introduced as an enhanced oil recovery method to improve waterflood performance especially in oil-wet reservoirs by changing the wettability to a more water-wet state and possibly lead to increased oil recovery (Feng et al., 2007 and Moon, 2008; Nasiri et al. 2009). Feng et al. (2007), Moon (2008) and Nasiri et al. (2009) reported increased oil production by injection of modified enzyme solutions in both laboratory core floods and a field scale pilot test.

Enzymes are a specific group of proteins that are synthesized by living cells to work as catalysts for the many thousands of biochemical reactions (Copeland, 2000). Enzymes may be used in solutions to either degrade unwanted chemicals or produce desired chemicals (Harris and McKay, 1998). Like all catalysts, enzymes work by lowering the activation energy for a reaction, thus dramatically accelerating the rate of the reaction (Reiner, 1969; Bickerstaff, 1987). Enzymes are used for different industrial applications, such as detergents, textile and food industry. However, use of enzymes in the oil and gas industry has been suggested recently.

The research presented in this work addresses using enzyme-proteins in order to improve oil recovery. The main motivation of this work is to investigate the potential and feasibility of this method as well as understanding the mechanism by which these molecules contribute to increased oil recovery through a mechanistic study of the effect of enzymes on oil-brine-solid interactions. The thesis consists of two main parts. In the first part, a discussion of the underlying mechanism/s of enzyme-brine injection is presented based on experimental investigations of the effect of enzyme-brine solutions on different oil/water and oil/water/solid interactions such as IFT and wettability. In the second part, experiments are made through core floods of different enzyme-protein solutions (added to the injection brine) and also combined surfactant-enzyme solutions, for reducing the residual oil saturation after conventional waterflooding. Core flooding experiments were done to investigate the potential of improved oil recovery by enzyme and enzyme-surfactant in sandstone and carbonate rocks.

In chapters 2 through 6 the fundamental theories are thoroughly reviewed. Chapter 2 gives a brief introduction to enhanced oil recovery (EOR) methods while a brief introduction of enzymes and EOR surfactants is given in Chapter 3 and 4, respectively. Chapter 5 is devoted to wettability issues and finally chapter 6 discusses interactions at oil/water and oil/water/solid interfaces

The experimental results and observations are presented in chapters 7-10. To investigate further by which mechanism/s the enzymes may contribute to enhanced recovery, groups of enzymes with different properties and catalytic functions, known to be interfacially active, were chosen to cover a wide range of possible effects. Chapter 7 describes a comprehensive investigation of the effect of the enzymes on oil-water-solid interactions by means of adhesion tests, contact angle measurements and adsorption measurements. Chapter 8 of this thesis has experimentally studied changes in oil-water interfacial properties by addition of enzymes and proteins, including measurements of interfacial tension and electrophoretic mobility. Attempts were also made to study changes in both oil and water phase composition after equilibration with enzymes. However, since the chemical composition of crude oil is highly complex, a model oil was used in some of the experiments.

Chapter 9 presents results of core flooding experiments including both sandstone and carbonate rocks using enzyme-brine and enzyme/surfactant-brine injection as the secondary and tertiary modes. The main objectives of the core flooding experiments were to evaluate the improvement in oil recovery after enzyme or enzyme-surfactant treatment. The rationale behind combining enzyme and surfactant flooding was based on previous positive results from combined low salinity and surfactant injection (Alagic and Skauge, 2010), as discussed further in this chapter.

To further improve our understanding of the underlying mechanisms of enzymes, glass micromodel experiments were conducted using enzyme-brine to be injected after water flooding. The results are presented in chapter 10. Chapter 11 of the thesis summarized the main results obtained from all experiments and visualizations. Concluding remarks are presented in chapter 12. Materials which are used in all experiments are listed in Appendix A. Explanations of the experimental procedures as well as some theory behind some of the experiments are listed in Appendix B.

Chapter 2 Enhanced oil recovery mechanisms

Enhanced oil recovery (EOR) processes are studied to increase oil production from depleted oil reservoirs after primary production in which oil is produced by energy naturally existing in a reservoir. Willhite (1986) defines enhanced oil recovery as any processes that helps recover more oil from a reservoir than what the reservoir can produce by its own energy. This definition is quite general and also includes injection of gas and water for pressure maintenance. But Lake (1989) defines EOR more specific as an oil recovery process by injecting materials not normally present in the reservoir.

2.1 Displacement efficiency

Considering any oil recovery process, the total displacement efficiency can be divided into two groups; microscopic and macroscopic displacement efficiencies. In equation form,

$$E = E_D \times E_V \quad (2.1)$$

where E is the total displacement efficiency, and E_D and E_V are the microscopic and volumetric (macroscopic) displacement efficiencies, respectively.

For a typical waterflood the average total displacement efficiency, i.e. the average oil recovery, is usually on the order of one-third (Green and Willhite, 1998). This one-third figure is by no means a universal result applicable to all reservoirs. Depending on the oil and reservoir characteristics, individual reservoirs can yield higher or lower recovery efficiencies. However, the figure indicates that after the completion of a waterflood a significant amount of

oil remains in the reservoir. This remaining oil is the target for EOR processes. In an EOR process, it is desirable that the values of E_D and E_V and consequently E approach 1.0.

2.1.1 Volumetric sweep efficiency

Macroscopic displacement efficiency (E_V) is a measure of how efficiently the displacing fluid sweeps out the volume of a reservoir, both areally and vertically, as well as how efficiently the displacing fluid moves the displaced oil toward production wells. Both areal and vertical sweeps must be considered, and it is often useful to further subdivide E_V into the product of areal and vertical displacement efficiencies.

Macroscopic displacement efficiency is strongly influenced by the stability of the front, which in turn is defined by the mobility of the fluids. The mobility of a fluid, λ is defined as the ratio between the permeability of the porous media, K and the viscosity of the fluid, μ . The mobility ratio, M , is the ratio between the mobility of the displacing and displaced fluid, respectively.

$$M = \frac{\lambda_w}{\lambda_o} = \frac{[K_{rw}(S_w)/\mu_w]}{[K_{ro}(S_o)/\mu_o]} \quad (2.2)$$

where M is the mobility ratio, λ_w and λ_o are the mobilities of water and oil, K_{rw} and K_{ro} are the relative permeabilities to water and oil and μ_w and μ_o are water and oil viscosities, respectively.

In a conventional waterflood, if the mobility ratio is unfavorable (>1), the water tends to finger into the oil and take the shortest path to the production well. This effect is amplified by reservoir geological heterogeneities. Favorable mobility ratios contribute to improved areal and vertical sweep. It can be provided by using chemicals such as polymer to add to water (displacing fluid).

Another factor which can be important to good macroscopic efficiency is the density difference between displacing and displaced fluids. Large density differences can result in gravity segregation i.e., the underriding or overriding of the fluid being displaced. The effect is that fluid is bypassed at the top or bottom of a reservoir, thus reducing E_V . If density differences do exist between fluids, this might be used to advantage by flooding in an updip or downdip direction.

2.2 Microscopic displacement efficiency

Microscopic displacement relates to the displacement or mobilization of oil at the pore scale (Green and Willhite, 1998). As such, E_D is a measure of the effectiveness of the displacing fluid in mobilizing oil in the regions contacted by the displacing fluid. Oil entrapment is a result of complex interactions between viscous, gravity and capillary forces. Improving recovery from hydrocarbon fields typically involves altering the relative importance of the viscous and capillary forces.

2.2.1 Capillary forces

Capillary forces are responsible for aiding or opposing the displacement of a fluid by another in a porous medium. In a porous medium, capillary forces are the result of the combined effect of the interfacial tensions between the rock and fluids, the pore size and geometry and the wetting characteristics of the system (Ahmed, 2001). Capillary pressure (P_c) refers to the pressure difference across a curved interface between two immiscible fluids. By convention, capillary pressure is defined as the pressure difference between the non-wetting phase (p_{nw}) and the wetting phase (p_w) (Anderson, 1987-a). For a system consisting of water as the wetting and oil as the non-wetting phase, the capillary pressure is defined as:

$$P_c(S_w) = P_o(S_w) - P_w(S_w) \quad (2.3)$$

where P_o and P_w are the pressures in the oil and water phase, respectively.

The general expression for calculating the capillary pressure at any point on an interface between oil and water is given by the Laplace equation (Dake, 1978):

$$P_c = P_o - P_w = \sigma_{ow} \left[\frac{1}{R_1} + \frac{1}{R_2} \right] \quad (2.4)$$

In equation 2.4, σ_{ow} is the interfacial tension between oil and water and R_1 and R_2 are the principal radii of curvature at any point on the interface, respectively.

2.2.2 Viscous forces

The term viscous forces in a petroleum reservoir refer to the pressure gradients associated fluid flow through the porous medium (Green and Willhite, 1998). It can be expressed in terms of Darcy's Law as follow:

$$\Delta P = -\frac{\bar{v}\mu L\phi}{k} \quad (2.5)$$

where ΔP is pressure drop across the porous medium, \bar{v} is average velocity of fluid in the pores of the porous medium, μ is fluid viscosity, L is length of the porous medium, and ϕ is porosity of the porous medium and k is permeability of the porous medium.

2.2.3 Capillary number

The capillary number, N_C is a dimensionless number defined as the ratio of viscous to capillary forces. N_C depends on the velocity (v), viscosity (μ) and interfacial tension (σ) of the wetting fluid and is commonly defined as (Brownell and Kats, 1949; Lake, 1989)

$$N_C = \frac{\mu v}{\sigma} \quad (2.6)$$

The magnitude of the capillary number reflects the relative importance of viscous to capillary forces.

2.2.4 Trapping of oil at the pore scale

Primary oil recovery by reservoir pressure depletion and secondary oil recovery by waterflooding usually result in poor displacement efficiency. As a consequence there is always some trapped oil that is remained behind in oil reservoirs. Trapping of oil in a porous medium depends on the pore structure of the porous medium, fluid/rock interactions related to wettability and fluid/fluid interactions reflected in IFT (Green and Willhite 1998). There are basically two mechanisms at pore scale by which residual oil is trapped in oil reservoirs, bypassing and snap-off of oil (Chatzis et al., 1983). In a porous media, unfavorable pore geometries such as heterogeneity in pore sizes and pore throat, pore-wall roughness and coordination number can cause bypassing of oil (see Figure 2.1) (Mohanty et al. 1987).

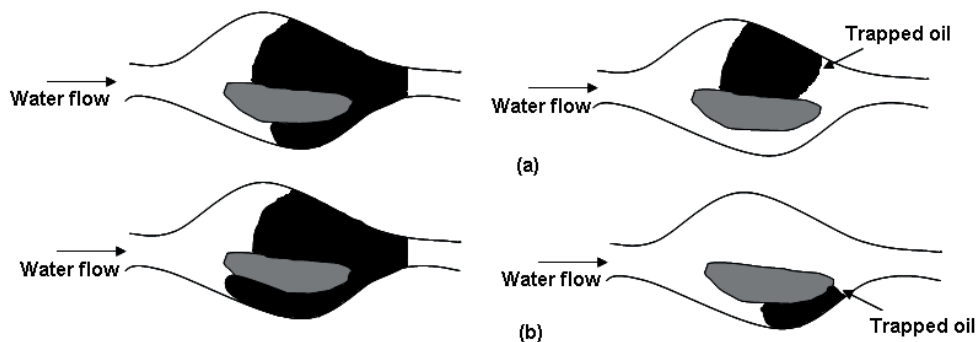


Figure 2.1: Schematic of the bypassing mechanism in imbibition for water-wet (a) and oil-wet (b) conditions. In water-wet system oil-water interface moving faster in small pore than in large pore and in oil-wet system is vice versa (Redrawn from Chatzis et al., 1983).

The second mechanism, snap-off, which is more dominant in water-wet systems is associated with the flow of wetting phase, which is water in water-wet case, through films. Water thus (at an appropriate capillary pressure) occupy the space by swelling around the oil and trapped the oil in the pore by detaching the oil droplet from the bulk oil. By estimation, 80% of the trapped oil in Berea sandstone cores occurred in snap-off geometries (see Figure 2.2) (Chatzis et al., 1983; Sorbie and Van Dijke, 2005).

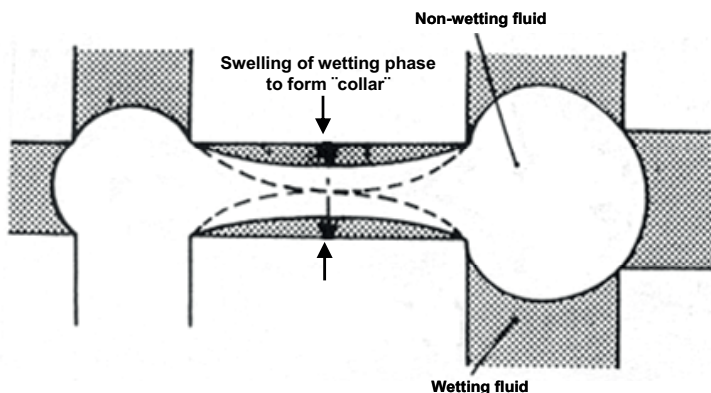


Figure 2.2: Schematic of the snap-off mechanism in imbibition (Sorbie and Van Dijke, 2005).

Enzymes-proteins can be introduced to improve waterflood performance especially in oil-wet reservoirs by changing the wettability to a more water-wet state and possibly lead to increased oil recovery (Feng et al., 2007). A discussion of the effect of wettability on oil recovery can be found in section 5.4. Surfactants are used to decrease oil-water interfacial tension such that physical mobilization of the oil takes place (Skjæveland and Kleppe, 1992).

2.2.5 Capillary desaturation curve (CDC)

Many authors (e.g. Amaefule and Handy, 1982; Kumar et al., 1985; Maldal et al. 1997; Nasiri and Abdi, 2005; Shen et al., 2006; Hamouda and Karousi, 2008) have studied the effect of capillary number on residual oil saturation at the core and reservoir scale. The relationship is typically shown through a capillary desaturation curve (CDC) as shown schematically in Figure 2.3. The CDC is a plot of capillary number on the x-axis and residual oil saturation on the y-axis. These curves typically show a residual oil saturation plateau region from very low capillary numbers through approximately $N_c \approx 10^{-6}$, after which residual oil saturations drop with increasing capillary number. The point at which residual oil saturation starts to drop with increasing capillary number is called the critical capillary number (N_{CC}). The N_{CC} varies from region to region due to numerous factors such as rock structure, rock wettability, test conditions and fluid types (Skjæveland and Kleppe, 1992).

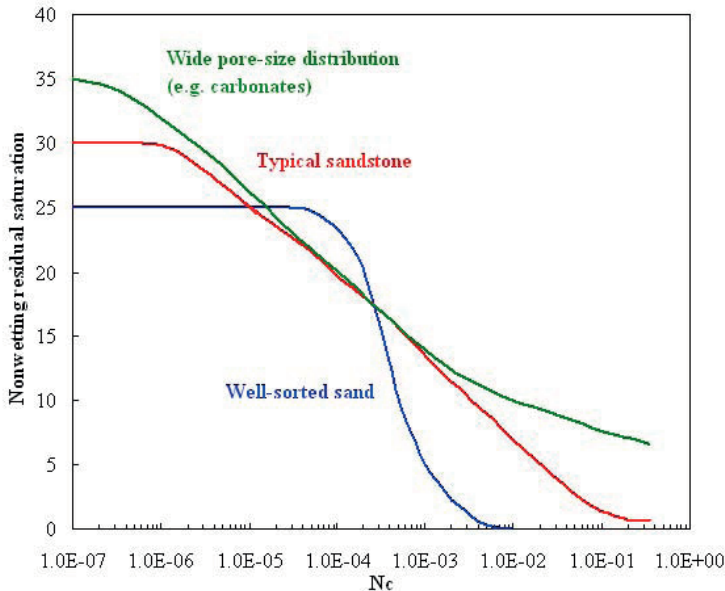


Figure 2.3: The Capillary Desaturation Curves for the non-wetting phase, for different types of porous media. The curves are reconstructions of those presented by Lake (1984).

Most displacement processes are designed to increase the viscous forces and/or reduce the capillary forces in order to reduce the residual oil saturation and increase the oil recovery. For this purpose we need to use some materials to add to injecting water to change reservoir rocks and fluid characteristics such as rock wettability and interfacial tension between oleic and aqueous phases favorably.

2.3 Classification of enhanced oil recovery methods

Marle (1991) classified EOR processes into three main categories; chemical, miscible and thermal processes. Figure 2.4 shows these different processes and the physical parameters involved. Each method is aimed to either improve the volumetric sweep efficiency or act at the pore scale to increase microscopic displacement efficiency. Of course, some of the methods can act on both the microscopic and macroscopic sweep efficiencies.

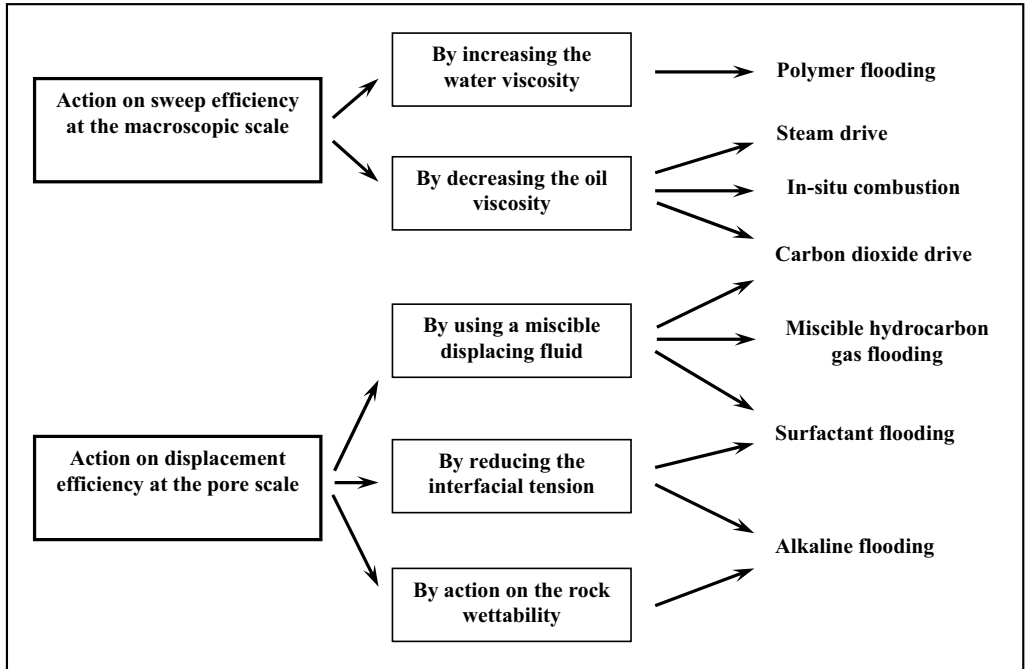


Figure 2.4: Main EOR methods classification (chemical, miscible and thermal) upon macroscopic and microscopic sweep efficiency. The table is reconstruction of that presented by Marle (1991).

The classification made by Marle (1991) is based on established enhanced oil recovery methods, and does not include novel processes which are under development such as microbial and enzyme based (Feng et al., 2007; Moon, 2008) enhanced oil recovery. This thesis investigates the possible effect of enzyme and combined enzyme-surfactant flooding mainly on microscopic displacement efficiency.

Chapter 3 Enzymes

Enzymes are a specific group of proteins that are synthesized by living cells to work as catalysts for the many thousands of biochemical reactions (Copeland, 2000). Enzymes may be used in solutions to either degrade unwanted chemicals or produce desired chemicals (Harris and McKay, 1998). Like all catalysts, enzymes work by lowering the activation energy for a reaction, thus dramatically accelerating the rate of the reaction. The disintegration of foodstuff by the digestive system is an example. It is normally accomplished within 3 to 6 hours, depending on the amount and type of food, but in the absence of enzyme catalysis it takes 30 years or more to achieve (Reiner, 1969; Bickerstaff, 1987).

3.1 Enzyme structure and function

Enzymes are generally globular proteins. Proteins are linear polymers of amino acids. Each amino acid has an amino group, a carboxylic acid group, a hydrogen atom and an R-group all surrounding a central carbon atom (see Figure 3.1). This R-group can simply be a hydrogen atom or more complex. The major division of amino acids is between those with hydrophilic (water loving) or hydrophobic (water hating) R-groups. Enzymes' function is determined by their complex structure. The reaction takes place in a small part of the enzyme called the active site, while the rest of the protein acts as "scaffolding". The amino acids around the active site attach to the substrate molecule and hold it in position while the reaction takes place (Copeland, 2000).

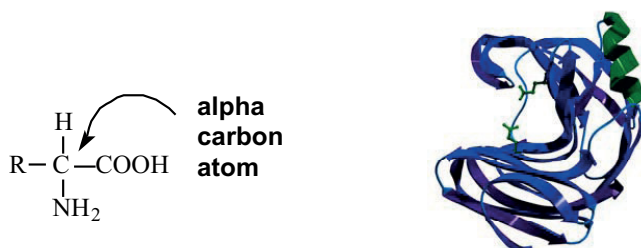


Figure 3.1: Left: General amino acid structure. Right: An example of three-dimensional structure of an enzyme.

Enzyme activity can be affected by different variables. These variables include temperature, chemical environment (e.g., pH), and the concentration of substrate. Other molecules can also affect enzymes activity such as inhibitors that decrease enzymes activity; and activators that increase activity. Many drugs and poisons are enzyme inhibitors (Reiner, 1969; Copeland, 2000).

Since enzymes act as catalysts, they are not consumed during the reaction, and so relatively few molecules are capable of catalysing the reaction a great many times. While enzymes cannot change the equilibrium position of a reaction, they can reduce the time required to reach equilibrium. Enzymes possess two special attributes that are not found to any great extent in other catalyst, and these are specificity and high catalytic power (Reiner, 1969; Blackburn, 1976; Bickerstaff, 1987; Copeland, 2000).

3.2 Mechanism of enzyme action

There are two major considerations with regards to the mechanism of enzyme action: substrate specificity and catalytic power.

Chemical catalysts display only limited selectivity whereas enzymes show specificity for the substrates and also products. This ensures that the final product is not contaminated with by-products. In the enzyme catalysis the reaction takes place in a particular region that is designed to accommodate the specific participants involved in the reaction. The region, which is known as the active site, binds the substrate and then carries out the reaction. Enzymes with broad specificity have more flexible active site requirements and can therefore accept a wider

range of substrate molecules (Reiner, 1969; Blackburn, 1976; Bickerstaff, 1987; Copeland, 2000).

During any reaction there is a state which is called "transition state". In this state the susceptible substrate bonds are not completely broken and new bonds in the product are not completely formed. The state is energy dependent because it requires energy to make and break chemical bonds. This represents an energy barrier to successful reaction, and is the reason why the vast majority of reactions proceed extremely slowly in the absence of external help. By providing heat energy, high pressure or extreme pH to weaken bonds, or by the addition of catalysts, reactants can be helped toward the transition state. To reduce the energy barrier, enzymes catalysts are more effective than other catalysts to facilitate transition state formation and thereby increase the rate of reaction (Reiner, 1969; Blackburn, 1976; Bickerstaff, 1987; Copeland, 2000).

The catalytic power of enzymes is due to the precise molecular interactions that occur at its active site. These interactions lower the energy barrier and make formation of the transition state easier. There are at least four types of interactions that can accomplish this effect, and they may operate singly or in combination.

- First, the active site in many enzymes provides a non-polar micro-environment. The removal of the substrate molecule from an aqueous polar solution into a non-polar phase may alter the conformation of the substrate towards the transition state. Also, a non-polar environment is useful for excluding water molecules, which may interfere in a reaction.
- Second, the precise alignment of substrate molecules in the active site presents the susceptible bonds at the correct angle so that a collision between reactants will result in the formation of a transition state.
- Third, the substrate molecule is normally held firmly in the active site by a number of non-covalent interactions, and small movements in the conformation of the enzyme molecule can be transmitted to active site causing a distortion of substrate structure, weakening the susceptible bond and reducing the amount of energy required to form a transition state.
- Lastly, the site amino acid residues contribute catalytic functional groups to participate directly in the reaction.

The basic mechanism by which enzymes catalyze chemical reactions begins with the binding of the substrate (or substrates) to the active site on the enzyme. The binding of the substrate to the enzyme causes changes in the distribution of electrons in the chemical bonds of the substrate and ultimately causes the reactions that lead to the formation of products. The products are released from the enzyme surface to regenerate the enzyme for another reaction cycle (see Figure 3.2).

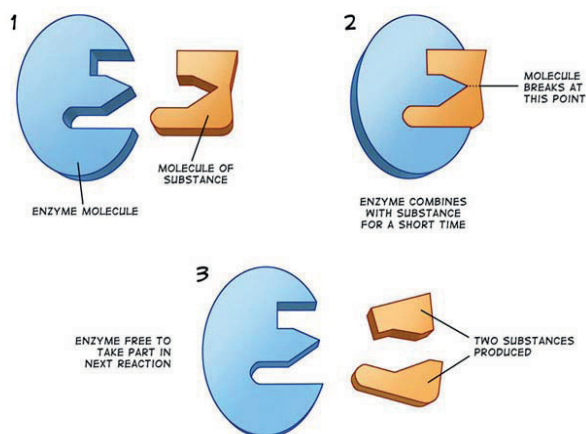


Figure 3.2: General mechanism of enzymes to catalyze chemical reactions.

The active site has a unique geometric shape that is complementary to the geometric shape of a substrate molecule, similar to the fit of puzzle pieces. This means that enzymes specifically react with only one or a very few similar compounds. There are two theories which describe the binding of enzymes and substrates. The first one is the lock and key theory, and the second one is the induced fit theory, which is a modification of the lock and key model.

3.2.1 Lock and Key Theory

The specific action of an enzyme with a single substrate can be explained using a Lock and Key analogy first postulated in 1894 by Emil Fischer (Meyer, 1995). In this analogy, the lock is the enzyme and the key is the substrate (see Figure 3.2). Only the correctly sized key (substrate) fits into the key hole (active site) of the lock (enzyme).

Smaller keys, larger keys, or incorrectly positioned teeth on keys (incorrectly shaped or sized substrate molecules) do not fit into the lock (enzyme). Only the correctly shaped key opens a particular lock.

3.2.2 Induced Fit Theory

Not all experimental evidence can be adequately explained by using the so-called rigid enzyme model assumed by the lock and key theory. For this reason, a modification called the induced-fit theory has been proposed by Koshland (1958).

The induced-fit theory assumes that the substrate plays a role in determining the final shape of the enzyme and that the enzyme is partially flexible. In this theory substrate binding induces a change in enzyme conformation which cause enzyme and substrate fit together better and so that groups in the active site which are required for catalysis are properly positioned (see Figure 3.3). This theory can also explain why sometimes certain compounds can bind to the enzyme but do not react properly, because the enzyme has been distorted too much.

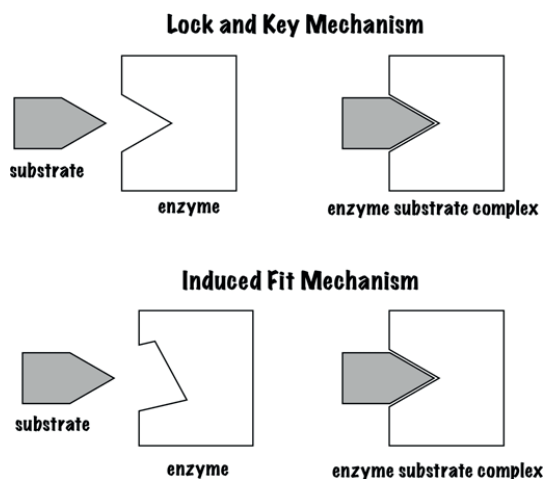


Figure 3.3: Mechanisms which describe the binding of enzymes and substrates.

3.3 Classification of enzymes

The names of enzymes, both common and systematic, are controlled by the Enzyme Commission. The common name is often derived by simply adding the suffix '-ase' to the name of the substrate upon which it works.

The systematic scheme of classification was adopted by the International Union of Biochemistry in 1961 (Baker and Chaykin, 1962). An enzyme is designated by four numbers,

main class, subclass, sub-subclass, and serial number, separated by periods. The six main classes of enzymes are presented in Table 3.1.

Table 3.1: Classes of enzymes (Baker and Chaykin, 1962).

Class	Function
1. Oxidoreductase	Catalyze redox (reduction-oxidation) reactions
2. Transferases	Catalyze transfer of a molecular group from one molecule to another
3. Hydrolases	Catalyze bond cleavage by the introduction of water
4. Lysases	Catalyze reactions involving the removal of a group to form a double bond or addition of a group to a double bond
5. Isomerases	Catalyze reactions involving intramolecular rearrangements
6. Ligases/Synthetases	Catalyze reactions joining together two molecules

3.4 Different enzymes and their uses

Enzymes are used for different applications with respect to their catalytic function. Using different types of enzyme started many years ago in industry, however, only a limited number of all the known enzymes are commercially available and even smaller amount is used in large quantities. More than 75% of industrial enzymes are hydrolases. They can hydrolyze peptides (protease enzymes), amides (amidase enzymes) and halides (halidase enzymes) in addition to esters (esterase enzymes) and triglycerides (lipase enzymes) (Fojan et al., 2000; Leisola et al., 2001).

Detergents were the first large scale application for enzymes. Esterases and lipases are used in detergents to decompose fats into more water-soluble compounds by hydrolyzing the ester bonds between the glycerol backbone and fatty acid (Leisola et al., 2001; Panda and Gowrishankar, 2005). Amylases are used in detergents to remove starch based stains.

Enzymes are used in food industry in large scale. Amylases and glucose isomerases are used to degrade starch and convert it to glucose and fructose. Esterases, pectinases, cellulases and xylanases are used in fruit juice manufacturing to improve juice liberation from the pulp. Similarly hydrolase enzymes are widely used in wine production to obtain a better extraction of the necessary components and thus improving the yield. Alpha-amylases and proteases

have been most widely studied in connection with improved bread quality in baking manufacturing (Leisola et al., 2001; Panda and Gowrishankar, 2005).

Enzymes are used in textile, leather and paper industries. Cellulases and laccases are used in textile industry in order to removal of microfibril and also color brightening. Leather industry uses proteolytic and lipolytic enzymes in leather processing to remove unwanted parts. Paper industry uses xylanases in pulp bleaching to liberate lignin fragments by hydrolyzing residual xylan (Leisola et al., 2001).

Enzymes are also used in personal care products. One application is cleaning of contact lenses by using protease and lipase enzyme solutions. Some toothpaste contains glucoamylase and glucose oxidase. The reasoning behind this practice is that glucoamylase liberates glucose from starch-based oligomers produced by alpha-amylase and glucose oxidase converts glucose to gluconic acid and hydrogen peroxide which both function as disinfectants (Leisola et al., 2001).

3.5 Enzyme applications in relation to oil and gas production

The use of enzyme processes in oil and gas industry has been suggested recently. The modern biotechnology industry can provide robust enzymes capable of tolerating oil reservoir environments.

Harris and McKay (1998) reported some applications of enzymes in oil and gas production. The applications included: enzyme pre-treatment of biopolymers to improve biopolymer handling characteristics; gel breaking in drilling to disrupt filter cake formation; desulphurization of hydrocarbons; and enzyme-based acid production for different purposes like formation damage treatment and matrix acidizing of carbonate, etc. They have also reported some other application for enzymes in the oil industry, like water shut-off and sand consolidation. Some of the mentioned applications by Harris and McKay (1998) will be discussed further in more detail.

3.5.1 Permeability modification

Modification of porous media permeability in conventional and fractured reservoirs by using enzymes was proposed by various researchers (e.g. Nemati and Voordouw, 2003; Larsen et al., 2008). The efficiency of water flooding is influenced by heterogeneity of the reservoir permeability. High permeability zones in the reservoir facilitate the transport of a large fraction of injected water to create “water fingers” that result in oil being bypassed. This problem can be overcome by selectively plugging water encroachment zones. Plugging of high permeability zones would force the injection fluid into oil bearing zones and result in increased oil production.

Nemati and Voordouw (2003) have used enzyme to modify porous media permeability. They showed that enzymatically catalyzed formation of CaCO_3 is an effective alternative for reducing porous media permeability. The results of their study indicate that an increase in enzyme concentration enhanced the extent of CaCO_3 precipitation and led to a significant decrease in permeability.

3.5.2 Removal of formation damage

Using enzyme as a means to remove formation damage induced by drilling fluids has been reported by several authors (e.g. Suhy et al., 1998; Hanssen et al., 1999; Battistel et al., 2005; Siddiqui and Nasr-El-Din, 2005; Samuel et al., 2009). Some of the polymer in drill-in fluids invades the near wellbore formation and creates skin damage. In this case, suitable enzymes can be used to degrade the polymers and remove most of this kind of polymer damage.

3.5.3 Pre-treatment of biopolymers

Using enzymes together with polymer has been reported by Kohler et al. (1987). They used enzymes to improve the injectivity of Xanthan gums (type of polymer). They stated that insoluble bacterial cells resulting from the fermentation process, and molecular aggregates or microgels, can be destroyed by the synergetic action of the enzymes. Consequently, flow behavior of treated xanthan gum solutions through reservoir rocks can be improved.

3.5.4 Breaker

Several authors (e.g. Moore et al., 1996; Tayal et al., 1997; Armstrong et al., 2010) have reported using enzymes as breakers in hydraulic fracturing. Usually high viscosity formulations of guar are used as fracturing fluids. Generally, a high viscosity fluid, as well as solid proppants, is used to pump into the production wells at sufficient pressure to fracture the formation to enhance oil and gas production by increasing permeability of the formation near the wellbore. Afterward, breakers like enzymes which are most common are used to reduce the fluid's viscosity (by breaking the polymer) which allows the proppant to settle into the fracture and facilitate fluid flow back to the wells.

3.5.4 Improved oil recovery

Feng et al. (2007) have used an enzyme to improve oil production. They performed experiments to examine the compatibility of the modified enzyme with different parameters such as type of oil, temperature, and salinity. Thereafter core flooding laboratory experiments were conducted. They concluded that at optimal conditions, recovery can be increase by 16.9% on average. Feng et al. (2007) also reported a field scale pilot test which was carried out with the same modified enzyme. Results showed decreasing water production and increasing oil production.

Moon (2008) reported enhanced oil recovery by Greenzyme injection. According to the report, coreflood tests were carried out, using Berea sandstone cores, synthetic brine and crude oil. Enzyme solutions with 3-7% concentration were injected through the core samples after waterflooding step and were halted after 5 PV injections. 48 hours soak was conducted afterward and injection of brine without adding enzymes was resumed. 3% and 13 % OOIP incremental oil recovery were obtained for 3% and 7% enzyme concentrations, respectively.

3.6 Surfactant-enzyme interactions

Surfactant-enzyme interactions in aqueous and reverse micellar solutions have been extensively studied for both technical applications (drug delivery, cosmetics and detergency, etc.) and a variety of reactions. The latter include various synthesis and hydrolysis reactions, as well as redox reactions (Savelli et al., 2000; Paul and Moulik, 2001). The potential advantages of employing enzymes in combination with water/oil microemulsions can be: (1)

increased solubility of non-polar reactants; (2) changing thermodynamic equilibrium possibly in favour of condensation (in cosmetic and medical products); (3) thermal stability improvement of the enzymes, enabling reactions to be occurred at higher temperature (Paul and Moulik, 2001)

According to Savelli et al. (2000), understanding the relationship between the surfactant chemical structure and the catalytic properties of the enzyme requires an extensive investigation. They proposed that the effect of surfactant on enzyme structure and activity is the result of chemically selective interactions that may be influenced by the enzyme structure, chemistry of the surfactant, and by other factors such as pH and ionic strength. The surfactant can interact with the enzyme and cause a conformational change for enzyme to a more active form and/or stabilize its native folded structure. Although the surfactant head group seems to have a determining role, other structural features of the detergent, such as its hydrophobic/hydrophilic balance, are also important in influencing the catalytic properties of an enzyme.

Interaction of enzymes with anionic and non-ionic surfactants was investigated by Jurado et al. (2007). They used a commercial lipase enzyme in order to assess its interaction with commercial non-ionic and anionic surfactants. According to the authors, non-ionic surfactants seem to prevent or delay enzyme penetration at the oil-water interface, thereby decreasing lipase activity. On the other hand, no inhibitory effect of the anionic surfactants on lipase action was found. Instead, a higher degree of enzymatic hydrolysis was found in the presence of anionic surfactants. They explained this by formation of an enzyme-surfactant complex which increases the catalytic properties of the enzyme. Another factor which may explain the effect of surfactant on lipase activity is the alteration of the interfacial properties of the oily phase due to surfactant adsorption.

3.7 Potential enzymes to use for enhanced oil recovery

Feng et al. (2007) reported use of enzymes in laboratory and pilot scale to improve oil recovery. This was a starting point to initiate a study to investigate potential enzymes which may improve oil recovery and study possible mechanisms which may contribute in this improvement. For this purpose group of enzymes known as interfacially active enzymes from hydrolases class were chosen. Effectiveness of hydrolase enzymes at oil-water and oil-water-solid interfaces has been reported by several authors (e.g. Marangoni, 1994; Hlady and Buijs,

1996; Beverung et al., 1999; Fojan et al., 2000; Nakanishi et al., 2001; Wertz and Santore, 2002).

Seven types of enzyme-proteins, Greenzyme, Zonase1 and 2; NZ2, 3 and 6 and Alpha-lactalbumin were used in this study. Greenzyme is a commercial water-soluble enzyme made from DNA-modified proteins extracted from hydrophobic microbes in a batch fermentation process. Using Greenzyme in order to improve oil recovery from Brea sandstone cores is reported by Moon (2008). Zonase1 and 2 are protease enzymes. They are active on catalysing break down of peptide bonds. NZ2, 3 and 6 are esterase enzymes and whose catalytic functions are to cleaving ester bonds. Alpha-lactalbumin is a whey protein. Several authors reported activity of this protein at oil, water and solid interfaces by means of different methods such as adsorption measurements (e.g. Halskau et al., 2002; Glomm et al., 2007).

Chapter 4 Surfactants for EOR

Surface active agents, or surfactants, are chemical agents that alter the properties of solution interfaces. Surfactants can be added to an aqueous solution to bring about decrease in oil-water interfacial tension. The use of surfactant for oil recovery is not a recent development in petroleum technology. Degroot was granted a patent in 1929 claiming water-soluble surfactants as an aid to improve oil recovery. Since then, thousands of studies have been published on surfactant flooding EOR, and numerous field operations have been going on around the world.

The success of surfactant flooding EOR depends on many factors such as formulation, cost, availability of chemicals, environmental impact, and oil prices in the market. In order for surfactants to be cost effective, several criteria also have to be met. The structure should increase the chemicals' affinity for the interface and produce ultra low IFT and it should be sufficiently simple to minimize the number of synthesis steps for commercial production.

4.1 Surfactant structures, types and properties

Surfactants are amphiphilic molecules composed of two parts (see Figure 4.1), a hydrophilic and a hydrophobic group. The hydrophobic portion of the surfactant monomer is typically a long hydrocarbon chain which can be saturated, unsaturated, straight, branched, or aromatic, frequently referred to as the "tail" of the molecule. The hydrophilic group often referred to as the "head" of the molecule, can be charged or non-charged (Lake, 1989). Surfactants are usually classified according to the charge of the hydrophilic group in the molecule. If the

hydrophilic part is negatively or positively charged the surfactant is called anionic or cationic, respectively. If the hydrophilic part only contains polar groups, the surfactant is called non-ionic. Surfactants can also contain both negatively and positively charged groups within the same molecule and are then classified as zwitter-ionic surfactants (Green and Willhite, 1998).

The hydrophilic group of the surfactant monomer provides most surfactants with a high solubility in water. The hydrophobic group of the monomer, however, prefers to reside in a hydrophobic phase. These competing effects result in the formation of micelles in aqueous solution, and accumulation of surfactant monomers at oil-water interfaces. In the case of micelles, the hydrophilic group is oriented towards the water phase and the hydrophobic groups create a hydrophobic environment in the core of the micelle. Similarly, at the oil-water interface, the surfactant is oriented with the hydrophobic group embedded in the oil phase and the hydrophilic head group oriented toward the water phase. This accumulation of surfactant at the oil-water interface reduces the oil-water interfacial tension.

Once a sufficient amount of surfactant has been added to aqueous solution, aggregates of surfactant monomers referred to as micelles will form. At relatively low surfactant concentrations, micelles are spherical in shape and can contain several hundred surfactant monomers with the charged head of the molecule oriented towards the water phase and the hydrophobic ends creating a hydrophobic environment in the core of the micelle (Hiemenz and Rajagopalan, 1997). Figure 4.2 shows a spherical micelle as well as a cylindrical micelle which can be created at higher surfactant concentration. The threshold concentration at which micelles begin to form is termed the critical micelle concentration (CMC) which is shown in Figure 4.3. Beyond the CMC, any surfactant added to aqueous solution will not increase the number of monomers in aqueous solution, but rather contribute to the formation of additional micelles (Lake, 1989).

The concentration of surfactant required to form micelles is typically small, between 10 mg/L and 2000 mg/L (Hiemenz and Rajagopalan, 1997) and depends on factors such as surfactant type, temperature, and water hardness. For ionic surfactants, the formation of micelles is usually an exothermic process, i.e. a reaction in which energy is released in the form of heat. CMC will therefore generally increase with increasing temperature (Zana, 1990). For non-ionic surfactants the trend of CMC is usually opposite to that of ionic surfactants (Evans and

Wennerstrom, 1999). As the hydrophobicity of the surfactant increases, its CMC in aqueous solution will generally decrease.

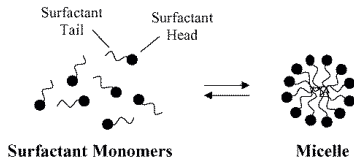


Figure 4.1: Surfactant structure.

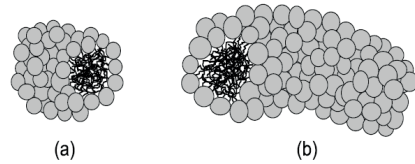


Figure 4.2: Micelles with different structures. (a) Spherical micelle (b) Cylindrical micelle.

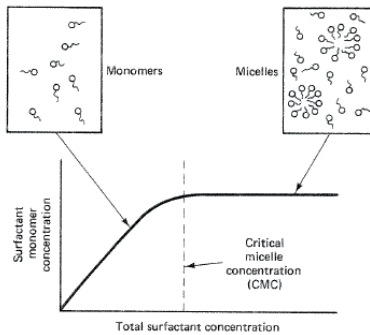


Figure 4.3: Schematic definition of the critical micelle concentration (Lake, 1984).

The hydrophile-lipophile balance (HLB) number is an indication of the relative strength of the hydrophilic and hydrophobic portions of the molecule and can be used to characterize the relative affinity of surfactants for aqueous and oleic phases. A high HLB number generally indicates good surfactant solubility in water, while a low HLB number indicates a lower aqueous solubility and higher relative affinity for the oleic phase. For a particular oleic phase, optimum aqueous phase solubilization will generally occur at a specific HLB number. Less hydrophobic oil phases generally require a higher HLB number surfactant to bring about sufficient solubilization (Garrett, 1972).

4.2 Increased oil recovery by surfactant flooding

The aim of surfactant flooding is to recover the capillary-trapped residual oil after waterflooding (Skjæveland and Kleppe, 1992). The reduction in oil-water interfacial tension arising from the addition of a surfactant to an aqueous solution will reduce the influence of capillary forces. If the interfacial tension can be lowered sufficiently, physical mobilization of oleic phase can occur. Interfacial tension between mineral oils and water is typically in the

range from 35-60 mN/m. By adding surfactant to the system these values can be lowered significantly. Ultra-low oil-water interfacial tension values down to about 1×10^{-3} mN/m have been reported by several researchers (e.g. Foster, 1973; Wilson and Brander, 1977; Milter and Austad, 1996; Nasiri and Abdi, 2005).

The degree of lowering of oil-water interfacial tension that will occur upon exposure to surfactants depends strongly on the particular oil-surfactant combination. While all conventional surfactants bring about some degree of interfacial tension lowering, only certain surfactants are capable of lowering interfacial tension by the amount necessary to mobilize significant quantities of residual oil. The use of blended surfactant combinations, co-solvents such as alcohol and salinity modification are often required to bring about significant lowering of interfacial tension (Rosen, 2004). The degree of interfacial tension reduction required to mobilize residual oleic phase can be best characterized by the capillary number and capillary desaturation curve which are explained in chapter 2 in details.

A major problem in determining the efficiency and economic feasibility of surfactant flooding for enhanced oil recovery is the unanticipated loss of surfactant. Up to 90% of the injected surfactant is believed to be retarded by the formation when passing through the target rock (Austad, 1993). The retention of surfactant may lead to a local increase in the interfacial tension and cause the process to be less effective (Zhang et al., 2005). Extensive research on surfactants for EOR has been done in the past decade to better understand the interplay between surfactant structures on low interfacial tension, and to achieve a surfactant formulation that gives good solubility, low retention and low interfacial tension.

4.3 Phase behavior

The oil-recovery effectiveness of a chemical flood is related to the phase behavior of the brine-oil- surfactant system. The important phenomenon in such systems is the ultra-low interfacial tension (IFT) that can occur. If we consider an aqueous phase (brine) containing surfactant with a concentration above the CMC together with an oleic phase, several different scenarios in term of phase behavior can take place which can be thermodynamically stable (Bourrel and Schechter, 1988; Winsor, 1954). A number of variables affect the phase behavior and solubilization parameters, and thus IFT. These variables include salinity of the brine, temperature, pressure, divalent ions, surfactant structure, co-surfactant and co-solvents

concentrations (Healy et al., 1976; Glover et al., 1979; Novstad, 1982; Puetro and Reed, 1983; Nelson, 1983; Skauge and Fotland, 1990; Skjæveland and Kleppe, 1992; Green and Willhite, 1998; Levitt et al., 2009).

Surfactants used in chemical flooding processes, typically exhibit good aqueous-phase solubility and poor oil-phase solubility at low brine salinities. Thus at low brine salinities, an overall composition in the two phase region will split into: an excess oil phase and a water external microemulsion phase. The excess oil phase is essentially pure oil and the microemulsion phase consists of brine, surfactant and solubilized oil in the center of micelles. This phase environment is referred to as a Winsor's Type I system, a lower-phase microemulsion or a Type II(-) system. The last terminology is due to the fact that the system consists of two phases and the slope of the tie lines in the two phase region is negative (Winsor, 1954; Nelson and Pope, 1978; Lake, 1989; Green and Willhite, 1998). Figure 4.4(a) shows a schematic for phase behavior of a Type II(-) system.

At high brine salinities, surfactant solubility in the aqueous phase is drastically reduced due to electrostatic forces. Thus at high brine salinities, an overall composition in the two phase region will split into an oil external microemulsion phase and an excess brine phase. In this case the brine phase would essentially contain no surfactant and some of the brine phase is solubilized in the microemulsion phase at the center of the micelles. This system is referred to as a Winsor's Type II, an upper-phase microemulsion or a Type II(+) system (Winsor, 1954; Nelson and Pope, 1978; Lake, 1989; Green and Willhite, 1998) (Figure 4.4(b)).

At the brine salinities between the two extremes discussed above, there exists a third type of phase behavior in which three phases (a brine phase, a microemulsion phase and an oil phase) coexist. The middle microemulsion phase is often referred to as bicontinuous, i.e. continuous in both oil and water. This system is known as a Winsor's Type III, a middle-phase microemulsion or a Type III system (Winsor, 1954; Nelson and Pope, 1978; Lake, 1989; Green and Willhite, 1998) (Figure 4.4(c)).

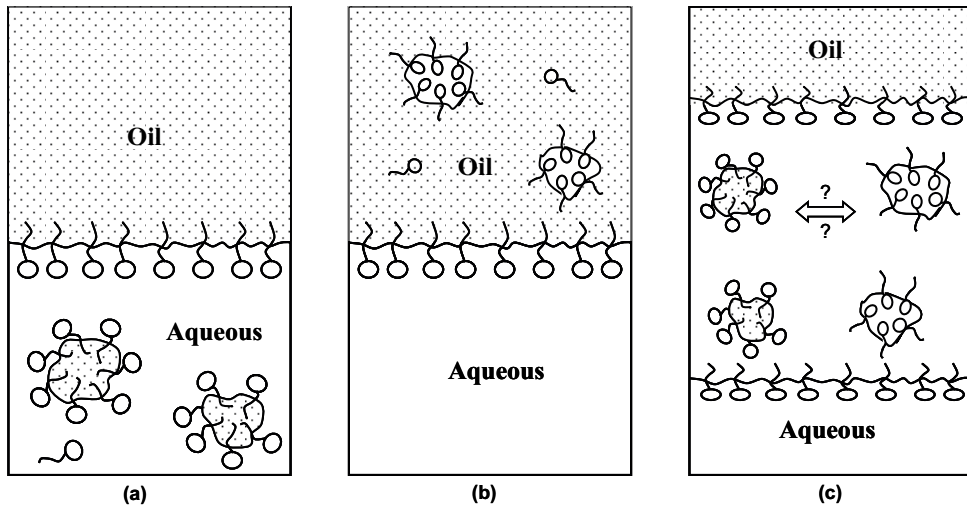


Figure 4.4: Schematic representation of phase behavior generated upon mixing oil, brine and surfactant. (a) Type II(-). (b) Type II(+). (c) Type III. The figures are reconstructions of those presented by Lake (1984).

4.3.1 The role of alcohol

For a surfactant system to be soluble and avoid gel-structure at reservoir conditions and low injection temperature, co-solvents like short-chained (C3-C5) alcohols are added to the system (Skjæveland and Kleppe, 1992). By incorporation of alcohol in the surfactant system, it makes the surfactant less rigid and thereby increases the rate of equilibration. The direction of phase change will depend on the hydrophilic/lipophilic balance of the alcohol compared with the surfactant. When the alcohol is most water soluble, the transition II(+) to II(-) occurs, and the drop in optimal solubility is significant. An oil soluble alcohol will move the phase behavior in the II(+) direction, and lowering in solubility will decrease as the molar volume of the alcohol approaches that of the oil.

Due to its effect on optimal salinity, alcohol may also be used to control phase behavior. In this case the alcohol behaves as a co-surfactant. By adding an appropriate alcohol to the surfactant system the alteration in optimum salinity with surfactant concentration may be less or even go in the opposite direction (Skjæveland and Kleppe, 1992).

4.4 IFT and phase behavior

IFT between the aqueous and oleic equilibrium phases is strongly dependent on the phase behavior of the microemulsion system (Green and Willhite, 1998). Among all parameters which affect phase behavior of the microemulsion, salinity is the most pronounced. Figure 4.5 shows correlation of the interfacial tension (IFT), solubilization parameter and phase behavior of microemulsion systems as a function of salinity by Healy and Reed (1974). In this figure $\sigma_{m/o}$ and $\sigma_{m/w}$ are interfacial tensions between the microemulsion/excess oil and microemulsion/excess brine respectively and V_o/V_s and V_w/V_s are solubilization parameters (where V_o , V_w , and V_s are volumes of oil, water and surfactant in microemulsion respectively). As it is seen in the figure, as brine salinity increases $\sigma_{m/o}$ decreases and $\sigma_{m/w}$ increases drastically. As either interfacial tension decreases, the appropriate solubilization parameter increases. So, optimal salinity is defined to be the salinity at which the water and oil solubilization ratios coincide. This optimal salinity also normally coincides with the salinity where $\sigma_{m/o}$ and $\sigma_{m/w}$ intersect. Low interfacial tensions correspond to the Type III environment where micelles swelled with internal phase.

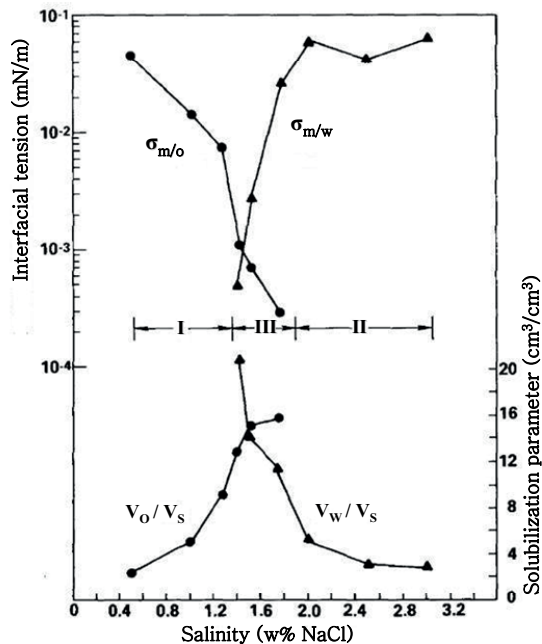


Figure 4.5: interfacial tension (IFT), solubilization parameter and phase behavior of microemulsion systems versus salinity (Healy and Reed, 1974).

Chapter 5 Wettability

Wettability is defined as the ability of one fluid to spread or adhere on a rock surface in the presence of other immiscible fluids (Anderson, 1986a). Wettability has a strong influence on the distribution and flow of fluids in the reservoir rock, and it thus affects oil recovery by waterflooding (Anderson, 1986a; Morrow, 1990; Cuiec, 1991). It is also a significant issue in multiphase flow problems ranging from oil migration from source rocks to such enhanced recovery processes as chemical flooding or alternate injection of CO₂ and water (Morrow, 1990).

For flat surfaces, contact angle is a commonly used measure of wettability. Figure 5.1 shows an oil drop at equilibrium on a solid in an oil-water-solid system.

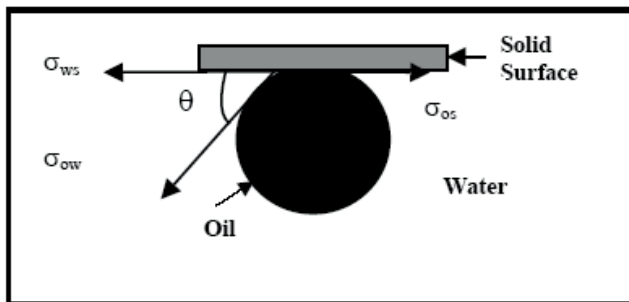


Figure 5.1: Contact angle in an oil-water-solid system.

At equilibrium, the interfacial energies are related by Young's equation:

$$\sigma_{os} = \sigma_{ws} + \sigma_{ow} \cos \theta \quad (5.1)$$

where;

σ_{os} = Interfacial energy between oil and solid

σ_{ws} = Interfacial energy between water and solid

σ_{ow} = Interfacial energy between oil and water

θ = Contact angle

The contact angle is the angle between the tangent to the solid surface and the tangent to the oil-water interface in the three phase contact point (see Figure 5.1).

5.1 Types of Wettability

5.1.1 Homogeneous wettability

In a porous media, wettability is generally classified as either homogenous (uniform) or heterogeneous (non-uniform) (Anderson, 1986a; Radke et al., 1992). In the homogeneous case, depending on the specific interactions of rock, oil, and brine, the entire rock surface has a uniform molecular affinity for either water or oil. On the other hand, heterogeneous wettability indicates distinct surface regions that exhibit different affinities for oil or water.

The wettability of a system can range from strongly water-wet to strongly oil-wet. When the rock has no strong preference for either the oil or water, the system is defined as having “neutral- (or intermediate-) wettability”. In a strongly water- or oil-wet reservoir, the wetting phase completely covers the rock surfaces. Historically, all petroleum reservoirs were believed to be strongly water-wet (Anderson 1986a; Morrow, 1990). This was based on two major facts. First, almost all clean sedimentary rocks are strongly water-wet. Second, sandstone reservoirs were deposited in aqueous environments into which oil later migrated (Morrow, 1991; Chernicoff, 1999). It was assumed that the connate water would prevent the oil from touching the rock surfaces. However, experience and observations from wettability tests on different reservoir rocks type shows that there are other conditions than only water-wet condition

5.1.2 Heterogeneous wettability

Intermediate wettability is used to describe different local wetting configurations including fractional wettability and mixed wettability. The term mixed wettability was introduced by Salathiel (1973), and used to describe a special type of intermediate wettability in which the

oil-wet surfaces form continuous paths through the larger pores, and smaller pores remain water-wet and contain no oil. This type of wettability is defined as “mixed-wet large” (see Figure 5.2) by Skauge et al. (2007). They also defined a wettability condition called “mixed-wet small”, where the large pores are water-wet and the small pores are oil-wet, and a fractionally-wet state where oil- and water-wet sites are random with respect to size (see Figure 5.2).

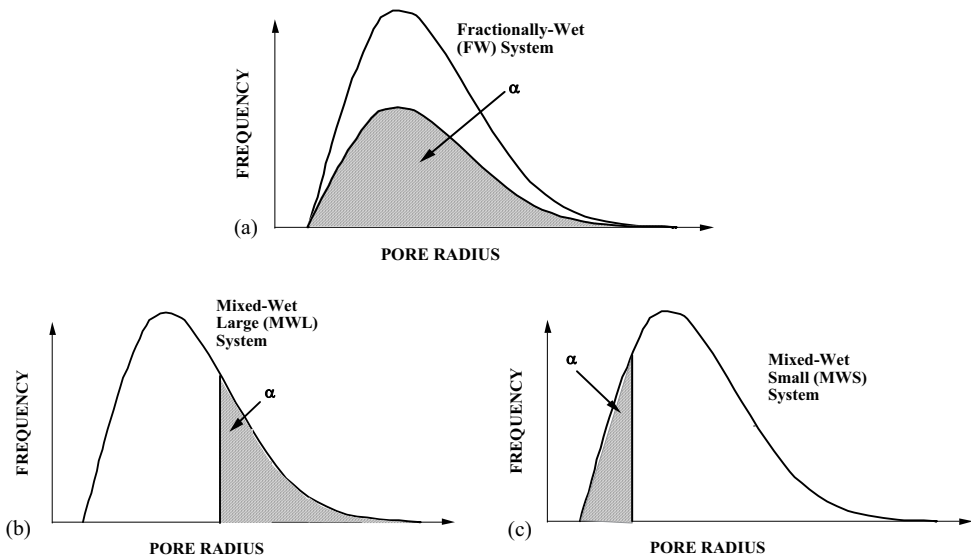


Figure 5.2: Pore size distributions showing the fraction of oil wet pores (a) and their distribution for (a) a fractionally-wet (FW) system; (b) a mixed-wet system where the large pores are oil wet (MWL); and (c) a mixed-wet system where the small pores are oil wet (MWS).

5.2 Factors affecting wettability

The wetting characteristics of reservoir rocks depend on several factors including composition of crude oil, brine and rock mineralogy. Heavy compounds in the crude oil such as asphaltenes, resins and high molecular weight hydrocarbons are believed to be responsible for wettability changes. An important characteristic of these components is the amount of polar functionality they contain. Polar functionalities can act as acidic or basic sites and thus affect charge density at the oil-water interface.

Several researchers discussed the role of acidic and basic compounds in crude oil to alter the wettability of a rock to more oil-wet (Cuiec, 1984; Anderson, 1986a&b; Crocker and

Marchin, 1988). The acidic and basic groups, which include phenols, carboxylic acids, sulfur and nitrogen components, are more or less present in all crude oils (Seifert and Teeter, 1970; Anderson, 1986a; Somerville et al., 1987; Frye and Thomas, 1993). It should be noted that the amount of acidic and basic compounds is not necessarily related to the content of asphaltenes in the crude oil (Skauge et al., 1999; and Standnes, 2002).

Temperature, pressure, initial water saturation, water solubility of polar oil components and the ability of the oil to stabilize heavy components have also been taken into consideration by several researchers as parameters that affect wettability alteration (Buckley, 1993; Jadhunandan and Morrow, 1995; Buckley et al., 1995&1996; Kaminsky and Radke, 1998; Al-Maamari and Buckley, 2000; Zhou et al., 2000; Hamouda and Gomari, 2006; Gomari, 2009).

Interactions at the oil-water and solid-water interfaces will be discussed in more detail in chapter 6. Interactions between ionized acidic and basic sites can occur between the oil-water and solid-water interfaces in the presence of water films (Buckley, 1996). They are governed by the charges of the oil-water and solid-water interfaces. Reservoir brines typically have close to neutral pH. At these values of pH, brine-carbonate interfaces are typically positively charged while brine-silica interfaces are typically negatively charged (Benner and Bartel, 1942; Denekas, et al. 1959; Anderson, 1986a; Skauge et al., 1999; Skauge and Fosse, 1996; Wesson and Harwell, 2000; Gomari, 2009). As a result, acidic components are more likely to affect carbonate rock wettability through acid-base interactions, while basic components affect silica wettability. Austad and Standnes (2003) confirmed that the negatively charged carboxyl groups of the crude oil are responsible for wetting behavior in chalk. They concluded that crude oils with high acidity have a high potential to alter the chalk wettability to more oil-wet.

5.3 Methods of wettability measurement

Many different methods have been proposed for measuring the wettability of a system (Anderson, 1986b). They include quantitative and qualitative methods. Quantitative methods include contact angles, imbibition and forced displacement (Amott, 1960), and the USBM wettability method (Donaldson et al., 1969). The contact angle measures the wettability of a flat surface, while the Amott and USBM methods measure the average wettability of a porous media like rock core plugs. Qualitative methods include methods like imbibition rates,

microscope examination, flotation, glass slide method, relative permeability curves, and permeability/saturation relationships (Anderson, 1986a).

5.3.1 Flat surfaces

When a drop of oil is placed on mineral surface immersed in water, a contact angle is formed which can range from 0° to 180° (see Fig. 5.1). The contact angle formed at the three-phase boundary defines the wetting or non-wetting behavior of a liquid on a solid surface, and is a measure of the equilibrium between adhesive and cohesive forces that exist between the molecules at the liquid-solid interface.

Contact angle is the most universal measure of the wettability of a surface (Morrow, 1990). The method is also used to determine whether a crude oil can alter wettability and to examine the effects of temperature, pressure and brine chemistry on wettability (Anderson, 1986b). Many methods of contact-angle measurement have been used. They include the tilting plate method, sessile drops or bubbles, vertical rod method, tensiometric method, cylinder method, and capillary rise method (Anderson, 1986b). The methods that are generally used in the petroleum industry are the sessile drop method and a modified form of the sessile drop method described by Leach et al. (1961) and Treiber et al. (1972). There are several challenges involved in interpreting contact angle measurements, including contact angle hysteresis. It is generally found experimentally that a liquid drop on a surface can have many different stable contact angles. Johnson and Dettre (1962) state that there appears to be three causes of contact-angle hysteresis: (1) surface roughness, (2) surface heterogeneity, and (3) surface immobility on a macromolecular scale.

5.3.2 Porous media

5.3.2.1 The Amott Method:

The Amott method proposed by Amott (1960), combines natural imbibition and forced displacement to measure the average wettability of the core. This method is based on the fact that the wetting fluid will generally imbibe spontaneously into the core, displacing the non-wetting one. The wettability indexes to water, I_w and oil, I_o are given by

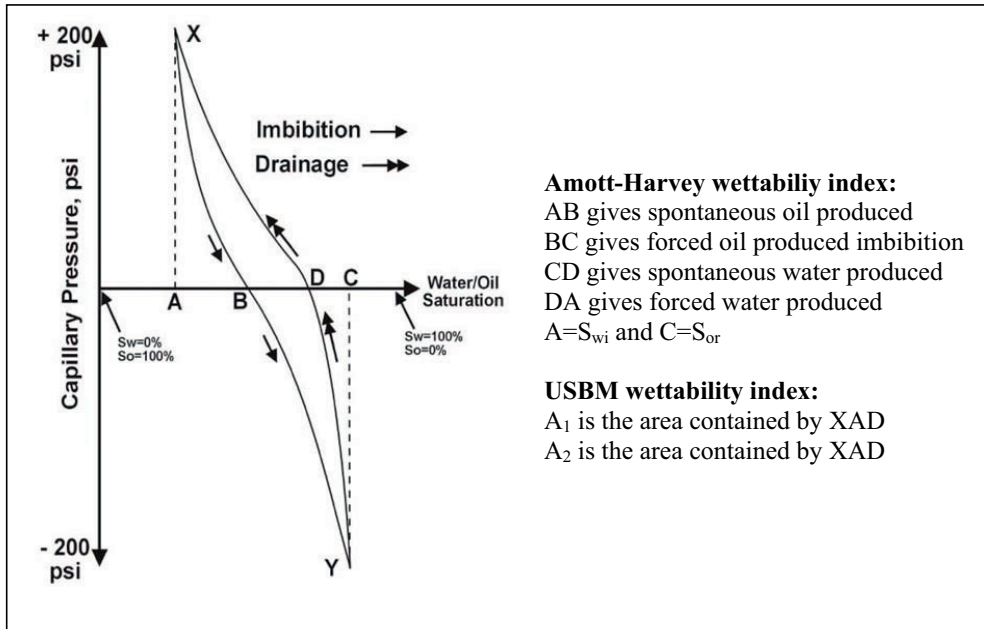


Figure 5.3: Imbibition and drainage capillary pressure curve required determining the Amott-Harvey and USBM wettability indices.

2.3.2.2 The USBM Method

The US Bureau of Mines (USBM) method proposed by (Donaldson et al., 1969), like the Amott test, measures the average wettability of the core. This wettability index is based on the fact that the work required for the wetting fluid to displace the non-wetting fluid from the core is less than the work required for the opposite displacement, and the required work is proportional to the area under the capillary pressure curve. In the USBM method, drainage and imbibition capillary pressures are measured using a centrifuge. The wettability number is defined by

$$I_{USBM} = \log\left(\frac{A_1}{A_2}\right) \quad (5.4)$$

where A_1 , A_2 , as illustrated in Figure 5.3, are the areas under the capillary versus saturation curves obtained during oil and brine drives, respectively. For a strongly water-wet system I_{USBM} is large and positive, while for an intermediate-wet system, I_{USBM} is around zero. A strongly oil-wet system will have a large and negative I_{USBM} . An advantage, which the USBM method has over the Amott test, is its sensitivity near neutral wettability. The disadvantage is

that the USBM wettability index can only be measured on plug sized samples because the samples must be spun in a centrifuge (Anderson, 1986b).

5.4 Wettability and oil recovery

Reservoir wettability and its effect on oil recovery have been extensively investigated for many years, and numerous authors have reported experimental work relating to the role of wettability in various aspects of oil recovery. Early examples of laboratory waterfloods show an increase in oil recovery with increasing water-wetness. In water-wet reservoirs most of the oil is typically displaced before water breakthrough with little or no oil flowing after breakthrough Anderson (1987b). But in oil-wet reservoirs, early water breakthrough occurs and appreciable amounts of oil are recovered after breakthrough. Much of the residual oil will be trapped by capillary forces in the smaller pores. Consequently, waterfloods are less efficient in oil-wet systems than in water-wet systems because more water must be injected to recover the same amount of oil. Donaldson et al. (1969) implemented waterflood tests using sandstone and crude oils to determine the effect of wettability on oil recovery. Wettability was changed by treating the cores with silicone. The recoveries obtained from silicone treated cores showed the effect of change in wettability from a water-wet system to an oil-wet system. The results showed a decreasing trend of oil recovery from water-wet to oil-wet cores. This means that more oil is produced from water-wet cores-

Several authors reported improved waterflood recovery with shift from strongly water-wet conditions to intermediate and weakly oil-wet condition. Investigation by Morrow (1990) showed that the oil recovery is optimum at neutral wettability for laboratory waterfloods on crude oil /brine/rock systems. Later, the results of experimental work on sandstone rocks by several researches (e.g. Jadhunandan and Morrow, 1991; Owolabi and Watson, 1993; Tweheyo et al., 1999, Skauge and Ottesen, 2002; Hamon and Bennes, 2003, Chen et al., 2004) also confirmed this fact. However, Karimaei et al. (2006) carried out an experimental study on sandstone cores. They used different aging time in order to get different wettability states. They employed the Amott method to classify the cores' wettability and concluded that the more water-wet conditions with a higher Amott index give greater oil recovery.

Graue et al. (1999a and b); Kamath et al (2001); Tie and Morrow (2005) and Karousi (2008) have performed oil displacement tests by water injection using carbonate rocks. They reached

the same conclusion as for sandstone rocks: the highest ultimate oil recoveries are obtained for the neutral-wet cores and the lowest recoveries for the oil-wet cores.

Several studies have considered the effect of wettability on chemical flooding and effects of chemical injection such as surfactants and alkali on wettability alteration and ultimate oil recovery. Ayirala and Rao (2004) conducted displacement experiments using surfactants in different rock-fluid systems to see the effect on wettability alteration and IFT. The results indicated an increase in oil recovery by using surfactant that was attributed to alteration of wettability from water-wet to mixed-wet system as the main mechanism for increasing oil recovery. Delshad et al. (2009) modeled chemical processes leading to wettability alteration in naturally fractured reservoirs. They proposed that using surfactants can change the wettability in mixed-wet matrix rocks in fractured reservoirs to water-wet condition and thereby increase the oil recovery by increased imbibition of the water into the rock matrix. Cationic surfactants were used by many researchers as a wettability modifier to alter wettability of carbonate formation to a more water-wet condition which leads to more oil recovery (Austad and Milner, 1997; Austad et al., 1998; Standnes et al., 2002; Xie et al., 2005). Dong et al. (2006) studied the effect of wettability on oil recovery of alkaline/surfactant/polymer. They found neutral-wettability as the optimum condition in terms of wettability for displacement efficiency of water flooding. A systematic study of surfactant-alkali system also was done by Gupta et al. (2009) for oil-wet fractures reservoirs. They identified that alkali-surfactants can alter wettability of oil-wet carbonate rocks toward more water-wet conditions and consequently lead to increased oil recovery.

Reservoir wettability is a complex area of study the results obtained by different researchers, it is observed that although oil recovery is a strong function of the reservoir wettability, its effect on oil recovery is still not completely understood. Researchers stated different wettability states as the best condition to achieve more oil recovery from reservoirs. However, most of them agree that oil-wet is the least favorable condition for oil recovery by waterflood and intermediate-wet conditions are the most favorable. Figures 5.4-5.6 show some of the experimental data on residual oil saturation as a function of Amott-Harvey wettability index obtained for sandstone and carbonate rocks. The residual oil saturation is lowest when the wettability is close to mixed-wet conditions, corresponding to an index near zero.

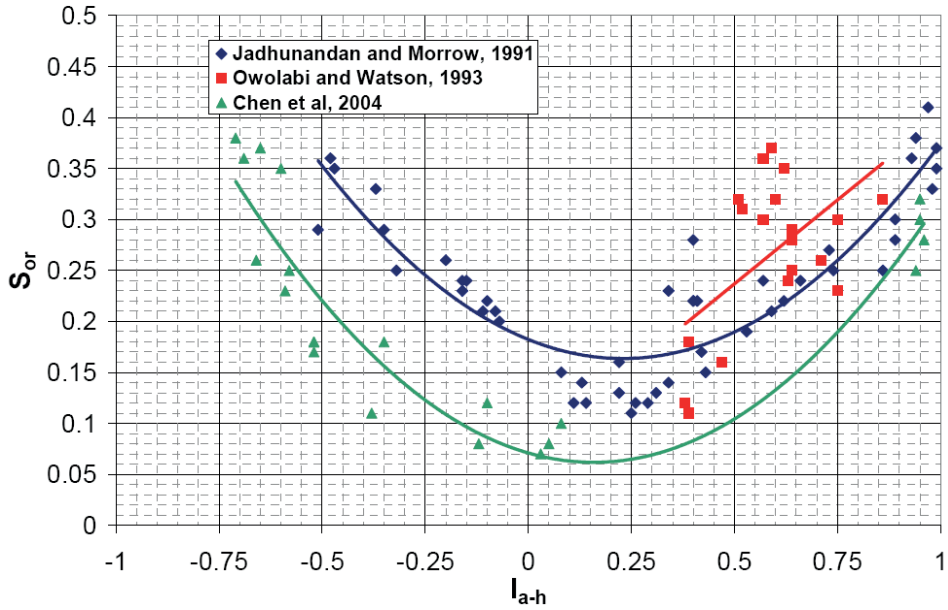


Figure 5.4: Residual oil saturation vs. I_{a-h} for Berea sandstone (Anderson, 2006).

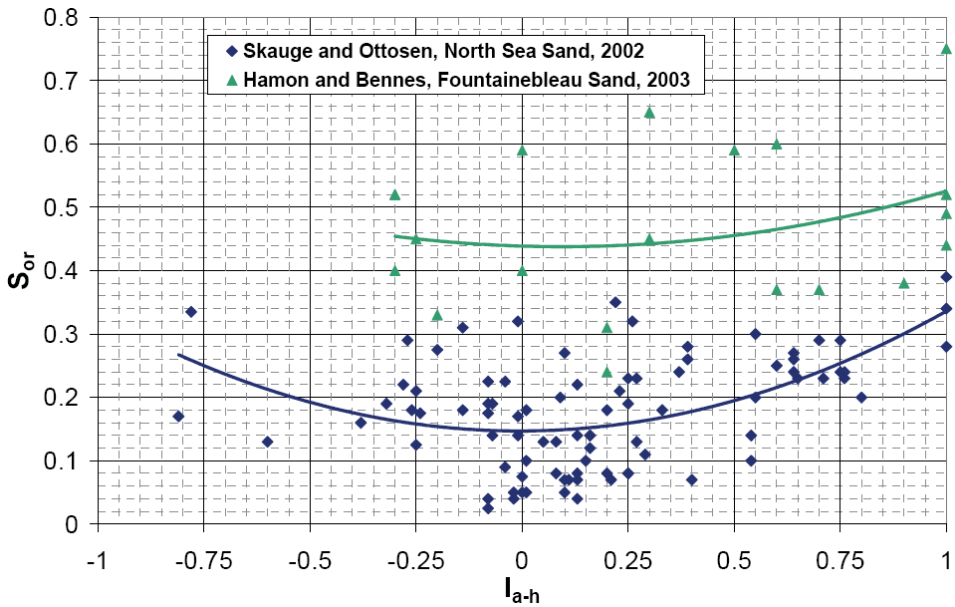


Figure 5.5: Residual oil saturation vs. I_{a-h} for several other sandstones (Anderson, 2006).

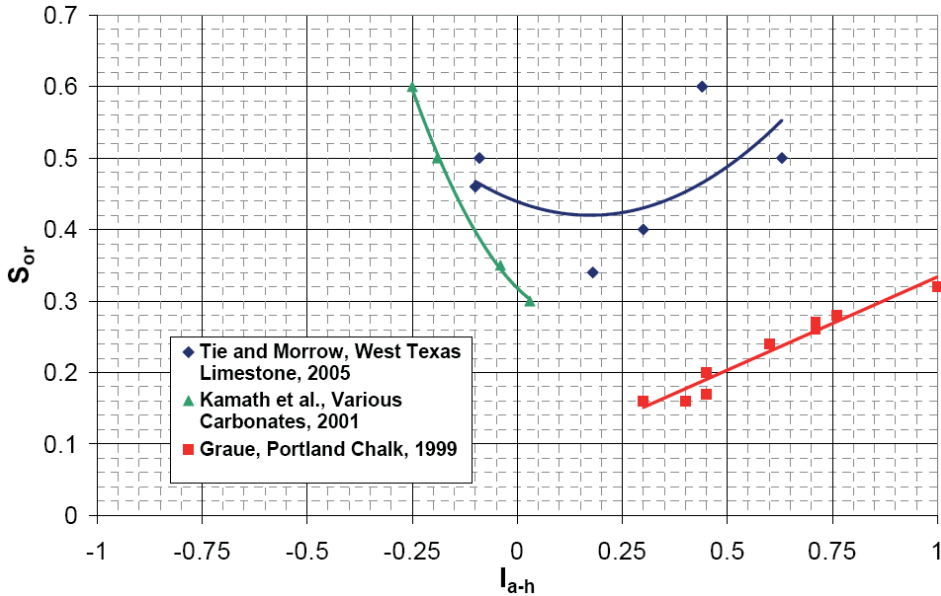


Figure 5.6: Residual oil saturation vs. I_{a-h} for several carbonates (Anderson, 2006).

5.5 Effect of wettability on Capillary Desaturation Curve (CDC)

Capillary desaturation curve was described and discussed previously in chapter 2. Since effect of wettability on CDC is important, it will be discussed here.

Wetting behavior of a rock is the key factor of the different phase distributions in a porous media. Since the rock surface tends to attract the wetting phase and repel the non-wetting phase, the non-wetting phase is easier to be mobilized and the reduction in its residual saturation will start to occur at a lower critical capillary number, N_{CC} . Conversely, for the wetting phase there is an affinity between the rock surface and the phase and therefore a higher N_{CC} is required in order to mobilize its residual saturation. Simply, it means that if a rock is strongly water-wet, then N_{CC} of water is higher than N_{CC} of oil and it is easier to mobilize oil than water.

The effect of wettability changes on the CDC for Berea sandstone is shown in Figure 5.7. This figure shows the variation of the critical capillary number, N_{CC} for the oil phase and its residual oil saturation at low capillary number for different wettability conditions. Oil mobilization seems to happen at lower N_{CC} in water-wet condition than other conditions.

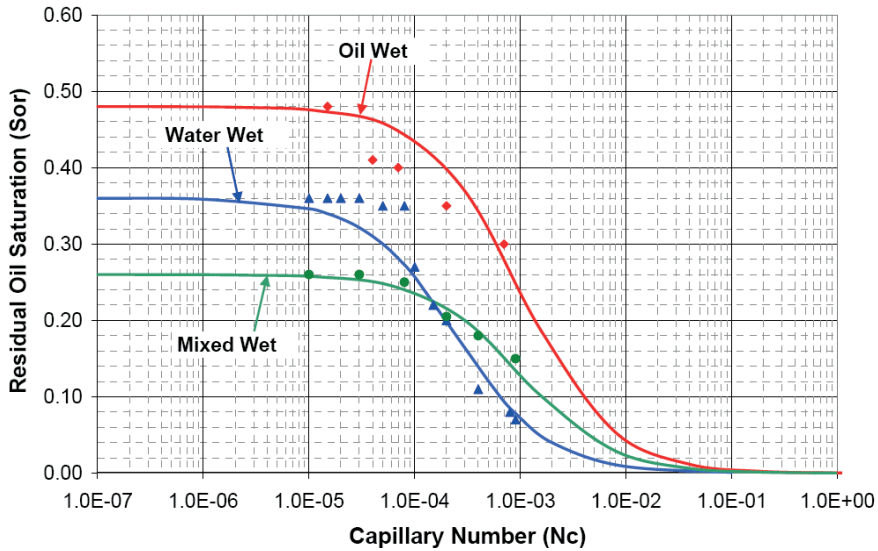


Figure 5.7: Effect of wettability on CDCs for Berea Sandstone (Mohanty and Salter, 1983). Figure regenerated by Anderson (2006).

Changes in the CDC for weakly oil-wet and intermediate-wet carbonate rocks are also shown in Figure 5.8. The main observation is extremely lower (about three orders of magnitude) critical capillary numbers for carbonate rocks compared to the Berea sandstone with approximately same wettability condition. Tie and Morrow (2005) also obtained similar results for grainstone carbonate rocks. They concluded that the low critical capillary number was due to wide pore-size and pore shape distributions. This different behavior could be also due to different fluid distributions, porosity and permeability of the two rock types (Hirasaki et al., 2004).

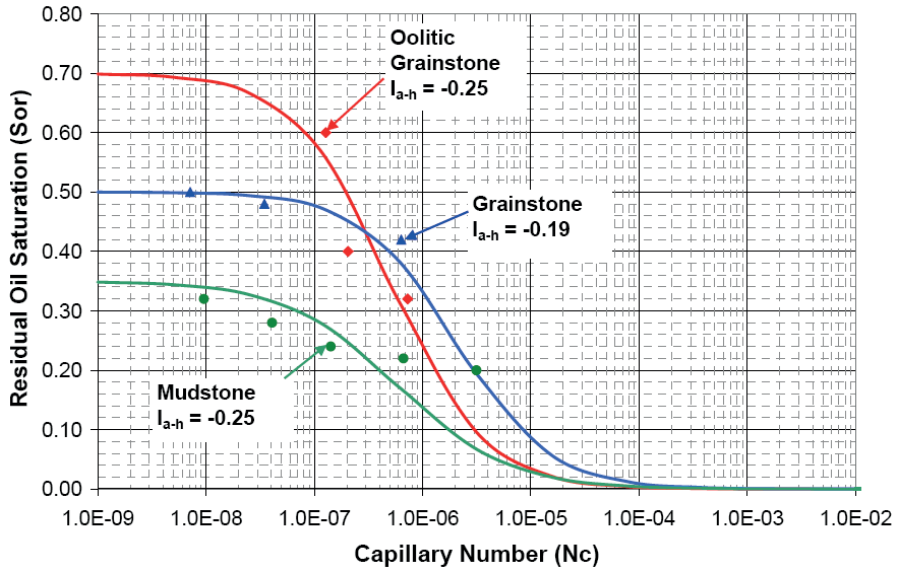


Figure 5.8: Effect of wettability on CDCs for carbonates (Kamath et al., 2001). Figure regenerated by Anderson (2006).

Chapter 6 Interactions at interfaces

An interface is the area which separate two phases from each other. An understanding of the surface forces acting between solid-liquid and liquid-liquid interfaces is a critical factor in many scientific and technological fields such as emulsification, flotation, coating, detergency, lubrication, dispersion of powders etc. Historically, the interactions between surfaces have been described by measurements of isolated properties, such as the macroscopic contact angle, surface tension and electrophoretic measurements.

6.1 DLVO theory and the electrical double layer

Electrostatic forces are the key factor to determine the surface properties of solids and their behavior in an electrolyte solution. They influence all intermolecular interactions between molecules, particles or surfaces which can be repulsive or attractive or combination of both (Butt et al., 2006). The interactions of the attractive van der Waals (F_a) and repulsive double layer forces (F_r) in the vicinity of a charged colloidal surface in an electrolyte solution is described by DLVO theory developed by Derjaguin and Landau (1941); Verwey and Overbeek, (1948). The force balance, F_t , is given as a function of the distance, h , from the charged colloid particle.

$$F_t(h) = F_a(h) + F_r(h) \quad (6.1)$$

6.1.1 The electrical double layer

Charged surfaces in an electrolyte solution attract ions of opposite charge (counter-ions) and repel ions with similar charge (co-ions). The counter-ions distribute to neutralize the surface by forming an ion layer that is a different from the bulk electrolyte solution (Butt et al. 2006).

This region of counter-ions is referred to as the electrical double layer which typically has a thickness in range of few nanometers. Figure 6.1 shows a schematic of the electrical double layer. The immobile layer is called the Stern layer whereas the region adjacent to the Stern layer is called the diffuse layer. The density of the counter-ions decreases with increasing distance from the particle. Finally the electrical potential becomes zero when the ion concentration is the same as in the bulk electrolyte solution. The potential curve is useful because it indicates the strength of the electrical force between particles and the distance at which this force comes into play. A charged particle will move with a fixed velocity in a voltage field. This phenomenon is called electrophoresis. The particle's mobility is related to the dielectric constant and viscosity of the suspending liquid and to the electrical potential at the boundary between the moving particle and the liquid. This boundary is called the shear plane and is usually defined as the point where the Stern layer and the diffuse layer meet.

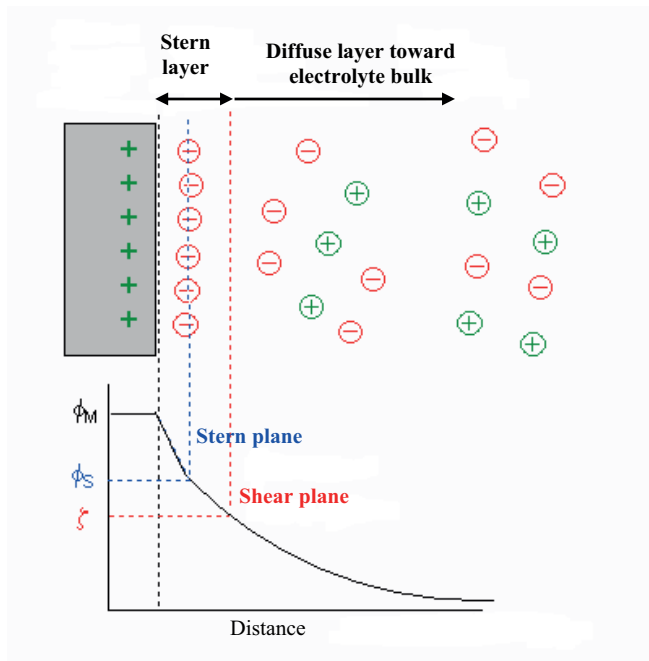


Figure 6.1: A typical schematic of electrostatic double layer structure for a positively charged surface in an electrolyte and corresponding electrostatic potential profile, where decays from a maximum value at the surface through zero in the bulk solution.

6.2 Disjoining pressure and water film stability

In a three phase system consisting of oil, water and solid rock, the interaction between charged interfaces separated by a water film can be explained by the concept of disjoining pressure. Disjoining pressure is defined as the change in energy per unit area as a function of the distance of two interfaces as they approach each other. Mathematically, disjoining pressure is defined by an augmented Young-Laplace equation:

$$P_c = \Pi + 2\sigma_{ow}J \quad (6.2)$$

where P_c is the capillary pressure between wetting (water) and non-wetting (oil) phases; Π is the disjoining pressure; σ_{ow} is interfacial tension between oil and water and J is the mean surface curvature. J is positive for concave surfaces and negative for convex surfaces.

Changes in oil reservoir wettability can be understood in terms of the stability of a thin wetting film separating the oil and solid phases. Initially, the rock surface is coated by a wetting film of water (i.e. connate water), preventing the oil in contacting the reservoir rock (Anderson, 1986-a). The generic disjoining pressure isotherm (right hand side of equation 6.2) determines the capillary pressure at which the water film is destabilized. The water film remains stable as long as the disjoining pressure (i.e. capillary pressure) does not exceed a maximum (critical) value. When a critical capillary (disjoining) pressure exceeded, the water film ruptures result in direct contact of the crude oil with the pore wall and consequently may affect the wetting behavior of the rock.

6.3 The crude oil-water interface

Crude oils have both basic (positive) and acidic (negative) species. These polar functional groups contain either nitrogen or oxygen or both that can provide acidic, basic or even zwitterionic character at the interface between crude oil and water. Electrical properties of the crude oil/water interface were explained by Buckley et al, (1989) by using the ionizable surface group (ISG) model. The ISG model assumes that the negative or positive charge of the interface is caused by dissociation of acidic and/or basic groups at the interface. The ISG model provided an adequate description of the electrical property of crude oil/water interface

by considering bulk concentration of the ions in solution, the number of ionizable sites and bulk pH.

The numbers of interfacially active sites can not be measured directly, but they can be deduced by changes in interfacial properties including IFT and electrophoretic mobility with brine composition (Buckley, 1996). Results of electrophoresis measurements of emulsified droplets of crude oil in brines of varying composition show that crude oil interfaces have net positive charge at low pH and net negative charge at high pH (Buckley et al., 1989). Several authors have shown that interfacial tension between acidic and basic crude oil and water changes with changing pH of the aqueous phase, and it is generally agreed that this is related to ionization of polar groups at the interface (see e.g. Buckley et al., 1989; Spildo and Høiland, 1999; Buckley and Fan, 2005). IFT decreases in the case of acidic oil and increases in the case of basic oil with increasing pH. When pH of the aqueous phase is very high or very low, the acidic and basic functional groups of crude oil components can react leading to the generation of in-situ surfactants. These surfactants can further alter the IFT as a function of time (Buckley and Fan, 2005).

6.4 Partitioning of organic acids and bases between oil and water

Partitioning of organic acid and bases between oleic and aqueous phase can be expressed as the ratio of the concentration of acid in oleic phase to the concentration of acid in the aqueous phase (Goodman, 1958):

$$P = \frac{[HA]_{o,tot.}}{[HA]_{w,tot.}} \quad (6.3)$$

where P is the partition ratio, while $[HA]_{o,tot.}$ and $[HA]_{w,tot.}$ are the total concentration of the component (moles/liter) in the bulk oleic and aqueous phase, respectively.

Partition ratio depends on different parameters such as aqueous phase pH and brine chemistry (Spildo, 1999). The partition ratio of organic acids between oil and water decreases with increasing pH and decreasing of pH results in increasing of P for organic bases. Partition ratio also increases by increasing the salinity of aqueous phase and introducing of divalent ions to the system (Spildo, 1999).

6.5 Adsorption at the liquid-liquid interface

A liquid/liquid interface can be modified by the addition of soluble and insoluble materials which results in either an adsorbed film or a deposited film. Some very few macromolecules have properties which are compatible with both types of solvents, polar and organic and even fewer macromolecules have properties which demand that they either have access to both solvents or organize themselves to compensate for the absence of one of these phases. Such amphiphilic compounds such as surfactants and enzymes will necessarily be exclusively distributed along the interfaces between two such solvents. If present in sufficient quantities they will coat the surface of one phase in such a manner as to alter the interactions between the two solvent phases. The effect is to expand the interface which in turn must be balanced by the tendency for the interface to contract under normal interfacial tension forces. The result is a lowering of interfacial tension according to the following:

$$\gamma = \gamma_0 - \pi \tag{6.4}$$

where;

γ_0 = initial interfacial tension before addition of surfactant

γ = final interfacial tension

π = expanding (interfacial) pressure

Ideal conditions for spontaneous emulsification and miscibility of liquids exist when $\pi > \gamma_0$.

6.5.1 Adsorption of enzymes and proteins at the oil/water interface

Enzymes are macro molecules that contain both hydrophobic and hydrophilic groups. In aqueous soluble enzymes, the core of the enzyme molecule consists mainly of hydrophobic groups, while the hydrophilic residues are predominantly on the surface. The solubility of enzymes in organic solvent is determined by the overall surface hydrophobicity of the enzyme. Enzymes that are active at interfaces often contain large fractions of hydrophobic moieties present at the surface which have low solubility in water (Beverung et al., 1999). The oil-water interface allows hydrophobic residue of the enzyme to be dissolved in, and interact favorably with the oil phase. Enzymes assembled at an organic-aqueous interface could provide the maximum accessibility to chemicals dissolved in both phases across the interface. Interfacial enzymes act on insoluble substrates. Esterases and lipases (subclasses of

hydrolases enzymes) are two important examples from this group of enzymes. They both hydrolyze ester bonds. Esterases typically show highest activity towards the soluble state of its substrate whereas the lipases display high activity towards the aggregated state of its substrate. (Marangoni, 1994; Fojan et al., 2000; Al-Zuhair et al., 2007).

In nature, interface binding enzyme-proteins can interact with the surface in great number of ways. This is mainly due to the complexity of the protein molecule which comprises positive and negative charges, groups with hydrogen bond capacity and hydrophobic/hydrophilic regions. Interface binding can thus occur via electrostatic interactions, hydration forces, acid-base interactions, hydrogen bonding, hydrophobic, ionic and the van der Waals interactions (Privalov and Gill 1988; Dill 1990). These interactions with the gain in entropy due to conformational changes of enzyme-proteins are often regarded as the driving forces for their presence at the interface (Prime and Whitesides 1991).

6.6 The solid-liquid interface

Solid surfaces are complex, both chemically and physically. Solid surfaces may be constituent of many different minerals. Interactions within oil/water/rock are characterized by surface properties of the mineral rock. The details of interaction between oil component and water and each mineral may differ (Buckley 1996). Mineral surfaces can broadly be divided into high- and low-energy surfaces. The surface energy of the solid dictates the chemical nature of the components with which it will interact. A high energy surface show a strong affinity for water because of the polar hydrophilic groups attached to its surface. As a result, high-energy surfaces thus considered to be strongly water-wet. Most of the minerals, including silica and calcite, that are of main components of petroleum reservoir rocks are high-energy minerals. Low energy surfaces are considered to be oil-wet, and typical examples include Teflon and wax (Spildo, 1999).

6.6.1 The solid/water interface

Electrical property of the mineral surfaces is the key factor determining electrostatic forces between the mineral surface and any ionized molecules in their surrounding environment. Silica and calcite are two important minerals which are of the main components of sandstone and carbonate rocks respectively (Zolotukhin and Ursin, 2000). The pH at which the solid

surface carries no net electrical charge is known as the point of zero charge (pzc). H^+ is the potential determining ion in silica and calcite (Spildo 1999). Therefore, the net charge on the mineral surface/water is affected by pH of their surrounding aqueous phase and can become more positively or negatively charged due to the loss (deprotonation) or gain (protonation) of protons (H^+). Silica has a pzc around 2 (Iler, 1979) and in any $pH > 2$ silica surface has negative net charge. The pzc for calcite is close to 9.5 (Somasundaran and Agar, 1967) and in any pH value < 9.5 calcite surface has positive net charge.

Another important mineral (clay mineral) which may be found in some extent in both sandstone and carbonate rocks is kaolin. Kaolin has a heterogeneous surface charge where the basal surface is believed to carry a negative constant structural charge which is attributed to the isomorphous substitution of Si^{4+} by Al^{3+} . While the charge on the edges is due to the protonation/deprotonation of surface hydroxyl groups and therefore depends on pH (Zhou and Gunter, 1992). At pH values higher than the pzc (around 4) the surface charge becomes negative (Schroth and Sposito, 1997).

6.6.2 Adsorption at the solid/liquid interface

Adsorption is a general term that refers to the disappearance of solutes (adsorbate) from solution with the presumption of adsorption on a solid phase (adsorbent). Adsorption is the accumulation at the solid-solution interface, and may result from either physical or chemical interaction with the surface. Physical adsorption (physisorption) is a relatively weak bonding (van der Waals type of forces) to the surface while chemical (chemisorption) is a stronger interaction which involves ionic or covalent bonding in addition to van der Waals and dispersion forces operative in physical adsorption (Butt et al. 2006).

The extent of adsorption at a solid-liquid interface is described by the adsorption function $\Gamma = f(P,T)$, which is determined experimentally (Butt et al. 2006). It indicates the number of adsorbed moles per unit area. In general, it depends on the temperature and the pressure. Adsorption increases at low temperature conditions and with the increases in pressure, it increases up to a certain extent till saturation level is achieved. After saturation level is achieved no more adsorption takes place no matter how high the pressure is applied. A plot of Γ versus P at constant temperature yields the adsorption isotherm. For better understanding of adsorption and to predict the amount adsorbed, adsorption isotherm equation are derived.

There are a large number of factors which complicate adsorption process at the solid-liquid interface. Both adsorbate-adsorbent interactions and those between the components in solution, as well as the surface structure of the adsorbent, are important in determining the extent of adsorption. Furthermore, adsorption from nonpolar media onto polar surfaces is affected by the amount of water present in the system (Stokes and Evans, 1997; Butt et al., 2006).

6.6.3 Adsorption of enzymes and proteins at solid/liquid interface

As mentioned before, most proteins and enzymes are large amphiphilic molecules. This characteristic makes them intrinsically surface-active molecules (Hlady and Buijs, 1996).

Adsorption of proteins and enzymes on a solid surface is a generally observed phenomenon in various fields and functional and structural changes of proteins and enzymes upon adsorption as well as the adsorbed amounts sometimes have very important consequences (Nakanishi et al., 2001). Adsorption of enzymes and proteins at solid-liquid interfaces and their interaction are major concerns in a number of fields, such as biology, medicine, biotechnology, and food processing.

In general, the adsorption of proteins and enzymes from aqueous solutions onto a solid surface occurs via three major steps: (1) transport of protein molecules from the bulk to the interface, (2) contact of the protein molecules to the solid surface and (3) conformational changes of the protein molecules during adsorption (Déjardin, 2006).

Although there are numerous exceptions, most proteins prefer to adsorb to a hydrophobic surface rather than to a hydrophilic surface (Malmsten, 1998). The preference for hydrophobic surfaces may be related to differences in conformation of the adsorbed protein on the two types of surfaces (Gray, 2004).

During adsorption, a protein may rapidly unfold to conform to the new environment of the surface. If the protein's structure is changed due to the adsorption process and/or the new local micro-environment, then it is said to be fully or partially "denatured", meaning that its properties are no longer those of the native protein. After adsorption, the protein layer may relax, achieving a new conformation with lower energy. Desorption of the adsorbed proteins

depends on populations of proteins which have been relaxed on the solid surface. Relaxed proteins bind to the surface tightly while weakly bound proteins attach loosely to the surface and may desorb easily (Wertz and Santore, 2002). The adsorption event itself occurs within microseconds to milliseconds, but relaxation occurs over a much longer timeframe, of the order of hours or even days (Malmsten, 1998). As a general rule, the thickness of many adsorbed protein layers on many surfaces is of the order of a few tens of nanometers (Gray, 2004). So, measurement of the amount of adsorbed proteins and enzymes requires high accuracy. Nakanishi et al. (2001) reviewed some methods such as depletion, radiotracer, Quartz crystal microbalance (QCM) etc. to measure amount of adsorbed proteins and enzymes at the solid surfaces.

The effects of protein–surface interaction on protein adsorption are rather complex due to the large number of contributions to the total interaction (Malmsten, 1998). There are different factors affecting adsorption process at solid-liquid interfaces such as protein net charge and charge distribution, the solution medium, the decay length of the electrostatic interactions, the occurrence of hydrophobic domains in the protein surface and the size of the protein (Malmsten, 1998).

The adsorption process is determined by a delicate balance between several attractive and repulsive forces. Duinhoven et al. (1995) studied adsorption process of different enzymes such as lipases, proteases and esterases and divided interactions that determine the adsorption of enzymes and proteins in four categories. (1) Protein-surface interactions which deal with electrostatic attraction or repulsion between the protein/enzyme and the interface and/or Van der Waals attraction. (2) Dehydration of interfaces on the outside of the protein and on the solid surface: protein and enzyme adsorption is promoted by dehydration of hydrophobic interfaces and opposed by dehydration of hydrophilic interfaces. (3) Structural changes in the protein and enzyme molecules upon adsorption which deal with unfolding of the globular protein by changing the balance between involved forces when they are brought into contact with a hydrophobic interface. (4) Surface coverage-dependent lateral interactions due to accumulation of protein and enzyme molecules at the interface: dipole-dipole interaction between the proteins and enzymes on the surface which can be either repulsive or attractive can oppose completion of monolayer coverage.

6.7 The crude oil-water-solid interface

Interactions in crude oil/water/solid depend on all involved ingredients. Composition of the oil and water and physical and chemical properties of the solid are important to determine the mechanisms involved in the system.

Water plays an important role in mediating oil/solid interactions. In the absence of water, neither the polar components nor the solid surfaces are charged. But in aqueous environments both oil/water interfaces and solid surfaces are charged. The charge at the interfaces depends on brine composition (Spildo, 1999). Chemical components of the crude oil that contribute in the interactions at the interfaces also play a crucial role in the crude oil/water/solid system. Electrostatic interactions between the charged surface of the reservoir rocks and the existing polar components in crude oil, determines type, extent and strength of adsorption of polar groups on the ionized mineral surfaces, which influence the wetting status of the rock.

Adhesion test was introduced by Buckley et al. (1989) to characterize interactions between a crude oil and brines of varying composition. The adhesion test provides an indication of water film stability in crude oil/water/solid system. In their work, Buckley et al. (1989) calculated the disjoining pressure as the sum of repulsive electrostatic double layer forces, London-van der Waals attractive forces, and short-range repulsive forces such as hydration forces. This was used to predict adhesion behavior on a glass surface for different crude oils at varying conditions of pH and salinity. The hypothesis was that if the value of Π is positive (by convention positive values are repulsive) for all values of separation distance, the water film is stable and non-adhesion behavior can be maintained. At the other end of the spectrum are unstable disjoining pressures when Π is positive (attractive) which result in adhesion behavior of the solid. In between is a transition zone where the disjoining pressure changes from positive (repulsion) to negative values (attraction) depending on the separation distance. Later, Hirasaki et al. (1991) and Basu and Sharma (1996) also discussed the stability of water films on the basis of disjoining pressure. Further, Basu and Sharma (1996) have shown that disjoining pressure is directly related to contact angle via the following equation:

$$\cos\theta = 1 + \frac{1}{\sigma_{ow}} \int_0^h hd\Pi \quad (6.5)$$

where θ is contact angle and h is the film thickness between oil and solid phases.

Interactions of crude oil/water/solid depend also on other environmental conditions such as temperature and pressure. Based on all parameters that mentioned, four different interaction mechanisms between crude oil-brine-solid in porous media were suggested by Buckley (1996) by which polar components are adsorbed to mineral surfaces (see Figure 6.2): (1) Polar interactions which can occur between dry surfaces and oil when no water is present. (2) Acid-base interactions which can occur between the oil-water and solid-water interfaces in the presence of water films. (3) Ion binding interactions that mask the purely acid-base interactions in the presence of divalent or multivalent ions. (4) Surface precipitation which can occur when the oil is a poor solvent for its asphaltenes.

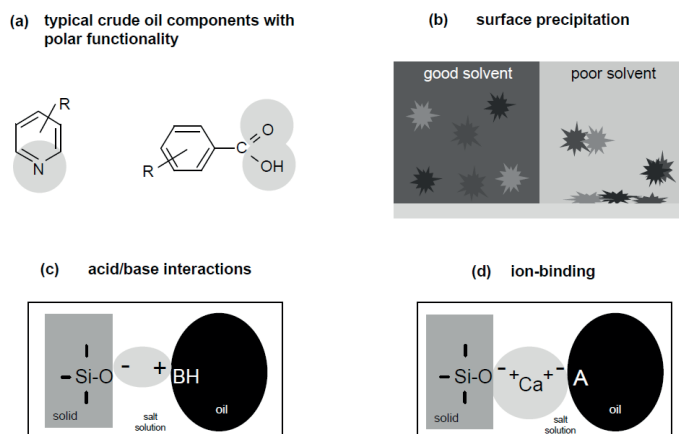


Figure 6.2: Mechanisms of interaction between crude oil components and solid surfaces (Buckley et al., 1998).

Chapter 7 Experimental study of oil-water-solid interfaces

The potential of EOR methods depends on their influence on oil, water and solid interactions at interfaces. If the method has potential to change the interactions favorably, it may consider using for further investigation, i.e. core flooding experiment, pilot and reservoir implementation. An important part of this thesis is to investigate how selected enzymes may influence wettability and capillary forces in a crude oil-brine-rock system, and thus possibly contribute to enhanced oil recovery.

To investigate further by which mechanisms selected enzymes may contribute to enhance oil recovery, groups of enzymes with different properties and catalytic functions, known to be interfacially active, were chosen to cover a wide range of possible effects. These groups include (1) Greenzyme (GZ) which is a commercial EOR enzyme and consists of enzymes and stabilizers, (2) Zonase group consists of two types of pure enzyme, Zonase1 and Zonase2 which are protease enzymes and whose catalytic functions are to hydrolyze (breakdown) peptide bonds, (3) Novozyme (NZ) group consists of three types of pure enzyme, NZ2, NZ3 and NZ6 which are esterase enzymes and whose catalytic functions are to hydrolyze ester bonds, and (4) Alpha-Lactalbumin (α -La) which is an important whey protein. This chapter describes a comprehensive investigation of the effect of the enzymes on oil-water-solid interactions by means of adhesion tests, contact angle measurements and adsorption measurements

7.1 Adhesion tests

As discussed in chapter 6, adhesion tests can be used to characterize crude oil/brine/solid interactions. We thus studied the adhesion behavior of two different crude oils, crude oil A

and B, as a function of pH and salt concentration and how this was affected by adding different enzymes. Solutions with pH ranging from 3 to 12 and concentrations of NaCl from 0 to 1 M were used in the experiments. A drop of crude oil is formed under brine solution by using a micro syringe with an inverted needle. After some period of contact between oil and solid surface (about 2 min), the oil droplet is drawn back into the needle. At this stage three different behavior, adhesion, non-adhesion and temporary adhesion may observe. The standard procedure for the adhesion experiments is provided in more detail Appendix B.

























It has been shown by adhesion map for clean glass slides that the pH and salt concentration of the brine, as well as the crude oil composition, affect the wetting behavior of the original water-wet glass surface (Skauge et al., 1996; Buckley et al., 1998). Tables 7.1 and 7.2 show adhesion maps for crude oil A and B, respectively. According to the adhesion maps, adhesion occurs at low pH and low NaCl concentration, in agreement with other experimental studies (e.g. Buckley and Morrow, 1990; Buckley et al., 1995; Skauge et al., 1996). Figure 7.1 shows an example of oil droplet which adheres to a clean glass surface.

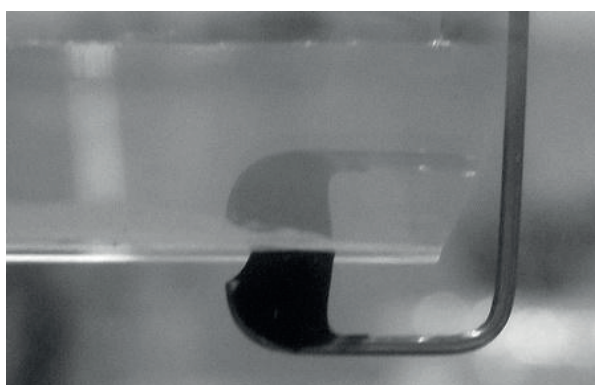
Table 7.1: Adhesion map for crude oil A with clean glass.

[NaCl] pH	0 M	0.1 M	0.5 M	1.0 M
12				
9				
6				
3				

Adhesion	
Non-adhesion	
Temporary adhesion	

Table 7.2: Adhesion map for crude oil B with clean glass.

[NaCl] pH	0 M	0.1 M	0.5 M	1.0 M
12				
9				
6				
5				
4				
3				

**Figure 7.1:** Photo of an oil droplet that adherer to the clean glass surface.

















At low salinity, where electrostatic forces are important, pH is the dominant variable for adhesion. Buckley and Morrow (1990) found a characteristic pH above which adhesion does not occur. This can be explained by considering double layer forces. At low pH, the basic functional groups at the crude oil-water interface are positively charged. The glass-water interface, on the other hand, is negatively charged above pH 2 (Iler, 1979; Anderson 1986-a). This likely result in crude oil adhesion by thinning of the water film separating the two oppositely charged interfaces.

Non-adhesion was observed at high pH (≥ 9) for both crude oils at all salinities. This is likely due to both the glass-brine and crude-oil brine interfaces being negatively charged. At pH 12 it was not possible to test adhesion for crude oil B as the physical properties of the oil was altered so that it would not form droplets at the syringe tip. This behavior may be attributed to a high fraction of acidic functional groups for crude oil B which would be completely ionized at this high pH, this giving rise to a very low oil-brine interfacial tension.

At pH 6, however, adhesion or temporary adhesion was observed at low salinities for crude oil A, while non-adhesion was found at all salinities for crude oil B. Both crude oils showed adhesion or temporary adhesion at low pH (pH 3) and salinities. At higher salinities, however, crude oil B gave adhesion while crude oil A showed temporary adhesion. This is likely due to differences in oil composition between crude oil A and B which, according to Buckley and Morrow (1990), can have a major effect on adhesion behavior, especially at high salinities. At high salinities, electrostatic forces are less important and the influence of DLVO forces in stabilizing the thin film of water between solid and crude oil is not significant. In this condition the adhesion behavior depends on the net charge at the interfaces of oil/water and solid/water (Buckley and Morrow, 1990). For a given crude oil or solid surface, the surface charge depends on the extent of acid/base dissociation reactions. If both oil/water and solid/water interfaces have like charge, it results in repulsion of interfaces and consequently the stabilization of intervening water film (non-adhesion behavior).

Adhesion map for crude oil B was also provided using aged glass as the solid surface. This was done to provide a qualitative measure of whether or not the surface properties of the glass slide were changed upon aging. Table 7.3 shows the adhesion map of crude oil B when aged glass was used as the solid surface. As the map shows oil droplet was adhered to the glass slide in all conditions and effect of different pH and salt concentration were overshadowed by wetting behavior of the solid surface. It should be pointed out that glass slides were washed first with toluene and then with decane prior to the experiments. Attempt was done to treat all the glass slides identical respect to washing procedure.









Table 7.3: Adhesion map for crude oil B with aged glass.

[NaCl] pH	0 M	0.1 M	0.5 M	1.0 M
12				
9				
6				
3				

7.1.1 Effect of enzymes on adhesion

The effect of a selected enzyme (NZ2) on the adhesion behavior of crude oil B was examined. A condition in which crude oil B showed adhesion behavior, pH 3 and 0.5M NaCl concentration was chosen as the initial condition. NZ2 enzyme was added to the brine in 0.1 wt% concentration. Crude oil droplets were introduced at the surface in 2 minutes time interval sequence i.e. droplet number 1 is the first drop in the measurement series, two minutes later, drop number two is tested etc. Table 7.4 shows the results from the experiment. The oil droplet starts to destabilize and move toward a non-adhesion condition after about 6 minutes (droplet 5). Thereafter the oil droplets did not adhere to the glass. As will be discussed in more detail in section 7.4, reasons why adding NZ2 may shift the crude oil B/0.5 M NaCl, pH 3/glass from adhesion to non-adhesion include adsorption of protein and cleaving of ester bonds which may change the crude oil/brine/solid interactions.

Table 7.4: Adhesion behavior of crude oil B at pH 3 and 0.5M NaCl concentration by NZ2 enzyme introduction.

Time (min)	0	2	4	6	8	10	12	14
Adhesion behavior								

7.2 Contact angle measurements involving different enzymes

The concept of wettability is generally illustrated using the sessile drop technique to measure contact angle. A drop of crude oil is placed on the solid surface immersed in water or brine. As the oil drop is placed on the surface, the drop makes an angle with the solid surface. The angle between the surface and the tangent at the drop boundary is then measured. This angle is referred to as the contact angle. Wettability often refers to the water advancing contact angle, but here in this technique water recedes to make way for the oil, thus actually depicting the water receding angle.

Figure 7.2 shows typically different states of wettability in terms of the contact angle by sessile drop technique. The detailed procedure of contact angle measurements is described in Appendix B.

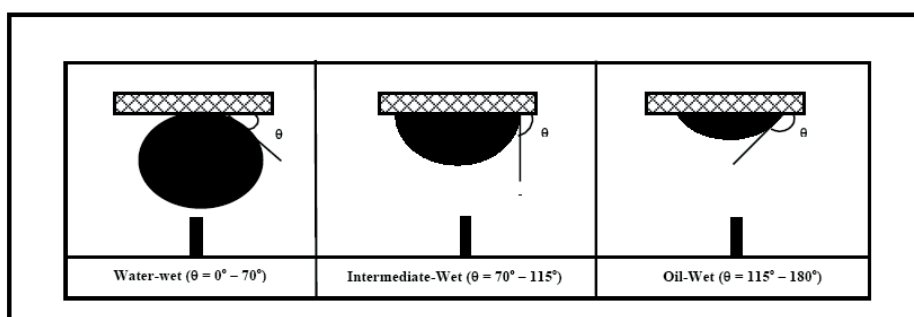


Figure 7.2: The conventional sessile drop contact angle technique.

The dimensionless term $\Delta\theta/\theta_{\text{REF}}$ was defined, where $\Delta\theta$ is $\theta_{\text{REF}} - \theta_{\text{ENZYME}}$ and θ_{REF} is the contact angle measured with an untreated brine phase without added enzyme, to account for both differences in the reference contact angle measured without added enzyme and the contact angle measured after adding enzymes. The results of these tests are summarised in the following sections for the different groups of enzymes and the two crude oils tested.

7.2.1 Greenzyme

7.2.1.1 Crude oil A

Table 7.5 shows the results for crude oil A with glass slides without any aging as the solid surface and brines with different Greenzyme concentration as the aqueous phase. As the

results clearly show, the difference in contact angle with and without enzyme is in some cases about 30° which is quite significant. As the concentration of Greenzyme increases, the change in contact angle is more pronounced. $\Delta\theta/\theta_{REF}$ increases accordingly to reach a plateau of roughly 0.5 at 0.75 wt% Greenzyme (see Figure 7.3).

Table 7.5: Contact angle measurements for crude oil A-Brine+GZ-Glass.

Type of enzymes	Enzyme conc. (wt%)	Ref. contact angle, θ_{Ref} (degree)	Average contact angle after adding enzyme, θ_{Enzyme} (degree)	$\Delta\theta = \theta_{Ref} - \theta_{Enzyme}$ (degree)	$\Delta\theta/\theta_{Ref}$
Greenzyme	0.01	62	46	16	0.26
Greenzyme	0.05	62	43	19	0.31
Greenzyme	0.1	62	42	20	0.32
Greenzyme	0.25	62	38	24	0.39
Greenzyme	0.5	62	36	26	0.42
Greenzyme	0.75	62	32	30	0.48
Greenzyme	1	62	32	30	0.48
Greenzyme	2	62	32	30	0.48

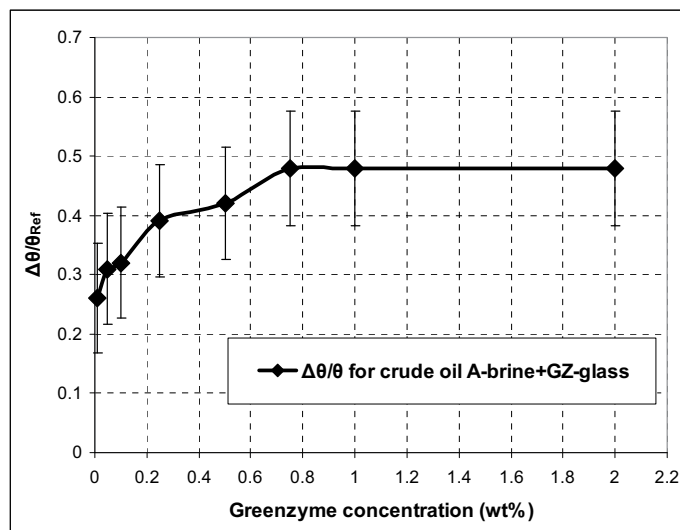


Figure 7.3: $\Delta\theta/\theta_{Ref}$ vs. GZ concentration when ordinary glass without aging was used as the solid surface and crude oil A as the oleic phase.

In the second group of experiments, glass aged in crude oil A for about 30 days at 80°C was used as the solid surface. In this group the enzymes had an even more pronounced effect on the contact angle. Different concentrations of Greenzyme were examined in this group of

experiments, and the results are summarized in Table 7.6 and Figure 7.4. Unlike the first group of experiments, the reference contact angle in the second group is different in all cases. The main reason for this is the washing procedure for the aged glass plates as described in measurement procedure in Appendix B.

Table 7.6: Contact angle measurements for crude oil A-Brine+GZ-Aged Glass (aged at 80°C).

Type of enzymes	Enzyme conc. (wt%)	Ref. contact angle, θ_{Ref} (degree)	Average contact angle after adding enzyme, θ_{Enzyme} (degree)	$\Delta\theta = \theta_{\text{Ref}} - \theta_{\text{Enzyme}}$ (degree)	$\Delta\theta / \theta_{\text{Ref}}$
Greenzyme	0.05	68	45	23	0.34
Greenzyme	0.1	65	34	31	0.48
Greenzyme	0.5	84	45	39	0.46
Greenzyme	1	84	50	34	0.40

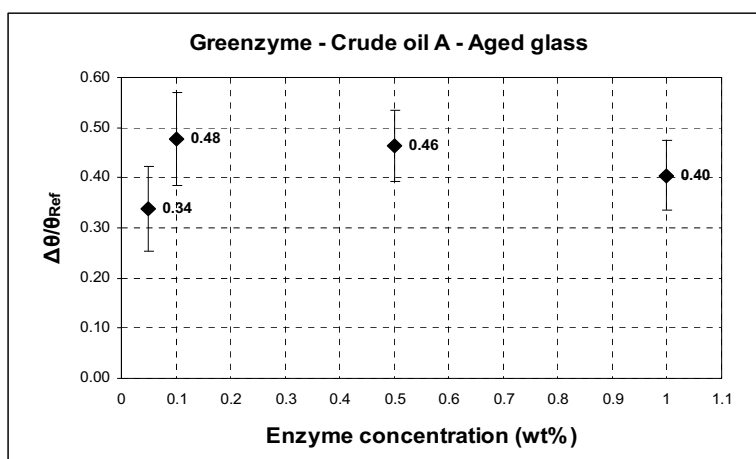


Figure 7.4: $\Delta\theta/\theta_{\text{Ref}}$ vs. GZ concentration when aged glass in crude oil A (aged at 80°C) was used as the solid surface and crude oil A as the oleic phase.

To examine the effect of enzyme on glass slides with different initial wettability states, identical concentration of Greenzyme was used for different reference contact angles. Table 7.7 and Figure 7.5 show the contact angle results for concentrations of 0.1 and 0.5 wt%. They show wettability alteration for different wetting states where the initial contact angles range from water-wet (0 to 75°) to intermediate-wet (75 to 105°); and oil-wet (105 to 180°) (Treiber et al. 1972). As the results show the effect of enzyme on the contact angle seem to depend on the reference contact angle. The change in contact angle is lower when the initial contact

angle is < 60 degrees or >100 degrees. The intermediate wetting state (60-100 degrees) appears to be the best condition for enzyme in terms of alteration of surface wettability.

Table 7.7: Contact angle measurements for crude oil A-Brine+GZ-Aged Glass (aged at 80°C), identical concentration of GZ in the solution.

Type of enzymes	Enzyme conc. (wt%)	Ref. contact angle, θ_{Ref} (degree)	Average contact angle after adding enzyme, θ_{Enzyme} (degree)	$\Delta\theta = \theta_{Ref} - \theta_{Enzyme}$ (degree)	$\Delta\theta / \theta_{Ref}$
Greenzyme	0.1	50	43	7	0.14
Greenzyme	0.1	65	34	31	0.48
Greenzyme	0.1	87	57	30	0.34
Greenzyme	0.5	50	43	7	0.14
Greenzyme	0.5	68	40	28	0.41
Greenzyme	0.5	84	45	39	0.46
Greenzyme	0.5	93	48	45	0.48
Greenzyme	0.5	126	122	4	0.03

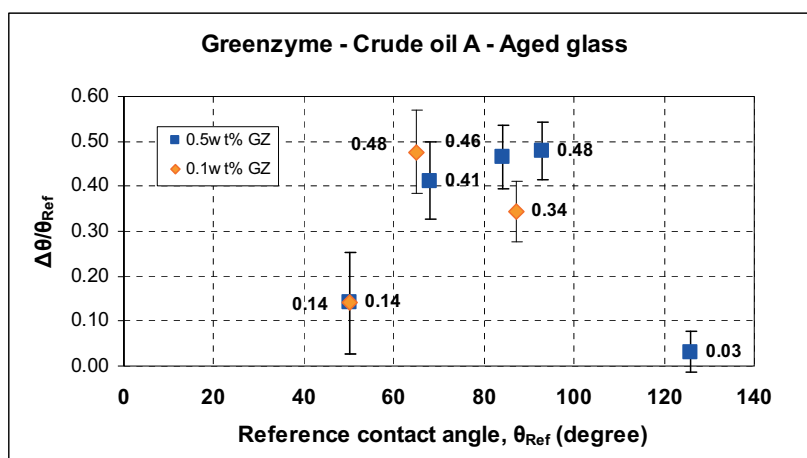


Figure 7.5: $\Delta\theta/\theta_{Ref}$ vs. different wetting state when identical concentration (0.1 and 0.5 wt%) of GZ was used as the aqueous phase, crude oil A as the oleic phase and aged glass (aged at 80° C) as the solid surface.

7.2.1.2 Crude oil B

Crude oil B has higher acid-to-base number than crude oil A, and consequently may be more efficient in changing the wettability of the solid surface towards more oil-wet conditions in the aging period (Skauge et al., 1999). Tables 7.8-7.9 and Figures 7.6-7.7 show the results for glass and aged glass (30 days at 80° C) as solid surfaces, respectively. According to the

results, unlike the contact angle for crude oil A, crude oil B gave almost the same contact angle changes independent of concentration when clean glass plates was used. For the case of aged glass plates, reference contact angles vary. Glass slides with almost similar reference contact angle gave changes in the contact angle that were almost identical and independent of Greenzyme concentration. As an example, for 0.01 and 1 wt% of Greenzyme in the aged glass experiments, $\Delta\theta/\theta_{REF}$ shows almost the same value irrespective of the Greenzyme concentration (see Figure 7.7). According to data for crude oil A and B involving aged glass, average contact angles after adding enzyme are roughly the same, however, they seem less scattered for crude oil B. The reason why contact angle changes are less scatter independent of enzyme concentration for crude oil B (clean and aged glass) can be ascribed to more acidic and basic functional groups in crude oil B, which may cause more interactions of the crude oil and the enzyme in the aqueous solution.

Table 7.8: Contact angle measurements for crude oil B-Brine+GZ- Glass.

Type of enzymes	Enzyme conc. (wt%)	Ref. contact angle, θ_{Ref} (degree)	Average contact angle after adding enzyme, θ_{Enzyme} (degree)	$\Delta\theta = \theta_{Ref} - \theta_{Enzyme}$ (degree)	$\Delta\theta / \theta_{Ref}$
Greenzyme	0.01	62	33	29	0.47
Greenzyme	0.05	62	33	29	0.47
Greenzyme	0.1	62	33	29	0.47
Greenzyme	0.25	62	34	28	0.45
Greenzyme	0.5	62	34	28	0.45
Greenzyme	1	62	34	28	0.45

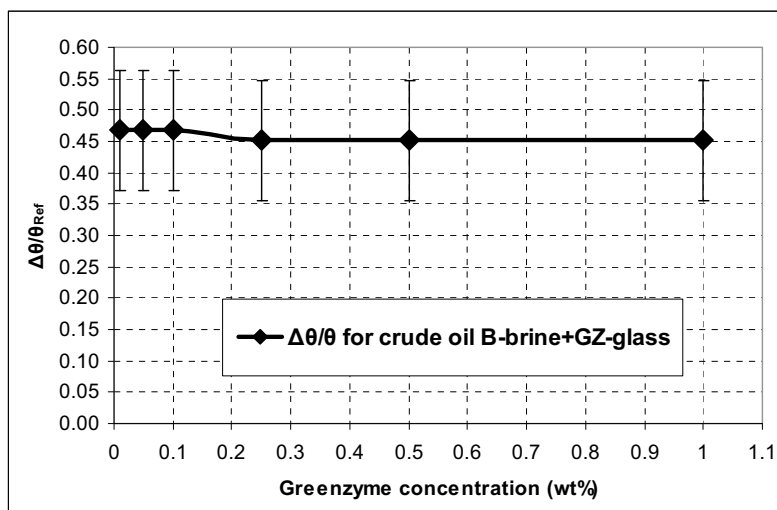


Figure 7.6: $\Delta\theta/\theta_{Ref}$ vs. GZ concentration when ordinary glass without aging was used as the solid surface and crude oil B as the oleic phase.

Table 7.9: Contact angle measurements for crude oil B-Brine+GZ-Aged Glass (aged at 80°C).

Type of enzymes	Enzyme conc. (wt%)	Ref. contact angle, θ_{Ref} (degree)	Average contact angle after adding enzyme,		$\Delta\theta = \theta_{Ref} - \theta_{Enzyme}$ (degree)	$\Delta\theta/\theta_{Ref}$
			θ_{Enzyme} (degree)			
Greenzyme	0.01	79	37		42	0.53
Greenzyme	0.05	72	37		35	0.49
Greenzyme	0.1	61	41		20	0.33
Greenzyme	0.5	65	41		24	0.37
Greenzyme	1	81	39		42	0.52

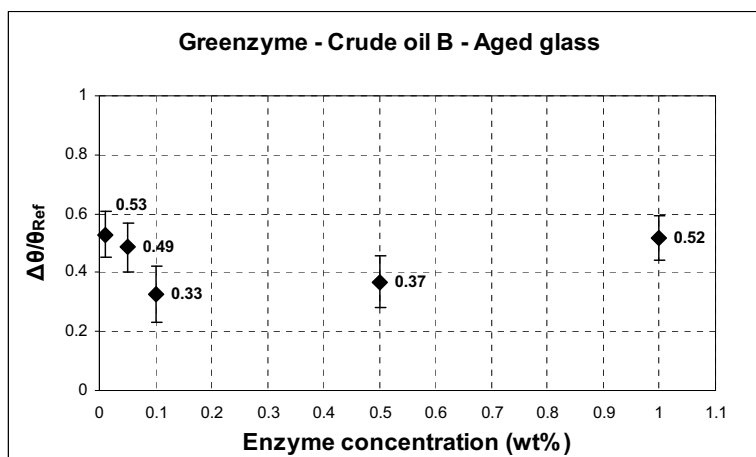


Figure 7.7: $\Delta\theta/\theta_{Ref}$ vs. GZ concentration when aged glass in crude oil B (aged at 80° C) was used as the solid surface and crude oil B as the oleic phase.

7.2.2 Zonase enzymes

In this group of experiments, the enzymes Zonase1 and 2 were added to the brine in different concentrations. Crude oil A was used as the oleic phase and glass aged in crude oil A for about 30 days at 80° C was the solid surface. Table 7.10 and Figure 7.8 show the results of the experiments. Zonase1 only gave changes in the contact angle when used in high concentrations (≥ 1 wt%). Zonase2 resulted in changes in contact angle, but less pronounced than for Greenzyme at the same concentration for comparable reference contact angles.

Table 7.10: Contact angle measurements for crude oil A-Brine+Zonase 1 & 2-Aged Glass (aged at 80°C).

Type of enzymes	Enzyme conc. (wt%)	Ref. contact angle, θ_{Ref} (degree)	Average contact angle after adding enzyme, θ_{Enzyme} (degree)	$\Delta\theta = \theta_{Ref} - \theta_{Enzyme}$ (degree)	$\Delta\theta/\theta_{Ref}$
Zonase1	0.1	128	120	8	0.06
Zonase1	0.5	48	44	4	0.08
Zonase1	1	54	44	10	0.19
Zonase1	2	129	107	22	0.17
Zonase2	0.1	86	86	0	0.00
Zonase2	0.5	92	64	28	0.30
Zonase2	1	82	58	24	0.29
Zonase2	2	107	64	43	0.40

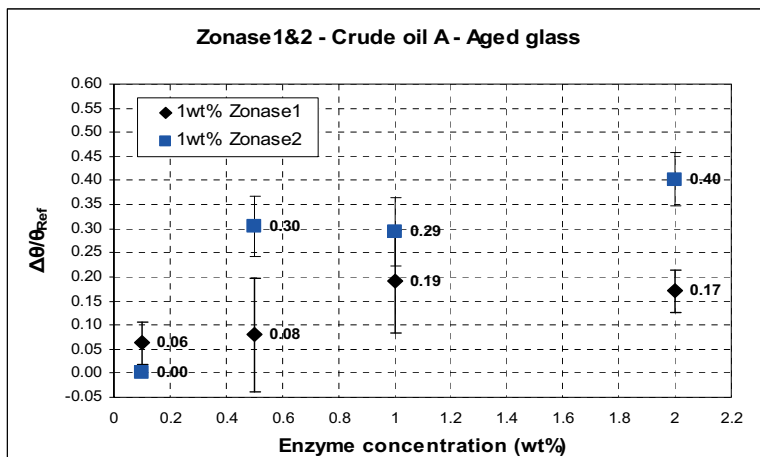


Figure 7.8: $\Delta\theta/\theta_{\text{Ref}}$ vs. Zonase 1 & 2 concentration when aged glass in crude oil A (aged at 80° C) was used as the solid surface and crude oil A as the oleic phase.

7.2.3 Esterase enzymes

Three different enzymes, NZ2, NZ3 and NZ6, from Novozyme were used. All experiments were performed using crude oil B both for measurements and aging (30 days at 80° C). Different concentrations of enzymes were examined in the contact angle experiments. Table 7.11 show the results for the three enzymes. As the results clearly show, the difference in contact angle with and without enzyme is in some cases more than 60°. This change is even more pronounced than for Greenzyme at the same concentration and for comparable reference contact angles.

Table 7.11: Contact angle measurements for crude oil B-Brine+NZ2, NZ3 & NZ6-Aged Glass (aged at 80°C).

Type of enzymes	Enzyme conc. (wt%)	Ref. contact angle, θ_{Ref} (degree)	Average contact angle after adding enzyme, θ_{Enzyme} (degree)	$\Delta\theta = \theta_{\text{Ref}} - \theta_{\text{Enzyme}}$ (degree)	$\Delta\theta / \theta_{\text{Ref}}$
NZ2	0.01	59	26	33	0.56
NZ2	0.1	90	27	63	0.70
NZ2	0.5	68	29	39	0.57
NZ2	1	86	28	58	0.67
NZ3	0.01	88	27	61	0.69
NZ3	0.1	72	26	46	0.64
NZ3	0.5	62	41	21	0.34
NZ3	1	82	29	53	0.65
NZ6	0.01	59	44	15	0.25
NZ6	0.1	69	54	15	0.22
NZ6	0.5	83	65	18	0.22
NZ6	1	86	29	57	0.66

Figure 7.9 shows the change in $\Delta\theta/\theta_{\text{REF}}$ for the three enzymes with changes in concentration. The results show a significant change in contact angle for all three enzymes, independent of enzyme concentration. Even at very low concentrations (0.01wt%), like in the case of NZ3, the change in contact angle is quite significant. In cases with similar reference contact angles the changes in contact angle are almost identical and apparently independent of enzyme concentration.

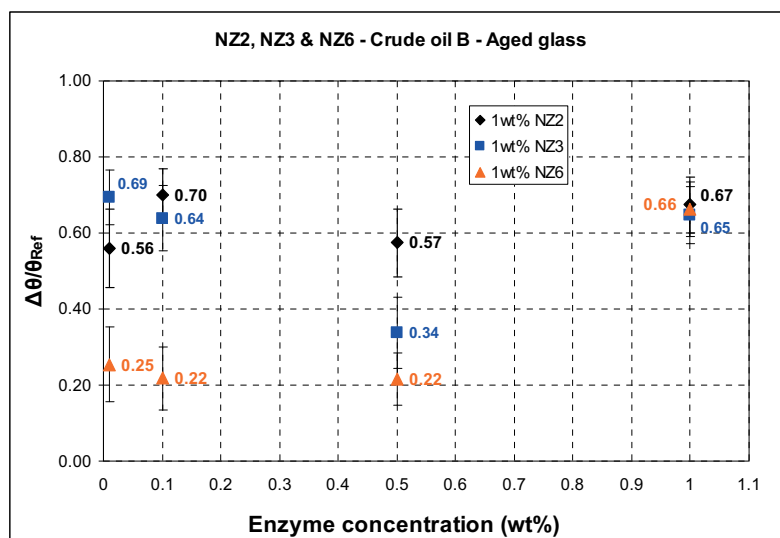


Figure 7.9: $\Delta\theta/\theta_{\text{Ref}}$ vs. NZ2, NZ3 & NZ6 concentration when aged glass in crude oil B (at 80° C) was used as the solid surface and crude oil B as the oleic phase.

7.2.4 Alpha-Lactalbumin

The whey protein Alpha-Lactalbumin (α -La) was also tested. Again, Crude oil B was used as the oleic phase and glass aged in crude oil B for about 30 days at 80° C was the solid. Table 7.12 and Figure 7.10 show the results of the experiments. As can be seen from the results, Alpha-Lactalbumin had a significant effect on the contact angle. The wettability alteration following addition of Alpha-Lactalbumin is close to the results obtained with Greenzyme for similar concentrations and reference contact angles.

Table 7.12: Contact angle measurements for crude oil A-Brine+ α -La -Aged Glass (aged at 80°C).

Type of enzymes	Enzyme conc. (wt%)	Ref. contact angle, θ_{Ref} (degree)	Average contact angle after adding enzyme, θ_{Enzyme} (degree)	$\Delta\theta = \theta_{\text{Ref}} - \theta_{\text{Enzyme}}$ (degree)	$\Delta\theta/\theta_{\text{Ref}}$
α -La	0.01	67	38	29	0.43
α -La	0.1	68	32	36	0.53
α -La	1	63	27	36	0.57

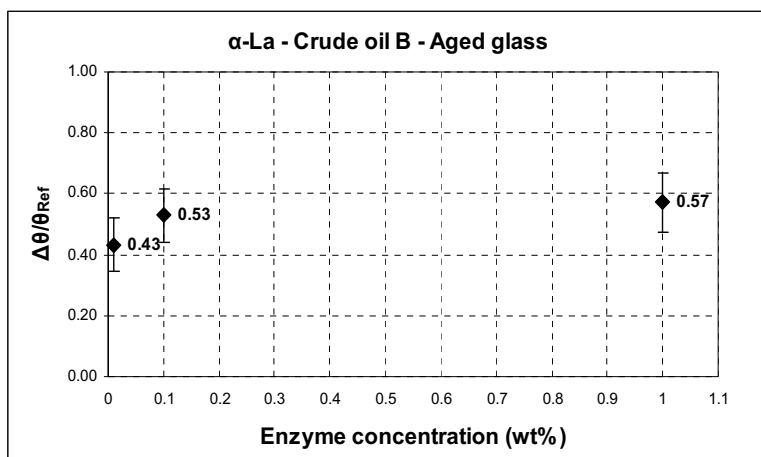


Figure 7.10: $\Delta\theta/\theta_{Ref}$ vs. α -La concentration when aged glass in crude oil B (at 80° C) was used as the solid surface and crude oil B as the oleic phase.

7.2.5 Effect of enzyme exposure time on measured contact angle

Contact angles were also measured as a function of time for selected enzymes to investigate the effect of enzyme exposure time on resulting contact angles. An example of this is shown in Figure 7.11 for NZ2 on clean glass slides with crude oil B used in the contact angle measurements. As can be seen from the figure, the contact angle is around 45 at time 0 but decreases to about 30 after 6 minutes. Note that each measurement is made with a fresh drop of crude oil.

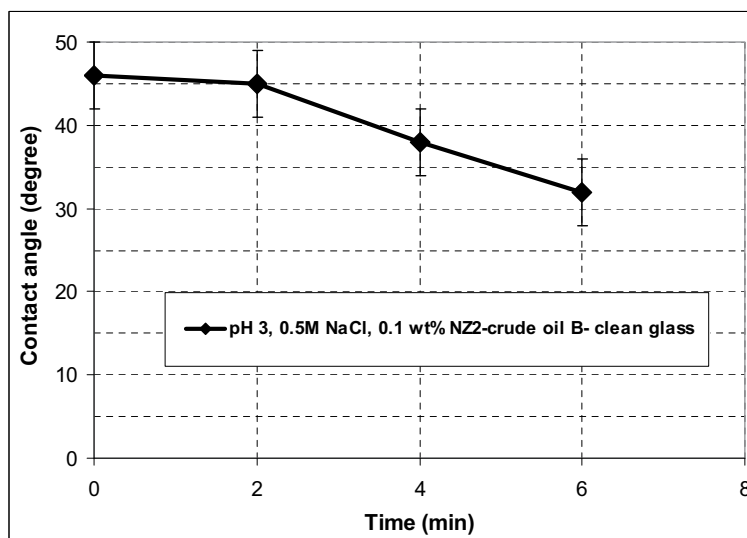


Figure 7.11: Contact angle change by introduction of enzyme to the system.

In another series of experiments, contact angle was measured as a function of time of exposure to 1wt% GZ-brine using crude oil B and aged glass slides (aged in crude oil B for more than 2 months at 80°C). In this case, all measurements were made on the same oil drop deposited on the glass surface. Measurements were done as a function of time for about 20 hours (see Figure 7.12). At time 0 the contact angle was 111 degree, however, and after 800 minutes it had decreased to 96 degrees. After that the decreasing trend leveled off.

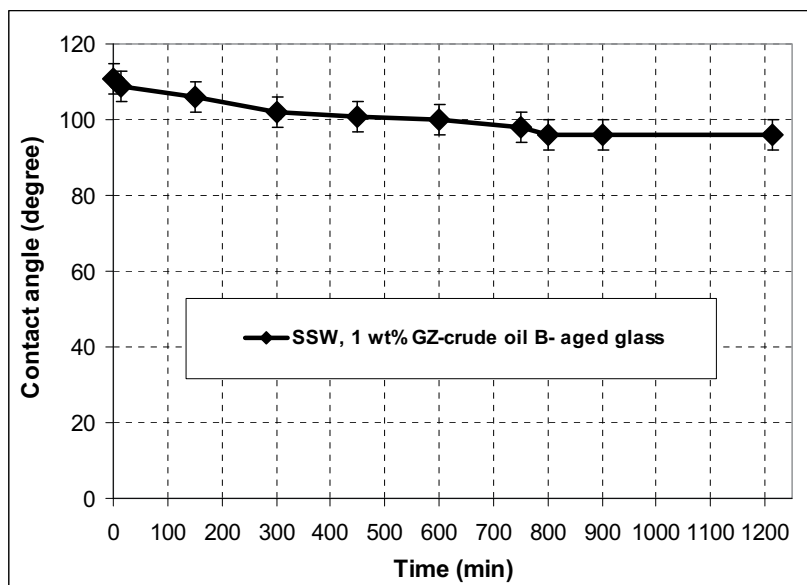


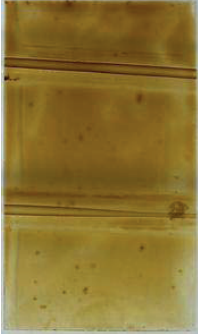
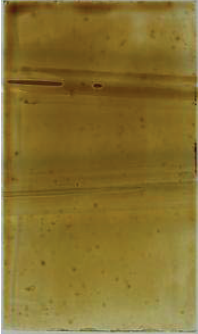
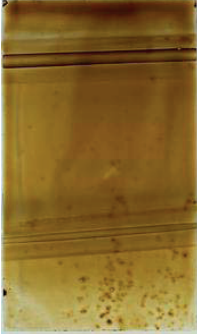
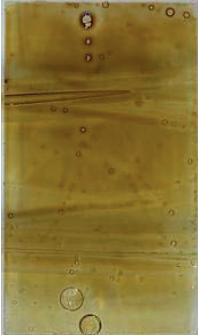
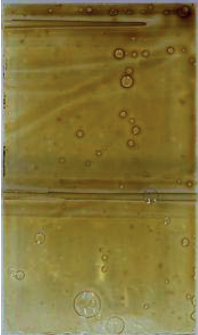
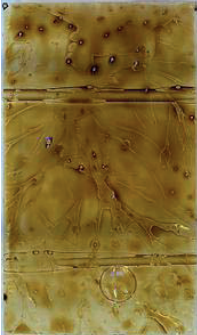
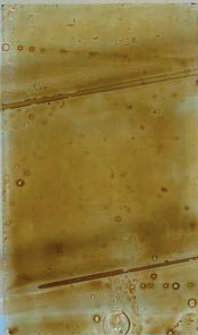
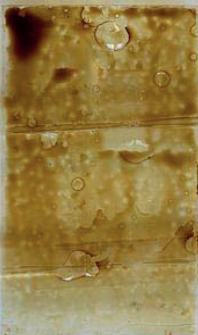
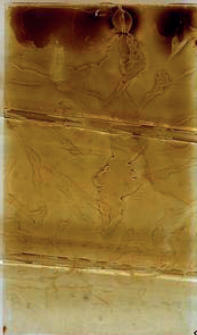



Figure 7.12: Contact angle measurements as a function of time corresponding to washing effect of enzymes.

7.3 Visual observations of the enzyme effect

Glass slides that have been aged in crude oil and then removed without further treatment have a visible crude oil “coating” on their surface. This is illustrated in the first pictures shown in Table 7.13. To visually observe the effect of enzymes on this surface “coating”, glass slides aged in crude oil B for more than 2 months at 80°C were put into containers of enzyme-brine solutions to study the effect of enzymes as a function of time. In these experiments, two enzymes, GZ and NZ2 in 1wt% concentration were used. One glass slide was also exposed to brine without enzyme to act as a blank sample. The glass slides were photographed prior to immersion and after selected exposure times. This is illustrated in Table 7.13.

In the experiment, glass slides were placed vertically in aqueous phase. Crude oil is less dense than water, thus buoyancy causes excess crude oil to migrate up along the glass plates. Since glass plates are unevenly saturated with crude oil after aging, it is difficult to assess the enzyme effect with respect to how much crude oil has migrated upward on the glass surface. In the evaluation of the enzyme effect two factors may be considered: (1) how much crude oil has migrated upward on the glass surface and (2) how much of the oil layer has been stripped off by enzyme solution. As it can be seen in the table there seem to be a visible effect of the enzymes on the oil “coating”.

Table 7.13: Photos show the washing effect of enzymes for different time intervals. Glass slides are pre-aged in crude oil B, and are not washed prior to immersion in the enzyme-brine solutions.

Time	SSW	SSW+1% GZ	SSW+1%NZ2
Before immersing to the solutions			
After 5 minutes			
After 17 hours			
After 5 days			

7.4 Proposed mechanism for wettability alteration by enzyme-proteins

Enzymes can catalyze cleaving of certain bonds in the crude oil and thereby change the interaction at the interfaces of crude oil/water/glass. In this study protease enzymes (Zonase enzymes) and esterase enzymes (Novozyme enzymes) were used, which catalyze breakdown of peptide and ester bonds, respectively. The esterase enzymes were found to have the most pronounced effect on contact angles. Figure 7.13 shows schematically how esterase enzymes may contribute to altering the wettability of the solid surface. By catalyzing breakdown of ester bonds which may exist in the crude oil and production of more acidic components, they contribute to increasing the repulsive electrostatic forces between the crude oil/brine/glass interfaces. This process may result in contact angle change toward more water-wet condition. A model oil containing a water insoluble ester was used to confirm the break down of the ester bonds by the esterase enzymes. Results of the measurements is presented and described in detail in chapter 8. Greenzyme had also significant effect on changing the contact angle. Adding GZ changes contact angle in case of using both type of glasses, glass an aged glass. Greenzyme according to the supplier (Greenzyme material safety data sheets) consists of enzyme and stabilizers. The enzyme itself is made from oleophilic microbes where the oil digesting properties have been neutralized, but the ability to seek hydrocarbons is kept and the added stabilizers are likely surfactants. Therefore, the effect of Greenzyme on contact angle alteration can not be a direct effect of enzyme alone. It means that other substantive existing in the GZ solution may also be in charge of contact angle alteration.

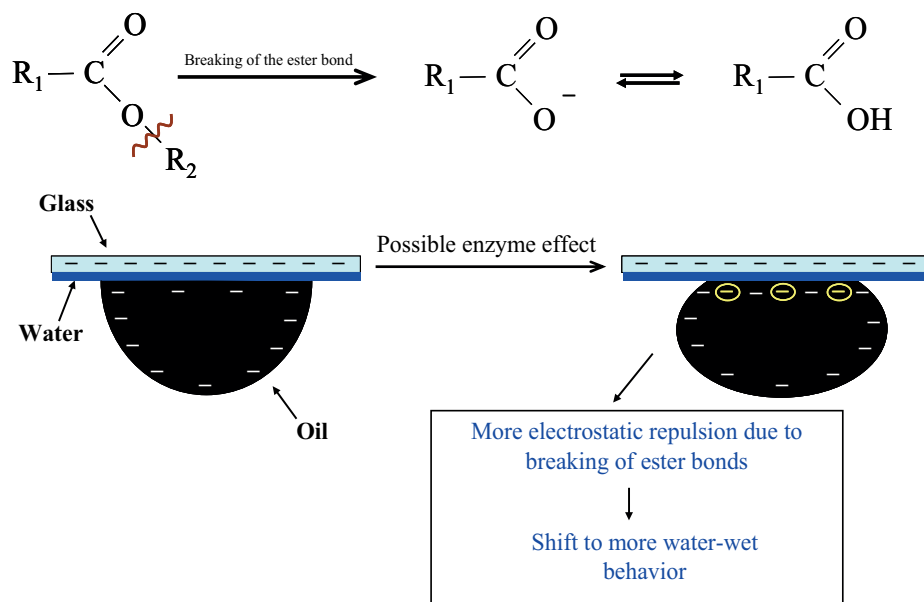


Figure 7.13: Breaking down of ester bonds by NZ group enzymes and alter the wetting behavior of the solid surface.

In addition to the catalytic effect of enzymes, the enzymes are also proteins which may adsorb onto a solid surface and thus cause changes in its properties. The process by which proteins adsorb onto solid surfaces and the interactions involved has been discussed in detail in chapter 6. In our experiments, we found a significant effect of the protein Alpha-Lactalbumin (α -La) on crude oil-water contact angles. This is likely due to surface modification by protein adsorption. Adsorption of α -La to adsorb onto different solid surfaces has been reported by several authors (e.g. Halskau et al., 2002; Glomm et al., 2007).

7.5 Adsorption measurements

To investigate whether adsorption could be an important mechanism contributing to contact angle changes by enzymes and proteins, adsorption studies were undertaken. Greenzyme (GZ) and NZ2, which were known to have a significant effect on crude oil-brine contact angle, were selected for this study. UV spectroscopy was used to measure changes in concentration of the enzymes after contact with the solid substrate.

Initially, a scan to determine the UV absorbance spectrum for the enzyme solutions was performed. For GZ solutions, the spectrum showed large fluctuations and limited

reproducibility. This could indicate that GZ is not a pure enzyme, but rather consists of several different components.

Unlike GZ, NZ2 showed a systematic behavior for different wavelengths and concentrations of the enzyme, and thus we proceeded with adsorption measurements using UV spectroscopy to detect changes in enzyme concentration. To examine adsorption of the NZ2 enzyme onto solid surfaces, kaolin and two types of silica powder, silica 1 and silica 2 with total surface area of 10.6, 3.65 and 650 m²/g, respectively were selected as the solids to use for the measurements. Silica is the main component in the sandstone rocks and glass plates and kaolin is an important clay mineral that may be found in carbonate and sandstone rocks in some extent. The effects of protein–surface interaction on protein adsorption are rather complex due to the large number of factors that contribute to the total interaction (Malmsten, 1998). These factors include temperature and pressure, protein net charge and charge distribution, the solution medium and the size of the protein (Malmsten, 1998; Butt et al., 2006). The net charge on the mineral surface/water is also important in this process which is affected by pH of their surrounding aqueous phase and can become more positively or negatively charged due to the loss (deprotonation) or gain (protonation) of protons (H⁺). pH of the solution in our experiments was around 8. Silica has a pzc around 2 (Iler, 1979) and in any pH > 2 silica surface has negative net charge. Kaolin has a heterogeneous surface charge where the basal surface is believed to carry a negative constant structural charge while the charge on the edges depends on pH (Zhou and Gunter, 1992). At pH values higher than the pzc (around 4) the surface charge becomes negative (Schroth and Sposito, 1997). So, both minerals have almost the same surface charge at given pH.

The results of silica 1 showed no adsorption of NZ2 at the investigated solid-to-liquid ratio (0.01, 0.05 and 0.1). Table 7.14 shows the results of the experiments for the silica2 and kaolin. Note that all the adsorption data in the table is average of two parallel measurements. Sample preparation and procedure of the measurements by UV technique is described in Appendix B.

Table 7.14: Adsorption measurements of NZ2 enzyme by silica and kaolin.

NZ2 Con. (wt%), Silica2				NZ2 Con. (wt%), Kaolin			
Reference Value	Solid/Liquid			Reference Value	Solid/Liquid		
	0.01	0.05	0.1		0.01	0.05	0.1
0.1	no ads.	no ads.	no ads.	0.1	no ads.	no ads.	no ads.
0.5	0.45	0.37	0.32	0.5	no ads.	no ads.	no ads.
1	0.74	0.68	0.63	1	0.93	0.81	0.86
2	1.52	1.38	1.29	2	no ads.	1.68	1.76

According to the results concentration of the NZ2 enzyme decreases by adding the silica2 to the system. Higher solid-to-liquid ration giving rise to more adsorption of the enzyme and lower concentration of enzyme into the solution. Since among different factors affecting adsorption of enzyme at the solid surfaces, all of them are kept identical with respect of doing experiment with kaolin silica1 and silica2, the difference in amount of enzyme adsorption may be attributed to the difference in surface area. Surface area of silica2 is 650 m²/g which is much higher than of that in silica1 and kaolin, 3.65 and 10.6 m²/g, respectively.

Chapter 8 Experimental study of oil-water interface

In chapter 7 we studied interactions in the oil/brine/solid system. It was found that enzymes can change the adhesion behavior of the crude oil on glass surfaces from adhesion to non-adhesion when they are added to the brine solution. This was confirmed by contact angle measurements, which showed that contact angles became more water-wet (i.e. decreased) after exposure to enzyme solutions. Possible mechanisms giving rise to these observations, including of catalysis of ester hydrolysis and enzyme adsorption, were discussed and to some degree tested.

The following chapter presents an experimental study of changes in oil-water interfacial properties by addition of enzymes and proteins, including measurements of interfacial tension and electrophoretic mobility. Attempts were also made to study changes in both oil and water phase composition after equilibration with enzymes. However, since the chemical composition of crude oil is highly complex, a model oil (refer to appendix A for detailed composition) was used in some of the experiments. The model oil was chosen to be a water insoluble ester (ethyl decanoate) solved in mineral oil in an effort to verify the possible role of catalysis of ester hydrolysis.

8.1 Interfacial tension (IFT) measurement

Interfacial tension (IFT) between crude oil and brine is an important variable in water/oil displacement which can be dependent on components of the crude oil, pH and composition of the aqueous phase. Adsorption of organic acid and/or bases at the oil/water interface results in lowering of interfacial tension. Oils with different properties were used in the experiments to

see the effect of oil composition on IFT. Further, groups of enzymes known to be interfacially active were tested to see their effect on IFT between oil and water.

In most of the IFT measurements oleic and aqueous solutions were equilibrated prior to the experiments. It was done because IFT values between crude oil and aqueous solutions are time dependent. This may be due to either slow diffusion of some components across the interface or molecular rearrangement at the interface with interface age (Buckley and Fan, 2005). Sample preparation and measurement procedure are presented in detail in Appendix B.

8.1.1 Effect of enzymes and proteins on crude oil-brine interfacial tension

The interfacial tension between crude oil B and brine containing 1wt % (0.5wt % for α -La due to availability) of enzyme or protein was measured as a function of equilibration time. Equilibration (2 or 4 weeks) was done by putting a container containing crude oil and enzyme-brine solutions with (1:1 volume ratio) horizontally, with occasional shaking, for the designated time interval. Figure 8.1 shows the results of the measurements. According to the results, interfacial tension between crude oil and enzyme-brine solutions was not significantly different from that between crude oil and brine. An exception is GZ which decreased the oil-brine IFT by a factor 3. GZ is a commercial enzyme which has been modified according to the crude oil complexity and is a compound of enzyme and stabilizers (surfactants) (Greenzyme material safety data sheets). The existence of stabilizers (surfactants) in the solution seems to make it exception among all tested enzymes and protein to be more interfacially active. NZ group enzymes are pure esterase enzymes which are known as interfacially active material and typically show activity towards the soluble state of their substrate (Fojan et al., 2000; Al-Zuhair et al., 2007). Although these esterase enzymes are interfacially active, it appears that their adsorbance on the crude oil-brine interface could not change the IFT. High concentration of interfacially active components in the crude oil can be the reason behind that. The affinity of the esterase enzymes for the interface seems to be not strong enough to replace the crude oil components. The result of IFT measurements using mineral oil and enzyme-brine solution which will be discussed further in section 8.1.3 shows good agreement with this argument. Adding enzyme to the brine solution could lower the IFT to some degree. It means that esterase enzymes are interfacially active when their substrate changes from crude oil to mineral oil. Increasing the equilibration time, from 2 to 4 weeks did not have a significant effect on interfacial tension.

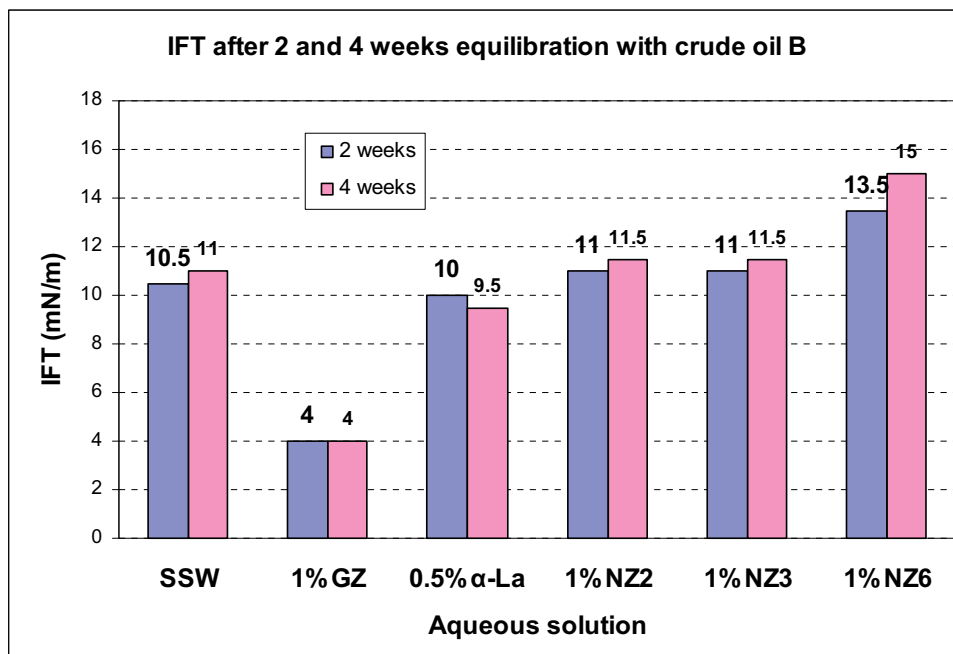


Figure 8.1: IFT for different concentration of different enzyme-brine solutions and crude oil B after 2 and 4 weeks equilibration.

Using GZ, which was found to have the largest effect on crude oil-brine IFT, the effect of enzyme concentration on interfacial tension was tested. Further, to investigate the possible influence of crude oil composition on the extent of IFT lowering, measurements with crude oil A was also included in this experimental series. Figure 8.2 shows the results of these experiments. As can be seen from the figure, both the extent IFT reduction and change of IFT with increasing GZ concentration is similar for crude oils A and B: IFT decreases with increasing Greenzyme concentration levelling off at 5mN/m at 1 wt% concentration.

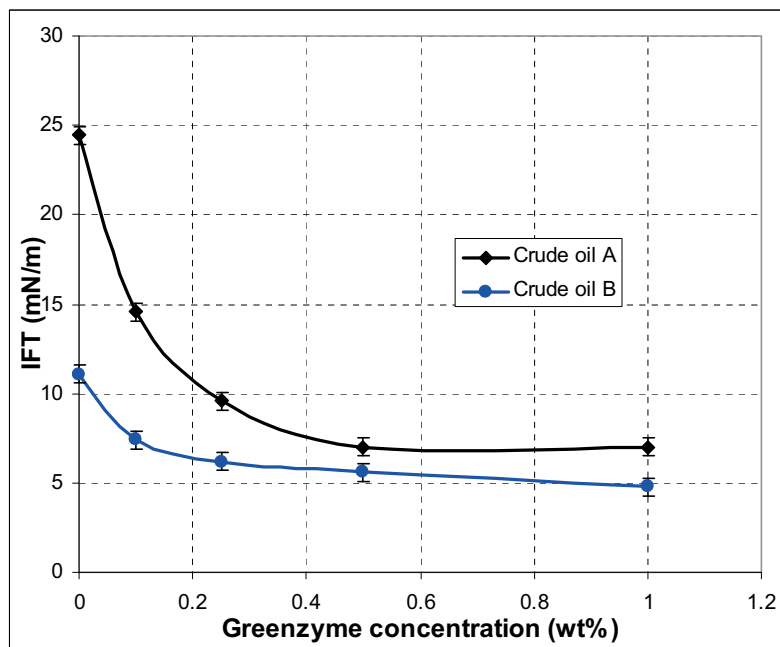


Figure 8.2: IFT between different concentrations of GZ solution and crude oil B.

8.1.2 Effect of enzyme on crude oil-brine interfacial tension at high and low pH

Interfacial tension between brine and crude oil B was measured after equilibration of the phases for brine compositions showing distinct adhesion (pH 3, no added salt) and non-adhesion (pH 9, 1M NaCl) behavior. Tests were performed both with and without enzyme added to the brine phase, using two different enzymes: GZ, which lowered the IFT, and NZ2 which had no effect on IFT, in the crude oil-brine system at sea water pH (pH ~ 6-7). The measured interfacial tensions are listed along with the initial and equilibrium pH values in Table 8.1. A graphical presentation of the IFT data is given in Figure 8.3, while Figure 8.4 shows a photo of the six samples.

Table 8.1: Overview of the samples, the pH change and measured interfacial tension.

Sample No.	Enzyme (1 wt%)	NaCl (M)	Initial pH	pH after equilibration	IFT (mN/m)
1	---	0.0	3.0	3.29	20.5
2	GZ	0.0	3.0	5.74	12.5
3	NZ2	0.0	3.0	3.53	23.0
4	---	1.0	9.0	5.80	14.0
5	GZ	1.0	9.0	5.83	4.0
6	NZ2	1.0	9.0	5.69	11.5

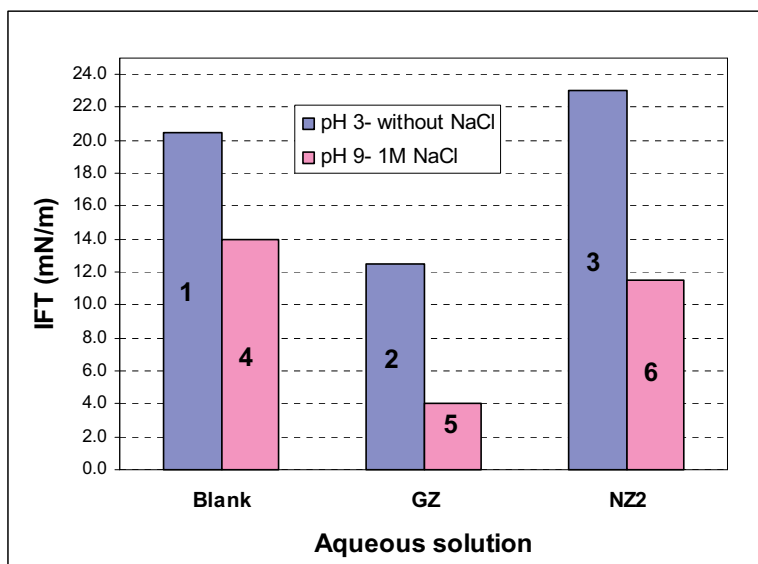
**Figure 8.3:** IFT between crude oil B and brine with varying pH and NaCl concentration with and without enzyme.



Figure 8.4: Photo of the samples immediately after the equilibrating in the rotator (number in accordance with sample numbers in Table 8.1.

In accordance with the adhesion tests reported in section 7.1, only sample 1 (pH 3, no added salt or enzyme) shows adhesion (see Figure 8.4). Adding NZ2 to the aqueous phase prior to equilibration appears to lead to the formation of a middle phase in sample 3 (pH 3, no added salt, 1 wt% NZ2), while in sample 6 (pH 9, 1M NaCl, 1 wt% NZ2) it seems to give solubilization of oil in the water phase as seen by the darker color.

As expected, IFT decreases with increasing pH, which is likely related to ionization of acidic functional groups (Buckley, 1996). It should, however be noted that the ionic strength of the high pH brine is different from that of the low pH brine, which may well affect IFT (Buckley 1996; Buckley and Fan, 2005).

Adding GZ to the brine phase lowers the interfacial tension at both high and low pH (see Figure 8.3). Since interfacial tension is lowered in both high and low pH, it can be speculated that added stabilizers in the GZ may contain surface active components which can adsorb on the interface and thus decrease interfacial tension. Adding NZ2 enzyme does not significantly affect IFT. However, it causes more crude oil to dissolve in the water phase (see Figure 8.4), which may be ascribed to hydrolysis of ester bonds in the crude oil.

Table 8.1 shows also changes in pH after equilibration of oil and water. Changing in pH of water phase can be explained by the theory of ionization of surface active groups (ISG) in the

crude oil (Buckley et al., 1989). Crude oil contains various polar organic compounds with acidic or basic properties, which may become ionized (acids) or protonated (bases) when equilibrated with brine. This ionization process at the oil-water interface depends on pH of the water phase. At high pH, crude oil acidic components are ionized. This increases the negative charge of the interface, and lowers the pH of the brine phase since H^+ ions are generated when the acids ionize. However, at low pH, crude oil acidic components may become protonated. This decreases the negative charge of the interface and increases the pH of the brine phase since H^+ ions are consumed by protonation of the bases. Such an increase in the pH after equilibration at low pH and a decrease after equilibration at high pH is in accordance with the observed results.

8.1.3 Effect of enzyme and proteins on model oil-brine interfacial tension

The NZ enzymes are known to be esterase enzymes. Thus, to investigate the effect of ester hydrolysis on oil-brine interfacial tension, two different model oils were equilibrated with brine solutions with added enzyme: one consisting of a pure mineral oil and one of the same mineral oil but with 1 wt% of a water insoluble ester added. In addition to the NZ enzymes, a test was performed with GZ added to the brine phase for comparison. The results of the measurements are shown in Figure 8.5.

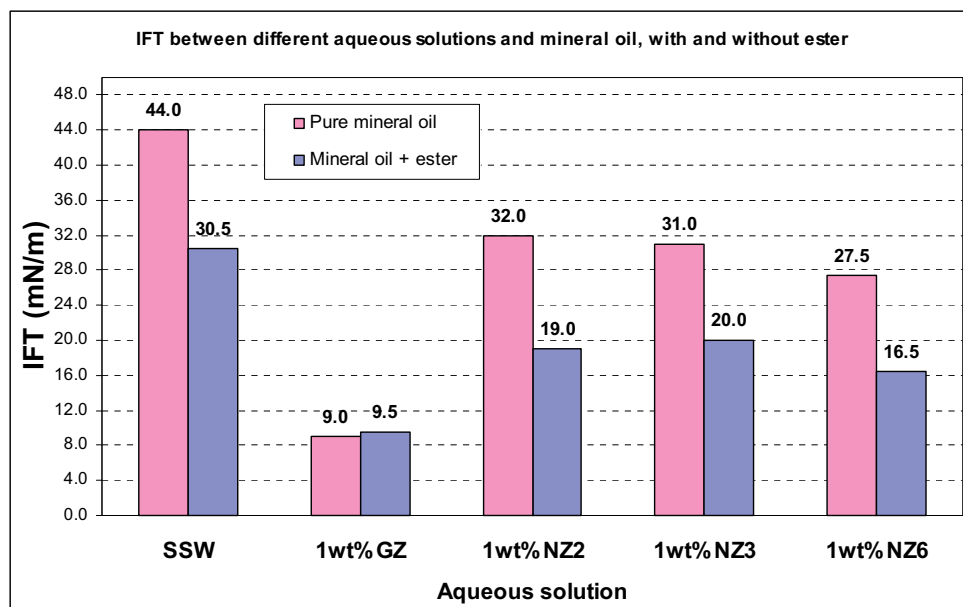


Figure 8.5: IFT between identical concentration (1wt%) of different enzyme-brine solutions and model oil, with and without ester.

Considering an oil phase consisting of a pure mineral oil (iso-octane), adding esterase enzymes to the brine decreased the oil-water IFT by roughly 10 mN/m. Decreasing in IFT value between mineral oil and water by adding enzyme-proteins to the aqueous phase has been reported by several authors. As an example, Beverung et al. (1999) performed IFT measurements between heptane and different enzyme-protein (globular proteins and lipases) solutions and reported decrease in IFT by adding enzyme-protein to the solution. They explained it by order/disorder transition in the globular protein molecule which permitting significant unfolding of the proteins at the oil/water interface. Effect of enzymes on IFT in mineral oil-brine system is contrary to what was seen for the crude oil-brine system where adding the esterase enzymes had no effect on IFT. This can be explained by high concentration of interfacially active components at the crude oil-brine interface whose activities overshadowed the interfacial activity of enzyme at the interface. In the case of GZ, however, the effect of adding the enzyme was roughly the same in the mineral oil-brine system as for the crude oil-brine system which can likely be related to the compound composition of GZ as already discussed.

Adding ester to the oil phase decreased the oil-water IFT both in the presence and absence of esterase enzymes. In the absence of enzymes, the observed decrease in IFT can likely be attributed to adsorption of polar ester groups at the oil-water interface. Adding esterase enzymes (i.e. NZ2, 3 and 6) to the brine phase decreased the IFT further. The additional lowering of IFT can be explained by action of enzymes on catalyzing break down of ester bonds (to form acid and alcohol) and production of acidic components at the oil/water interface which giving rise to increasing of the electrostatic interactions at the interface. However, the results of electrophoretic mobility measurements that will be explained in section 8.2 are in contrary to this hypothesis. In this regard, as mentioned, interfacial activity of the enzymes which comes from the protein nature of the enzymes can not be discarded since IFT values decreased to some extent in the cases when there was no ester in the oleic phase.

8.1.4 Effect of surfactants on crude oil-brine interfacial tension

As already discussed in chapter 4 different variables affect the phase behavior and solubilization parameters, and thus IFT in brine/oil/surfactant system. Optimal salinity and its variation with temperature are among these parameters. In our experiments, temperature (ambient) and injection water salinity (sea water) was fixed, and screening for surfactants was consequently done for these conditions only. Given the high salinity and presence of divalent ions in sea water, solubility of the surfactant was a critical issue. Based on the surfactants available in our laboratories, their optimal salinities and solubilization parameters, four internal olefine sulfonate surfactants (O332, O342-l, O342-h and O342-c) were selected for testing. The aim was to find a surfactant that would lower IFT as much as possible given our experimental conditions.

Good solubility and stabilized solution are also desirable to decrease retention of the surfactant inside the porous media as low as possible (Gupta et al. 2009). Surfactants were added to the brine at 1wt% concentration. Co-solvents are often added to increase surfactant solubility. Therefore, 2-butanol and 2-pentanol (IAA) as co-solvents were added in different concentrations (1-4 wt%) into the surfactant solutions. IFT between aqueous solutions and crude oil B were measured for all the samples to investigate the suitable surfactant, co-solvent and their concentrations which result in the lowest value of IFT. Table 8.2 shows all results for different surfactant, co-solvent and concentrations. All IFT measurements were done

without any equilibration between aqueous and oleic phases prior to the measurements. Among four tested surfactants, surfactant O342-c seems to give the lowest IFT when 1wt% 2-pentanol was used as the co-solvent. Further increasing of co-solvent concentration did not give additional lowering of IFT (see Table 8.2). So, this surfactant and co-solvent with 1wt% concentration were used further in displacement experiments.

Table 8.2: IFT measurements with different types and concentrations of surfactants and co-solvent.

Surfactant (1 wt%)	Co-solvent	Solution appearance	IFT (mN/m)
O332	4 wt% 2-butanol	Clear	0.158 ± 0.001
O342-h	1 wt% 2-pentanol	Turbid	0.360 ± 0.001
O342-l	1 wt% 2-pentanol	Turbid	0.191 ± 0.001
O342-c	1.5 wt% 2-pentanol	Turbid	0.04
O342-c	1 wt% 2-pentanol	Turbid	0.005 ± 0.001

8.1.5 Combined effect of surfactants and enzymes on crude oil-brine IFT

Using a combination of enzymes and surfactants for different purposes has been reported by several authors (see chapter 3). In this study, a new approach of combining enzyme and surfactants for use in coreflooding experiments was tested (see chapter 9). Prior to the coreflooding experiments the combined effect of enzyme and surfactant on crude oil-brine interfacial tension was tested, as well as their compatibility in aqueous solution. The results for the enzymes selected for the coreflooding experiments (GZ and NZ2) combined with the most promising surfactant (O342-c) are displayed in Table 8.3.

In the presence of 1 wt% alcohol co-solvent, the crude oil-brine IFT was the same for the surfactant and NZ2-surfactant solutions irrespective of enzyme concentration. For the GZ enzyme, however, this was only true at low enzyme concentrations (1 wt%). At high enzyme concentration (5 wt%) the crude oil-brine IFT was higher for the GZ-surfactant solution than for the surfactant solution.

Contrary to the NZ2-surfactant solutions, the GZ-surfactant solutions were clear in the presence of 1 wt% alcohol co-solvent. It thus seems that GZ in part acts as a co-solvent. Since

the presence of alcohol is generally thought to contribute to higher oil-water interfacial tensions in surfactant systems (see chapter 4), measurements were performed for GZ-surfactant solutions in the absence of alcohol. In this case the aqueous solutions were turbid, and the resulting crude oil-brine interfacial tension increased relative to the measurements with added alcohol. Based on these results, 1 wt% surfactant solutions with 1 wt% alcohol co-solvent and GZ or NZ2 enzyme added were chosen for the coreflooding experiments.

Table 8.3: IFT measurements for surfactant (1 wt% O342-c) -enzyme solutions.

Co-solvent	Enzyme	Enzyme concentration (wt%)	Solution appearance	IFT (mN/m)
1 wt% IAA	---	---	Turbid	0.005 ± 0.001
1 wt% IAA	GZ	1	Clear	0.008 ± 0.002
1 wt% IAA	GZ	5	Clear	0.026 ± 0.003
---	GZ	1	Turbid	0.060 ± 0.003
---	GZ	5	Turbid	0.173 ± 0.001
1 wt% IAA	NZ2	1	Turbid	0.005 ± 0.001
1 wt% IAA	NZ2	5	Turbid	0.003 ± 0.001

8.2 Electrophoretic mobility measurements

Three types of oil including crude oil A, crude oil B and model oil were used in electrophoretic mobility measurements. Different type of enzymes, Greenzyme, NZ2, NZ3 and NZ6 were used to make the enzyme-brine solutions. Because of high conductivity of the SSW, the instrument was not able to measure electrophoretic mobility in the case of using SSW as the aqueous phase. So, all the measurements for electrophoretic mobility were done using 0.5 wt% of NaCl into the distilled water however 3 times diluting of SSW made it possible to perform the electrophoresis measurement which will be discussed in next section. Figure 8.6 shows the results of the measurements. Sample preparation and measurement procedure are presented in detail in Appendix B.

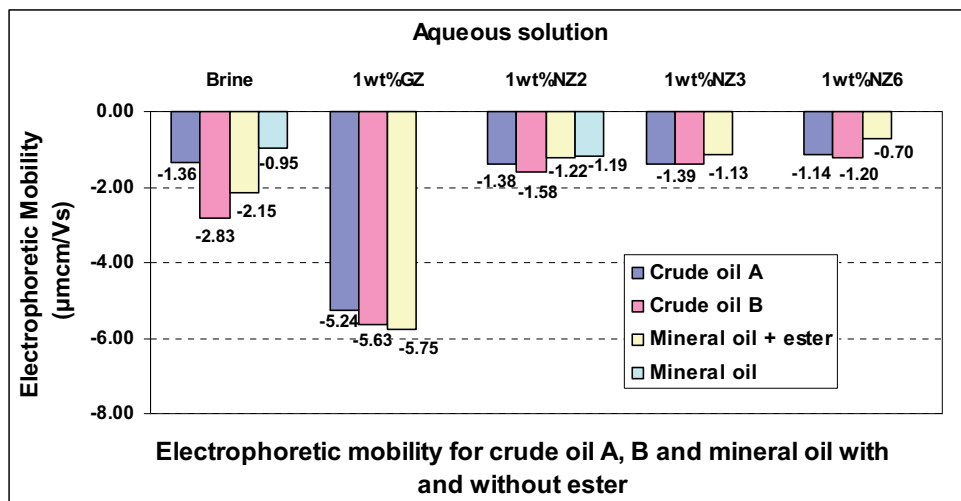


Figure 8.6: Electrophoretic mobility for emulsion of crude oil A, B and model oil in different enzyme-brine solution.

Crude oil A, Crude oil B and mineral oil with and without ester show different values for the reference electrophoretic mobility without adding any enzymes which are, -1.36, -2.83, -2.15 and -0.95 $\mu\text{mcm/Vs}$ respectively. The reason could be different acid and base functional groups of the oils. Crude oil B contains more acidic functional groups which can explain its higher value of electrophoretic mobility compare to the others. Mineral oil, suspended in water has also negative electrophoretic mobility due to the adsorption of negative ions, i.e. they migrate towards the positively charged electrode (Huotari et al. 1998).

Adding Greenzyme to the brine cause an increase in the electrophoretic mobility (more negative). Although the two crude oils and the mineral oil with added ester have different electrophoretic mobilities initially, the values are almost identical when GZ is added to the brine phase, meaning that adding GZ into the solution overshadowed the effect of other substances. Existence of stabilizers (surfactants) in GZ solution can explain this behavior, meaning that the increase in electrophoretic mobility to the more negative values might be the result of added stabilizers in the GZ solution. While the esterase enzymes seemed to have limited effect on the electrophoretic mobility of crude oil A, the mobility was decreased for crude oil B and mineral oil with added ester. This can be explained by the amount of acid to base functional group in crude oil B which is more compare to crude oil A and existence of ester in the mineral oil that cause more electrical charges at the oil-water interface and thereby more interaction of enzyme at the interface.

Electrophoretic mobility can be influenced by pH of the aqueous solution (Buckley et al., 1989; Huotari et al. 1998). Results of electrophoresis measurements of emulsified droplets of crude oil in brines of varying composition show that crude oil interfaces have net positive charge at low pH and net negative charge at high pH (Buckley et al., 1989). To investigate whether pH variations could be influencing our results, the pH of the relevant enzyme brine solutions was measured (see Table 8.4). Results did not show any significant change on pH by adding enzyme to the brine compare to the case of untreated brine. So, it can be inferred that the observed change in electrophoretic mobility does not seem to be related to changing of pH in solutions.

Table 8.4: pH values for brine and enzyme-brine solutions.

Sample	Brine	1wt% GZ	1wt% NZ2	1wt% NZ3	1wt% NZ6
pH	8.41	8.22	8.43	8.42	8.31

8.2.1 Effect of salinity on Electrophoretic mobility:

All the measurements of electrophoretic mobility discussed above were done using 0.5 wt% NaCl. To consider the effect of salinity, and also the presence of divalent ions (Ca^{2+} and Mg^{2+}), experiments were conducted with crude oil B and dilutions of SSW. Performing measurements with dilutions of SSW instead of sodium chloride solutions makes the experimental conditions more representatives of those encountered during core floodings and contact angle measurements.

As expected, the electrophoretic mobility increases with increasing dilution from 3 to 100 times (see Figure 8.7). Although electrophoretic mobility increased with increasing dilution of SSW in all cases, the effect was largest for the system with GZ added for which the electrophoretic mobility was doubled from 3 to 100 times dilution.

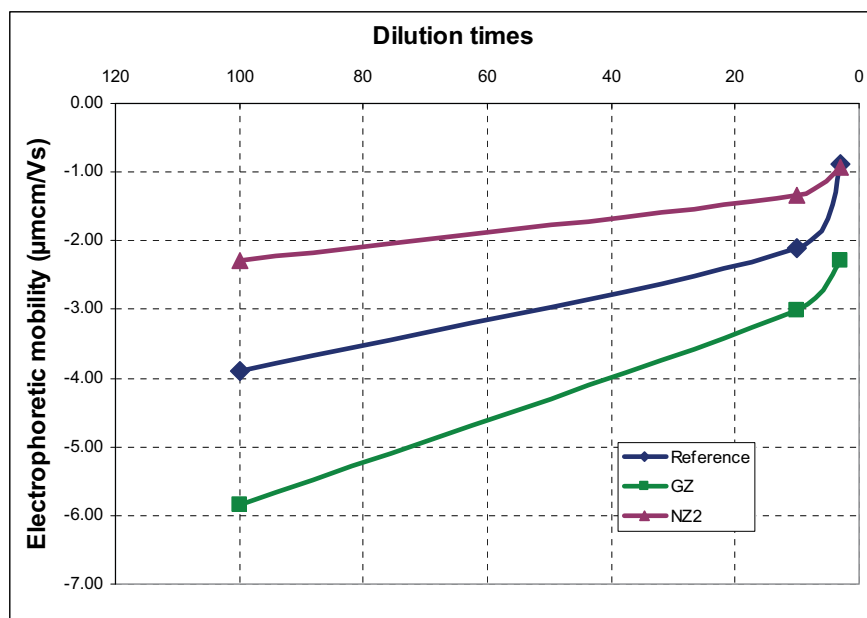


Figure 8.7: Electrophoretic as a function of dilution times of SSW.

The mobility of a charged colloid depends not only on its charge, but also on the salinity of the surrounding electrolyte solution: electrophoretic mobility is higher in low salinity solutions when the electrical double layer (see section 6.1) is expanded. However, in the case of diluted synthetic sea water, specific adsorption of divalent ions may also influence electrophoretic mobility. Further, specific interactions of divalent calcium and magnesium cations with ionizable species at the crude oil/water interface may also influence the mobility of dispersed crude oil droplets (Buckley 1996; Buckley and Fan, 2005).

8.3 Detection of changes in oil and water phase composition by enzyme action

In this section we report on tests performed to investigate possible changes in oil composition by enzymatic action, i.e. breakdown of the heavier components into smaller ones or partitioning of organic acids between oil and brine. The tests were performed by equilibrating oil (crude oil or mineral oil with added ester) and brine with enzyme added and then measuring changes in the oil and water phase compositions, respectively.

8.3.1 Gas chromatography

Sample preparation and experimental procedures are described in Appendix B. Initially, tests were performed with crude oil. Crude oil B which was equilibrated with different enzyme-brine solutions (GZ, NZ2 group and α -La) was examined in gas chromatograph to analyze different components of the crude and compositional changes resulting from enzyme-proteins action. However, due to the complexity of crude oil, compositional changes, if any, after exposure to brine solutions containing different enzymes could not be detected within the experimental limitations.

In the case of the pure mineral oil with added ester, however, comparison of compositional changes after equilibration with different enzymes were possible. Table 8.5 shows the amount of the different components in the mineral oil after equilibration with different enzyme solutions. As can be seen from the table (see also Figure 8.8), there is a significant change in the amount of ester detected in the mineral oil after equilibration with brines containing esterase enzymes (i.e. NZ2, NZ3 and NZ6). This is not surprising since esterase enzymes (NZ group) are known to catalyze the hydrolysis of ester bonds to form an acid and an alcohol, and consequently decrease the amount of ester in the oil. In the case of adding Greenzyme, the change in ester concentration is comparatively low. This indicates that Greenzyme is not dominantly involved in ester hydrolysis.

Table 8.5: Amount of different components in the model oil after equilibrated with the enzymes.

Component (%)	Reference	GZ	NZ2	NZ3	NZ6
i-C8	98.63	98.64	98.97	99.00	99.02
n-C10	0.90	0.97	0.98	0.88	0.84
Ester	0.47	0.39	0.05	0.11	0.14

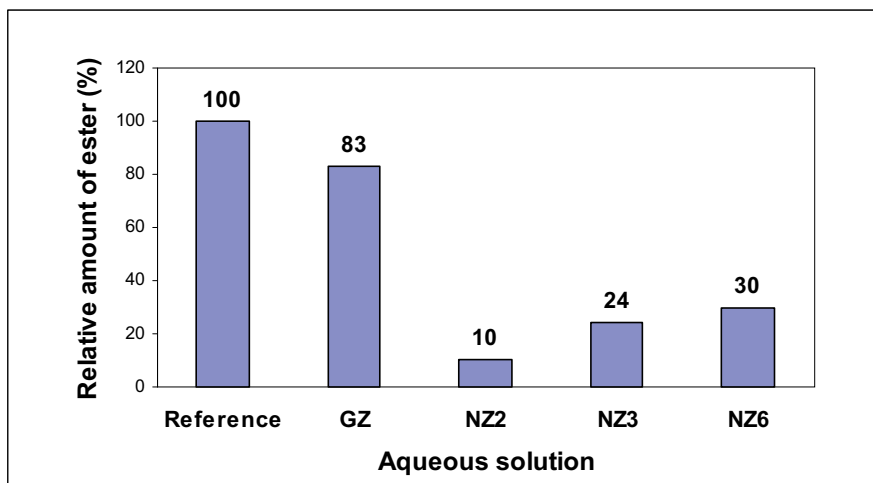


Figure 8.8: Relative amount of the ester to the reference case without adding any enzyme for model oil after equilibration with different enzyme-brine solutions.

8.3.2 Isotachophoresis (ITP) measurements

Brine with added different enzyme-proteins (GZ, NZ groups and α -La) were equilibrated with crude oil B and used in ITP apparatus to detect any compositional change resulting from enzyme-proteins action. Sample preparation and experimental procedure are described in Appendix B. Water phase analysis indeed, can determine the amount of any organic acids components which may result from enzymes-proteins activity when they were equilibrated with the oil. However, in our case testing the aqueous phase with ITP techniques were not conclusive with respect to its compositional changes.

Chapter 9 Core displacement experiments

In chapter 7 and 8 potential of enzymes to change the oil-water-solid and oil water properties was investigated. In chapter 7 it was found that adding enzymes to brine solution can change the adhesion behavior of the crude oil from adhesion to non-adhesion and further change the contact angle to a more water-wet behavior. It was found also that enzymes are more effective to change wettability at initial intermediate wettability. In chapter 8 it was found that effect of enzymes to change the oil-water properties are minor compare to their effect on oil-water-solid properties. Their contribution to change interfacial tension between oil and water is not significant while they affect electrophoretic mobility of emulsified oil in enzyme-brine solution to some extent.

The following chapter studies dynamic core displacements using sandstone and carbonate rocks to investigate the potential of improved oil recovery by enzyme and enzyme-surfactant. Most of the core flooding experiments commenced with water flooding at initial water saturation, S_{wi} , (established with synthetic sea water) which will be referred to as secondary mode displacements. Accordingly, tertiary oil recovery processes are assigned to injection of enzyme and/or enzyme-surfactant solutions initiated at the residual oil saturation, S_{or} , established by the secondary displacements. The core flooding conducted on various core of the same type to check the reproducibility of the experiments.

9.1 Effect of enzymes on oil recovery

Displacement tests using sandstone and carbonate cores were preformed to study the effect of enzymes on oil recovery. The preparation of the core samples prior to the experiments is

explained in Appendix B. The synthetic seawater brine and reservoir crude oil was used in the core flooding experiment as the aqueous and oleic phases, respectively. Different types of enzyme, Greenzyme and NZ2 which were found to have the largest effect on contact angle change (refer to chapter 8) were selected among available enzymes for displacement tests as secondary and tertiary modes to displace crude oil in the cores.

The results of the displacement experiments are divided in two main parts; sandstone and carbonate cores. Sandstone cores include four short and two long cores. Carbonate cores include five cores. Properties of the rocks, crude oils and brines are presented in Appendix A.

9.1.1 Sandstone cores

Four short (approximately 6 cm), B1-B4, and two long (approximately 30cm), LB1 and LB3, Berea sandstone cores were prepared to study the effect of enzyme solution on oil recovery in sandstone rocks. Table 9.1 shows all steps of flooding scenarios with brine and enzyme-brine for sandstone cores.

Table 9.1: Dynamic displacement scenarios for sandstone cores.

Core ID	Step1	Step 2	Step 3
B1	SSW flooding	1 wt% GZ flooding	---
B2	SSW flooding	1 wt% GZ flooding	1 wt% GZ flooding
B3	SP. Imbibition of SSW	SSW flooding	1 wt% GZ flooding
B4	SP. Imbibition of 1 wt% GZ	1 wt% GZ flooding	---
LB1	SSW flooding	1 wt% GZ flooding	5 wt% GZ flooding
LB3	SSW flooding	1 wt% NZ2 flooding	---

9.1.1.1 Brine Flooding Followed by Greenzyme-Brine Flooding, Cores B1 and B2

Brine injection into cores B1 and B2 was performed at an initial flow rate of 0.1 cc/min (nominal) followed by a 0.5 cc/min bump rate. For both cores, most of the oil was produced before WBT. However, more oil was produced after WBT from core B2 compared to core B1. This could be an indication of a less water-wet condition for core B2 as compared to core B1.

The initial waterflood was followed by flooding with brine containing 1wt% Greenzyme (GZ-brine). Different injection rates (0.1-0.7 cc/min) were examined in this flooding scenario. Oil production by enzyme-brine injection was continues independent of the injection rate and differential pressure was constant during designated injection rate. The resulting oil production profiles are shown in Figures 9.1-9.2 for core B1 and 9.3-9.4 for core B2. Table 9.2 summarizes the time to water breakthrough (WBT) waterflood (WF), Greenzyme (GZ) and total recovery in percent original oil in place (OOIP) and the number of pore volumes (PV) injected.

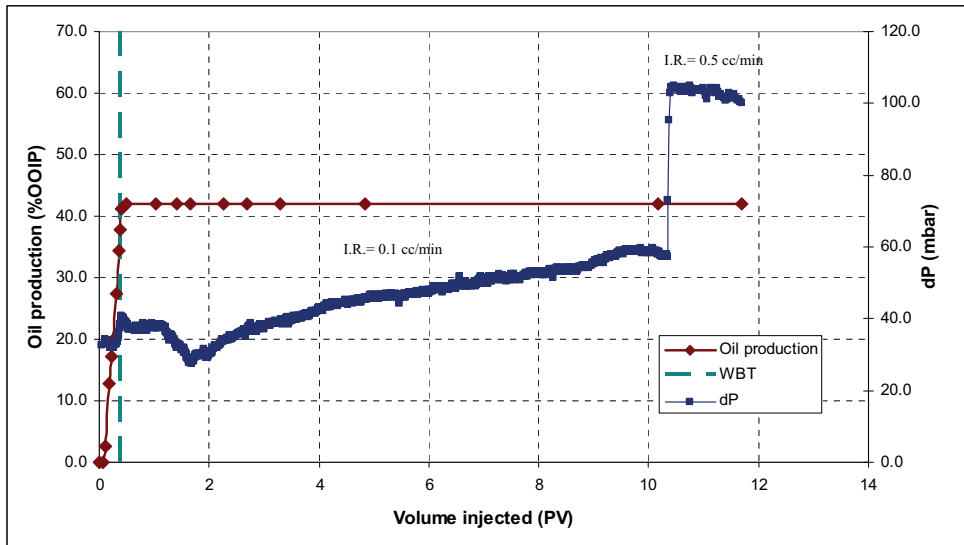


Figure 9.1: Oil production, differential pressure profiles and WBT time for water flooding core B1.

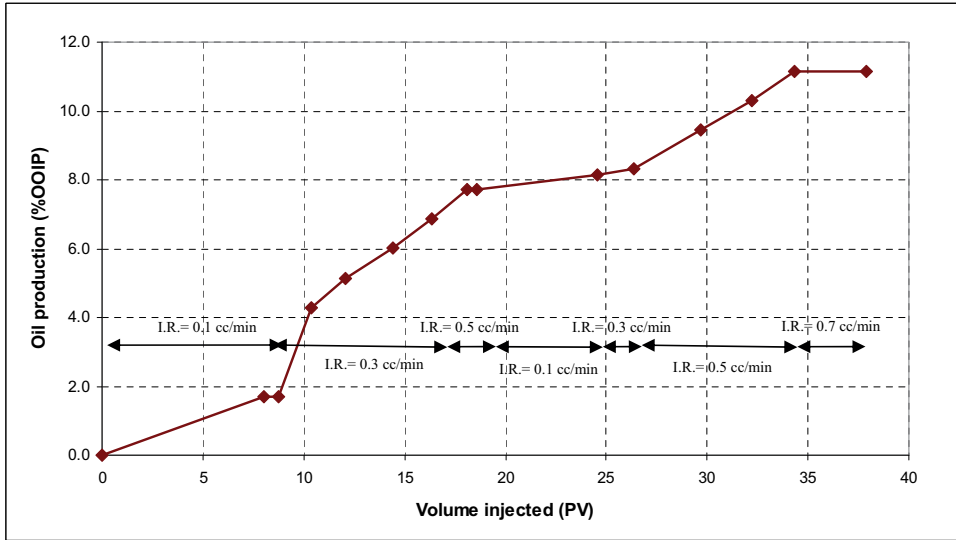


Figure 9.2: Oil production during different injection rates for 1wt% GZ flooding core B1.

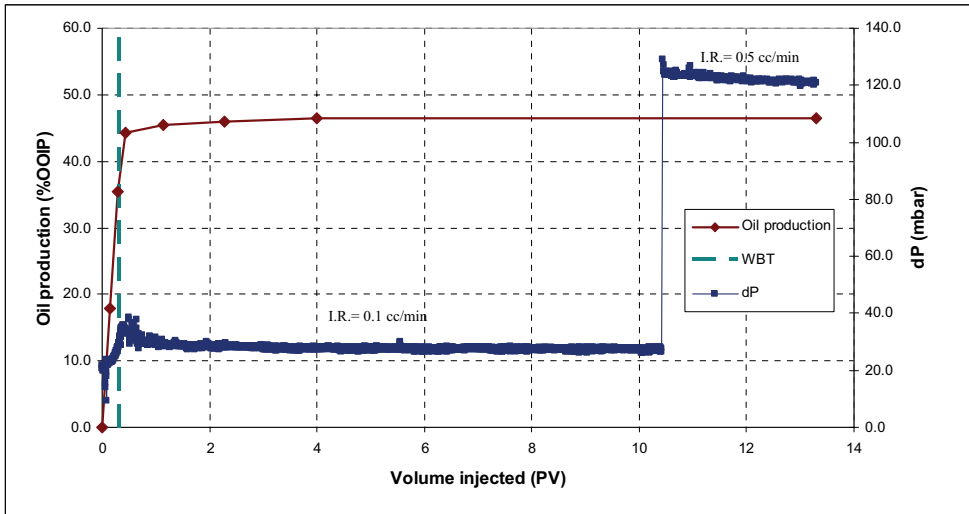


Figure 9.3: Oil production, differential pressure profiles and WBT time for water flooding core B2.

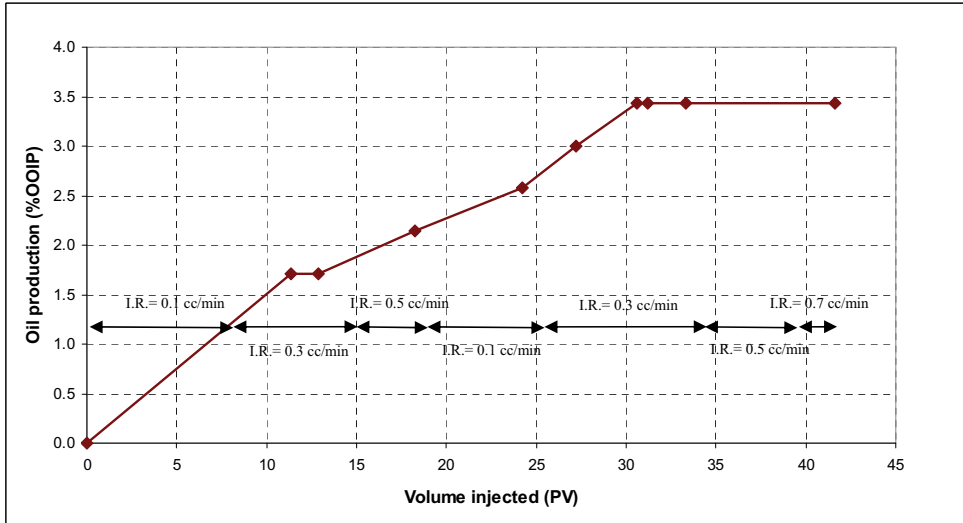


Figure 9.4: Oil production during different injection rates for 1wt% GZ flooding core B2.

Table 9.2: Summary of production data for cores B1 and B2.

Core ID	B1	B2
WBT (PV)	0.37	0.33
WF recovery (% OOIP)	42	47
PV injected	12	13
GZ recovery (% OOIP)	11	4
PV injected	34	32
Total oil recovery (% OOIP)	54	51

9.1.1.2 Spontaneous Imbibition and Flooding Scenario, Cores B3 and B4

Figure 9.5 shows the results of spontaneous imbibition of brine and GZ-brine into cores B3 and B4 vs dimensionless time, t_D . This scaling group was introduced by Ma et al. (1997) to obtain a dimensionless time, t_D , which compensates for differences in rock and fluid properties:

$$t_D = t \sqrt{\frac{k}{\phi}} \frac{\sigma}{\sqrt{\mu_w \mu_o}} \frac{1}{L_C^2} \quad (9.1)$$

Where t is imbibition time, k permeability, Φ porosity, σ interfacial tension, μ_w and μ_o viscosity to water and oil, respectively, and L_C is the characteristic length (all quantities in consistent units).

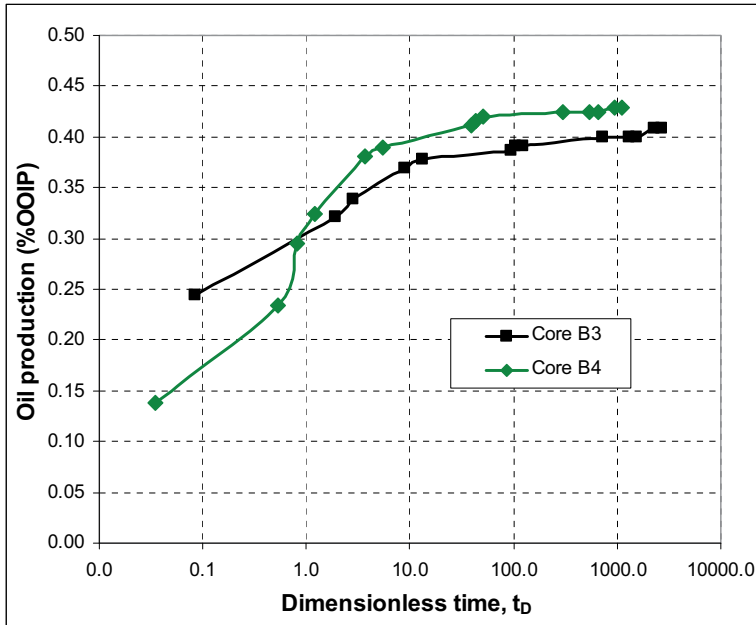


Figure 9.5: Oil production by imbibition vs dimensionless time cores B3 and B4.

In the early stages of oil production by spontaneous imbibition of brine and GZ-brine into the cores, the production rate in core B3 is larger than in core B4. Consequently, after the first minute, oil recovery in core B3 is about 24% OOIP compared to 14% OOIP in core B4. This delay in oil production could be related to Greenzyme reaction time. The figure shows larger total oil production by spontaneous imbibition of GZ-brine in core B4 (43 % OOIP) compared to core B3 (41% OOIP). However the oil recovery difference is 2 % OOIP which is not significant.

Cores B3 and B4 were flooded using different slugs of brine and GZ-brine after spontaneous imbibition. Core B3 was continuously flooded with different injection rates (0.1-1 cc/min) by brine but, no further oil production was attained. The initial waterflood was followed by flooding with brine containing 1wt% Greenzyme (GZ-brine) with different injection rates (0.1-0.5 cc/min) for core B3. Continuous injection of GZ-brine was also applied for core B4 after spontaneous imbibition using different rates of injection (0.1-0.5 cc/min). The resulting

oil production profiles are shown in Figure 9.6. As the figure shows, unlike the core B1 and B2, with the first nominal injection rate (0.1 cc/min) no further oil production was observed, but increase in the rate of injection (0.3-0.5 cc/min) resulted in additional oil production. Table 9.3 summarizes recovery by spontaneous imbibition (SP. Imb.), waterflood (WF), Greenzyme (GZ) and total recovery in percent original oil in place (OOIP) and the number of pore volumes (PV) injected.

Table 9.3: Summary of production data for cores B3 and B4.

Core ID	B3	B4
Recovery by SP. Imb. (%OOIP)	41	43
WF recovery (% OOIP)	0	---
PV injected	15	---
GZ recovery (% OOIP)	5.2	5.2
PV injected	26	35
Total oil recovery (% OOIP)	46.2	48.2

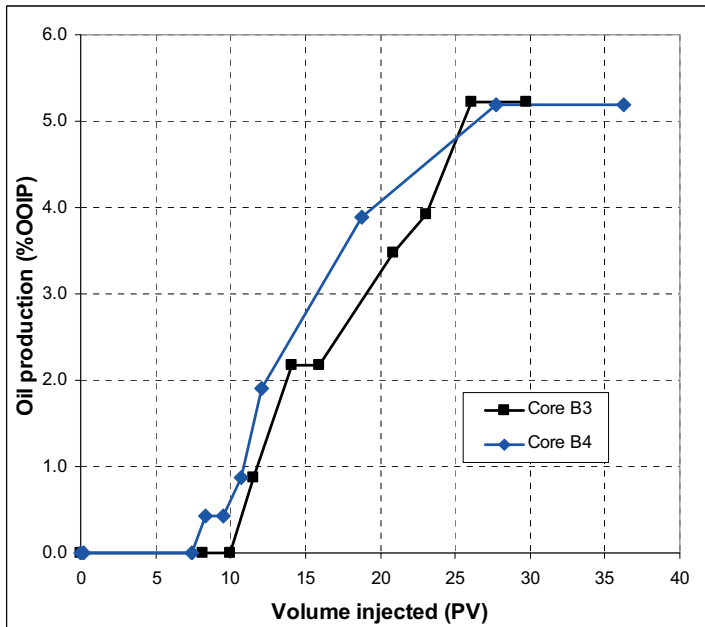


Figure 9.6: Production profile for GZ-brine flooding cores B3 and B4.

9.1.1.3 Brine Flooding Followed by Enzyme-Brine Flooding, Cores LB1 and LB3

Brine was continuously injected into core LB1 and LB3 at a nominal initial injection rate of 0.1 cc/min followed by bump rates of 0.3-1 cc/min. Although most of the oil was produced before water break through (WBT) for both cores, both cores showed significant two-phase production after WBT (see Figures 9.7 and 9.8). Extensive two-phase production after WBT (about 20% OOIP) could be an indication of wettability alteration toward less water-wet behavior as a result of aging in elevated temperature. Compared to the short Berea cores, which showed no oil production after WBT, this could be an indication of a less water-wet condition for cores LB1 and LB3.

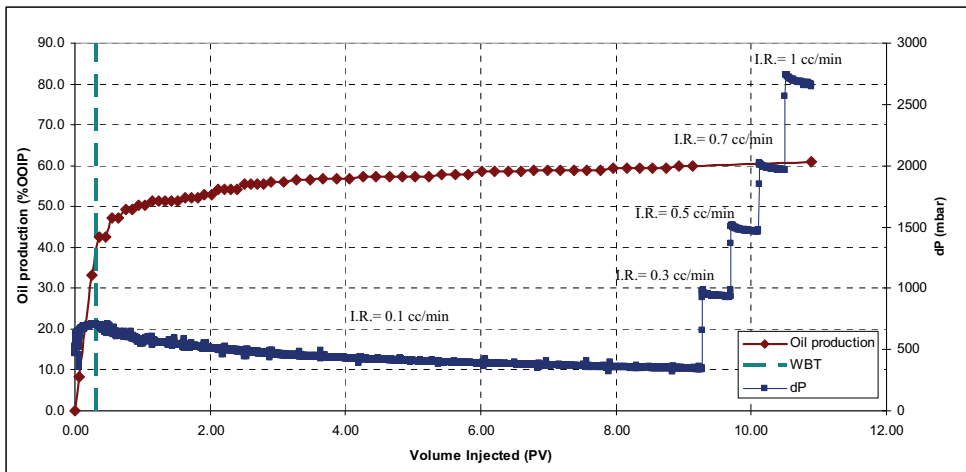


Figure 9.7: Oil production, differential pressure profiles and WBT time for water flooding core LB1.

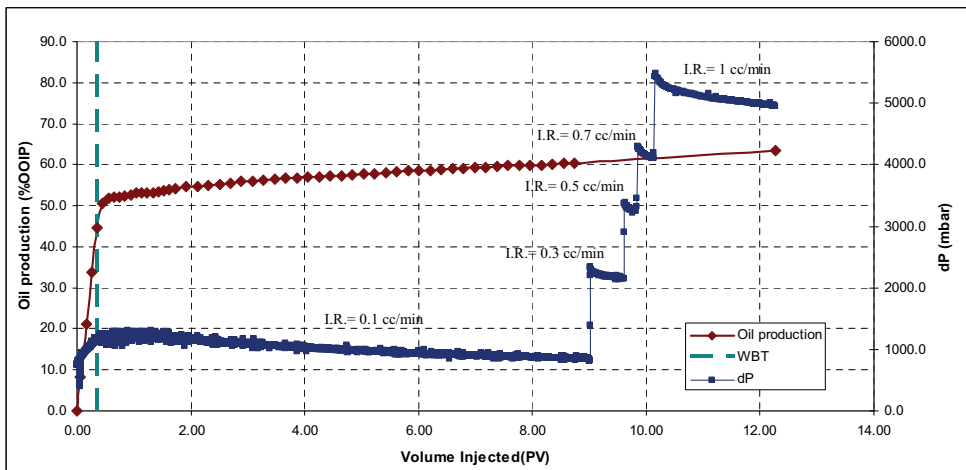


Figure 9.8: Oil production, differential pressure profiles and WBT time for water flooding core LB3.

For core LB1, initial brine flooding was followed by flooding with brine containing 1wt% Greenzyme (GZ-brine). To test the effect of high GZ concentration, this was followed by injection of 5wt% GZ-brine with different injection rates (0.1-1 cc/min). Core LB3, however, was injected with 1%wt NZ2-brine (with injection rates 0.1-1 cc/min), to compare the oil recovery potentials of the two enzymes. GZ injection (1 and 5 wt% concentration) into core LB1 recovered approximately 3.5% OOIP incremental oil, while NZ2 injection into core LB3 gave 3% OOIP incremental oil. Table 9.4 summarizes the time to water breakthrough (WBT), waterflood, enzyme and total recovery in %OOIP and the number of pore volumes injected.

Table 9.4: Summary of production data for cores LB1 and LB3.

Core ID	LB1	LB3
WBT (PV)	0.32	0.35
WF recovery (% OOIP)	61	66
PV injected	10	12
Enzyme recovery (% OOIP)	3.4	3
PV injected	30	13
Total oil Recovery (% OOIP)	64.4	69

The oil recovery after water flooding seems fall in two groups, one for LB1 and LB3 and one for B1 and B2. There are several factors that may contribute to this. LB1 and LB3 are from a more low permeable Berea material ($K_w \sim 150$ mD) than B1 and B2 ($K_w \sim 650$ mD). This is likely due to higher clay content for the low permeable Berea material, which in turn may affect its interactions with crude oil and brine. An indication of this is that LB1 and LB3 has less water-wet oil production profiles than B1 and B2 (see discussion in section 5.4 including Fig. 5.4 and 5.5). Less water-wet conditions are often associated with higher oil recoveries (see for example Morrow, 1990; Jadhunandan and Morrow, 1991; Skauge and Ottesen, 2002). Further, even though, bump rates were applied after initial injection rate in all cores, capillary end effects may contribute to lower recovery from the short core plugs (B1 and B2) compared to recovery from long cores. However, this is probably a minor effect.

9.1.2 Carbonate cores

Five carbonate cores from different fields in Middle East were used to examine the effect of enzyme on oil production after water flooding step. Table 9.5 shows all steps of flooding scenarios with brine and enzyme-brine for carbonate cores.

Table 9.5: Dynamic displacement scenarios for carbonate cores.

Core ID	Step1	Step 2	Step 3
S-889	Measuring I_{a-h}	SSW flooding	1 wt% GZ flooding
Th1	1 wt% GZ flooding	---	---
Th2	SSW flooding	1 wt% GZ flooding	---
Th3	SP. Imbibition of 1 & 10 wt% NZ2 @ room temperature and 40°C	SSW flooding	1 wt% NZ2 flooding
Th4	SP. Imbibition of brine @ room temperature and 40°C	SSW flooding	1 wt% NZ2 flooding

9.1.2.1 Brine Flooding Followed by GZ-Brine Flooding, Core S-889

Amott-Harvey wettability index, I_{a-h} was used to characterize wettability state of the carbonate core (Morrow, 1990). This method combines natural imbibition and forced displacement to measure the average wettability of the core. For detailed description of the method refer to Chapter 5. The difference between I_w and I_o ($I_w - I_o$) is called I_{a-h} . This index for the core is about 0.2. According to the classification made by Morrow (1990) this core is intermediate-wet. After characterizing of the wettability, core S-889 which was saturated with crude oil A was continuously injected by brine at S_{wi} condition. The nominal rate of injection was 0.1 cc/min and continued by 0.15 and 0.2 cc/min as the bump rates. About 17 PV was injected into the core. Total oil production of 48% OOIP was attained by brine injection (see Figure 9.9). There was a delay between start of brine injection and oil production which was about 2 PV injections. The reason of this delay could be the low permeability of the rock. The injection water needs enough pressure to overcome the resistance forces and push the oil out of the core. Water break through (WBT) was happened after 2.35 PV. Unlike the short sandstone core plugs, most of the oil (more than 25% OOIP) was produced after WBT.

Combined with the measured Amott-Harvey wettability index, this indicates an intermediate wet core. The core was injected by brine containing 1wt% Greenzyme (GZ-brine) after brine flooding. Very low rate of oil production was observed after starting the GZ-brine injection. 6 % OOIP incremental oil were produced after more than 15 PV injections. Table 9.6 summarizes the waterflood, enzyme and total recovery in %OOIP and the number of pore volumes injected.

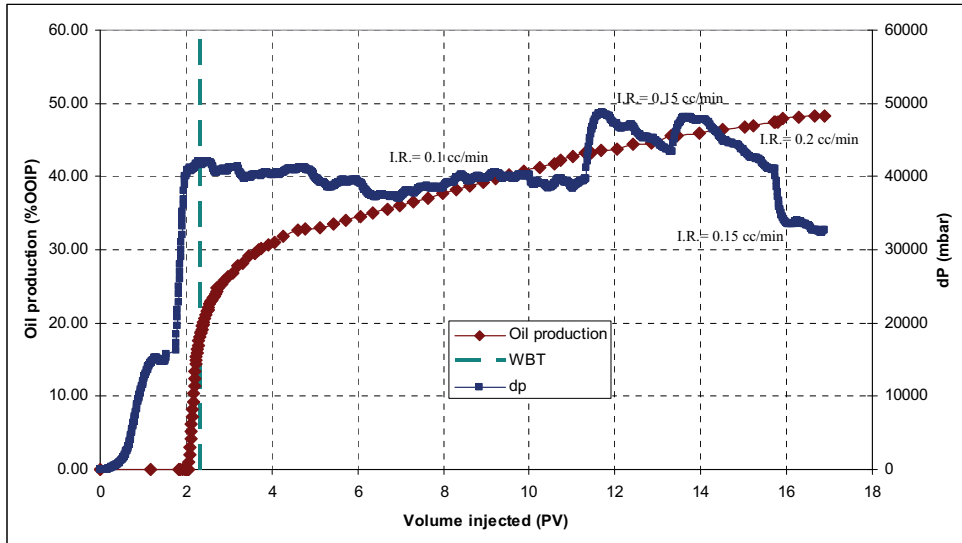


Figure 9.9: Oil production, differential pressure profiles and WBT time for water flooding core S-889.

Table 9.6: Summary of production data for core S-889.

Core ID	S-889
WBT (PV)	2.35
WF recovery (% OOIP)	48
PV injected	17
Enzyme recovery (% OOIP)	6
PV injected	15
Total oil Recovery (% OOIP)	54

9.1.2.2 Brine Flooding Followed by Enzyme-Brine Flooding. Cores Th1-Th4

Reservoir crude oil was used in the experiments, and the brine used in the experiments was prepared in the lab according to the salt concentrations of original formation brine. Properties

of the rocks, crude oil and formation brine are presented in Appendix A. The initial rate of brine injection was 0.1 cc/min for all cores. After oil production stopped the rate was increased in stepwise manner up to 1 cc/min (bump rates) to ensure that there is no more producible oil by brine flooding. Thereafter enzyme-brine was injected to the cores with different injection rates (0.1-1 cc/min) to see the effect of enzymes on oil recovery.

Core Th1 was injected by 1%wt GZ-brine without any prior injection of brine. Core Th2 was flooded first by brine and injection scenario was followed by 1wt% GZ-brine. Cores Th3 and 4 were used to test the effect of enzyme on spontaneous imbibition of enzyme-brine. Core Th3 and Th4 surrounded by 1wt% GZ-brine and brine (as the reference), respectively. Since there was no oil production after 7 days by spontaneous imbibition of 1wt% enzyme-brine, the concentration of enzyme increased to 10wt%. The test was done in room temperature (7days) and elevated temperature to 40°C (7 days). There was no oil produced in both cases, with and without enzymes. This can be a qualitative indication of the wettability conditions of the cores: since there was no oil production by spontaneous imbibition, it can be inferred that the cores were in non water-wet condition.

Table 9.7 summarizes the waterflood, enzyme and total recovery in %OOIP and the number of pore volumes injected. According to the results, adding enzymes to the injected brine can lead to more oil production from 1 to more than 7 %OOIP. The results show almost the same amount of incremental oil production for both types of enzymes, GZ and NZ2.

Table 9.7: Summary of production data for cores Th1-Th4.

Core ID	Th1	Th2	Th3	Th4
WF recovery (% OOIP)	---	80.7	66.7	64.2
PV injected	---	34	14	12
Enzyme recovery (% OOIP)	82.3	7.2	1	7.3
PV injected	32	31	13	10
Total oil recovery (% OOIP)	82.3	87.9	67.7	71.5

9.1.3 Proposed mechanism for enhanced oil recovery by enzymes

According to the results of the core flooding experiments, by injecting enzyme-brine solution into the cores after water flooding step, some incremental oil was produced. Important factors

to consider in relation to enhanced oil recovery processes are, viscosity of the displaced and displacing fluids and relation between those (mobility ratio); interfacial tension between displaced and displacing fluids; and wettability of the porous media. According to the results reported in chapter 8, adding Greenzyme to the water decrease the interfacial tension between the oil and water to some extent. But the increase in interfacial tension can not be the dominant mechanism underlying the more oil recovery from the cores. The reason could be described by considering the capillary desaturation curve which was explained in detail in chapter 2. In section 9.3 also the capillary number regarding to brine and enzyme-brine flooding are calculated. According to the result, calculated capillary number is far behind the N_{CC} (around 5×10^{-4}) reported in the literature (Mohanty and Salter, 1983; Garnes et al., 1990) for the same type of rock. To shift the curve toward less residual oil area, capillary number needs to increase by several times in order of ten. So, decreasing of the IFT by only 3-4 times can not be enough to shift the CDC. This fact is also true for changing viscosity by adding enzymes into the brine solution. Viscosity of the untreated brine is about 1.1 mPa·s. According to measurements adding enzyme into the brine solution had almost no effect on viscosity and was observed to be Newtonian even in the case of adding 10 wt%. Therefore the only factor which can be the dominant parameter to increase oil recovery is changing rock wettability toward more water-wet condition. Wettability alteration by use of different method which result in enhancement of oil recovery reported in both sandstone and carbonate rocks (e.g. Austad et al., 1998; Austad and Standnes, 2003; Zhang et al., 2006). In general, wettability of sandstone rocks is a result of electrostatic interactions at oil-water-solid interfaces and disjoining pressure plays an important role in this matter (refer to chapter 6). However in carbonate rocks wettability of the rock is a result of chemisorption type of reaction at the oil-solid interface (Buckley, 1996). The change in wettability by enzyme-proteins toward more water-wet condition by measuring contact angle on silica glass surface that can be the representative of sandstone rocks is well documented in chapter 7. However, no attempts at investigating mechanisms have been made in the case of carbonate surfaces. The contact angle results indicate that the intermediate wetting condition is the best condition for enzyme-protein effectiveness on silica surfaces. Observations by Feng et al. (2007) also confirm the wettability change toward more water-wetness by enzymes. They stated that enzymes can change wettability of reservoir rock from oil to water-wetness, reducing interfacial tension and reduce the flow resistance through a porous medium. Figure 9.10 shows a photo taken by Feng et al. (2007), where the enzyme changes the rock wettability to more water-wet status.

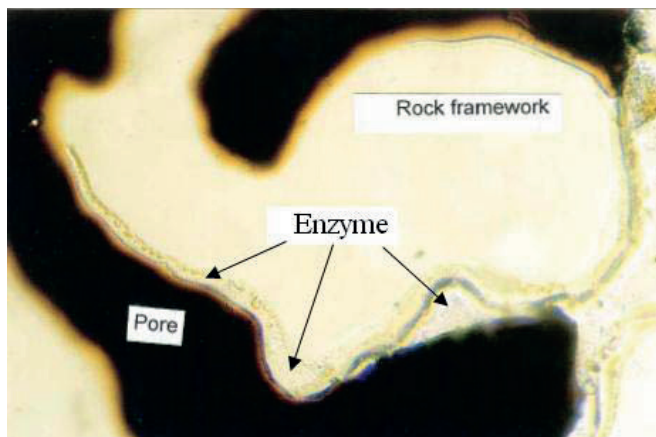


Figure 9.10: Enzymes that moves forward along the pore channels and change the oil-wet sections to water-wet (Feng et al., 2007).

According to coreflooding results, using enzyme-proteins may alter wettability of both rock types, sandstone and carbonate and consequently lead to more oil recovery while the other reported techniques may work either in carbonate or sandstone rocks. This characteristic of enzymes makes them unique and special between all methods which have been proposed in order to increase oil recovery. Among other methods we can point out to low salinity water flooding. In the past decade, there is a strong interest in use of this technique to enhanced oil recovery. Several researchers reported using this technique and proposed different underlying mechanisms for it (e.g. Morrow, 1990; Tang and Morrow, 1997; Filoco and Sharma, 1998; Lager et al., 2006; Agbalaka et al., 2009). One of the reported mechanisms is wettability alteration toward more water-wet condition by lowering salinity relative to the content in formation water. All the reported results are in sandstone rocks and unlike the enzymes; it seems that this technique can not have beneficial impact on oil recovery in carbonate rocks.

9.2 Combined enzyme-surfactant injection

As already discussed in the literature review in chapter 3, enzymes and surfactants can be used together in the solution to improve performance of each other. Enzyme can improve the performance of the surfactant and as a catalyst, decrease the reaction time of the surfactant in the solution and also may increase solubility of the surfactant. Surfactant in return can improve stability of the enzymes in terms of tolerate higher temperature, enabling reactions to occur at higher temperature (Savelli et al., 2000; Paul and Moulik, 2001; Jurado et al. 2007).

This may indeed be the rationale behind adding surfactants as stabilizers in the commercial EOR enzyme, Greenzyme.

Another possibility is to consider enzyme and surfactant as two distinct methods of obtaining increased oil recovery which may, when combined, provide added benefit of either of the two applied alone. As an example of this, Alagic and Skauge (2010) combined low salinity brine injection and with surfactant flooding. The surfactant system used produced low (10^{-2} mN/m), but not ultralow (10^{-3} - 10^{-4} mN/m) interfacial tensions. While lowering the injection brine salinity probably leads to destabilisation of oil layers and their subsequent release from mineral surfaces, this oil is probably easily re-tapped in a high capillarity environment. However, when this process occurs in an environment where capillary forces that tend to trap oil are weak, this oil is likely to stay mobile instead of becoming re-trapped. The combined effect of low salinity and surfactant is thus to recover additional oil by two distinctly different mechanisms, with low capillary forces facilitating oil bank formation and propagation.

To investigate the benefit of both enzymes and surfactants, combination of sea water, surfactant and enzyme were examined on long Berea sandstone cores in the lab and compared with the results of surfactant flooding without added enzyme. Table 9.8 shows the flooding sequence of the cores. Surfactant and co-solvent were selected according to their contribution in IFT reduction. Section 8.1.4 is described the selection of surfactant and co-solvent used in displacement experiment.

Table 9.8: Dynamic displacement scenarios for sandstone cores, LB1, LB2 and LB3.

Core ID	Step1	Step 2	Step 3	Step 4	Step5
LB1	SSW flooding	1 wt% GZ flooding	5 wt% GZ flooding	5wt% GZ + 1wt% Surf. flooding	1 wt% Surf. flooding
LB2	SSW flooding	1 wt% Surf. flooding	---	---	---
LB3	SSW flooding	1 wt% NZ2 flooding	5wt% NZ2 + 1wt% Surf. flooding	---	---

9.2.1 Enzyme-Surfactant-Brine Flooding, Core LB1 and LB3

After 5wt% enzyme-brine flooding for core LB1, surfactant (1 wt%) and co-solvent (1 wt%) was added to enzyme-brine solution and was injected by different nominal rate of 0.1-1 cc/min into the core to see the effect of the combined solution on the oil recovery. Although more oil production was expected from the core by hybrid process, 1.5% OOIP incremental oil recovery was produced after about 15 PV injections. The reason could be the increasing of the IFT after adding enzyme into the solution. IFT between brine and crude oil B showed the value of 0.005 mN/m after adding 1wt% concentration of surfactant and co-solvent. Adding GZ concentration into the solution increased the IFT. The IFT value was 0.026 mN/m for 5wt% GZ-surfactant solution (see Table 8.3). Capillary number seems to be not enough to reach to its critical point by this IFT and cause oil to be produced from the core (see Table 9.11). To investigate the effect of the surfactant itself on the oil recovery, the core was flushed by brine for about 4 PV and then injected by surfactant and co-solvent solution at 1wt% concentration. No oil was produced after more than 8 PV injection with different rates of injection (0.1-1 cc/min). It showed that even by surfactant solution without added enzyme the capillary number was not enough to expel the oil from the core.

For core LB3, combination of NZ2 enzyme (1 wt%), surfactant (1 wt%) and co-solvent (1 wt%) was examined. The solution was injected with different rates of injection (0.1-1 cc/min) into the core after 1wt% enzyme-brine injection. Incremental oil recovery of 4% OOIP was the result of this flooding. According to the result of IFT measurements (see Table 8.3) adding NZ2 enzyme into the surfactant solution did not affect significantly the IFT between brine and crude oil. The IFT in both cases with and without added enzyme were almost the same, 0.005 mN/m. It could be the reason that adding NZ2 into surfactant solution resulted in more incremental oil recovery than GZ.

Table 9.9 summarizes the time to water breakthrough (WBT), waterflood, enzyme, surfactant-enzyme and total recovery in %OOIP and the number of pore volumes injected.

Table 9.9: Summary of production data for cores LB1 and LB3.

Core ID	LB1	LB3
WF recovery (% OOIP)	61	66
PV injected	10	12
Enzyme recovery (% OOIP)	3.4	3
PV injected	30	13
Enzyme-surfactant recovery (% OOIP)	1.5	4
PV injected	15	13
Total oil Recovery (% OOIP)	65.9	73

9.2.2 Surfactant-Brine Flooding, Core LB2

Results of the enzyme-surfactant injection in cores LB1 and LB3 did not result in significant oil production. Adding enzyme to the surfactant solution may prevent the oil to be produced from the core. This idea could be true in case of adding Greenzyme into the surfactant solution, because, it increased the IFT between crude oil and brine. In case of adding NZ2 enzyme, IFT did not change significantly but oil production did not increase as was expected. To clarify this situation core LB2 was selected and used as the reference case to inject surfactant solution without adding enzyme and compare with the cases, LB1 and LB3 when enzyme-surfactant-brine solution was used as the injection solution.

Brine was continuously injected into core LB2. The nominal initial injection rate was 0.1 cc/min and it was followed by 0.3-1 cc/min as the bump rates. 62.2 % OOIP total oil recovery was produced after about 14 PV injections (see Figure 9.11). Water breakthrough (WBT) happened after injection of 0.28 PV. 20% OOIP was produced after WBT which is significant amount of production.

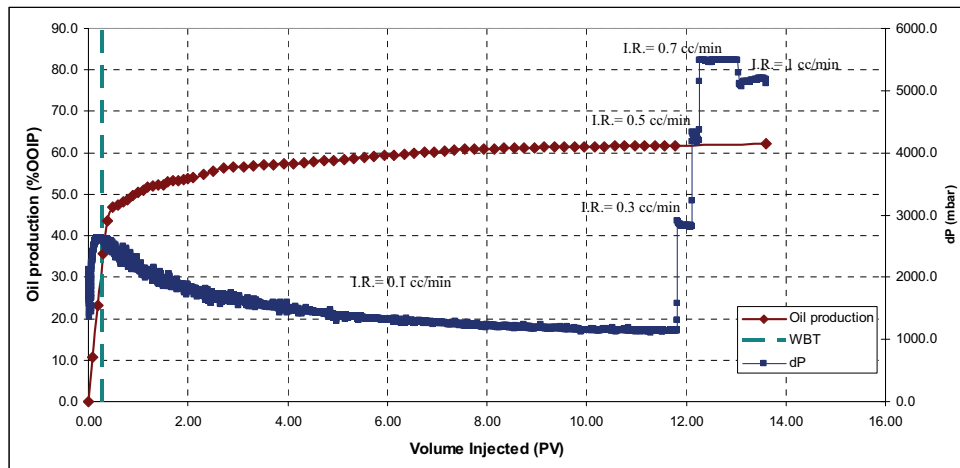


Figure 9.11: Oil production, differential pressure profiles and WBT time for water flooding core LB2.

The flooding scenario was followed by injecting of surfactant and co-solvent at 1wt% concentration into the core. By nominal injection rate of 0.1 cc/min only 1% OOIP was produced from the core after more than 2 PV injections. To increase the order of capillary number to its critical value and expelling the oil out of the core, injection rate was increased by 5 and 10 times respectively. After increasing of the injection rate from 0.1 to 0.5 cc/min, oil started to produce and residual oil saturation began to decrease but, the oil production was too slow. 1% OOIP incremental oil was the result of this flooding. Increasing the injection rate to 1cc/min caused the crude oil to be expelled from the core by a good production rate. 15.8% OOIP incremental oil was produced after less than 3 PV injection of the surfactant solution. Table 9.10 summarizes the time to water breakthrough (WBT), waterflood, enzyme, surfactant-enzyme and total recovery in %OOIP and the number of pore volumes injected.

Table 9.10: Summary of production data for cores LB2.

Core ID	LB2
WBT (PV)	0.28
WF recovery (% OOIP)	62.2
PV injected	14
Surfactant recovery (% OOIP)	15.8
PV injected	3
Total oil Recovery (% OOIP)	78

9.3 Capillary number analysis

Capillary numbers for all flooding scenarios in cores LB1, LB2 and LB3 were calculated using equation 2.6 based on IFT reported in Tables 8.2 and 8.3. Table 9.11 summarizes capillary numbers (N_C) for the different modes of oil recovery when enzyme, surfactant or combination of both was added to injection water. Capillary numbers were analyzed to get the critical value when oil is starting to produce by enhanced oil recovery processes.

Table 9.11: Calculated capillary numbers (for injection rate of 1 cc/min) and corresponding S_{or} (fraction OOIP) for aged Berea cores, LB1, LB2 and LB3.

Core ID	LB1	LB2	LB3
N_C , Brine flooding / S_{or}	7.73E-06 / 0.39	8.04E-06 / 0.38	7.70E-06 / 0.34
N_C , Enzyme flooding / S_{or}	1.70E-05 / 0.36	---	7.70E-06 / 0.31
N_C , Surfactant flooding / S_{or}	---	1.77E-02 / 0.20	---
N_C , Enzyme-surfactant flooding / S_{or}	3.27E-03 / 0.34	---	1.57E-02 / 0.27

Figure 9.12 depicts the capillary number versus residual oil saturation. This curve is known as CDC curve which was described in Chapters 2 and 5 in detail. CDC curve for aged Berea cores (see Figure 9.12) shows that the critical capillary number (N_{CC}) for the cores is estimated to be about $7 \cdot 10^{-4} \pm 2 \cdot 10^{-4}$. This number is in agreement with the value reported by other researchers (Mohanty and Salter, 1983; Garnes et al., 1990) for the same rock type (refer to chapter 5). At this point the slope of the curve changes and residual oil saturation begins to decrease. Slope of the curve after N_{CC} shows the decreasing trend of residual oil saturation, the steeper the slope, the easier mobilization of the trapped oil. In core LB2, N_{CC} achieved by low injection rate (0.1 cc/min) of surfactant flooding, but the decreasing trend of residual oil was slow. Further increasing of injection rate to 0.5 and 1 cc/min which in fact strengthens viscous forces increased the decreasing trend of the CDC curve after N_{CC} and caused mobilization of the trapped oil inside the porous media.

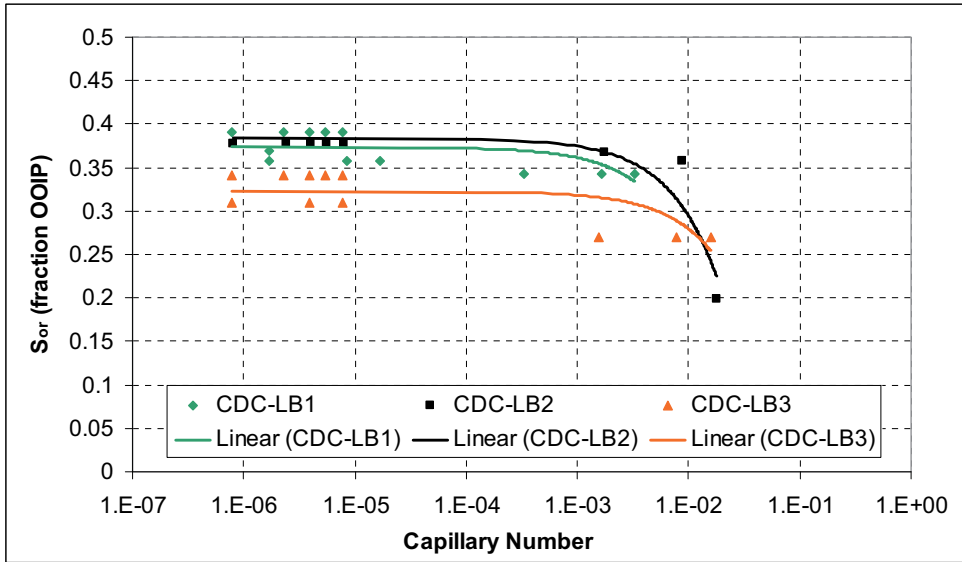


Figure 9.12: Capillary desaturation curve (CDC) cores LB1, LB2 and LB3.

For cores LB1 and LB3 (see Figure 9.12), low (0.1 cc/min) and high (1 cc/min) injection rates of enzyme-surfactant solutions, respectively, resulted in $N_C > N_{CC}$. As a result the slope of the S_{or} vs N_C curves began to decrease, especially for core LB3 where NZ2 enzyme was added to the injected solutions. Higher capillary numbers were reached during injection at 1 cc/min of surfactant or enzyme-surfactant solutions in cores LB2 and LB3, respectively, compared to enzyme-surfactant flooding of core LB1 at the same rate. The reason is that, unlike NZ2 which was used for core LB3, GZ appears to have a negative effect on the interfacial tension (see section 8.1.5) during enzyme-surfactant injection in core LB1. However, although the same capillary number was applied in core LB2 and LB3, significantly lower S_{or} was obtained for core LB2. A possible reason could be the configuration of the remaining oil after enzyme flooding which is different than that after waterflooding due to wettability changes induced by the enzymes. This phenomenon will be discussed in more detail in chapter 10.

9.4 Wettability and water end point permeability

Comparison of brine end point permeability can be used as an indication of wettability. More water-wet behavior shows lower water end point permeability at the same water saturation, S_w . Table 9.12 shows water endpoint permeabilities at residual oil saturations representative of the different stages of the flooding, i.e. after waterflooding (S_{or1}) and flooding with

different concentrations of enzyme-brine solution (S_{or2} and S_{or3}). Comparison of the endpoints before and after 1wt% enzyme-brine flooding shows no significant wettability change for cores B1, B2, B3, LB1 and LB3.

Table 9.12: End point permeabilities and S_{or} for different stages of the sandstone cores.

Core ID	Abs. K_w (mD)	Waterflood			1wt% enzyme injection		> 1wt% enzyme injection	
		S_{or1}	K_w at S_{or1} (mD)	K_{rw} at S_{or1} (mD)	S_{or2}	K_w at S_{or2} (mD)	S_{or3}	K_w at S_{or3} (mD)
B1	621	47.7	43	0.07	38.5	67	---	---
B2	632	43.8	51	0.08	41.0	60	41.0	29
B3	576	50.7	42	0.07	46.2	52	---	---
B4	619	---	---	---	43.3	38	---	---
LB1	140	30.3	19	0.14	29.0	23	27.7	13
LB2	89	28.8	7	0.08	---	---	---	---
LB3	138	25.9	10	0.07	24.0	14	---	---

Core B4 which was not exposed to the untreated brine in all stages shows lower end point permeability than other cores with respect to related S_{or} which is almost in the same range of others. Core B2 showed lower end point permeability (29 mD) after 10wt% enzyme-brine flooding compared to after flooding with 1wt% enzyme-brine (60 mD), even though no additional oil was produced. Decrease in the water endpoint permeability in the case of 10wt% enzyme-brine flooding without any change in saturation unit of residual oil may indicate that the core was becoming more water-wet. Core LB1 also showed almost the same behavior as core B2 when the concentration of the enzyme increased in the solution to 5 wt%. The end point permeability decreased from 23 to 13 mD by increasing the enzyme concentration from 1 to 5wt% where the residual oil saturation has decreased more than one unit. It should be pointed out that although the cores were aged in elevated temperature, according to their endpoint relative permeability after waterflood, they show water-wet behavior. In general, endpoint relative permeability (K_{rw}) < 0.1 is characteristic of water-wet system that is true for all cores except core LB1 which is slightly less water-wet ($K_{rw} = 0.14$). However, LB1, LB2, and LB3 cores had a large two phase production after water breakthrough which indicates less water-wet condition in the cores and it is in contrary of the relative permeability results.

Chapter 10 Micromodel experiments

In Chapter 7 we showed that adding enzymes to the brine phase gave a significant decrease in contact angle for Greenzyme and the three different esterase enzymes tested. However, only Greenzyme was found to have an effect on oil-water interfacial tension, which was reduced by a factor of approximately 3 when Greenzyme was added (see Chapter 8). Flooding aged Berea sandstone cores, waterflooded to residual oil saturation, with Greenzyme added to the water phase gave an additional recovery of between 3 and 11 % OOIP. One experiment performed with one of the esterase enzymes also showed a reduction in residual oil in the same area as that observed for Greenzyme.

From a capillary desaturation point of view, the reduction in interfacial tension obtained by adding Greenzyme is not sufficient to induce mobilization of residual oil. Further, a reduction in residual oil saturation was found after flooding with one of the esterase enzymes, which did not affect the oil-water interfacial tension. Based on these observations, we expect wettability changes to be the main factor contributing to mobilization of oil remaining after regular waterflood. To explore this hypothesis further, micromodel experiments were undertaken.

10.1 Glass micromodels

Glass micromodels are two-dimensional models of pore system which can be made in glass by use of a photo-imaging technique followed by chemical etching of the glass (McKellar and Wardlaw, 1982). Such models are useful to study fluid flow behavior within pore spaces and observe the effects of pore and fluid variables on the trapping and subsequent mobilization of residual phases during simulated secondary and tertiary recovery processes. Glass micromodels have proven to be very useful for studying variety of oil recovery processes such as water and gas flooding, miscible and immiscible displacements, surfactant floods, foam

injection, microbial EOR and solution gas drive (Danesh et al., 1987; Nguyen et al., 2002; Sohrabi et al., 2004; Sayegh and Fisher, 2008; Crescente et al., 2008). Micromodels have also been used to study specific aspects relating to flow in porous media such as wettability, capillary pressure, interfacial tension, asphaltene deposition and heterogeneity (Donaldson and Thomas, 1971; Sayegh and Fisher, 2008).

In fact, using micromodel technique can improve understanding of basic mechanisms involved in oil recovery techniques by providing us a direct observation of pore level events. Although it is not possible to visually examine all processes occurring at the pore level in actual reservoir rocks, a very close approximation can perhaps be achieved in micromodel experiments.

10.2 Study of enzyme-brine injection by glass micromodel

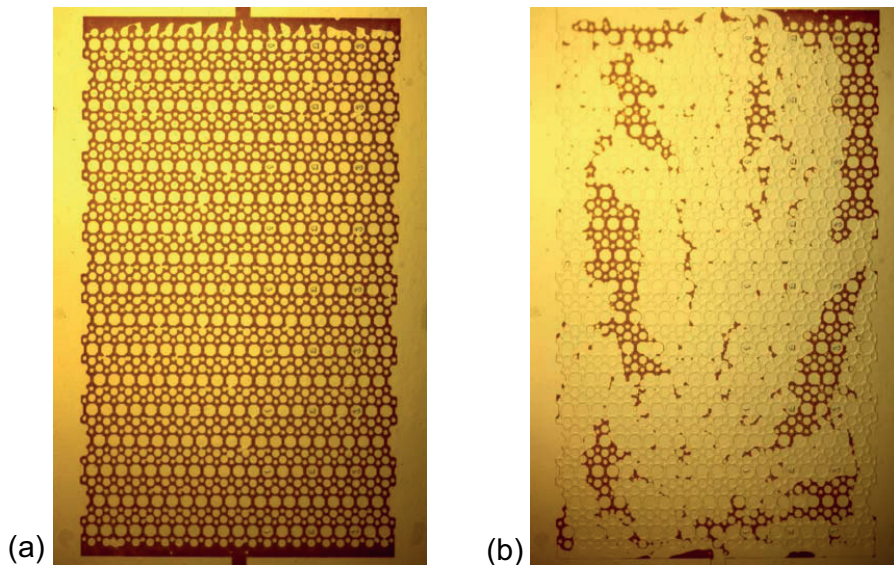
To investigate how the residual oil saturation changes during enzyme-brine flooding (EnF), 1 wt% solutions of Greenzyme (GZ) and NZ2 in sea water were injected into a micromodel after waterflooding (WF). A detailed description of the micromodel and experimental procedure is presented in Appendix B. The same model was reused in multiple experiments, necessitating effective cleaning after exposure to crude oil (for cleaning procedure, refer to Appendix B).

Five sets of experiments, three sets with GZ and two with NZ2, applying the same procedure were performed. Table 10.1 shows the different steps in the flooding cycle for the micromodel experiments. To compare oil recovery efficiencies in different experiments, it was decided to keep the experimental variable such as the pattern of the micromodel, flow rate and concentration of the enzyme unchanged in all experiments. Images of the model were taken after each flooding stage and analyzed with "Image J software" to calculate the oil saturation for each individual image.

Table 10.1: Dynamic displacement scenarios for micromodel experiments.

Exp.	Step1	Step 2
N0.1	SSW flooding	1 wt% GZ flooding
N0.2	SSW flooding	1 wt% GZ flooding
N0.3	SSW flooding	1 wt% GZ flooding
N0.4	SSW flooding	1 wt% NZ2 flooding
N0.5	SSW flooding	1 wt% NZ2 flooding

Examples of oil and water saturations in the micromodel prior to and after the waterflooding, i.e. at irreducible water saturation (S_{wi}) and waterflood residual oil saturation (S_{or}), respectively, are shown in Figures 10.1. To ensure that any change in residual oil is related to the effect of enzyme, the model was waterflooded for more than 24 hours with a nominal injection rate of 1 ml/hr. After water flooding, continuous injection of 1 wt% of enzyme-brine solution was performed with identical injection rate as waterflooding i.e. 1 ml/hr.

**Figure 10.1:** Micromodel (a) @ S_{wi} and (b) @ S_{or} after waterflooding No.1.

10.2.1 Waterflooding

Figures 10.1-10.2 show pattern of the residual oil saturation after waterflooding step. Table 10.2 also shows the amount of oil saturation after waterflooding. According to the figures and table residual oil saturation after waterflooding varies in micromodel experiments i.e. the

residual oil saturation can not precisely reproduce, although the same procedure was applied for all experiments. This observation was also reported by Chatzis et al. (1983). They found that residual oil saturation after waterflooding were closely similar in appearance but does not give a precise reproduction.

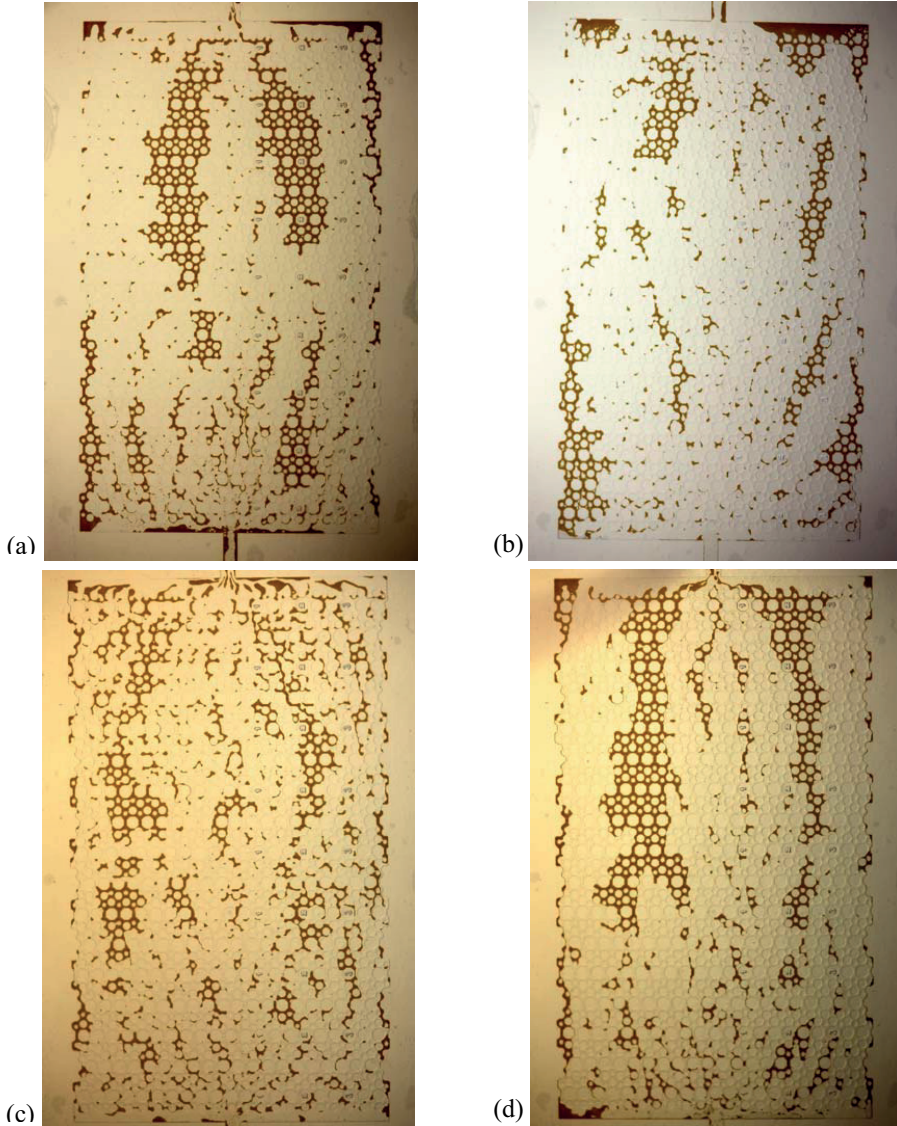


Figure 10.2: Micromodel @ S_{or} after waterflooding (a) experiment No.2 (b) experiment No. 3 (c) experiment No.4 (d) experiment No. 5.

As can be seen from Figures 10.1-10.2, the pattern of residual oil saturation after the initial waterflood consists of large clusters of the oil phase along the model and some areas with

relatively small blobs of oil distributed. Among different factors affecting the amount and pattern of residual oil in the micromodel, pore structure and wettability of the model are in a great importance.

Chatzis et al. (1983) have considered the effect of different variables such as aspect ratio, coordination number and pore size distribution to study how pore structure affect the residual oil saturation after waterflooding. According to them, among different parameters, aspect ratio can have a significant effect on trapping of oil phase after waterflooding. The aspect ratio is defined as the ratio between the diameter of the pore body and the pore throat. The trapping mechanism goes through a transition from bypassing to snap-off as aspect ratio increases.

The micromodel used in this study is designed with the pores of various sizes which make a semi-symmetric or semi-regular pattern with three aspect ratios, 2,3 and 5 (Shabni Afrapoli, 2009). This range of aspect ratios in the model results in contribution of different trapping mechanism at the pore scale, i.e. bypassing and snap-off event (which was discussed in more detail in chapter 2). In general, at high aspect ratio, the recovery of oil is low and comes mostly from the volume contributes by the throat pores (Chatzis et al. 1983). In the area with high aspect ratio (> 3) i.e. in the large pores connected by narrow throats, the dominant trapping mechanism is snap-off. In these areas the size of the trapped cluster decreases and entrapment of oil as a large number of relatively small blobs increases. Whereas in the area with lower aspect ratio i.e. in the pores connected by wider throats the dominant trapping mechanism of oil phase would be bypassing.

Another important factor affecting the pattern of residual oil in the micromodel is wettability. Glass micromodels are usually considered strongly water-wet because their surface chemistry is similar to that of clean sandstone (Grattoni et al., 2002). The mechanism of flow into oil pores can be changed by rendering the wettability of the glass micromodel from water-wet to oil-wet or mixed-wet. Mixed-wet state arises because water is the first fluid present and occupies corner wedge in the model (Buckley, 1996). In glass micromodels, wettability alteration of the high energy silica pore surfaces by interactions with crude oil components should be similar to the interactions reported on flat glass surfaces and depends on the nature of the oil, aging time and temperature and brine composition, as discussed in chapter 6. In the oil-wet system the flow mechanism changes more to piston-type flow. A direct consequence of this change is a change in the pattern of the residual oil saturation. Oil trapped in water-wet

systems is in the form of small, isolated pockets, while the size of the pockets of oil increased as the water-wetness of the system decreased (Donaldson and Thomas 1971, Sohrabi et al. 2000 and 2004). In the mixed-wet system, during the initial waterflood, both piston-type and film flow of water were taking place depending on the wettability of the pores (Sohrabi et al., 2004). Investigation about effect of wettability on oil recovery from micromodels by Morrow et al. (1986) also showed that in a water-wet system, residual oil is mainly trapped in pore bodies while in a micromodel aged in crude oil at S_{wi} the residual oil was mainly trapped in pore throats.

In our experiments, micromodel has been aged in crude oil prior the waterflooding which has been explained in detail in Appendix B. Although the same procedure was performed for all experiments, it seems that different wettability state has been arisen. As discussed above, wettability state affects the amount and the pattern of the residual oil saturation after waterflooding. Comparison of the residual oil saturation in different experiments in Figures 10.1-10.2 shows the difference in wettability state. For instance, residual oil pattern in exp. 4 shows more water-wet state than the other experiments where the size of the residual oil pockets seems smaller than the other cases. This difference in wettability by aging has been also addressed in chapter 9 of this thesis for core materials.

While glass micromodels have been used mostly as tools for qualitative study, some researchers have used image-analyzing techniques to measure the oil saturation for each step of flooding (e.g. Jeong et al., 2000; Sohrabi et al., 2000 and 2004) In this study, a computerized image processing system was employed for oil saturation measurement before and after enzyme-brine treatment (see Table 10.2). Table 10.2 shows that the amount of the residual oil after waterflooding varies between 15 and 22 %. The effect of wettability on the remaining oil after waterflooding can be more highlighted when it is taken into consideration that the same micromodel with identical pore structure has been used in all experiment. It means that effect of pore structure (aspect ratio) can not be discarded but may be overshadowed by wettability effect in our experiments.

10.2.2 Enzyme-brine flooding

Injection of enzyme-brine into the waterflooded micromodel produced additional oil from the model. Table 10.2 shows oil saturation after enzyme-brine flooding in different stage of flooding. According to the table, the changes in oil saturation range from 2 to more than 6

saturation unit, with an estimated error of ± 2 saturation units. Reduction in oil saturation by enzyme-brine injection is consistent with the results of the core flooding experiments which are presented in chapter 9. In the micromodel flooding the incremental oil recovery by enzyme flooding is independent of the amount of the residual oil after waterflooding. Exp. 5 produced almost the same amount of incremental oil as Exp. 1 and 2 where the S_{or} after water flooding is about 16 for exp. 5 and about 22 for Exp. 1 and 2. This independence of incremental oil has been also seen in the core flooding experiments where different sandstone cores with different S_{or} produced almost the same amount of the oil after enzyme-brine injection.

Table 10.2: Residual oil saturation at different stage of flooding for different experiments.

Exp.	S_{or} (%)	WF	EnF (20 PV inj.)	EnF (35 PV inj.)	EnF (50 PV inj.)
N0.1		21.8	19.7	15.6	15.5
N0.2		21.6	16.6	15.4	---
N0.3		16.0	12.4	11.6	---
N0.4		14.8	13.0	12.5	---
N0.5		16.4	12.1	11.7	11.5

As discussed in the core flooding chapter, wettability alteration may be the main factor contributing to mobilization of oil remaining after waterflood. Investigation by use of the high quality photos taken from different stages of the micromodel flooding provided us some evidence about wettability change in the system that ended up to more oil recovery from the model. The evidences will be discussed further in this chapter.

Figure 10.3 and 10.4 show examples of GZ- and NZ2-brine injection into the micromodel after brine flooding in different time steps of the flooding. In addition to being injected with different enzymes, the oil distribution in the GZ injection experiment (exp. 1) was qualitatively different from that of the NZ2 experiment (exp. 4). As discussed previously, the distribution of residual oil in experiment 4 indicated a more water-wet system than that in exp. 1. As discussed in chapter 7, effect of enzymes on contact angles is larger when the initial wettability of the solid surface is in the range of intermediate wetting. This indicates that for exp. 4 the effect of enzyme is likely more pronounced which can be seen in Figures 10.3-10.4. This is also confirmed by the values of S_{or} after enzyme flooding given in Table

10.2. Residual oil saturation after enzyme-brine flooding has been decreased more than 6 % for exp. 1 while this value for exp. 4 reduced about 2.5 %. This fact i.e. less water-wet state can also be true for experiments 2 and 5, by considering the residual oil pattern after waterflooding (see Figure 10.2) and the amount of the remaining oil after enzyme-brine injection (see table 10.2).

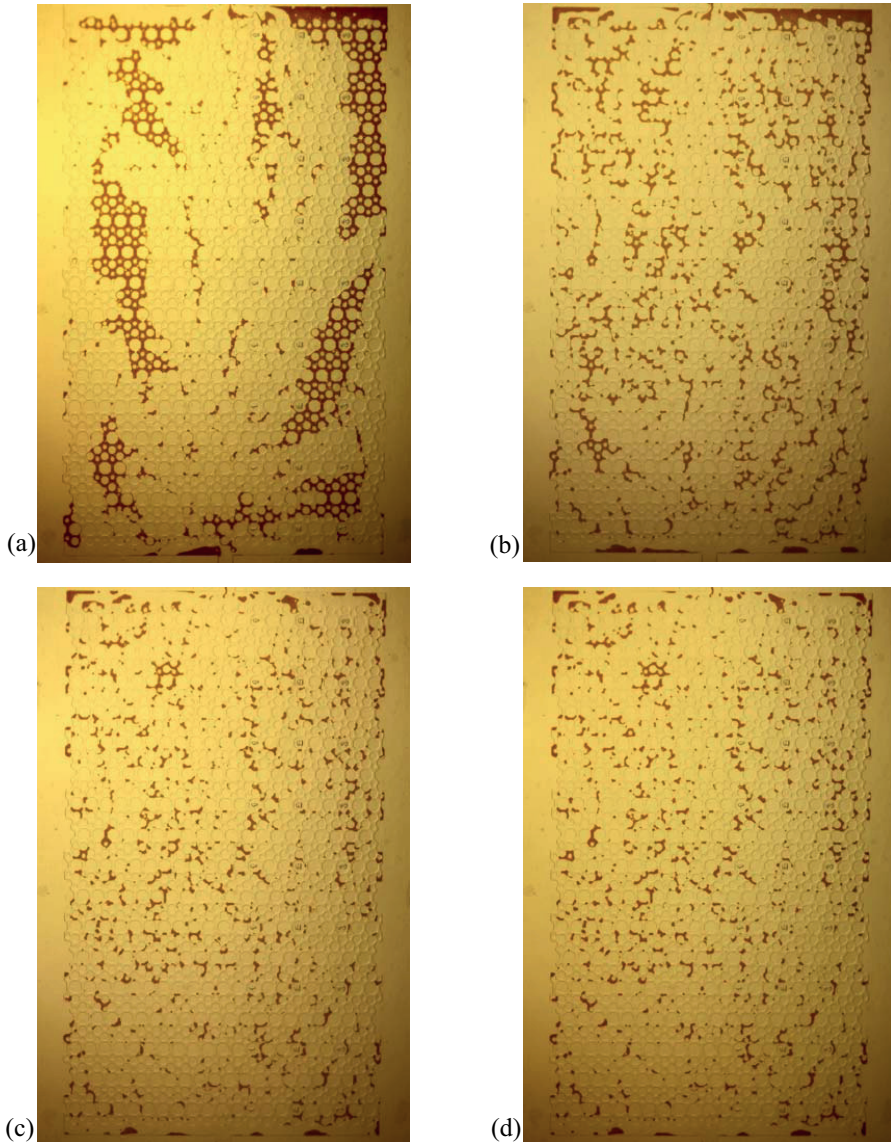


Figure 10.3: Micromodel (experiment No.1) @ S_{or} after different stages of flooding (a) waterflooding (b) 1 day enzyme-brine, (c) 2 days enzyme-brine and (d) 3 days enzyme-brine.

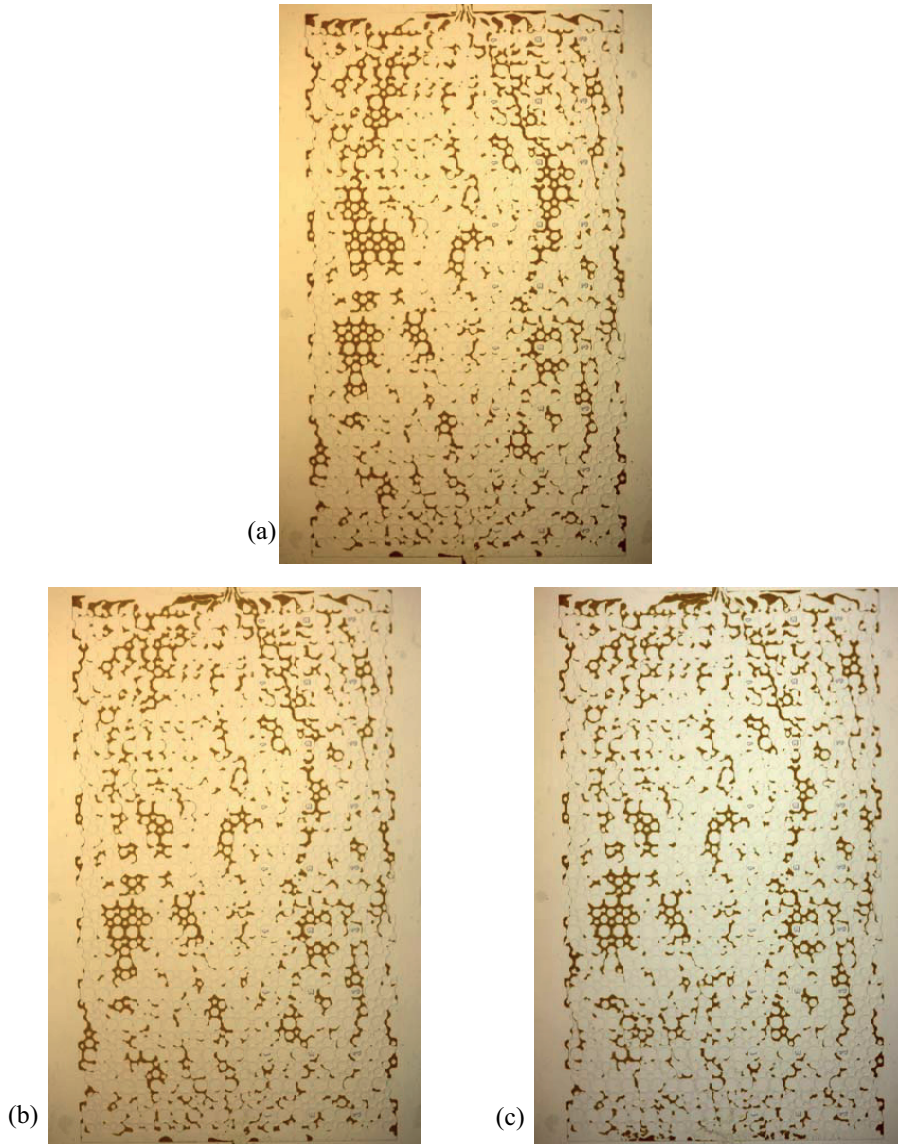


Figure 10.4: Micromodel (experiment No.4) @ S_{or} after different stages of flooding (a) after waterflooding, (b) after 1 day NZ2-brine flooding and (c) after 2 days NZ2-brine flooding.

10. 2.3 Evidence of wettability change in the micromodel

Figure 10.5 shows the oil distribution in a section of the micromodel at different time intervals after the injection of 1wt% GZ flooding (GZF) into the model. As can be seen from the figure, the enzyme-brine solution can mobilize oil from areas which were not swept by water.

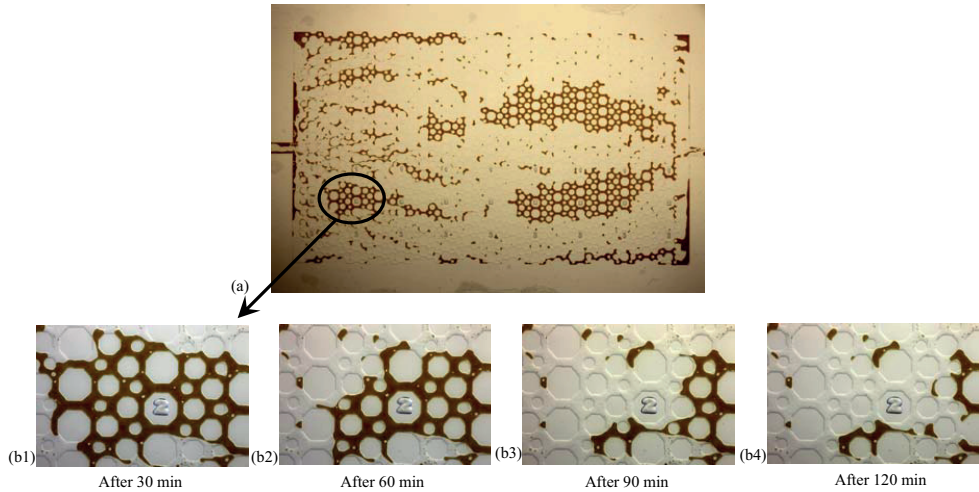


Figure 10.5: (a) S_{or} after water flooding No.2 (b) Focused area in different time steps of enzyme-brine flooding.

By injecting enzyme-brine in the second stage of the flooding scenario flow mechanism seemed to behave more as the water-wet system (especially, in the cases which the onset wettability seems less water-wet) and reach to the by-passed zones in the model through water films. By continuing the injection, at later stage of the flooding, the water filaments surrounding the oil present in the larger pore bodies, thicken progressively and leave oil filaments in the middle of pores and finally cause oil snap-off at the pore throats. Figure 10.6 shows some examples of snap-off which occurred at later stage (after about three PV injections) of enzyme-brine injection into the model.

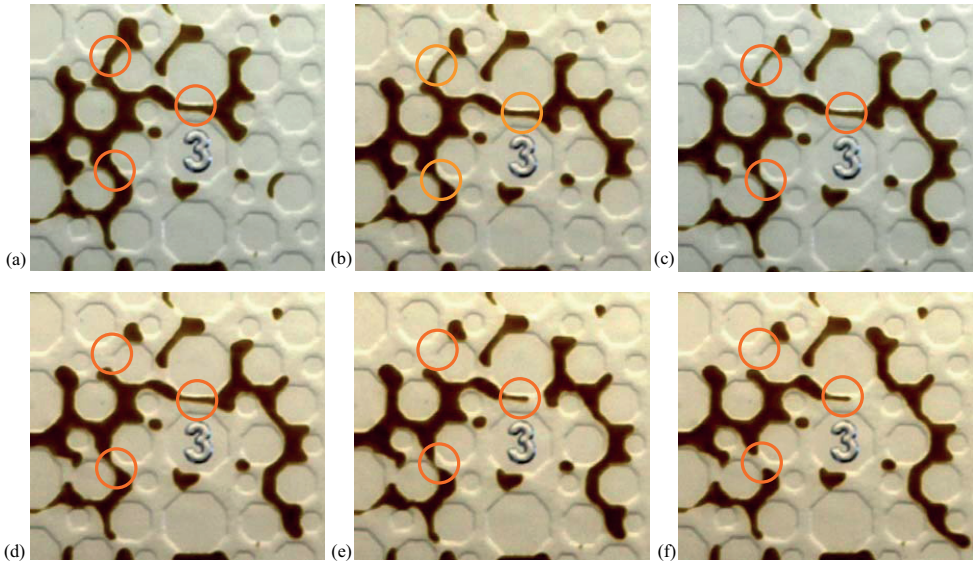


Figure 10.6: Examples of snap-off event by injection of enzyme-brine in experiment No.3. Time interval between images is about one minute.

At late stage of the enzyme-brine flooding, the pattern of residual oil saturation shows more water-wet behavior compare to initial waterflood. Figure 10.7 shows an example of this change in wettability condition. By injection of enzyme-brine into the model, by-passed oil started to move along the model and small oil patches are distributed and retrapped along the model. Figure 10.7-b shows distributed oil patches after injection of enzyme-brine solution. The pattern shows various oil droplets which can be the result of snap-off event.

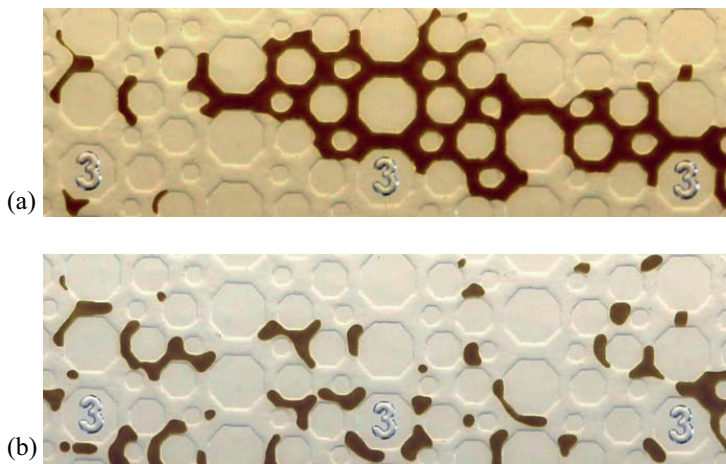


Figure 10.7: Example of effect of wettability change on residual oil saturation in micromodel experiments after enzyme-brine flooding (experiment NO.3). (a) after waterflooding (b) after about one day enzyme-brine flooding.

The curvature of the oil-water interface can also be an indication of wettability alteration by enzyme-brine injection. Some researchers (e.g. Buckley, 1996; Sohrabi *et al.*, 2000 and 2004) used oil-water interfaces to evaluate the wettability status of the micromodel. They have evaluated the wettability of the model by the shapes of moving oil-water interfaces and by snap-off of the advancing water phase. Sohrabi *et al.*, (2000 and 2004) counted the interfaces which show the water-wet, intermediate-wet and oil-wet behavior. The more of each state indicates the wettability status of the model. In mixed-wet systems where contact angle between oil and water is relatively low (around 90 degree), the oil-water interfaces are fairly flat (Buckley, 1996). In our study, comparison of Figure 10.7-a and b show the change in oil-water interfaces. In Figure 10.7-a, the majority of the interfaces show non-water-wet behavior i.e. the curvature of oil-water interface shows intermediate-wet behavior where oil-water interfaces are fairly flat or oil-wet behavior where the curvature of oil-water interface is toward oil. However, after exposing to enzyme-brine solution (see Figure 10.7-b) oil-water interfaces appears to be more water-wet i.e. the curvature at the interface is towards water. This change in behavior to more water-wet state was observed in all experiment at late stage of the enzyme-brine flooding.

Chapter 11 Summary of the main results

11.1 Scope of this study

Enzymes are used for different industrial applications, such as detergents, textile and food industry. However, use of enzymes in the oil and gas industry has been suggested recently. Feng et al. (2007) reported increased oil production by injection of modified enzyme solutions in both laboratory core floods and a field scale pilot test. However, data on the possible use of enzymes to increase recovery after waterflooding is very limited. Further, to our knowledge, there have been no comprehensive attempts at investigating the mechanisms by which enzymes contribute to enhanced oil recovery. The scope of the present work is thus to study how enzymes can affect oil recovery, and further to investigate the mechanism by which enzymes contribute to more incremental oil.

The experimental work started by examining the effect of enzymes on oil-water-solid and oil-water interactions as inferred from interfacial tension, electrophoretic mobility and wettability measurements (Chapter 7 and 8). The measurements were done with different types of enzyme added to the brine phase and compared with samples without enzyme. Following this initial phase, the effect of enzyme solutions on enhanced oil recovery from sandstone and carbonate rocks was tested (Chapter 9). Finally, an attempt to link the static and the dynamic measurements were made by studying the displacement process with and without added enzyme in micromodel experiments (Chapter 10).

11.2 What can enzymes do?

Enzymes are a specific group of proteins that catalyse many thousands of biochemical reactions by lowering the activation energy and thus dramatically accelerating the rate of the reaction. The question here is how using enzymes can lead to enhanced oil recovery?

Crude oils contain a large number of polar molecules such as phenols, carboxylic acids, sulphur and nitrogen. These polar functional groups can provide acidic, basic or even zwitterionic sites at the interface between crude oil and water and thus have direct impact on fluid/rock interactions related to wettability and fluid/fluid interactions related to interfacial tension (IFT). Wettability and IFT have a strong influence on the distribution and flow of fluids in the reservoir rock. Together with the structure of the porous medium they are the major parameters affecting the amount and distribution of capillary trapped oil in a reservoir after waterflooding. More details of these oil trapping mechanisms can be found in chapter 2.

Enzymes can contribute to changing the fluid-rock and/or fluid-fluid interactions mainly by catalysing the break down of crude oil components. As an example, hydrolase enzymes catalyse bond cleavage by introduction of water which may break these molecules down into (i) smaller molecules with increased water solubility and reduced interfacial activity and/or (ii) more polar molecules (e.g. ester hydrolysis to form acid + alcohol). These compositional changes may influence on wettability and interfacial tension. Besides, as discussed in detail in chapter 6, proteins are known to adsorb onto solid/liquid and liquid/liquid interfaces. The protein nature of the enzymes may thus give rise to changes in the interaction energy between crude oil, brine and rock.

11.3 “Evidence” of wettability alteration by enzymes

Adhesion tests and contact angle measurements were performed to evaluate the ability of enzymes to change the wettability of silica glass surfaces. Different types of enzyme from different classes, hydrolases, proteases, esterases, as well as a pure protein, were used in the experiments. The results of all contact angle and adhesion measurements were presented and discussed in detail in chapter 7. Using the adhesion method, it was shown that adding enzymes to the brine solution can change the adhesion behavior of the crude oil on the solid surface from adhesion to non-adhesion.

Contact angle measurements showed that enzyme-proteins affect the wettability of glass surfaces for both untreated glass and glass aged in crude oils at elevated temperature (80°C). All enzymes changed the wettability of the glass surfaces towards a more water-wet condition. Among the tested enzymes, protease enzymes was found to have the least effect while esterase enzymes had the most pronounced effect on the oil-brine-quartz contact angle. The latter changed contact angle independent of their concentration and all concentrations showed almost the same change in contact angle. Adding Greenzyme and pure protein also had significant effect on contact angle, comparable with the results obtained with esterase enzymes. The results showed that the wettability alteration of the glass surface appears to be most pronounced when we have a solid surface with more intermediate wettability i.e. contact angle between 65 and 100 degrees.

The mechanisms underlying contact angle change by enzymes can be discussed with two perspectives. As enzymes they catalyze the breakdown of certain bonds which may exist in the crude oil, and thereby change the interaction forces at the crude oil/brine/glass interface. However, the protein nature of enzymes should also be considered.

Esterase enzymes catalyze the hydrolysis of ester bonds to form acid and alcohol. Dissociation of the acid may lead to increasing repulsive electrostatic forces at interfaces of crude oil/brine/glass surface (see Figure 11.1).

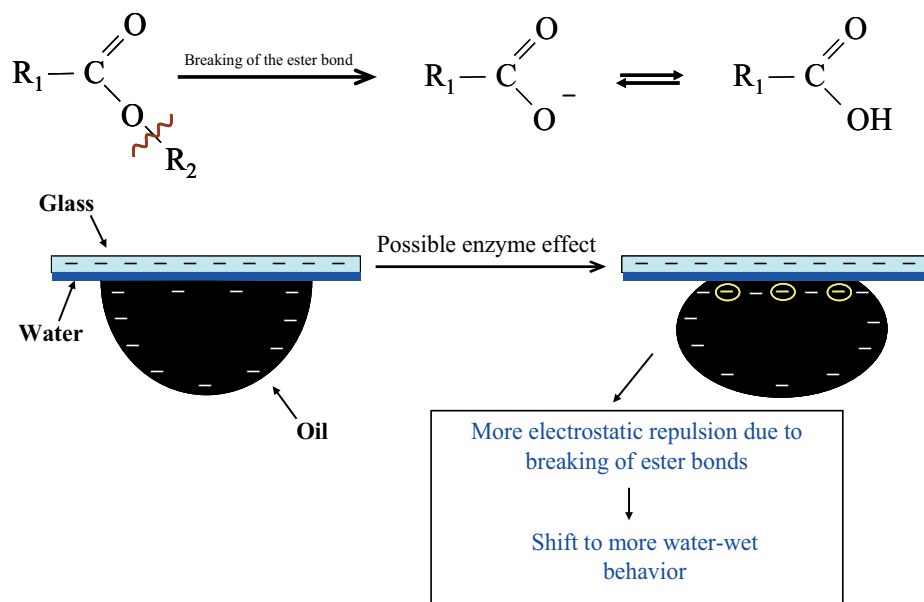


Figure 11.1: Breaking down of ester bonds by NZ group enzymes and alter the wetting behavior of the solid.

Gas chromatography measurements on mineral oil with added ester showed the breakdown of ester bonds and a significant decrease in amount of ester in the oil. This phenomenon was also investigated measuring the electrophoretic mobility of oil droplets dispersed in brine in the presence of enzymes (see chapter 8). The electrophoretic mobility is directly proportional to the magnitude of the charge on the oil droplets in the brine solution.

Enzymes affect the electrophoretic mobility of the oils in brine as a result of change in the electrostatic forces at oil-water interface. Adding Greenzyme to the brine cause an increase in the electrophoretic mobility (more negative). Although the two crude oils and the mineral oil had different electrophoretic mobilities initially, the values are almost identical when GZ was added to the brine phase, meaning that adding GZ into the solution overshadowed the effect of other substances. The reason can be due to added stabilizers (surfactants) to the Greenzyme which have the negative charge (Greenzyme material safety data sheets). Esterase enzymes seemed to have limited effect on the electrophoretic mobility of crude oil A, the mobility was decreased for crude oil B and mineral oil with added ester. This can be explained by the amount of acid and base functional group in crude oil B which is more compare to crude oil A and existence of ester in the mineral oil that cause more electrical charges at the oil-water interface and thereby more interaction of enzyme at the interface.

Adsorption of the protein at the crude oil-brine-glass interface, which has been discussed in detail in chapter 6 of this thesis, may change the wetting behavior of the glass. Alpha-Lactalbumin which is a pure protein showed strong effect on changing contact angle on its alteration toward more water-wet state (see chapter 7). This is likely due to surface modification by protein adsorption. Adsorption of α -La to adsorb onto different solid surfaces has been reported by several authors (e.g. Halskau et al., 2002; Glomm et al., 2007). Adsorption measurements by use of UV spectroscopy also showed adsorption of esterase enzymes on silica and kaolin (see chapter 7).

The interfacial tension between crude oil and brine containing enzyme or protein was measured as a function of equilibration time (see chapter 8). According to the results, interfacial tension between crude oil and enzyme-brine solutions was not significantly different from that between crude oil and brine. An exception was GZ which decreased the oil-brine IFT by a factor of approximately 3. GZ is a commercial enzyme which has been modified according to the crude oil complexity and is a compound of enzyme and stabilizers (surfactants) (Greenzyme material safety data sheets). The existence of stabilizers (surfactants) in the solution seems to make it exception among all tested enzymes and protein to be more interfacially active. Although esterase enzymes are interfacially active (Fojan et al., 2000; Al-Zuhair et al., 2007), it appears that their adsorbance on the crude oil-brine interface could not change the IFT. High concentration of interfacially active components in the crude oil can be the reason behind that. The affinity of the esterase enzymes for the interface seems to be not strong enough to replace the crude oil components. The result of IFT measurements using mineral oil and enzyme-brine solution which has been discussed further in section 8.1.3 shows good agreement with this argument. Adding enzyme to the brine solution could lower the IFT to some degree. It means that esterase enzymes are interfacially active when their substrate changes from crude oil to mineral oil

11.4 Enzymes and the potential for oil mobilization

To investigate the potential of enzymes to improve oil recovery, dynamic displacement experiments were performed using sandstone and carbonate rocks (see chapter 9). Core plugs with different lengths prepared and flooded first with brine (in most of the experiment) and then followed by with enzyme-brine. Combination of surfactant and enzyme also were tested in long sandstone (approximately 30 cm) after enzyme-brine flooding step to study the effect

of combining the two methods on oil recovery. Figure 11.2 shows oil recovery after each step for all cores. All cores were flooded with several PV of brine prior to any other processes to ensure that there is no more oil produced by water flooding.

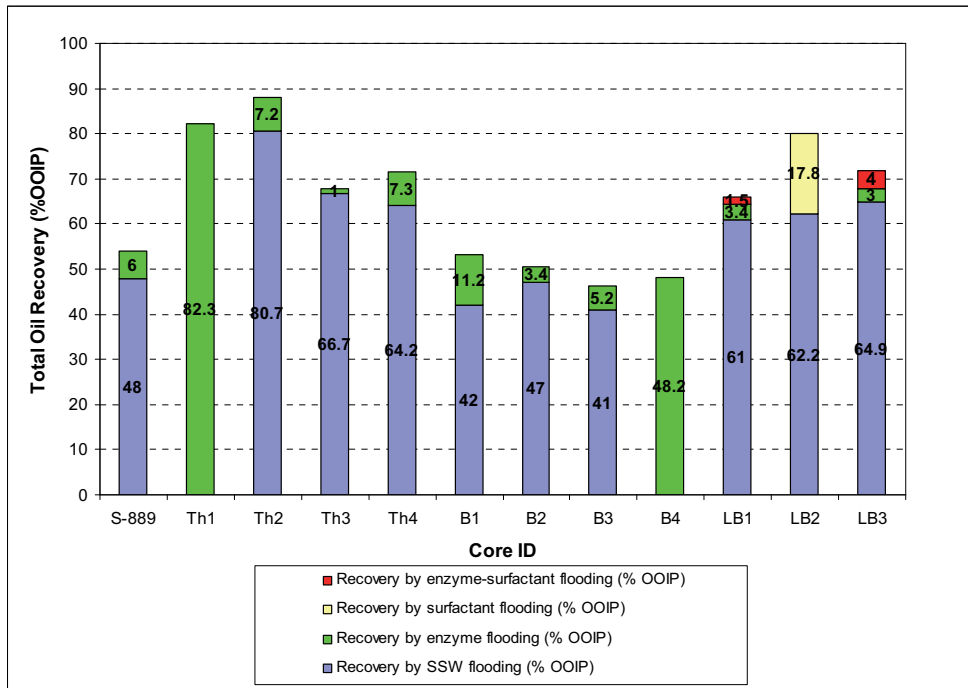


Figure 11.2: Oil recovery in different flooding scenario for all cores.

Injection of enzyme-brine solution was found to give an incremental increase in oil recovery of 1 to 11% OOIP. No significant difference was found between experiments in sandstone and carbonate cores. The results also show that different types of enzymes, GZ and NZ2 appear to have almost the same effect on oil recovery in the cores (see Figure 11.2). Further, judging from Figure 11.2, oil recovery by enzyme flooding also seems to be independent of the amount of residual oil after water flooding. Cores with more residual oil gave similar incremental oil recovery as long cores with less residual oil after water flooding.

There are two important mechanisms in relation to improved microscopic displacement efficiency: decreasing of the IFT between oleic and aqueous phases and destabilization of oil layers in porous medium. According to the results reported in chapter 8 adding enzyme to the brine showed no significant change in the IFT however GZ was an exception that lowered the IFT to some extent (about 3-4 times). The reduction of IFT in case of adding GZ, as already

discussed, is due to added stabilizers (surfactants) into the enzyme solution. But reduction of IFT by 3-4 times can not increase the capillary number enough to include significant mobilization of capillary trapped oil after waterflooding. This can be explained by taking capillary desaturation curve (CDC) into account. The capillary number needs to increase by several orders of magnitude to overcome its critical value. The calculated capillary numbers for enzyme-brine flooding are much smaller than the N_{CC} (around 5×10^{-4}) reported in the literature (Garnes et al., 1990 and Mohanty and Salter, 1983).

Destabilization of oil layers in porous media by enzyme-proteins, which can be the result of wettability change, was discussed in detail in chapter 7. Contact angle measurements were limited to silica glass surfaces, which can be representative of sandstone rocks. Enzyme-proteins changed the contact angle towards a more water-wet state (i.e. the contact angle decreased). Observations by Feng et al. (2007) also confirm a change in wettability towards a more water-wet state by enzymes. According to the authors, enzymes could change the wettability of reservoir rock from oil to water-wet and reduce the flow resistance through a porous medium. So, based on the experimental results presented in this work and results in reviewed literature it seems that the wettability alteration is the dominant underlying mechanism for enzyme flooding to improve oil recovery. This characteristic of enzymes makes them unique and special between all methods which have been proposed in order to increase oil recovery. Among other methods we can point out to low salinity water flooding. In the past decade, there is a strong interest in use of this technique to enhanced oil recovery. Several researchers reported using this technique and proposed different underlying mechanisms for it (e.g. Morrow, 1990; Tang and Morrow, 1997; Filoco and Sharma, 1998; Lager et al., 2006; Agbalaka et al., 2009). One of the reported mechanisms is wettability alteration toward more water-wet condition by lowering salinity relative to the content in formation water. All the reported results are in sandstone rocks and unlike the enzymes; it seems that this technique can not have beneficial impact on oil recovery in carbonate rocks.

To investigate how combination of enzymes and surfactants work, injection of combined enzymes and anionic surfactants was examined on two long Berea sandstone cores, LB1 and LB3 (see chapter 9). Destabilization of oil layers by enzyme action along with lowering the capillary forces as a result of using surfactants can be the advantages of the combined enzyme-surfactant method to increase oil recovery. In the case of adding GZ into the surfactant solution (core LB1), the IFT between the solution and crude oil increased and made

it unfavorable for the surfactant action. Unfavorable GZ action on IFT can be a result of added stabilizers (surfactants) into the GZ solution. So, combining GZ with the surfactant was not a good implementation to enhance oil recovery. Results of the core flooding on aged Berea sandstone cores showed 1.5% OOIP incremental oil recovery by performing the GZ-surfactant flooding (see chapter 9). However, Adding esterases enzyme into surfactant solution seems to have no effect on IFT and resulted in more incremental oil recovery (core LB3) which was 4% OOIP compare to that for the GZ-surfactant case.

A capillary number analysis has been made for long Berea sandstone cores LB1, LB2 and LB3 (see chapter 9). Capillary numbers were analyzed to get the critical value when oil is starting to produce by enhanced oil recovery processes. Core LB2 was used as a reference case to inject surfactant without adding any enzyme to compare the results with the cases when enzyme was added to surfactant solution (cores LB1 and LB3). Results of the analysis showed that the critical capillary number for the cores is estimated to be about $7 \cdot 10^{-4} \pm 2 \cdot 10^{-4}$ which is in agreement with other published data by different researchers such as Garnes et al. (1990) and Mohanty and Salter (1983) for the same type of rock. For cores LB1 and LB3 (see section 9.3), injection of enzyme-surfactant solutions resulted in $N_C > N_{CC}$. As a result the slope of the S_{or} vs N_C curves began to decrease, especially for core LB3 where estrases enzyme was added to the injected solutions. Higher capillary numbers were reached during injection at 1 ml/min of surfactant or enzyme-surfactant solutions in cores LB2 and LB3, respectively, compared to enzyme-surfactant flooding of core LB1 at the same rate. The reason is that, unlike NZ2 which was used for core LB3, GZ appears to have a negative effect on the interfacial tension (see section 8.1.5) during enzyme-surfactant injection in core LB1. However, although the same capillary number was applied in core LB2 and LB3, significantly lower S_{or} was obtained for core LB2 (about 13 saturation units compared to about 3 saturation units for the other cases). A possible reason for this could be different configuration of the remaining oil after enzyme flooding than that after waterflooding due to wettability changes induced by the enzymes. This phenomenon has been discussed in more detail in chapter 10. It should be pointed out that the same experimental conditions were applied for all core flooding.

11.5 Validation of results obtained from static and dynamic experiments

Liquid-Liquid and solid-liquid interactions were measured by using IFT and wettability measurements, respectively, in first part of experimental work to test the enzymes' effect on those properties. Adding enzymes to the brine phase gave a significant decrease in contact angle for Greenzyme and the three different esterase enzymes tested (see Chapter 7). However, only Greenzyme was found to have an effect on oil-water interfacial tension, which was reduced by a factor of approximately 3 when Greenzyme was added (see Chapter 8). In second part of experimental work, flooding aged Berea sandstone and carbonate cores waterflooded to residual oil saturation, with Greenzyme added to the water phase gave an additional recovery of between 3 and 11 % OOIP. Three experiments performed with one of the esterase enzymes also showed a reduction in residual oil in the same ranges as that observed for Greenzyme.

Using micromodels can contribute to improved understanding of basic mechanisms involved in oil recovery techniques by providing direct observations of pore level events. In this work, micromodels were used to gain insight into the mechanisms by which enzymes may contribute to recovering incremental oil (see chapter 10). Glass micromodels are two-dimensional models of pore system which can be a representative of porous media. Such models can connect our understanding from static measurements on flat surfaces and dynamic measurements in cores by providing visualization of flow within the pore space. The latter includes observations of the effect of pore and fluid variables on the trapping and subsequent mobilization of residual phases during simulated secondary and tertiary recovery processes.

While glass micromodels have been used mostly as tools for qualitative study, some researchers have used image-analyzing techniques to measure the oil saturation for each step of flooding (e.g. Jeong et al., 2000; Sohrabi et al., 2000 and 2004). In this study, a computerized image processing system was employed for oil saturation measurement before and after enzyme-brine treatment.

Micromodel experiments showed changes in the residual oil saturation by enzyme-brine flooding when 1wt% Greenzyme and NZ2 were added to the brine solution. The incremental oil recovery by enzyme-brine flooding seems to be independent of the amount of the residual oil after waterflooding. Experiments with S_{or} of 0.16 and 0.22 (saturation unit) after waterflooding, produced almost the same amount of incremental oil after injection of enzyme-

brine solutions. Reduction in oil saturation by enzyme-brine injection, as well as the apparent independency between incremental oil and initial residual oil saturation after water flooding was consistent with the results of the core flooding experiments which were presented in chapter 9.

As discussed in the core flooding chapter, wettability alteration may be the main factor contributing to mobilization of oil remaining after waterflood. Wettability alteration of flat surfaces by adding enzymes to the brine solution was shown and discussed in detail in chapter 7. Micromodel experiments showed that the pattern of residual oil saturation change significantly after enzyme-brine flooding, and that the observed changes can be the result of wettability alteration towards a more water-wet state. Figure 11.3 shows an example of the change in oil saturation distribution through the micromodel. As Figure 11.3 shows, the residual oil pattern is modified to more distributed oil patches by injecting of enzyme-brine although the additional oil production was relatively low.

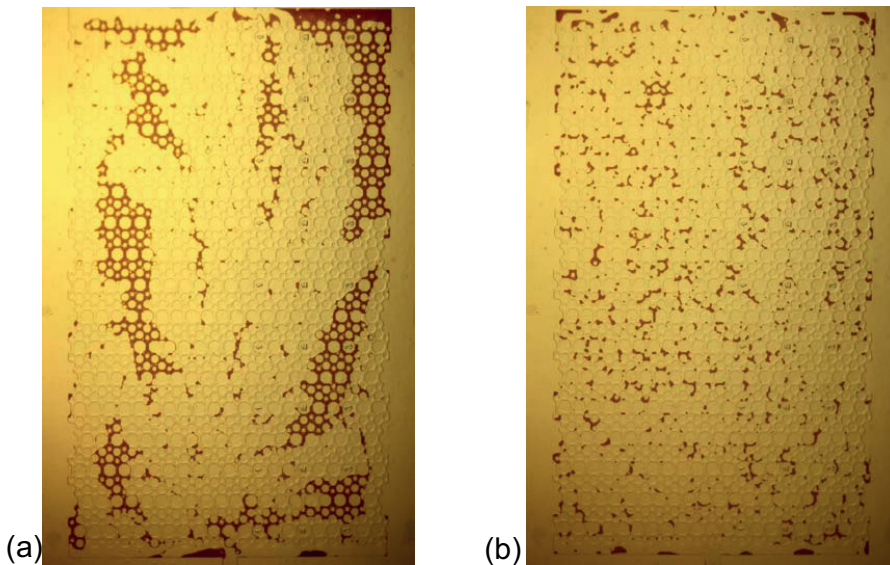


Figure 11.3: An example of micromodel @ S_{or} after different stages of flooding (a) after waterflooding and (b) after enzyme-brine flooding.

The enzyme-brine solution could mobilize oil from areas which were not swept by water in the waterflooding step. By injecting enzyme-brine solution in the second stage of the flooding, the flow mechanism seemed to behave more like the water-wet system and reach to

the by-passed oil zones in the model through water films. By continuing the injection the water filaments surrounding the oil present in the larger pore-bodies, thicken progressively and leave oil filaments in the middle of pores. This filling mechanism finally causes oil snap-off at the pore throats. At a later stage some of the by-passed oil starts to move along the model, which leads to the distribution and re-trapping of small oil patches along the model (see Figure 11.3). Figure 11.4 shows some examples of snap-off which occurred after about 3 PV enzyme-brine injections into the model.

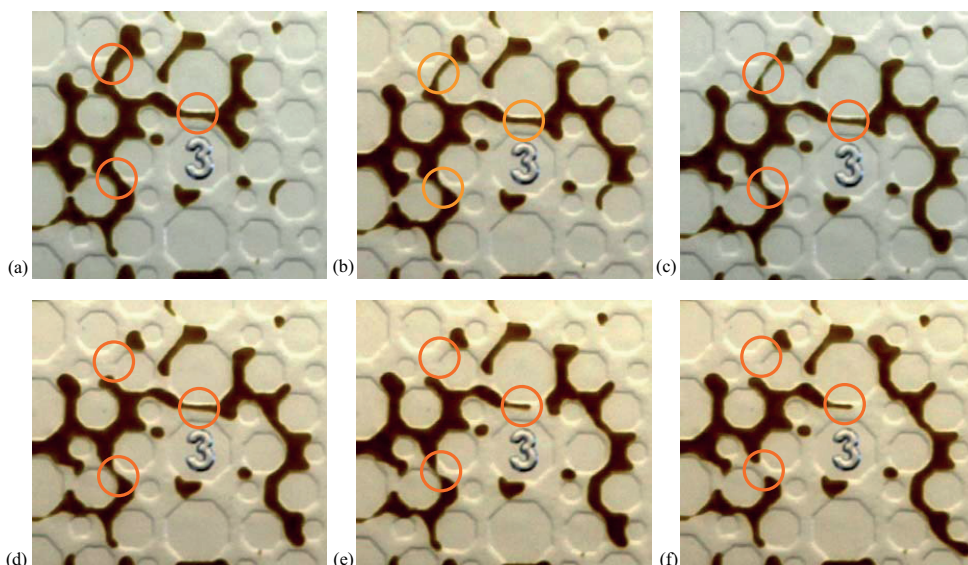


Figure 11.4: Examples of snap-off event by injection of enzyme-brine in experiment No.3. Time interval between images is about one minute.

Wettability alteration to a more water-wet state can also be investigated by considering the curvature of the oil-water interface (see e.g. Buckley, 1996; Sohrabi et al., 2000 and 2004). In mixed-wet systems where contact angle between oil and water is relatively low (around 90 degree), the oil-water interfaces are fairly flat (Buckley, 1996). Investigations of high resolution photos from the model showed significant changes in the curvature of oil-water interfaces from intermediate-wet (flat interfaces) to water-wet status after exposure of the model to enzyme solution. Comparison of Figures 11.5-a and b shows the change in oil-water interfacial curvature. In Figure 11.5-a the majority of the interfaces show non-water-wet behavior. The curvature of the oil-water interfaces display intermediate-wet behavior, where oil-water interfaces are fairly flat, or even more oil-wet behavior where the curvature of the oil-water interface is towards the oil phase. However, after exposing the micromodels to

enzyme-brine solution (see Figure 11.5-b), the oil-water interfaces appear to be more water-wet with the interfacial curvature towards the water phase. This change in behavior to a more water-wet state was observed in all experiments after flooding with several pore volumes of enzyme-brine solution.

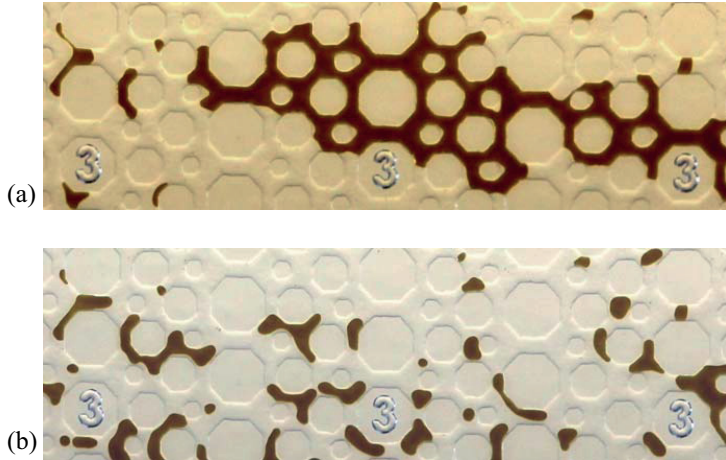


Figure 11.5: Example of effect of wettability change on residual oil saturation in micromodel experiments after enzyme-brine flooding (experiment NO.3). (a) after waterflooding (b) after about one day enzyme-brine flooding.

The evidences of wettability alteration made by micromodel experiments can validate our proposal, wettability alteration, as the main mechanism contributing to increasing oil recovery. Observations of wettability change were in agreement with contact angle measurements on glass surfaces and incremental oil recovery after enzyme-brine injection in micromodel experiments were also in agreement with core flooding experiments.

Chapter 12 Concluding remarks

The main finding of this thesis is that adding enzymes to the injection brine gives increased oil recovery from both sandstone and carbonate cores. Further, enzymes have been found to change the wettability of silica surfaces towards more water-wet conditions.

An important part of this thesis was to investigate how selected enzymes may influence wettability and capillary forces in a crude oil-brine-rock system, and thus possibly contribute to enhanced oil recovery. Considering interactions in the oil/brine/solid system, it was found that enzymes can change the adhesion behavior of the crude oil on glass surfaces from adhesion to non-adhesion when they are added to the brine solution. This was confirmed by contact angle measurements, which showed that contact angles became more water-wet (i.e. decreased) after exposure to enzyme solutions. Possible mechanisms giving rise to these observations, including catalysis of ester hydrolysis and enzyme adsorption, were discussed and tested.

The interfacial properties at oil-water interface have been studied. It was found that the effect of enzymes on the oil-water properties are minor compared to their effect on oil-water-solid properties. The contribution to change interfacial tension between oil and water is not significant while enzymes affect electrophoretic mobility of emulsified oil in enzyme-brine solution to some extent.

Results of dynamic core displacements using sandstone and carbonate rocks showed the potential of improved oil recovery by enzyme and enzyme-surfactant. Flooding carbonate and aged Berea sandstone cores, waterflooded to residual oil saturation, with Greenzyme added to the water phase gave an additional recovery of between 3 and 11 % OOIP. One experiment on

aged sandstone core and two on carbonate cores performed with one of the esterase enzymes also showed a reduction in residual oil in the same ranges as that observed for Greenzyme.

Judging from a capillary desaturation point of view, the reduction in interfacial tension obtained by adding Greenzyme is not sufficient to induce mobilization of residual oil. Further, a reduction in residual oil saturation was found after flooding with one of the esterase enzymes, which did not affect the oil-water interfacial tension. Based on these observations, we expect wettability changes to be the main factor contributing to mobilization of oil remaining after regular waterflood. To explore this hypothesis further, micromodel experiments were undertaken.

Micro model experiments showed change in amount of residual oil saturation by enzyme-brine flooding when 1wt% Greenzyme and NZ2 were added to the brine solution. The amount of change in residual oil saturation was consistent with the incremental oil recovery produced in the core flooding experiments. Micromodel experiments also showed that the pattern of residual oil saturation change to more distributed oil patches by injecting enzyme-brine solution although the additional oil production was relatively low. This change in pattern of residual oil saturation is likely related to wettability alteration toward more water-wet state induced by the enzyme-brine solution.

This thesis presents an experimental investigation of a new EOR technique for which only a limited amount of published data is available. While we have tried to investigate several possible mechanisms which may help explain why enzymes affect the wettability of silica surfaces and how this contributes to increased oil recovery, the amount of work needed to perform a comprehensive study of each of the mechanisms is beyond the scope of one PhD thesis. Directions for future work would be both to investigate whether it is mainly the protein nature or the enzyme nature (i.e. catalysis of chemical reactions) which contributes to wettability alteration, and to expand the study to cover more enzymes targeting other functional groups.

Appendix A Material

A.1 Solid

Core plugs:

Seven sandstone core plugs including four short, B1, B2, B3 and B4 and three long, LB1, LB2 and LB3 were cut from two blocks of Berea sandstone, respectively. Five carbonate cores from Middle East, S-889 and Th1-Th4 also used in core flooding experiments. Physical properties of all sandstone and carbonate cores are reported in Table A.1.

Table A.1: Physical properties of sandstone and carbonate core samples

Core ID	Length(cm)	Diameter(cm)	Porosity(%)	PV(ml)	Swi	Soi	Abs. Kw(mD)	Ko,Swi(mD)
B1	5.83	3.725	22.27	14.14	0.18	0.82	620.8	645.0
B2	5.91	3.725	21.81	14.04	0.18	0.82	632.4	662.2
B3	5.7	3.725	21.60	13.41	0.18	0.82	575.7	617.0
B4	5.9	3.725	21.66	13.85	0.18	0.82	618.5	555.3
LB1	29.9	3.775	18.40	61.55	0.22	0.78	140.4	166.6
LB2	30.2	3.770	17.67	59.54	0.19	0.81	88.6	101.0
LB3	30	3.775	18.45	61.91	0.24	0.76	137.6	151.2
S-889	4.42	3.725	23.40	11.38	0.12	0.88	28.0	2.5
Th1	4.52	3.770	27.00	13.60	0.23	0.77	11.4	4.6
Th2	5.04	3.780	27.30	15.50	0.19	0.81	5.0	3.1
Th3	5.03	3.800	24.40	13.90	0.21	0.79	5.4	4.4
Th4	5.05	3.790	26.80	15.25	0.19	0.81	5.4	3.7

Glass slides

Glass microscope slides (28×48) from Menzel-Gläser, Germany were used in the adhesion and contact angle experiments. Table A.2 shows chemical composition of the glass plates.

Table A.2: Chemical composition of the glass slides used for adhesion and contact angle experiments

Material	SiO ₂	Na ₂ O	K ₂ O	CaO	MgO	Al ₂ O ₃	Fe ₂ O ₃	SO ₃
Content (%)	72.2	14.3	1.2	6.4	4.3	1.2	0.03	0.3

Silica and Kaolin

Silica and kaolin powder were used in adsorption experiments. Table A.3 shows the specification of both.

Table A.3: Properties of silica and kaolin powder

Type of soild	Supplier	Product code	Mean particle size (μm)*	BET surface area (M^2/g)*
Silica1	US Silica	MIN-U-SIL	4.7	3.65
Silica2	Degussa	FK 310	5.5	650
Kaoline	Sigma-Aldrich	K1512	---	10.6

* obtained from supplier

A.2 Oil

Two types of stock tank oil, A and B (see Table A.4) from two oil reservoirs in the North Sea were used in the static experiments. Both oils were filtered through a 0.5 μm filter to remove any coarse particles prior to use. Crude oil A and B was used also for dynamic displacement in core S-889 and all sandstone core plugs, respectively. A crude oil from Middle East provided by Shell Oil Company was used for dynamic displacement in cores Th1-Th4. The composition of the crude oil was not provided.

Table A.4: Properties of the crude oil

Crude oil ID	Density at 20°C (g/ml)	Viscosity at 20°C (mPa·s)	Acid number (mg KOH/g oil)	Base number (mg KOH/g oil)
A	0.8436	51*	0.123	1.096±0.05
B	0.8784	13.8*	2.84±0.01	0.95±0.10

* at shear rate 100 (s^{-1})

Model oil (mineral oil) was also used in the measurements in this research study. The model oil consists of 98 wt% isooctane, 1wt% decane and 1% ester. Table A.5 shows specifications of the model oil contents.

Table A.5: Specification of model oil component

Type of soild	Supplier	Purity (%)	ρ (g/cm ³) @ 25° C
Isooctane	Rathburn Chemicals	99	0.692
Decane	Sigma-Aldrich	99	0.730
Ethyl decanoate (ester)	Sigma-Aldrich	99	0.862

A.3 Brine

Synthetic sea water (SSW) was used in all static and dynamic experiments (except in dynamic displacement of cores Th1-Th4). Table A.6 shows the composition of the used brines.

Table A.6: Composition of brine used for sandstone and carbonate cores

Chemical compound	Na ⁺	Ca ²⁺	Mg ²⁺	Cl ⁻	HCO ₃ ⁻	SO ₄ ²⁻	K ⁺
Concentration of ions (ppm), brine (SSW) used for static experiments and dynamic displacements of sandstones and S-889	11156	471	1330	20128	139	2743	350
Concentration of ions (ppm), brine used for Th1-Th4	49933	14501	3248	111810	162	234	---

A.4 Enzyme-Protein

Seven types of enzyme-proteins, Zonase1, Zonase2, Greenzyme, NZ2, NZ3, NZ6 and Alpha-lactalbumin were used in this study.

Zonase 1 and 2 were provided by a company located in Bergen, Norway. Zonase is a protease enzyme, derived from the hatching fluid of salmon. It helps the fish embryo getting out of its eggshell. The eggshells are made as a tough, fibrous protein structure, and the fish larva is not able to get out by using mechanical power. Zonase helps to digest the eggshell without harming the larva, and thereby allowing the fish to be born. According to ABT research study, Zonase is stable for years and works well in a range of different pH's, the optimum pH for

Zonase is around pH 7.5, however the Zonase is provided in a solution where it is still active at pH as low as 5.0.

Greenzyme is a commercial enzyme consists of enzymes, water and stabilizers (surfactants) (Greenzyme material safety data sheets) Greenzyme is a water-soluble formulation made from DNA-modified proteins extracted from hydrophobic microbes in a batch fermentation process (Moon, 2008).

NZ2, 3 and 6 were provided by a Novozyme, Denmark. They are esterase enzymes cleaving ester bonds. NZ2 and NZ3 are typical lipolytic enzymes attacking triglycerides in position 1 and 3. These enzymes normally work on oil/water interfaces and may thus modify the oil/water interactions occurring there. NZ6 has in addition a more general esterase activity. Alpha-lactalbumin is an important whey protein. Several authors reported activity of this protein at oil, water and solid interfaces by means of different methods such as adsorption measurements (e.g. Halskau et al., 2002; Glomm et al., 2007).

A.5 Surfactant

Four anionic surfactants (internal olefine sulfonate) from Shell research and development with codes O332, O342-c, O342-h and O342-l were used in the experiments. Two types of co-solvent, 2-butanol and 2-pentanol (Isoamyl alcohol) were used in surfactant solutions in the experiments.

Appendix B Method and procedure

B.1 Core displacement experiments

Core samples preparation

Cutting and cleaning:

In the case of sand stone rock: four short core plugs, B1, B2, B3 and B4 from the same block and three long core plugs, LB1, LB2 and LB3 were cut from another block of Berea sandstone.

In the case of carbonate rock: five limestone core plugs from Middle East were used. Since the core plugs were used before, they have to be washed prior to experiment. Therefore core plugs were placed in a soxhlet apparatus and cleaned using hot refluxing toluene and methanol to remove residual hydrocarbons and formation water salts.

All the cores were put in the oven at 80°C until constant weight was achieved.

Saturation, porosity and permeability:

- All the core plugs evacuated by vacuum pump to reach the vacuum pressure less than 2 mbar and then they were saturated 100 % with brine.
- Porosity of the cores was determined from the weight difference of the saturated and dried cores.
- All the cores were installed into proper core holders according to their lengths. Confining pressure was applied around the cores such that it should be at least 10 bars more than the maximum expecting differential pressure during flooding scenarios. For the short cores triaxial-type core holders and 20 bar confining pressure and for the

- Long cores hydrostatic core holders (RES-0011) from ResLab Norway and 30 bar confining pressure were used. It was assumed that brine displaced from the core plug when the initial confining pressure was applied was due to the conformance of the sleeve to the surface of the core plug, and not to any reduction in pore volume.
- To establish an initial water saturation, S_{wi} , high viscosity oil (Marcol 152) was used to displace the brine. After attaining a desirable S_{wi} , Marcol 152 were exchanged with the crude oil by injecting of at least five pore volumes of crude oil into the cores.
- Permeability to crude oil was determined for the cores in both cases, before and after establishing of S_{wi} . The saturation procedure and all the displacements were done at ambient temperature (22°C).

Aging:

In order to establish non water-wet condition in the sandstone cores, all of them were enclosed in core holders and aged in an oven at 90°C for one month. During the aging period, crude oil inside the cores was exchanged with fresh crude oil once a week. After the aging step, the cores were flooded with an additional four pore volumes of freshly filtered crude oil. Cores Th1-Th4 were also aged in the crude oil provided by Shell oil company with the same procedure as sandstone cores at 90°C for 2 weeks.

Spontaneous imbibition of brine and enzyme-brine

Two sandstone cores and two carbonate cores were used to examine spontaneous imbibition of brine, whereby the wetting fluid (brine) spontaneously imbibes into the pore spaces and displaces the less-wetting fluid (crude oil) from the pore spaces of a porous medium.

Cores B3 & Th4 and B4 & Th3 at S_{wi} status were immersed (see Figure B.1) in brine and enzyme-brine respectively to compare the oil production vs time behavior and to see the effect of the enzyme on spontaneous imbibition. The expelled oil was collected and its volume was measured. Results were recorded as the total amount of oil produced at various time intervals.

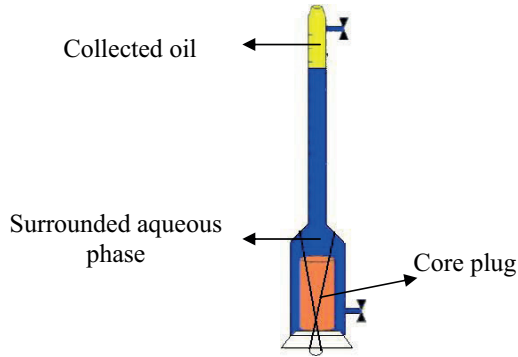


Figure B. 1: Sketch of the Amott-cell. The core sample is located at the bottom of the displacing fluid. Because of the lower density of oil, the displaced oil floats to the top of the Amott-cell.

Waterfloods to Sor:

The displacement tests were performed in all cores, except core B4 and Th1 using brine prior to inject any other solutions. The core flooding apparatus (see Figure B.2) consisted of a Quizix high pressure pump system equipped with a pair of cylinders to provide continuous flow of different fluids into the cores and a separator at the production line to collect and record volumetric production profiles of different phases from the cores. Back pressure regulator was utilized in all core floods for the purpose of avoiding formation of gas. Pressure changes during flooding were also monitored with a FUJI pressure transducer and were logged continuously during injection. All the flooding experiments were performed at ambient temperature (22°C).

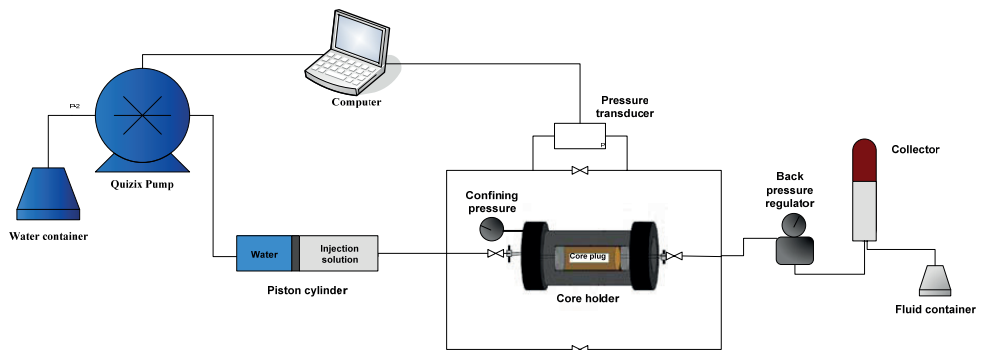


Figure B.2: Core flooding apparatus

The flooding procedure is as follow:

Waterfloods:

- Synthetic formation brine was injected into each core sample as the displacing fluid at a nominal flow rate of 0.1 ml/min.
- Injection flow rates were increased stepwise (bump rates) after 0.1 ml/min injection rate up to 1 ml/min to see the effect of injection rates on oil recovery and to ensure that there is no more oil production by water flooding. Increasing the injection rate also reduce or eliminate the "capillary end effect". This phenomenon may happen during water flooding and decrease oil production from the core.
- Incremental volumes of oil and water produced were recorded as a function of time.
- Waterfloods were terminated at water cuts in all injection steps in excess of 99.95%.
- Permeability to water at residual oil saturation ($k_w @ S_{or}$) was determined.

Waterfloods with added enzyme and surfactant:

- Enzyme-brine solution using different enzymes with various concentrations were injected to the cores with different injection rates and any additional oil production was recorded.
- Enzyme-brine solution was injected until a water cut of 99.95% was achieved.
- Permeability to water at residual oil saturation ($k_w @ S_{or}$) was determined.
- In some cases (core B2) the displacement test was preceded by further injecting of higher concentration of enzymes added to the brine.
- Enzyme-brine solution was injected until a water cut of 99.95% was achieved.
- Permeability to water at residual oil saturation ($k_w @ S_{or}$) was determined.
- In some cases (core LB1 and LB2) enzyme-surfactant-brine solution using identical enzyme as the one which was used in previous flooding step were injected to the cores and any additional oil production was recorded.

- Enzyme-surfactant-brine solution was injected until a water cut of 99.95% was achieved.
- Permeability to water at residual oil saturation ($k_w @ S_{or}$) was determined.

In the case of using enzyme and surfactant, a displacement experiment was performed on a control sample using formation brine-surfactant with no added enzyme. This was to differentiate between the oil productions caused by the enzyme.

B.2 Experiments on the glass plate

Adhesion test:

A drop of crude oil is formed under brine solution by using a micro syringe with an inverted needle as shown in Figure B.3. The volume of the oil droplet can vary, but usually is quite small in the order of few μl . The oil droplet is allowed to contact a smooth solid surface when is submerged in the aqueous phase. After some period of contact between oil and solid surface (about 2 min), the oil droplet is drawn back into the needle. At this stage different behavior may observed as follows:

- Adhesion: Oil droplet leaves the needle and forming a droplet on the underside of the glass.
- Nonadhesion: Oil droplet leaves the glass and hangs on the needle tip.
- Temporary adhesion: Oil drop adherer first to the glass but, leaves the glass and go over to the syringe tip. Adhesion temporary differs from non-adhesion by a small oil stain adherer the glass, although most of the oil has gone over to the syringe tip.

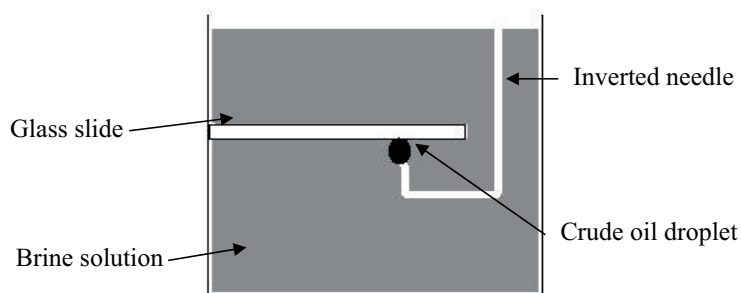


Figure B.3: Equipment setup for performing of adhesion test. An inverted needle pushes the crude oil contacting a glass surface.

Adhesion test was performed on clean and aged glass (at elevated temperature, 80° C). The experiments were performed on a CAM 200 (KSV Instruments, USA) so that oil-drop/water/glass contacts could easily observed. Adjusting the pH of the aqueous solution was done by using hydrochloric acid and sodium hydroxide.

Cleaning procedure of the glass slide

All the glass slides were cleaned and treated identically prior to adhesion measurements. Any contamination on the glass surface can affect the adhesion behavior. In addition, washing with various chemicals will give different surface charges which affect the adhesion behavior (Buckley, 1996). Thus, it is important that all the glass slides adjust to the same state before measurement.

To wash the glass slides using for adhesion measurements, a standard washing procedure given by Buckley (1996) was used. Using this procedure can also provide the opportunity to compare results with other works which have done by other researchers.

The washing procedure was as follow:

1. Glass plates were cleaned for 15 minutes in ultrasonic bath in the solution with 9 parts hydrogen peroxide (35%) and 1 part ammonium hydroxide (25%).
2. Glass plates were taken out of the cleaning solution and washed extensively with distilled water.
3. Glass plates were soaked in measurement brine solution for several days.

Contact angle measurement

Contact angle measurement method was used to estimate wetting properties of a localized region on the solid surfaces in presence of different types of liquid. Since this method can quantify the wettability, wettability alteration of a solid surface can be distinguished simply. The KSV camera 100 (see Figure B.4) was used to measure the water-oil contact angle based on sessile drop technique. A Hamilton micrometer (1 ml) inverted syringe was used to deposit the droplets on the glass slides. All experiments were performed at ambient conditions.



Figure B.4: KSV camera 100

Procedure

To see the effect of the enzymes on the contact angle, some experiments were done with different types of enzymes. The results were compared to reference contact angles performed with untreated brine, i.e. brine without added enzymes. In the experiments, different weight percentages (0-2%) of the enzymes were used as the heavier (aqueous) phase and crude oil A and B as the lighter phase. The oil droplets were deposited on the glass surface surrounded by the aqueous phase, and gave a dynamic water receding condition by displacing the water from the surface. In each experiment, after deposition of the oil droplet on the surface and waiting for a while (approximately 2 min) to stabilize the droplet, images of the water-oil contact angle were taken at 5 second intervals. For each concentration 7-10 parallel droplets have been examined, 10 images were taken of each droplet. It means that for each droplet there were about 70-100 measurements. So, each reported data point in reported tables in chapter 7 is the average of all measured data that represents a static equilibrated contact angle (θ_{ER}) initiated by a water receding angle. The experimental error of the contact angle is estimated to $\pm 4^\circ$.

In the second group of experiments, glass plates aged in crude oil A and B for about 30 days at 80°C were used as the solid surface when crude oil A and B were used as the probe respectively. Using aged glass plates had some advantages such as more stable oil droplets on the solid surface and more visible effect of the enzymes on the contact angles. To use the aged glass plates for the contact angle measurements, bulk crude oil must first be rinsed off. This was done by gently rinsing with Toluene, soaking in fresh Decane (about 2 min) and finally rinsing with distilled water (Liu and Buckley, 1997). It should be noted that this procedure is

not unique, as it depends to what extent adsorbed material is removed by rinsing with toluene. As a result, variation in the reference contact angle was observed.

B.3 Adsorption measurement

UV spectroscopy was done in the lab in order to measure adsorption of enzyme-proteins onto solid surfaces. This method deals with electromagnetic spectrum. The electromagnetic spectrum ranges from very short wavelengths (including gamma and x-rays) to very long wavelengths (including microwaves and broadcast radio waves). Most of the radiation that surrounds us cannot be seen, but can be detected by dedicated sensing instruments. The visible spectrum constitutes just a small part of the total radiation spectrum. On the immediate high energy side of the visible spectrum lays the ultraviolet, and on the low energy side is the infrared (see Figure B.5).

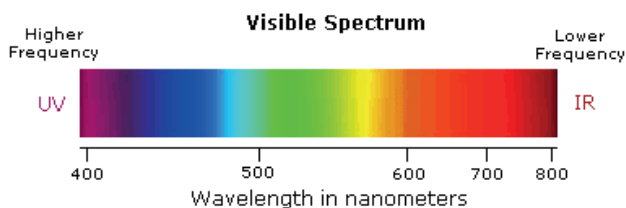


Figure B.5: The visible part of the electromagnetic spectrum and designated wavelengths

Theory and Procedure

Two types of enzyme were selected among all enzymes, Greenzyme and NZ2 from Novozyme group. First of all, absorbance of the UV light by enzyme should be checked. For this purpose Perkin Elmer-Lambda 25 UV/Vis spectrometer was employed. Figure B.6 shows the components of this spectrometer. The functioning of this instrument is relatively straightforward. A beam of light from a visible and/or UV light source (colored red) is separated into its component wavelengths by a prism or diffraction grating. Each monochromatic (single wavelength) beam in turn is split into two equal intensity beams by a half-mirrored device. One beam, the sample beam (colored purple), passes through a small transparent container (cuvette) containing a solution of the enzyme being studied in brine. The other beam, the reference (colored blue), passes through an identical cuvette containing only brine. The intensities of these light beams are then measured by electronic detectors and

compared. The intensity of the reference beam, which should have suffered little or no light absorption, is defined as I_0 . The intensity of the sample beam is defined as I .

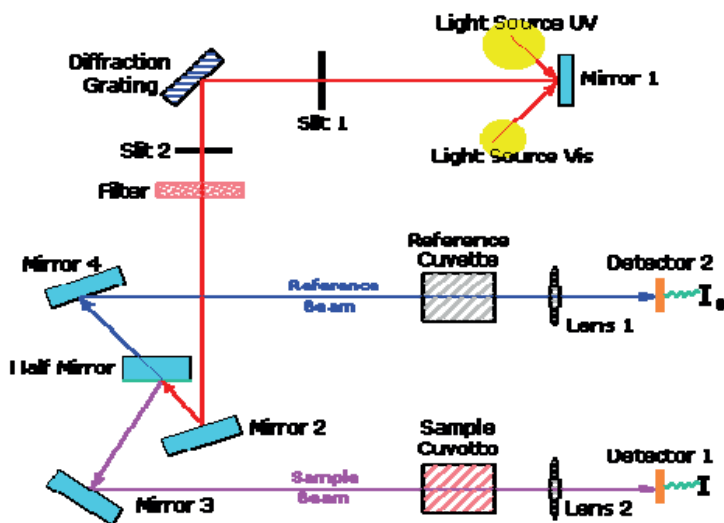


Figure B.6: components of UV spectrometer

Over a short period of time, the spectrometer automatically scans all the component wavelengths in the manner described. The ultraviolet (UV) region scanned is normally from 200 to 400 nm, and the visible portion is from 400 to 800 nm. If the sample compound does not absorb light of a given wavelength, then $I = I_0$. However, if the sample compound absorbs light then $I < I_0$, and this difference may be plotted on a graph versus wavelength, as shown in Figure B.7.

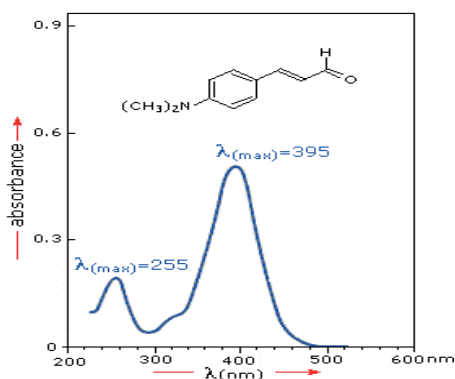


Figure B.7: Typical plot of absorbance vs wavelength

Absorption may be presented as transmittance ($T = I/I_0$) or absorbance ($A = \log I_0/I$). If no absorption has occurred, $T = 1.0$ and $A = 0$.

Different concentration of enzymes in brine were prepared and used in the spectrometer to see the behavior of the compound. Figure B.8 and B.9 are examples of the behavior of the Greenzyme and NZ2 solutions for 1wt% concentration respectively in UV spectrometer where different wavelengths has plotted versus absorbance, A.

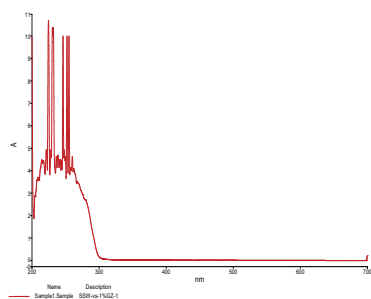


Figure B.8: UV spectroscopy for 1% Greenzyme-brine solution

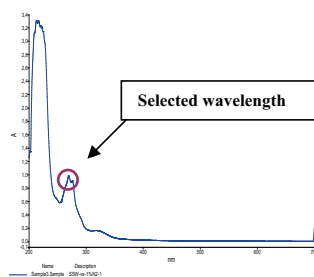


Figure B.9: UV spectroscopy for 1% NZ2-brine solution

As figures show, for the Greenzyme, there is no absorbance except for low wavelength (<200 nm) area that shows fluctuation in absorbance compare to NZ2 and the position of those fluctuations are not identical for different concentration of Greenzyme solution. However, for the NZ2 solution all the plots regarding to different concentration shows the same trend and identical peak locations. It could be resulted that Greenzyme solution is not suitable for UV spectrometer to study the enzyme absorbance on the solid surfaces. Since NZ2 shows a UV active behavior, we can make a reference curve which is correlation between different enzyme concentration and intensity for a specific wavelength.

To make a reference curve for the NZ2 solution, intensity of 269nm (see Figure B.9) wavelength were selected for different concentration of NZ2-brine solution and plotted versus adsorption. The correlation is shown in Figure B.10 below.

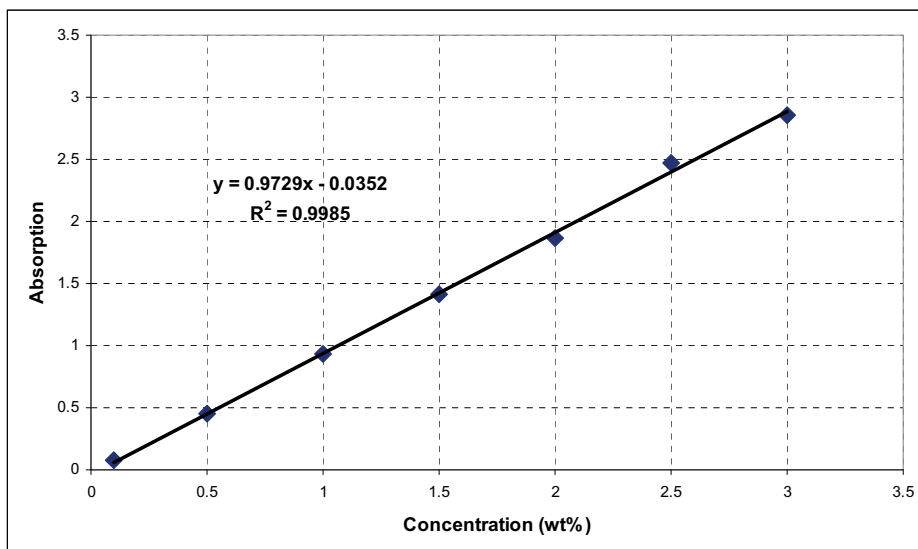


Figure B.10: Correlation between adsorption and NZ2 concentration at 269nm wavelength

To examine any adsorption of the NZ2 enzyme onto the solid surfaces, kaolin and two types of silica powder with total surface area of 10.6, 3.65 and 650 (m^2/g) respectively were selected to use for the static adsorption tests. Different weight percentage of the Silica and Kaolin were mixed with different concentration of the NZ2-brine. The mixtures were shaken for 48 hours. All the samples were centrifuged at 5000 rpm for about 30 min afterward and transparent liquid part were used for the measurements. The measurement error is estimated to be about 5%.

B.4 Interfacial tension (IFT) measurement

Interfacial tension (IFT) is the surface free energy that exists between two immiscible liquid phases, such as oil and water. IFT is an important factor that has influence over different forces in oil reservoirs and consequently oil recovery.

Two complementary techniques were used in this study to measure IFT. High to moderately low (around 1.0 mN/m) IFTs were measured by pendant drop technique whereas moderately low to ultralow IFTs were measured by spinning drop technique.

Procedure

Different types of enzyme-protein were used to add to the brine phase in different concentrations and contacted with different types of oil including crude oil and mineral oil to see the effect of enzyme-proteins on interfacial activity between aqueous and oleic phases. The oils were equilibrated with aqueous phase prior to measurements. Aqueous phase and oil with a 1:1 volume ratio were allowed be stabilization either by shaking for 3 days, and then storing horizontally for 2 days or only storing horizontally (and shaking occasionally) for a certain time at room temperature (it has mentioned in the text in this case). In case of using surfactant into solutions, spinning drop technique was used to measure IFT. All the measured IFT by this technique are first contact IFT without any prior equilibration of aqueous and oleic phases. By equilibration of two phases, measuring of IFT was difficult with the instrument because of too much dissolve oleic phase into the aqueous phase.

Pendant drop

The KSV camera 200 pendant drop instrument was used to measure the interfacial tension between oleic and aqueous phases. In this instrument interfacial tension is determined by analyzing the shape of the oil drop hanging from the tip of a syringe. The measurements were done by fitting of the Young-Laplace equation to the drop image. The interfacial tension at the liquid interfaces can be related to the drop shape through the following equation (Hansen and Rødsrud, 1991):

$$IFT = \frac{\Delta\rho \cdot g \cdot R_0^2}{\beta} \quad (B.1)$$

Where, $\Delta\rho$ is the difference in density between fluids at interface; g is gravitational constant; R_0 is radius of drop curvature at apex and β is the shape factor which can be defined through the Young-Laplace equation expressed as three dimensionless first order equations (see Figure B.11) and can be calculated by computational methods using iterative approximations.

$$dX / dS = \cos \phi$$

$$dZ / dS = \sin \phi$$

$$d\phi / dS = 2 + \beta Z - \sin \phi / X$$

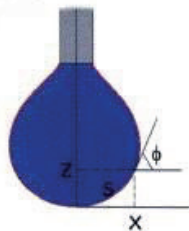


Figure B.11: three dimensionless first order equations to define the shape factor

In the experiments, for each concentration 6-8 parallel droplets have been examined, 10 images were taken of each droplet. It means that for each droplet there were about 60-80 measurements. So, each reported data is the average of all measured data that represents IFT between oleic and aqueous phases. The experimental error of the IFT is estimated to ± 0.5 mN/m.

Spinning drop

Krüß SITE100 (Germany) spinning drop tensiometer, with software DSA 2 (version 2.2) was employed to measure IFT between oleic and aqueous phases when its value is lower than the measurement range of pendant drop technique. Measuring range for SITE100 is 10^{-6} to 50 mN/m. The instrument has a circular measuring cell. All measurements were performed with the lens 3/0.07. SITE100 was connected to a Julabo 4 (Germany) bath for temperature control. All measurements were performed at $(25.0 \pm 0.1)^\circ \text{C}$.

Spinning drop method is based on the theory derived by Vonnegut (1942). A drop of a less dense liquid is injected into a container of the denser liquid, and the whole system is rotated with sufficient speed (horizontal). The drop elongates along the axis of rotation and is transformed into a cylindrical shape with hemispherical ends. The interfacial tension opposes the elongation because of the increase in area and a configuration which minimizes system free energy is reached. Measurement of radius, R of the cylindrical shape can be related to interfacial tension if the fluids are gyrostatic equilibrium and if each fluid is stationary relative to the rotating tube (Manning and Scriven, 1977). Gyrostatic equilibrium is achieved at high rotational speeds, so that gravitational forces perpendicular to the axis of rotation is negligible compared to the centrifugal forces.

If the fluid densities are ρ_A and ρ_B , and the angular velocity ω of rotation are known, then interfacial tension can be calculated from the measured drop profile by Vonnegut's formula:

$$\sigma = \frac{(\rho_A - \rho_B)\omega^2 r_m^3}{4} \quad (\text{B.2})$$

It applies to cases that the relationship between droplet length and droplet diameter is greater than 4. Manning and Scriver (1977) reported an uncertainty of 0.4% for the measurement of interfacial tension with a spinning drop.

To measure the IFT, measuring cell filled with the denser phase (aqueous) by using a 3 ml sterile plastic syringe with a 12 cm long needle. It was tilted and spun up to 3000 rpm to get out any air bubbles. Then it was tilted to the horizontal position, and the light phase were added (one drop or more, depending on the system) from a micro syringe with a 12 cm long needle to the system. Then measurement was done by spinning of the cell to the desired rotation speed (rotation speed that gives a minimum of 4 for the ratio of length / height of the droplet). Since phases were not equilibrated prior to measurements, IFT measurements were continued until consistent results achieved.

B.5 Electrophoretic mobility

One of the key factors that can help to illustrate the working mechanism of the enzymes is electrophoretic mobility of the crude oil particles when they are in contact with water at the interface. When an electric field is applied across an electrolyte, migration of electrically charged particles in solution or suspension will occur in a manner that they are attracted towards the electrode of opposite charge (Figure B.12). Viscose forces acting on the particles tend to oppose this movement. The charged particles move with constant velocity when equilibrium is reached between two opposing forces. This velocity commonly is referred to as electrophoretic mobility of the particles. The electrophoretic mobility is directly proportional to the magnitude of the charge on the particle.

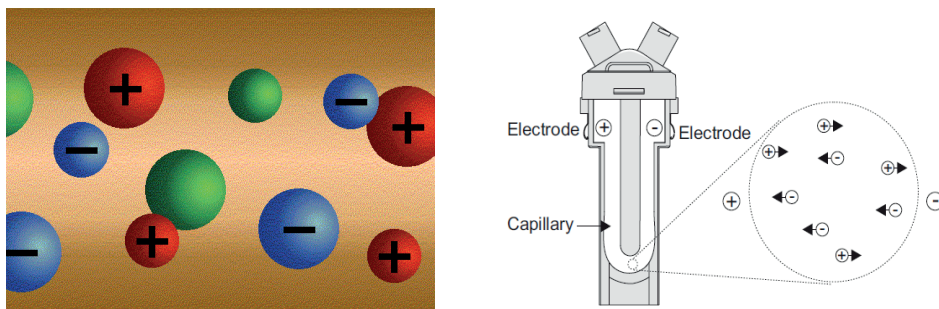


Figure B.12: Schematic of different charged particles in an electrolyte (left) motion of the charged particles by applying an electric field (right)

Procedure

Malvern's Zetasizer Nano instrument, United Kingdom was employed to measure electrophoretic mobility of the tiny crude oil particles in presence of different enzymes into aqueous solution. The essence of an electrophoresis measurement in this instrument is a cell with electrodes at either end to which a potential is applied (see Figure B.12). The velocity of particles which move towards the electrode of opposite charge is measured and expressed in unit field strength as their mobility. This velocity is measured based on Laser Doppler Velocimetry (LDV) technique. In this technique as illustrated in Figure B.13, a laser is used to provide a light source to illuminate the particles within the sample. For electrophoretic mobility measurements this light source is split to provide an incident and reference beam. The laser beam passes through the centre of the sample cell, and the scattering at an angle of 17° is detected. The light scattered at an angle of 17° is combined with the reference beam. This produces a fluctuating intensity signal where the rate of fluctuation is proportional to the speed of the particles. A digital signal processor is used to extract the characteristic frequencies in the scattered light.

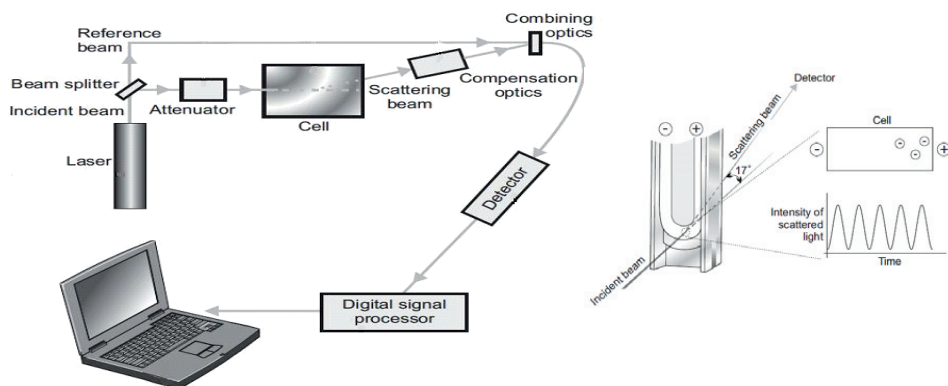


Figure B.13: Laser Doppler Velocimetry (LDV) technique in Malvern's Zetasizer Nano

For all measurements, first, samples of different enzymes with identical concentration of 1wt % in different salinity of brine were prepared. Emulsions of oil in brine were formed at room temperature using a small droplet of the oil in 15 ml of brine. Finally, to have a better emulsion of crude oil into enzyme-brine solutions, all the samples were put in the sonic mixer for about 10 minutes prior to measurements. Three parallels set of measurement were done for each sample, each set measured the electrophoretic three times, i.e. for each sample electrophoretic mobility was measured nine times and average was reported in the results. All the results then compared to the reference sample which was untreated brine without adding any enzyme.

B.6 Gas chromatography

Gas chromatography (GC) is a chemical analysis for separating chemicals components of a complex sample. A small amount of the sample to be analyzed is drawn up into a syringe. The syringe needle is placed into a hot injector port of the gas chromatograph which is at the head of the chromatographic column, and the sample is injected. The injector is set to a temperature higher than the components' boiling points. So, components of the mixture evaporate into the gas phase inside the injector. The gaseous components of the sample is transported through the column by the flow of a carrier gas (mobile phase), such as helium. It is within the column that separation of the components takes place. The column itself contains a liquid stationary phase which is adsorbed onto the surface of an inert solid. The rate at which the molecules progress along the column depends on the interaction of the molecules with the stationary phase which in turn depends on the type of molecule and the stationary

phase materials. The stronger the interaction is the longer the molecules remain attached to the stationary phase, and consequently more time to go through the column. So, the various components of the sample mixture are separated as they progress along the column and reach the end of the column at different times (retention time). A detector is used to monitor the outlet stream from the column to determine amount of each component and the time at which it reaches the outlet. Figure B.14 shows a schematic diagram of a gas chromatograph.

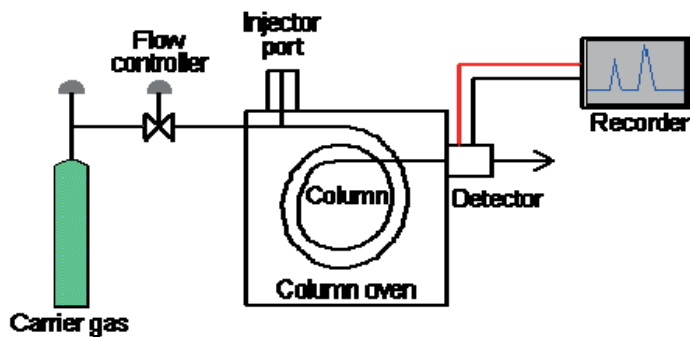


Figure B.14: schematic diagram of a gas chromatograph

Procedure:

Different oils including crude oil and mineral oil were mixed with brine and enzyme-brine solutions with portion of 1:1 and allow be equilibrated afterward. Equilibration was done for the cases of using crude oil just by putting the container of the samples horizontally for two weeks and shakes them occasionally. For the cases of using mineral oil, equilibration was done by shaking the samples continuously for three days. All the oil samples were analyzed by whole oil gas chromatography using a Trace GC (ThermoFinnigan, Germany) equipped with a HP-PONA column (50 m length, 0.2 mm i.d., 0.5 μm film thickness). Helium was used as carrier gas. The oils were injected into an injector at a temperature of 300°C. The flame ionization detector (FID) was kept at 350°C (15 min initial hold time) to 60°C at a rate of 2/3°C/min and then to 320°C (15 min final hold time) at a rate of 4°C/min. Assignment of peaks to specific compounds was done by analysis of the Norwegian Geological Standard oil (NSO-1) and identification of the peaks according to NIGOGA manual (Weiss et al., 2005).

B.7 Isotachophoresis

Isotachophoresis (ITP) is an electrophoretic separation technique used to separate ionic compounds in the water phase without special requirements of sample preparation (Barth

1987). The method is due to migration in an electric field of ion species of the same sign, all having a common counter-ion. The driving force of the separation is the electric current delivered from a constant current, high-voltage unit. An isotachopheric migration is one in which a mixture of ions of similar charge quality separate into discrete zones of regulated concentration in presence of two ionic zones of higher and lower mobility than all ions in the mixture (Holloway and Trautschold, 1982).

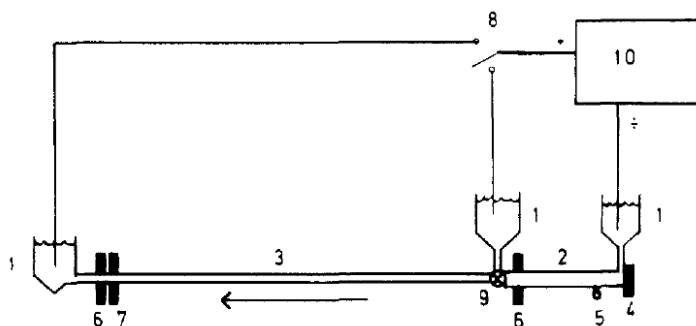


Figure B.15: The ITP apparatus (Tachophor): (1) electrolyte reservoirs; (2) pre-separation channel; (3) analytical capillary; (4) injection port; (5) draining valve; (6) conductivity detectors; (7) UV detector; (8) high-voltage switch; (9) three-way valve; (10) high-voltage, constant current unit (Barth 1987).

Figure B.15 shows a schematic diagram of the ITP apparatus. In ITP, a sample is introduced between two working electrolytes; the leading electrolyte (LE) is chosen to have the highest mobility in the system and the capillary is filled with this electrolyte whereas the second electrolyte, the terminating one (TE), is chosen to have the lowest mobility in the system which is lower than all the target compounds. When the current is applied, the ions are pulled through the system by the potential difference. The different components separate into zones of molecules with equal mobility, ideally consisting of just one compound per zone. The zones are separated in order of decreasing mobility and the separated compounds are detected using a conductivity detector (Barth 1987).

Procedure

Crude oil B was mixed with brine and enzyme-brine solutions with portion of 1:1 and allow be equilibrated afterward. Different type of enzymes-proteins, Greenzyme, NZ1, NZ2, NZ3 and α -La were used in this experiment. The amount of enzyme-protein in enzyme-brine solution was 1wt% except the α -La case which was 0.5wt%. Equilibration was done just by putting the container of the samples horizontally for one month and shakes them occasionally.

Aqueous phase were separated and examine in the ITP apparatus to determine existence of any organic acids caused by enzyme-proteins activity.

The analysis is performed on a LKB 2127 Tachophor (see Figure B.15) with 0.32 mm i.d. analytical quartz capillary. The Tachophor has been rebuilt with a precolumn. The precolumn is a wide-bore (2 mm) channel with a tell-tale conductivity detector at the junction with the capillary analytical column. The analytical column has two detectors, a conductivity detector with linear and differential signal output and a UV detector at 254 nm. A high capacity preseparation loop makes the setup usable for saline water samples with organic acids components detectable beyond a detection limit at approximately 0.1 mM.

B.8 Micromodel experiments

To visualize the effect of enzymes on oil recovery and investigate the mechanism underlying enzyme-brine flooding, micromodel experiments were implemented.

Experimental set-up

Figure B.16 depicts the experimental setup which was used for micromodel study. It can be divided in two main systems according to their functions: a system for flooding through the micromodel, and a system for capturing the images. Descriptions of the main components are as follow:

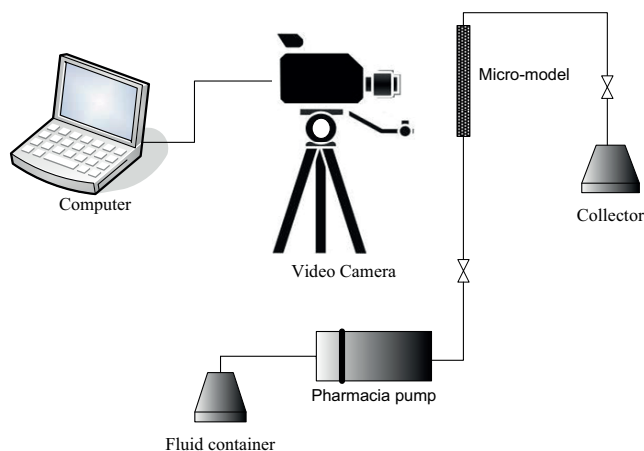


Figure B.16: Schematic diagram of the micromodel setup

Glass micromodel

Figure B.17 shows schematically the glass micromodel used in this study. Construction of the micromodels has previously been described by Chatzis (1982). Conceptually, it is simple in design. Two glass plates are held together where one of the glass plates has a two dimensional detailed flow pattern chemically etched onto it and the other plate is unetched and has parallel sides. This covering plate has inlet and outlet holes drilled at either end, allowing fluids to be displaced through the network of pores. Since the structure of the model is only one pore deep and it is all made of glass, fluids as they flow along the pore channels and their interaction with each other can be observed. It is also possible to observe how the geometry of the pore network affects the patterns of flow and trapping. (Sohrabi et al., 2000)

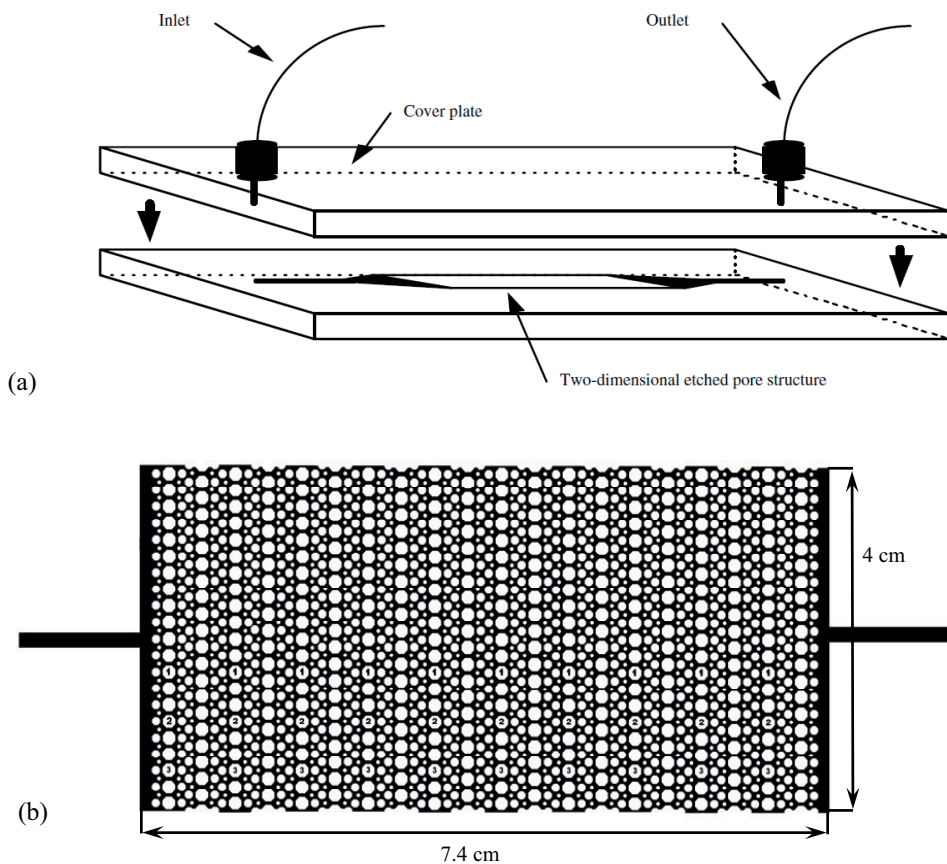


Figure B.17: (a) Schematic of the micromodel structure (Sohrabi et al., 2004) (b) Schematic of full length two-dimensional pore pattern in the micromodel

Various pore patterns can be designed with precise specification of the topology and geometry of the system and used in two-dimensional micromodel experiments. This is the advantage of such models over other idealized porous media, such as packs of glass beads. A disadvantage is that such models do not have topological properties like that in three-dimensional networks (McKellar and Wardlaw, 1982). In this study, an unsymmetrical pattern which is shown in Figures B.18-a and b was used. The pore structure contains pores and pore throats with various sizes. The average depth of etched flow channels was about 100 μm . The pore channels between adjacent grains have a width ranging from 350 to 570 μm . The diameters of small, medium and large grains are 400, 900 and 1450 μm , respectively. Table B.1 shows all the dimension of the micromodel.

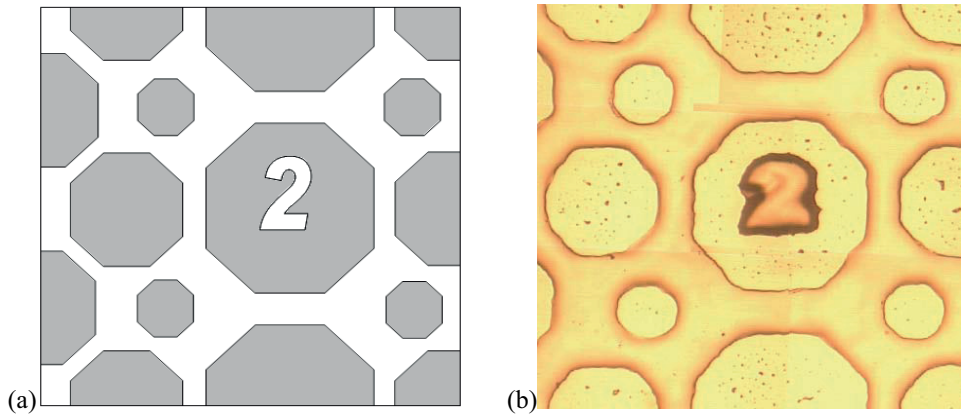


Figure B.18: Illustration of pore pattern in the micromodel; a) designed pore network and b) etched on the glass (Shabani Afrapoli, 2009).

Table B.1: Micromodel Characteristics

Parameter	Micromodel
Length (cm)	7.4
Width (cm)	4
Depth (cm)	1.0×10^{-2}
Porosity (ϕ)	0.44
PV (cm^3)	1.302

Pump

Pharmacia LKB Pump P-500 was used to inject the fluids into the glass micromodel. This pump was capable of a lower rate of 1 ml/hr.

Video Camera

A Canon (EOS 5D) video camera was placed on appropriate distance from the model and connected to a computer, allowing viewing and recording the images from the model. The video camera accompanying especial lenses enabled us to take photos with very high resolution.

Computer and software

A computer was used to store and process the images. Software accompanying the video camera enabled us to connect the camera to the computer and take pictures upon command, and could also be programmed to take pictures at time intervals, which allowed surveillance of one point during prolonged periods without human supervision. An open source image processing program, ImageJ was used to process the images and calculate the oil saturation.

Experimental procedure

Cleaning

The micromodel was cleaned with alternating cycles of methanol, toluene and distilled water prior to each experiment. In case of existence of air inside the micromodel, isopropanol was used into inject to the model and remove the air.

Establishment of the initial conditions

Micromodel was saturated 100 % with brine by continues flooding at the nominal flow rates up to 100 ml/hr. The injection was continued for at least 30 minutes to be sure that the model was completely saturated with brine. The irreducible water saturation (S_{wi}) was then established by injecting crude oil B at the rates up to 30 ml/hr. The Micromodel was kept at S_{wi} condition at ambient temperature for about three days to be aged. It was done to establish a less water-wet condition inside the model.

Flooding experiments

Different sets of experiments were carried out to test the effectiveness of enzyme to reduce oil saturation in micromodel. After establishment of irreducible water saturation, brine was continuously injected at the nominal rate of 1 ml/hr. The brine injection was continued until no more oil was produced and residual oil saturation was reached. The injection scenario was then continued by injecting of 1wt% of enzyme-brine into the model at identical injection rate

as waterflooding. With the continuous capturing of image of the model, it was possible to observe any changes in residual oil saturation and fluid flow patterns.

Appendix C SCA paper

USE OF ENZYMES TO IMPROVE WATERFLOOD PERFORMANCE

Hamidreza Nasiri, Kristine Spildo, and Arne Skauge
Center for Integrated Petroleum Research (CIPR), Bergen, Norway

This paper was prepared for presentation at the International Symposium of the Society of Core Analysts held in Noordwijk aan Zee, The Netherlands 27-30 September, 2009

ABSTRACT

A variety of enhanced oil recovery (EOR) methods have been developed and applied to improve waterflood efficiency. These methods aim at improving both microscopic displacement efficiency and macroscopic reservoir sweep. In addition to reducing residual oil saturation and increasing contact with unswept oil, fluid flow improvement has also been a focus of EOR technologies. A change in wettability may lead to a favorable change in fluid flow properties. Another significant focus has been to improve spontaneous imbibition to enhance oil recovery from matrix rock in fractured reservoirs.

We have been investigating to what extent enzymes-proteins can change the wettability state of an oil reservoir formation and possibly lead to increased oil recovery by waterflooding. Enzymes consist of water soluble proteins which may act as catalysts and encourage interactions between oil and water that may release oil from the grain faces of a porous medium.

This work reports the results of contact angle measurements to quantify the changes in wettability resulting from different concentrations of enzyme-in-brine solutions. Several different enzyme-protein mixtures have been investigated. The experimental results confirm a considerable decrease in contact angle with enzyme solutions compared to an untreated brine. In all cases, the change due to added enzymes was towards a more water-wet state. The paper will also discuss core flood results using enzyme-in-brine solutions for waterflooding Berea sandstone cores aged in crude oil.

INTRODUCTION

Wettability has been the object of much research. Several papers have discussed the influence of wettability on oil recovery. The major factor which controls the location, flow, and distribution of fluids in a reservoir is wettability [1]. Wettability is a significant issue in multiphase flow problems ranging from oil migration from source rocks to such enhanced recovery processes as chemical flooding or alternate injection of CO₂ and water [2]. Several researchers attempt to alter the wettability favorably in the oil reservoirs to improve spontaneous imbibition of water and also the waterflood in order to enhance oil recovery. Austad et al. [3] and Xu et al. [4] reported different production profiles using surface active agents to enhance spontaneous imbibition into chalk cores and ascribed this difference in behavior to the change of wettability by surface active agents. Several authors [5-7] have reported effects of brine composition on wettability change and Alagic and Skauge [8] demonstrated the use of low salinity water plus surfactant to change wettability and improve oil recovery.

Enzymes-proteins can be introduced to improve waterflood performance especially in oil-wet reservoirs by changing the wettability to a more water-wet state and possibly lead to increased

oil recovery [9]. Enzymes are a specific group of globular proteins that are synthesized by living cells to work as catalysts for the many thousands of biochemical reactions such as break down or synthesis of certain compounds. Like all catalysts, enzymes work by lowering the activation energy of a reaction, thus dramatically accelerating the reaction rate [10-11]. Chemical catalysts display only limited selectivity; whereas enzymes show specificity for the substrates and also products, which ensure that the final product is not contaminated with by-products. Enzymes with broad specificity have more flexible active site requirements and can therefore accept a wider range of substrate molecules [10-11].

Use of different types of enzymes in industrial application started many years ago. Use of enzyme processes in the oil and gas industry context has, however, only been suggested recently. Enzyme applications were reported in the oil industry in different categories such as removing damage by disrupting filter-cake formation in drilling; enzyme base acid production; sand consolidation; desulphurization of hydrocarbons containing high levels of sulphur; and water shut-off [12]. Feng et al. [9] also reported the use of enzymes to improved oil recovery at laboratory and field scales.

This paper presents the results of a study to provide improved insight into the impact of enzyme-protein type reactions in porous media. The specific objectives were to: (1) evaluate the results of the static experiments such as contact angle and interfacial tension measurements, (2) determine key parameters that may govern the process, and (3) perform core flood experiments to investigate wetting change and possible oil mobilization. The paper is divided into two parts; the first presents a review of static experiments and results thereafter, the paper presents and discusses the core flooding experiments.

EXPERIMENTAL

Materials

Solid

Four core plugs, B1, B2, B3 and B4 were cut from the same block of Berea sandstone. Physical properties of the cores are reported in Table 1.

Glass microscope slides (28×48) from Menzel-Gläser, Germany were used in the experiments to measure the contact angle.

Oil

Two types of stock tank oil, A and B (Table 2) from two oil reservoirs in the North Sea were used in the static experiments. Both oils were filtered through a 0.5 µm filter to remove any coarse particles prior to use. Based on acid and base numbers, cores were aged in crude Oil B and then waterflooded [13-14].

Brine

Synthetic sea water (SSW) was used in all static and dynamic experiments. Table 3 shows the composition of the used brine.

Enzyme-Protein

Three types of enzymes, Zonase1, Zonase2 and Greenzyme were used in the static experiments. Zonase 1 and 2 were provided by a company located in Bergen, Norway. Detailed specifications of Zonase 1 and 2 were not available because of company restrictions. Another type of enzyme, Greenzyme was also used in the experiments. Greenzyme is a water-

soluble formulation made from DNA-modified proteins extracted from hydrophobic microbes in a batch fermentation process [15]. Among mentioned enzymes, Greenzyme was selected for use in dynamic experiments.

Procedures

Contact Angle

The KSV camera 200 was used to measure the water-oil contact angle based on sessile drop technique. A Hamilton micrometer (1 ml) inverted syringe was used to deposit the droplets on the glass slides. All experiments were performed at ambient conditions. To see the effect of the enzymes on the contact angle, some experiments were done with three different types of enzymes. The results were compared to reference contact angles performed with untreated brine, i.e. brine without added enzymes. In the experiments, different weight percentages (0-2%) of the enzymes were used as the heavier (aqueous) phase and crude oil A and B as the lighter phase. The oil droplets were deposited on the glass surface surrounded by the aqueous phase, and gave a dynamic water receding condition by displacing the water from the surface. In each experiment, after deposition of the oil droplet on the surface and waiting for a while (approximately 2 min) to stabilize the droplet, images of the water-oil contact angle were taken at 5 second intervals. For each concentration 7-10 parallel droplets have been examined, 10 images were taken of each droplet. It means that for each droplet there were about 70-100 measurements. So, each reported data point in Tables 4-9 is the average of all measured data that represents a static equilibrated contact angle (θ_{ER}) initiated by a water receding angle. The experimental error of the contact angle is estimated to $\pm 4^\circ$.

In the second group of experiments, glass plates aged in crude oil A and B for about 30 days at 80°C were used as the solid surface when crude oil A and B were used as the probe respectively. Using aged glass plates had some advantages such as more stable oil droplets on the solid surface and more visible effect of the enzymes on the contact angles. To use the aged glass plates for the contact angle measurements, bulk crude oil must first be rinsed off. This was done by gently rinsing with Toluene, soaking in fresh Decane (about 2 min) and finally rinsing with distilled water [16]. It should be noted that this procedure is not unique, as it depends to what extent adsorbed material is removed by rinsing with toluene. As a result, variation in the reference contact angle was observed (see Tables 5-7 and 9).

IFT

The KSV camera 200 pendant drop instrument was used to measure the interfacial tension between crude oil and brine. The crude oils were equilibrated with brine prior to measurements. Brine and crude oil with a 1:1 volume ratio were shaken for 3 days, and then stored horizontally for 2 days at room temperature to allow be stabilization.

Viscosity

The MCR300 delivered by Physica, Anton Paar, which is a shear rate controlled rheometer equipped with two different sets of geometry was employed to measure viscosity.

For viscosity lower than $10\text{ mPa}\cdot\text{s}$ the concentric cylinder geometry, DG26.7/T200/SS, with 23.83 mm and 27.59 mm internal and external radius respectively was used. The temperature was controlled by a Peltier water circulating/heat-regulating apparatus ($\pm 0.1^\circ\text{C}$), mounted on 78210 TEZ 150 P cell.

For viscosities higher than 10 mPa·s which is rheological characterization of crude oil samples, CP75-1 cone plate-to-plate geometry with 74.987 mm diameter and 0.994 ° angle was used. This time, the Peltier element was coupled with CF80 TEK 150 P-C cell to stabilize temperature during measurements.

Dynamic Displacement Tests

Preparation

All the cores were put in the oven at 60°C for about 72 hours to ensure that they were totally dried. Vacuum pump was used to saturate the cores 100 % with brine. Porosity of the cores was determined from the weight difference of the saturated and dried cores. All the cores were installed into triaxial-type core holders with 20 bars confining pressure. To establish an initial water saturation, S_{wi} , high viscosity oil (Marcol 152) was used to displace the brine. After attaining a desirable S_{wi} , Marcol 152 were exchanged with the crude oil by injecting of at least five pore volumes of crude oil into the cores. Permeability of the cores was determined in both cases, before and after establishing of S_{wi} . The saturation procedure and all the displacements were done in ambient temperature (22°C).

In order to establish non water-wet condition in the cores, all the cores were enclosed in core holders and aged in an oven at 80°C for one month. During the aging period, crude oil inside the cores was exchanged with fresh crude oil once a week. After the aging step, the cores were flooded with an additional four pore volumes of freshly filtered crude oil.

Spontaneous Imbibition of Brine

Two cores were used to examine spontaneous imbibition of brine, whereby the wetting fluid (brine) spontaneously imbibes into the pore spaces and displaces the less-wetting fluid (crude oil) from the pore spaces of a porous medium.

Cores B3 and B4 at S_{wi} status were immersed in brine and enzyme-brine respectively to compare the oil production vs time behavior and to see the effect of the enzyme on spontaneous imbibition. The expelled oil was collected and its volume was measured. Results were recorded as the total amount of oil produced at various time intervals.

Core Flooding

The displacement tests were performed in four sandstone cores using brine, enzyme-brine and crude oil B. The core flooding apparatus consisted of a Quizix high pressure pump system equipped with a pair of cylinders to provide continuous flow of different fluids into the cores and a separator at the production line to collect and record volumetric production profiles of different phases from the cores. Pressure changes during flooding were also monitored with a FUJI pressure transducer and were logged continuously during injection.

A nominal flow rate of 0.1 ml/min was used to inject brine into cores B1-B3, followed by higher injection rates of brine to ensure that there is no more incremental oil production. While core B1 and B2 started from S_{wi} , core B3 had been used to measure spontaneous imbibition of brine prior to the waterflooding sequence. After waterflooding to residual oil saturation, 1wt% GZ-brine solutions were injected into the cores to see the effect of enzyme on the oil production. Core B2 was further flooded with a 10wt% GZ-brine solution to see if increasing the enzyme concentration had an effect on oil recovery. Core B4, for which spontaneous imbibition of 1wt% GZ-brine had been measured, was injected with the enzyme-brine solution directly. All the flooding experiments were performed in ambient temperature (22°C).

RESULTS AND DISCUSSION

Contact Angle Measurements

Crude oil A

Table 4 shows the results for crude oil A with glass slides without any aging as the solid surface and brines with different Greenzyme concentration as the aqueous phase. As the results clearly show, the difference in contact angle with and without enzyme is in some cases about 30° which is quite significant. The dimensionless term $\Delta\theta/\theta_{REF}$ was defined, where $\Delta\theta$ is $\theta_{REF} - \theta_{ENZYME}$ and θ_{REF} is the contact angle measured with a brine phase without added enzyme. As the concentration of Greenzyme increases, the change in contact angle is more visible and $\Delta\theta/\theta_{REF}$ increases accordingly to reach a plateau of roughly 0.5 at 0.75 wt% Greenzyme (Figure 1).

In the second group of experiments, glass aged in crude oil A for about 30 days at 80°C was used as the solid surface. This showed a more visible effect of the enzymes on change of the contact angle. Different enzymes with different concentration were examined in this group of experiment. Table 5-7 show the results for different types of enzyme. Unlike the first group of experiments, the reference contact angle in the second group is different in all cases. The main reason is the washing procedure for the aged glass plates as described earlier.

To examine the effect of enzyme on glass slides with different wettability states, identical concentration of enzymes was used in some cases for different reference contact angles. Results for Greenzyme (Table 5) show a significant change in contact angle by adding enzyme. However for reference contact angles > 90 degrees the effect of enzyme on the contact angle seems to decrease. Results for Zonase1 (Table 6) were not promising except for high concentrations. Using Zonase2 (Table 7) resulted in changes in contact angle, but less pronounced than for Greenzyme at the same concentration and for comparable reference contact angles.

Crude oil B

Greenzyme was selected for use in experiments with crude oil B. Tables 8 and 9 show the results for glass and aged glass as solid surfaces respectively. According to the results, contact angle changes are almost the same independent of concentration, for the case using ordinary glass without aging. For the case of aged glasses, reference contact angles vary. For the cases that have almost similar reference contact angle the changes in contact angle are almost identical and independent of Greenzyme concentration. As an example, for the concentration of 1 and 0.01 wt% of Greenzyme in aged glass experiments, $\Delta\theta/\theta_{REF}$ shows almost the same value irrespective of the Greenzyme concentration.

IFT Measurements

Interfacial tension between crude oil (A and B) and brine adding different concentration of Greenzyme was measured. Figure 2 shows the results of the measurements. The Figure shows IFT of 24 and 11 mN/m for the crude oil A and B respectively. According to the Figure, IFT decreases with decreasing Greenzyme concentration for both oils. For crude oil A, the trend levels off at 0.5 wt% concentration at 7mN/m IFT and for crude oil B at 5 mN/m at 1 wt% Greenzyme concentration.

Viscosity Measurements

Viscosity of crude oils, brine and different concentration of GZ-brine solution were measured. It was about 1.1 mPa·s for the brine. According to measurements adding Greenzyme into the

brine solution had no effect on viscosity and was observed to be Newtonian even in the case of adding 10 wt%. Table 2 also shows viscosity of the crude oils.

Dynamic Experiments

According to the results of contact angle measurements, Greenzyme seemed to have larger influence on changing the contact angle than the other two enzymes. So, it was selected among available enzymes for displacement tests. Even though lower concentrations showed good results in contact angle measurements, 1wt% concentration was selected in tests of the effectiveness of Greenzyme.

Brine Flooding Followed by Enzyme-Brine Flooding, Core B1

After continuous injection of brine into core B1, a total oil recovery of 42 % OOIP was obtained after about 10 PV injections. Most of the oil was produced before water break through (WBT) at 0.37 PV (Figure 3). This was followed by flooding with brine containing 1wt% Greenzyme (GZ-brine). Very low rate of oil production was observed after starting the GZ-brine injection. 11 % OOIP incremental oil were produced after 34 PV injections.

Brine Flooding Followed by Different wt% of Enzyme-Brine Flooding, Core B2

Core B2 gave a recovery of 47% OOIP total oil recovery after more than 10 PV of continuous brine injection (Figure 3). Water breakthrough (WBT) happened after injection of 0.33 PV. Although most of the oil was produced before WBT, more oil was produced after WBT compared to core B1. This could be an indication of a more oil-wet condition for core B2 as compared to core B1. The flooding was continued with injection of 1%wt GZ-brine injection. The rate of oil production was low with only 3.5% OOIP additional recovery after more than 40 PV injection. To test the effect of high GZ concentration, this was followed by injection of 10wt% GZ-brine with different injection rates (0.1-0.5 cc/min) into the core. No additional oil was produced after more than 22 PV injection.

Spontaneous Imbibition and Flooding Scenario, Core B3 And B4

Figure 4 shows the results of spontaneous imbibition of brine and GZ-brine into cores B3 and B4 vs dimensionless time, t_D . This scaling group was introduced by Ma et al. [17] to obtain a dimensionless time, t_D , which compensates for differences in rock and fluid properties:

$$t_D = t \sqrt{\frac{k}{\phi}} \frac{\sigma}{\sqrt{\mu_w \mu_o}} \frac{1}{L_c^2} \quad (1)$$

Where t is imbibition time, k permeability, Φ porosity, σ interfacial tension, μ_w and μ_o viscosity to water and oil, respectively, and L_c is the characteristic length (all quantities in consistent units).

In the early stages of oil production by spontaneous imbibition of brine and GZ-brine into the cores, the production rate in core B3 is larger than in core B4. Consequently, after the first minute, oil recovery in core B3 is about 24% OOIP compared to 14% OOIP in core B4. This delay in oil production could be related to Greenzyme reaction time. However, the Figure shows larger total oil production by spontaneous imbibition of GZ-brine in core B4 (43 % OOIP) compared to core B3 (41% OOIP). However the oil recovery difference is 2 % OOIP which is not significant.

Cores B3 and B4 were flooded using different slugs of brine and GZ-brine after spontaneous imbibition. Core B3 was continuously flooded by brine but, there was no further oil production after about 15 PV injection into the core. Injection of GZ-brine was then performed for core B3 using different injection rates. Incremental production of 5.2% OOIP (Figure 5) was attained after 26 PV injection. Core B4 was flooded continuously with GZ-brine using different rates of injection. 5 % OOIP (Figure 5) incremental oil was produced over about 35 PV injection. In both cases, as Figures 5 and 6 show, with the first nominal injection rate (0.1 cc/min) no further oil production was observed, but increase in the rate of injection (0.3-0.5 cc/min) resulted in additional production.

Wettability and Water End Point Permeability

Comparison of brine end point permeability can be used as an indication of wettability. More water-wet behavior shows lower water end point permeability at the same water saturation, S_w . Table 10 shows water endpoint permeabilities at water saturations representative of the different stages of the flooding, i.e. after waterflooding and after flooding with GZ-brine. Comparison of the endpoints before and after 1wt% GZ-brine flooding shows no significant wettability change for cores B1, B2, and B3.

Core B4 which was not exposed to the untreated brine in all stages shows lower end point permeability than other cores with respect to related S_w which is almost in the same range of others. Core B2 showed lower end point permeability (29 mD) after 10wt% GZ-brine flooding compared to after flooding with 1wt% GZ-brine (60 mD), even though no additional oil was produced. Decrease in the water endpoint permeability in the case of 10wt% GZ-brine flooding without any change in saturation unit of brine (no oil production) may indicate that the core was becoming more water-wet.

CONCLUSION

Contact angle measurements indicate more water-wet behavior with enzymes solution, especially for Greenzyme (GZ).

Interfacial tension between crude oil and brine solution containing enzymes shows somewhat lower values compared to untreated brine, but adding enzymes into the brine has no effect on brine viscosity.

Results of spontaneous imbibition of untreated brine and GZ-brine show delayed imbibition of GZ-brine in the early stages, but higher total oil production.

Additional oil recovery from 3.5% to 11% OOIP was obtained by injection of the enzyme solution into the cores.

Endpoint permeability of the cores indicate little change in wettability of the cores after flooding with GZ-brine, except for the core B4 that was never exposed to untreated brine and core B2 when 10% GZ concentration was used as the displacing fluid.

For the cores in this study, less change in wettability than expected was observed which could be due to the rather water-wet behavior being exhibited even after the aging period.

ACKNOWLEDGEMENTS

Thanks to the Petromaks program at the Norwegian Research Council for financial support.

NOMENCLATURE

PV	pore volume
OOIP	original oil in place
SSW	synthetic sea water
WBT	water breakthrough
S_{wi}	Irreducible water saturation
θ_{REF}	Contact angle measured with a brine phase without added enzyme
θ_{ENZYME}	Contact angle measured with a brine phase added different enzyme concentrations
$\Delta\theta$	difference between θ_{REF} and θ_{ENZYME}
θ_{ER}	static equilibrated contact angle initiated by a water receding angle
IFT	interfacial tension
t	imbibition time
k	permeability
Φ	porosity
σ	interfacial tension
μ_w	viscosity of water
μ_o	viscosity of oil
L_c	characteristic length

REFERENCES

- 1) Anderson, W.G., Wettability literature survey - Part 1-a: Rock/ Oil/ Brine interactions and the effects of core handling on wettability. JPT, 1986: p. 1125-44.
- 2) Morrow, N.R., Wettability and its effect on oil recovery. JPT, 1990: p. 1476-84.
- 3) Austad, T., et al., Chemical flooding of oil reservoirs 8. Spontaneous oil expulsion from oil- and water-wet low permeable chalk material by imbibition of aqueous surfactant solutions. Colloids and Surfaces, 1998. 137: p. 117-129.
- 4) Xu, W., S.C. Ayirala, and D.N. Rao, Experimental investigation of oil compositional and surfactant effects on wettability at reservoir conditions, in Society of Core Analysts. 2005, SCA: Toronto, Canada.
- 5) Morrow, N.R., et al., Prospects of improved oil recovery related to wettability and brine composition. Journal of Petroleum Science and Engineering 1998. 20: p. 267-276.
- 6) Yu, L., et al., Analysis of the Wettability alteration process during seawater imbibition into preferentially oil-wet chalk cores, in Society of Petroleum Engineering. 2008, SPE: Oklahoma, USA.
- 7) Zhang, P., M.T. Tweheyo, and T. Austad, Wettability alteration and improved oil recovery by spontaneous imbibition of seawater into chalk: Impact of the potential determining ions Ca^{2+} , Mg^{2+} , and SO_4^{2-} . Colloids and Surfaces, 2007. 301: p. 199-208.
- 8) Alagic, E. and A. Skauge, Change to low salinity brine in combination with surfactant flooding, in EAGE, IOR 2009. 2009, EAGE: Paris, France.
- 9) Feng, Q.-x., et al., EOR Pilot Tests with modified enzyme in China, in SPE Europe/EAGE. 2007, SPE: London, United Kingdom.
- 10) Blackburn, S., Enzyme structure and function. Enzymology. 1976, Leeds, England: Marcel Dekker INC.
- 11) Reiner, J.M., Behavior of enzyme systems. Second edition ed. 1969, Albany, New York: Van Nostrand Reinhold Company.
- 12) Harris, R.E. and I.D. McKay, New applications for enzymes in oil and gas production, in SPE European Petroleum Conference. 1998, SPE: Hague, Netherlands.

- 13) Skauge, A., et al., Effects of organic acids and bases, and oil composition on wettability, in SPE. 1999, SPE: Houston, Texas, USA.
- 14) Xie, X., N.R. Morrow, and J.S. Buckley, Contact angle hysteresis and the stability of wetting changes induced by adsorption from crude oil. *Petroleum Science and Engineering*, 2002. 33: p. 147-159.
- 15) Gray, J., Using enzymes to enhance oil recovery in JPT online. 2008, SPE.
- 16) Liu, Y. and J.S. Buckley, Evolution of wetting alteration by adsorption from crude oil in SPEFE. 1997, SPE: Texas, USA.
- 17) Ma, S., N.R. Morrow, and X. Zhang, Generalized scaling of spontaneous imbibition data for strongly water-wet systems. *Journal of Petroleum Science and Engineering*, 1997. 18: p. 165-178.

Table 1. Physical properties of Berea core samples

Core ID	Length (cm)	Diameter (cm)	Porosity (%)	PV(ml)	Swi	Soi	Abs. Kw(mD)	Ko, Swi(mD)
B1	5.83	3.7	22.27	14.14	0.18	0.82	621	645
B2	5.91	3.7	21.81	14.04	0.18	0.82	632	662
B3	5.7	3.7	21.6	13.41	0.18	0.82	576	617
B4	5.9	3.7	21.7	13.9	0.2	0.8	619	555

Table 2. Properties of the crude oil

Crude oil ID	Density at 20°C (g/ml)	Viscosity at 20°C (mPa.s)	Acid number (mg KOH/g oil)	Base number (mg KOH/g oil)
A	0.8436	51*	0.123	1.096±0.05
B	0.8784	13.8 *	2.84±0.01	0.95±0.10

*at shear rate 100 (s⁻¹)

Table3.Composition of brine

Chemical compound	Na ⁺	Ca ²⁺	Mg ²⁺	Cl ⁻	HCO ₃ ⁻	SO ₄ ²⁻	K ⁺
Concentration of ions (ppm)	11156	471	1330	20128	139	2743	350

Table 4. Contact angle measurements for crude oil A-Brine+GZ-Glass

Type of Enzyme	Enzyme concentration	Reference contact angle	Average contact angle with enzyme (degree)	Difference, Δθ (degree)	Δθ/θ
	(wt%)	without enzyme, θ (degree)			
Greenzyme	0.01	62	46	16	0.26
Greenzyme	0.05	62	43	19	0.31
Greenzyme	0.1	62	42	20	0.32
Greenzyme	0.25	62	38	24	0.39
Greenzyme	0.5	62	36	26	0.42
Greenzyme	0.75	62	32	30	0.48
Greenzyme	1	62	32	30	0.48
Greenzyme	2	62	32	30	0.48

Table 5. Contact angle measurements for crude oil A-Brine+GZ-Aged Glass (aged at 80°C)

Type of Enzyme	Enzyme concentration	Reference contact angle	Average contact angle with enzyme (degree)	Difference, Δθ (degree)	Δθ/θ
	(wt%)	without enzyme, θ (degree)			
Greenzyme	0.05	68	45	23	0.34
Greenzyme	0.05	77	53	24	0.31
Greenzyme	0.1	65	34	31	0.48
Greenzyme	0.1	87	57	30	0.35
Greenzyme	0.5	84	45	39	0.46
Greenzyme	0.5	126	122	4	0.03
Greenzyme	0.5	93	48	45	0.48
Greenzyme	0.5	50	43	7	0.14
Greenzyme	0.5	68	40	28	0.41
Greenzyme	1	84	50	34	0.40

Table 6. Contact angle measurements for crude oil A-Brine+Zonase1-Aged Glass (aged at 80°C)

Type of Enzyme	Enzyme concentration	Reference contact angle	Average contact angle with enzyme (degree)	Difference, Δθ (degree)	Δθ/θ
	(Wt%)	without enzyme, θ (degree)			
Zonase1	0.1	128	120	8	0.06
Zonase1	0.1	51	51	0	0.00
Zonase1	0.5	121	137	-16	-0.13
Zonase1	0.5	48	44	4	0.08
Zonase1	1	123	138	-15	-0.12
Zonase1	1	54	44	10	0.19
Zonase1	2	129	107	22	0.17

Table 7. Contact angle measurements for crude oil A-Brine+Zonase2-Aged Glass (aged at 80°C)

Type of Enzyme	Enzyme concentration (wt%)	Reference contact angle without enzyme, θ (degree)	Average contact angle with enzyme (degree)	Difference, $\Delta\theta$ (degree)	$\Delta\theta/\theta$
Zonase2	0.1	86	86	0	0.00
Zonase2	0.5	92	64	28	0.30
Zonase2	1	54	42	12	0.22
Zonase2	1	56	38	18	0.32
Zonase2	1	82	58	24	0.29
Zonase2	2	107	64	43	0.40

Table 8. Contact angle measurements for crude oil B-Brine+GZ-Glass

Type of Enzyme	Enzyme concentration (wt%)	Reference contact angle without enzyme, θ (degree)	Average contact angle with enzyme (degree)	Difference, $\Delta\theta$ (degree)	$\Delta\theta/\theta$
Greenzyme	0.01	52	33	19	0.37
Greenzyme	0.05	52	33	19	0.37
Greenzyme	0.1	52	33	19	0.37
Greenzyme	0.25	52	34	18	0.35
Greenzyme	0.5	52	34	18	0.35
Greenzyme	1	52	34	18	0.35

Table 9. Contact angle measurements for crude oil B-Brine+GZ-Aged Glass (aged at 80°C)

Type of Enzyme	Enzyme Concentration (wt%)	Reference contact angle without enzyme, θ (degree)	Average contact Angle with enzyme (degree)	Difference, $\Delta\theta$ (degree)	$\Delta\theta/\theta$
Greenzyme	0.01	79	37	42	0.53
Greenzyme	0.05	72	37	35	0.49
Greenzyme	0.1	61	41	20	0.33
Greenzyme	0.5	65	41	24	0.37
Greenzyme	0.5	67	45	22	0.33
Greenzyme	1	81	39	42	0.52

Table 10. End point permeabilities and Sw for different stages of the cores

Core ID	Sw (%) after brine flooding	Kw at Sor, (mD), after brine flooding	Sw (%) after 1%GZ-brine flooding	Kw at Sor, (mD), after 1%GZ-brine flooding	Sw (%) after 10%GZ-brine flooding	Kw at Sor, (mD), after 10%GZ flooding
	B1	52.26	43	61	67	---
B2	56.20	51	59	60	59	29
B3	49.29	42	54	52	---	---
B4	---	---	57	38	---	---

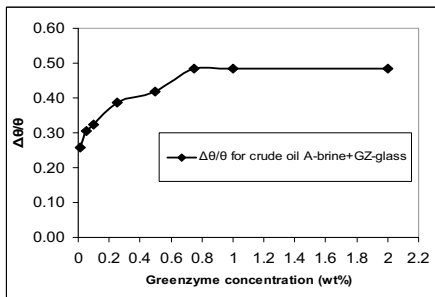


Figure 1. $\Delta\theta/\theta$ vs. Greenzyme concentration

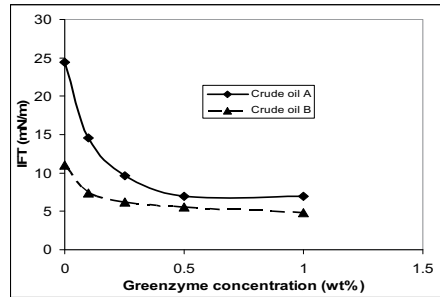


Figure 2. IFT for different concentration of GZ-brine and crude oil A and B

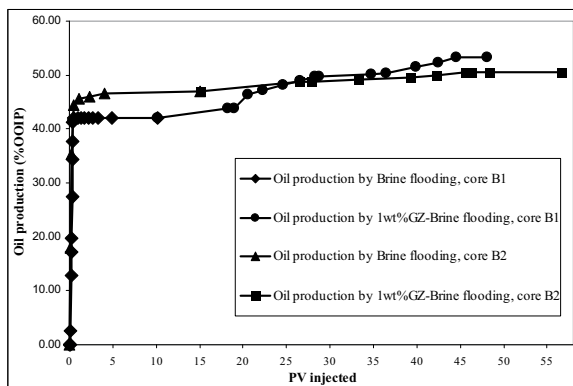


Figure 3. Production profile for different flooding scenarios Cores B1 and B2 (aged at 80°C)

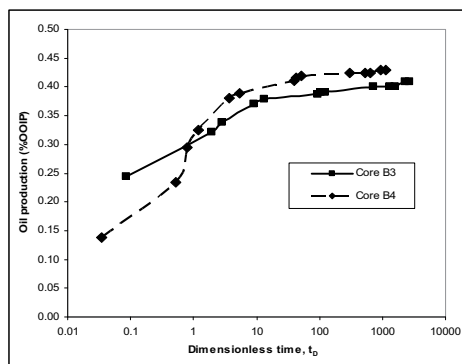


Figure 4. Oil production by imbibition vs dimensionless time and B4

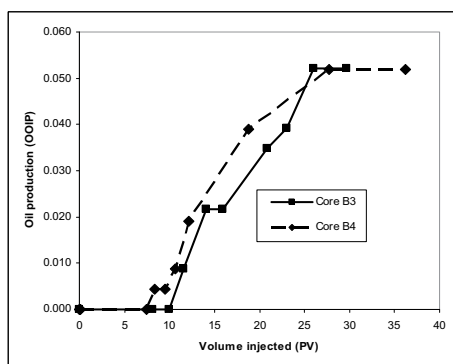


Figure 5. Production profile for GZ-brine flooding Cores B3 Cores B3 and B4

Bibliography

Agbalaka, C.C., Dandekar, A.Y., Patil, S.L., Khataniar, S. and Hemsath, J.R., 2009. Coreflooding studies to evaluate the impact of salinity and wettability on oil recovery efficiency. *Transport Porous Media*, 76(1): 77-94.

Ahmed, T., 2001. *Reservoir engineering handbook*. Gulf Professional Publishing, Houston, Texas.

Alagic, E., 2010. *Combination of low salinity water flooding with surfactant injection – a new hybrid EOR process*, University of Bergen, Bergen.

Al-Maamari, R.S. and Buckley, J.S., 2000. Asphaltene precipitation and alteration of wetting: Can wettability change during oil production?, *SPE/DOE Improved Oil Recovery Symposium*. SPE/DOE, Tulsa, OK, USA.

Al-Zuhair, S., Ramachandran, K.B. and Hasan, M., 2007. Effect of enzyme molecules covering of oil–water interfacial area on the kinetic of oil hydrolysis. *Journal of Chemical Engineering* doi:10.1016/j.cej.2007.08.030.

Amaefule, J.O. and Handy, L.L., 1982. The effect of interfacial tension on relative oil/water permeabilities of consolidated porous media. *SPEJ*.

Amott, E., 1960. Observations relating to the wettability of porous rock. *Petroleum Transactions, AIME*, 216: 156-162.

Anderson, G.A., 2006. *Simulation of chemical flood enhanced oil recovery processes including the effects of reservoir wettability*. Monograph Thesis, University of Texas at Austin.

Anderson, G.A., Delshad, M., Mohammadi, C.B. and Pope, G.A., 2006. Optimization of chemical flooding in a mixed-wet Dolomite reservoir, *SPE/DOE symposium on Improved Oil Recovery*, Tulsa, Oklahoma.

Anderson, W.G., 1986a. Wettability Literature Survey - Part 1: Rock/ Oil/ Brine interactions and the effects of core handling on wettability. *JPT*: 1125-44.

Anderson, W.G., 1986b. Wettability Literature Survey - Part 2: Wettability measurement. *JPT*: 1246-62.

Anderson, W.G., 1987a. Wettability Literature Survey - Part 4: Effects of wettability on capillary pressure. JPT: 1283-1300.

Anderson, W.G., 1987b. Wettability Literature Survey - Part 6: The Effects of wettability on waterflooding. JPT.

Armstrong, C.D., Stevens, R.F., Le, H., Stephenson, C. and Qu, Q., 2010. The next generation of regenerative catalytic breakers for use in alkaline and high-temperature fracturing fluids, SPE International Symposium and Exhibition on Formation Damage Control. SPE, Louisiana, USA.

Austad, T., 1993. A review of retention mechanisms of ethoxylated sulfonates in reservoir cores, SPE International Symposium on Oilfield Chemistry. SPE, New Orleans, LA, USA.

Austad, T., Matre, B., Milter, J., Sævareid, A. and Øyno, L., 1998. Chemical flooding of oil reservoirs 8. Spontaneous oil expulsion from oil- and water-wet low permeable chalk material by imbibition of aqueous surfactant solutions. Colloids and Surfaces, 137: 117-129.

Austad, T. and Milter, J., 1997. Spontaneous imbibition of water into low permeable chalk at different wettabilities using surfactants, International symposium on oilfield chemistry. SPE, Houston, USA.

Austad, T. and Standnes, D.C., 2003. Spontaneous imbibition of water into oil-wet carbonates. Journal of Petroleum Science and Engineering, 39: 363-376.

Ayrala, S.C. and Rao, D.N., 2004. Multiphase flow and wettability effects of surfactants in porous media. Colloids and Surfaces, 241: 313-322.

Baker, J.R. and Chaykin, S., 1962. The Biosynthesis of Trimethylamine-N-Oxide. Journal of Biological Chemistry, 237(4).

Barth, T., 1987. Quantitative determination of volatile carboxylic acids in formation waters by isotachopheresis. Analytical chemistry, 59: 2232-2237.

Basu, S. and Sharma, M.M., 1996. Measurement of critical disjoining pressure for dewetting of solid surfaces. Journal of Colloid and Interface Science, 181: 443-455.

Battistel, E. et al., 2005. Enzyme breakers for chemically modified starches, SPE European Formation Damage. SPE, Scheveningen, The Netherlands.

Benner, F.C. and Bartell, F.E., 1942. The effect of polar impurities upon capillary and surface phenomena in petroleum production. Drilling and Production Practice. API, New York, 341-348 pp.

Beverung, C.J., Radke, C.J. and Blanch, H.W., 1999. Protein adsorption at the oil-water interface: characterization of adsorption kinetics by dynamic interfacial tension measurements. Biophysical Chemistry, 81: 59-80.

Bickerstaff, G.F., 1987. Enzymes in Industry and Medicine. Studies in Biology. Edward Arnold, Renfrewshire, Scotland.

Blackburn, S., 1976. Enzyme Structure and Function. Enzymology. Marcel Dekker INC., Leeds, England.

Bourrel, M. and Schechter, R.S., 1988. Microemulsions and related systems: formulation, solvency, and physical properties. Marcel Dekker, New York, xii, 481 s. pp.

Brownell, L.E. and Katz, D.L., 1949. Flow of fluids through porous media, part II. Chemical Engineering Process, 43: 601-612.

Buckley, J., Liu, Y. and Monsterleet, S., 1998. Mechanisms of wetting alteration by crude oils. SPE journal, 3(1): 54-61.

Buckley, J.S., 1993. Asphaltene precipitation and crude oil wetting, SPE Annual Technical Conference and Exhibition SPE, Houston, TX, USA.

Buckley, J.S., 1996. Mechanisms and consequences of wettability alteration by crude oils, Heriot-Watt University, Edinburgh.

Buckley, J.S., Bousseau, C. and Liu, Y., 1995. Wettability alteration by brine and crude oil: From contact angles to cores, SPE Annual Technical Conference and Exhibition SPE, Dallas, TX, USA.

Buckley, J.S. and Fan, T., 2005. Crude oil/brine interfacial tension, International Symposium of the Society of Core Analysts, Toronto, Canada.

Buckley, J.S., Liu, Y., Xie, X. and N. R, M., 1996. Asphaltenes and crude oil wetting- The effect of oil composition, SPE/DOE Improved Oil Recovery Symposium. SPE/DOE, Tulsa, OK, USA.

Buckley, J.S. and Morrow, N.R., 1990. Characterization of crude oil wetting behavior by adhesion tests, SPE/DOE Seventh Symposium on Enhanced Oil Recovery. SPE, Tulsa, Oklahoma.

Buckley, J.S., Takamura, K. and Morrow, N.R., 1989. Influence of electrical surface charges on the wetting properties of crude oils. SPE Reservoir Engineering.

Butt, H.-J., Graf, K. and Kappl, M., 2006. Physics and chemistry of interfaces. Wiley-VCH, Weinheim, XII, 386 s. pp.

Chatzis, I., 1982. Photofabrication Technique of 2-D micromodels, New Mexico petroleum recovery research center, New Mexico.

Chatzis, I., N. R, M. and Lim, H.T., 1983. Magnitude and detailed structure of residual oil saturation. SPE Journal: 311-326.

Chen, J., Hirasaki, G. and Flaum, M., 2004. Study of wettability alteration from NMR: Effect of OBM on wettability and NMR responses, 8th International Symposium on Reservoir Wettability.

Chernicoff, S., 1999. *Geology: an introduction to physical geology*. Houghton Mifflin Co., Boston, XXVI, 596, 44 s. pp.

Copeland, R.A., 2000. *Enzymes: a practical introduction to structure, mechanism, and dataanalysis*. Wiley-VCH, New York, XVI, 397 s., pl. pp.

Crescente, C., Rekdal, A., Abraiz, A. and Torsæter, O., 2008. A pore level study of MIOR displacement mechanisms in glass micromodels using *Rhodococcus* sp. 094, SPE symposium on improved oil recovery. SPE, Tulsa, Oklahoma, USA.

Crocker, M.E. and Marchin, L.M., 1988. Wettability and adsorption characteristics of crude-oil asphaltene and polar fractions. *JPT*: 470-474.

Cuiec, E.L., 1991. Evaluation of reservoir wettability and its effect on oil recovery. In: N. Morrow (Editor), *Surfactant Science Series: Interfacial phenomena in petroleum recovery*. Marcel Dekker Inc., New York.

Cuiec, L., 1984. Rock/crude-oil interactions and wettability: An attempt to understand their interrelation, SPE Annual Technical Conference and Exhibition. SPE, Houston, TX, USA.

Dake, L.P., 1978. *Fundamentals of reservoir engineering*. ELSEVIER, The Hague, The Netherlands.

Danesh, A., Peden, J.M., Krinis, D. and Henderson, G.D., 1987. Pore level investigation of oil recovery by solution gas drive and gas injection, SPE Annual Technical Conference and Exhibition. SPE, Dallas, TX.

Degroot, M., 1929. Flooding process for recovering oil from subterranean oil-bearing strata. 1823439, USA.

Déjardin, P., 2006. *Proteins at solid-liquid interfaces*. Springer-Verlag Berlin Heidelberg, Berlin, Heidelberg.

Delshad, M., Fathi, N., Anderson, G.A., Pope, G.A. and Sepehrnoori, K., 2009. Modeling wettability alteration by surfactants in naturally fractured reservoirs. *SPE Reservoir Evaluation & Engineering*.

Denekas, M.O., Mattax, C.C. and Davies, G.T., 1959. Effects of crude oil components on rock wettability. *Petroleum Transactions, AIME*, 216: 330-333.

Derjaguin, B. and Landau, L., 1941. *Acta Physicoschim USSR*, 14: 633.

Dill, K.A., 1990. Dominant forces in protein folding. *Biochemistry*, 29(31): 7133-7155.

Donaldson, E.C. and Thomas, R.D., 1971. Microscopic observation of oil displacement in water-wet and oil-wet systems, 46th Annual Fall Meeting of SPE. SPE, New Orleans, USA.

Donaldson, E.C., Thomas, R.D. and Lorenz, P.B., 1969. Wettability determination and its effect on oil recovery. *SPEJ*: 13-20.

Dong, H., Hong, Y. and Rui, W., 2006. The effect of wettability on oil recovery of alkaline/surfactant/polymer flooding, SPE Annual Technical Conference and Exhibition. SPE, San Antonio, TX, USA.

Duinhoven, S. et al., 1995. Driving forces for enzymes adsorption at solid-liquid interfaces Journal of Colloid and Interface Science, 170: 340-357.

Evans, D.F. and Wennerström, H., 1999. The colloidal domain: where physics, chemistry, biology, and technology meet. Wiley-VCH, New York, XL, 632 s. pp.

Feng, Q.-x. et al., 2007. EOR Pilot Tests With Modified Enzyme in China, SPE Europe/EAGE. SPE, London, United Kingdom.

Filoco, P.R. and Sharma, M.M., 1998. Effect of brine salinity and crude oil properties on relative permeabilities and residual saturations. SPE Journal, 5(3): 293-300.

Fischer, E., 1894. Einfluss der configuration auf die wirkung der enzyme. Ber. Dtsch. Chem. Ges., 27: 2984-2993.

Fojan, P., Jonson, P.H., Petersen, M.T.N. and Petersen, S.B., 2000. What distinguishes an esterase from a lipase: A novel structural approach. Biochimie, 82: 1033-1041.

Foster, W.R., 1973. A low-tension waterflooding process. Journal of Petroleum Technology: 205-210.

Frye, G.C. and Thomas, M.M., 1993. Adsorption of organic compounds on carbonate minerals. 2. Extraction of carboxylic acids from recent and ancient carbonates. Chemical Geology, 109: 215-226.

Garnes, J.M., Mathisen, A.M., Scheie, A. and Skauge, A., 1990. Capillary Number Relations for Some North Sea Reservoir Sandstones Enhanced Oil Recovery Symposium. SPE/DOE, Tulsa, Oklahoma.

Garrett, H.E., 1972. Surface active chemicals. Pergamon, Oxford, X, 167 s. pp.

Glomm, W.R., Halskau, Ø., Jr., Hanneseth, A.-M.D. and Volden, S., 2007. Adsorption behavior of acidic and basic proteins onto citrate-coated Au surfaces correlated to their native fold, stability, and pI. Journal of Phys. Chem, 111: 14329-14345.

Glover, C.J., Puetro, M.C., Maerker, J.M. and Sandvik, E.L., 1979. Surfactant phase behavior and retention in porous media. SPEJ.

Gomari, K.A.R., 2009. Different approaches to understand mechanism of wettability alteration of carbonate reservoirs, SPE EUROPEC/EAGE. SPE, Amsterdam, The Netherlands.

Goodman, D.S., 1958. The distribution of fatty acids between n-heptane and aqueous phosphate buffers. American Chemistry Society, 80.

Grattoni, C.A., Al-Sharji, H.H., Dawe, R.A. and Zimmerman, R.W., 2002. Segregated pathways mechanism for oil and water flow through an oil-based gelant. *SPE Journal*, 35: 183–190.

Graue, A. et al., 1999a. Impacts of wettability on capillary pressure and relative permeability, International Symposium of the Society of Core Analysts. SCA.

Graue, A., Viksund, B.G., Eilertsen, T. and Moe, R., 1999b. Systematic wettability alteration by aging sandstone and carbonate rock in crude oil. *Journal of Petroleum Science and Engineering*, 24: 85-97.

Gray, J.J., 2004. The interaction of proteins with solid surfaces. *Current Opinion in Structural Biology*, 14: 110-115.

Green, D.W. and Willhite, G.P., 1998. Enhanced Oil Recovery. SPE textbook series, 6. SPE, Richardson, Texas, 545 pp.

Gupta, R., Mohan, K. and Mohanty, K.K., 2009. Surfactants screening for wettability alteration in oil-wet fractured carbonates, Annual Technical Conference and Exhibition. SPE, New Orleans, USA.

Halskau, Ø., Frøystein, N.Å., Muga, A. and Martinez, A., 2002. The membrane-bound conformation of alpha-Lactalbumin studied by NMR-monitored H exchange. *Journal of Molecular Biology*, 321: 99-110.

Hamon, G. and Bennes, M., 2003. Two-phase flow rock-typing: Another approach, International Symposium of the Society of Core Analysts. SCA.

Hamouda, A.A. and Gomari, K.A.R., 2006. Influence of temperature on wettability alteration of carbonate reservoirs, SPE/DOE Improved Oil Recovery Symposium. SPE/DOE, Tulsa, OK, USA.

Hamouda, A.A. and Karousi, O., 2008. Effect of Temperature, Wettability and Relative Permeability on Oil Recovery from Oil-wet Chalk. *Energies*, 1: 19-34.

Hansen, F.K. and Rødsrud, G., 1991. Surface tension by pendant drop 1. A fast standard instrument using computer image analysis. *Journal of Coll. Int. Sci.*, 141.

Hanssen, J.E., Jiang, P., Pedersen, H.H. and Jørgensen, J.F., 1999. New enzyme process for downhole cleanup of reservoir drilling filtercake, SPE International Symposium on Oilfield Chemistry. SPE, Houston, USA.

Harris, R.E. and McKay, I.D., 1998. New Applications for Enzymes in Oil and Gas Production, SPE European Petroleum Conference. SPE, Hague, Netherlands.

Healy, R.N. and Reed, R.L., 1974. Physicochemical aspects of microemulsion flooding. *SPEJ*, 14: 491-505.

Healy, R.N., Reed, R.L. and Stenmark, D.G., 1976. Multiphase microemulsion systems. *SPEJ*.

- Hiemenz, P.C. and Rajagopalan, R., 1997. Principles of colloid and surface chemistry. Marcel Dekker, New York, XIX, 650 s. pp.
- Hirasaki, G., 1991. Wettability: fundamentals and surface forces. SPE Formation Evaluation, 6: 217-226.
- Hirasaki, J.G., Miler, C.A., Pope, G.A. and Jackson, R.E., 2004. Surfactant based enhanced oil recovery and foam mobility control.
- Hirasaki, G., 1991. Wettability: fundamentals and surface forces. SPE Formation Evaluation, 6: 217-226.
- Hlady, V. and Buijs, J., 1996. Protein adsorption on solid surfaces. Current Opinion in Biotechnology, 7: 72-77.
- Holloway, C.J. and Trautschold, I., 1982. Principles of Isotachopheresis. Fresenius Z Analytical Chemistry, 311: 81-93.
- Huotari, H.M., Huisman, I.H. and Tragårdh, G., 1998. Electrically enhanced crossflow membrane filtration of oily waste water using the membrane as a cathode. Journal of Membrane Science, 156: 49-60.
- Iler, R.K., 1979. The chemistry of silica. Wiley, New York.
- Jadhunandan, P.P. and Morrow, N., 1991. Spontaneous imbibition of water by crude oil/brine/rock system. In situ, 15(4): 319-345.
- Jadhunandan, P.P. and Morrow, N., 1995. Effect of wettability on waterflooding recovery for crude-oil/brine/rock systems. SPE Reservoir Engineering: 40-46.
- Jeong, S.W., Corapcioglu, M.Y. and Roosevelt, S.E., 2000. Micromodel study of surfactant foam remediation for residual trichloroethylene. Environmental Science and Technology, 34: 3456-3461.
- Johnson, R.E. and Dettre, R.H., 1962. Wettability and contact angles. Journal of surface and colloid science, 2: 85-153.
- Jurado, E. et al., 2007. Hard-Surface Cleaning Using Lipases: Enzyme-Surfactant Interactions and Washing Tests. Journal of Surfactants and Detergents, 10: 61-70.
- Kamath, j., Meyer, R., Nakagawa, F. and Frank, M., 2001. Understanding waterflood residual saturation of four carbonate rock types, SPE Annual Technical Conference and Exhibition. SPE, New Orleans, LA, USA.
- Kaminsky, R. and Radke, C.J., 1998. Water films, asphaltenes, and wettability alteration, SPE/DOE Improved Oil Recovery Symposium SPE/DOE, Tulsa, OK, USA.
- Karimaie, H., Torsæter, O., M.R. Esfahani b, Dadashpour, M. and b, S.M.H., 2006. Experimental investigation of oil recovery during water imbibition. Journal of Petroleum Science and Engineering, 52: 297-304.

Karousi, O., 2008. Investigated wettability alteration of chalk in macro-, micro- and nanoscale with temperature and ions effect on oil recovery, University of Stavanger, Edinburgh.

Kohler, N., Lonchamp, D. and They, M., 1987. Injectivity Improvement of Xanthan Gums by Enzymes: Process Design and Performance Evaluation. JPT.

Koshland, D.E., 1958. Application of a theory of enzyme specificity to protein synthesis. Proceedings of the National Academy of Sciences of the USA, 44(2): 98-104.

Kumar, S., Torabzadeh, S.J. and Handy, L.L., 1985. Relative permeability function for high- and low-tension system at elevated temperatures, Society of Petroleum Engineers California Regional Meeting. SPE, Bakersfiel, CA, USA.

Lager, A., Webb, K.J., Black, C.J.J., Singleton, M. and Sorbie, K.S., 2006. Low salinity oil recovery - An experimental investigation, International Symposium of the Society of Core Analysts, Trondheim, Norway.

Lake, L.W., 1989. Enhanced Oil Recovery. Prentice Hall, Englewood Cliffs.

Lake, L.W., Pope, G.A., Carey, G.F. and Sepehrnoori, K., 1984. Isothermal, multiphase, multicomponent fluid-flow in permeable media. In Situ, 8: 1-40.

Larsen, J., Poulsen, M., Lundgaard, T. and Agerbæk, M., 2008. Plugging of fractures in chalk reservoirs by enzyme-induced calcium carbonate precipitation. SPE production and Operations: 478-483.

Leach, R.O., Wagner, O.R., Wood, H.W. and Harpke, C.F., 1961. A laboratory and field study of wettability adjustment in waterflooding, SPE International Petroleum Conference and Exhibition. SPE, Dallas, USA.

Leisola, M., Jokela, J., Pastinen, O., Turunen, O. and Schoemaker, H., 2001. Industrial use of enzymes. In: O.O.P. Hänninen and M. Atalay (Editors), Physiology and Maintenance. Department of Physiology, University of Kuopio, Finland.

Levitt, D.B. et al., 2009. Identification and evaluation of high-performance EOR surfactants. Reservoir Evaluation and Engineering.

Liu, Y. and J.S. Buckley, Evolution of wetting alteration by adsorption from crude oil in SPEFE. 1997, SPE: Texas, USA.

Ma, S., Morrow, N.R. and Zhang, X., 1997. Generalized scaling of spontaneous imbibition data for strongly water-wet systems. Journal of Petroleum Science and Engineering, 18: 165-178.

Maldal, T., Gulbrandsen, A.H. and Gilje, E., 1997. Correlation of capillary number curves and remaining of saturation for reservoir and model sandstone. In Situ, 21(3): 239-269.

Malmsten, M., 1998. Formation of adsorbed protein layers. Journal of Colloid and Interface Science, 207: 186-199.

- Manning, C.D. and Scriven, L.E., 1977. On interfacial tension measurement with a spinning drop in gyrostatic equilibrium. *Review of Scientific Instruments*, 48(12): 1699-1705.
- Marangoni, A.G., 1994. Enzyme kinetics of lipolysis revisited: The role of lipase interfacial binding. *Biochemical and Biophysical Research Communications*, 200(3): 1321-1328.
- Marle, C.M. (Editor), 1991. Basic concept of Enhanced Oil Recovery. *Critical reports on applied chemistry*, 33. Elsevier applied science, London.
- McKellar, M. and Wardlaw, N.C., 1982. A method of making two-dimensional glass micromodels of pore systems. *Journal of Canadian Petroleum Technology*, 21(4): 39-41.
- Meyer, E.F., 1995. Emil Fischer: then and now. *Pharmaceutics Acta Helvetiae* 69: 177-183.
- Milner, J. and Austad, T., 1996. Chemical flooding of oil reservoirs 7. Oil expulsion by spontaneous imbibition of brine with and without surfactant in mixed-wet, low permeable chalk material. *Journal of Colloids and Surfaces A: Physicochemical and Engineering Aspects*, 117: 109-115.
- Mohanty, K.K., Davis, H.T. and Scriven, L.E., 1987. Physics of oil entrapment in water-wet rock. *SPE Reservoir Engineering*: 113-128.
- Mohanty, K.K. and Salter, S.J., 1983. Multiphase flow in porous media III: Oil mobilization, transverse dispersion, and wettability,, *SPE Annual Technical Conference and Exhibition*. SPE, san Francisco, CA, USA.
- Moon, T., 2008. Using enzymes to enhance oil recovery, *JPT online*. SPE.
- Moore, W.R., Beall, B.B. and Ali, S.A., 1996. Formation damage removal through the application of enzyme breaker technology, *SPE International Symposium of Formation Damage*. SPE, Louisiana, USA.
- Morrow, N.R., 1990. Wettability and its effect on oil recovery. *JPT*: 1476-84.
- Morrow, N.R., 1991. Evaluation of reservoir wettability and its effect on oil recovery. In: N. Morrow (Editor), *Surfactant Science Series: Interfacial phenomena in petroleum recovery*. Marcel Dekker Inc., New York.
- Morrow, N.R., Lim, H.T. and Ward, J.S., 1986. Effect of crude Oil induced wettability changes on oil recovery. *SPE Formation Evaluation*: 89-103.
- Morrow, N.R., et al., Prospects of improved oil recovery related to wettability and brine composition. *Journal of Petroleum Science and Engineering* 1998. 20: p. 267-276.
- Nakanishi, K., Sakiyama, T. and Imamura, K., 2001. On the adsorption of proteins on solid surfaces, a common but very complicated phenomenon. *Journal of Bioscience and Bioengineering*, 91(3): 233-244.

Nasiri, H. and Abdi, R., 2005. Enhanced Oil Recovery by Surfactant Flooding. MSc. Thesis
Thesis, NTNU, Trondheim, 212 pp.

Nasiri, H., K. Spildo, and A. Skauge, Use of enzymes to improve waterflood performance, in
International Symposium of the Society of Core Analysts. 2009: Noordwijk, Netherlands.

Nasr-El-Din, H.A., Al-Otaibi, M.B., Al-Qahtani, A.A. and Al-Fuwaires, O.A., 2006. Filter-
cake cleanup in MRC wells using enzyme/surfactant solutions, SPE. SPE, Lafayette, LA,
USA.

Nasr-El-Din, H.A., Al-Otaibi, M.B., Al-Qahtani, A.A. and M.Samuel, 2006. An effective
fluid formulation to remove drilling-fluid mudcake in horizontal and multilateral wells. SPE
Drilling and Completion.

Nelson, R.C., 1983. Effect of live crude on phase behavior and oil recovery efficiency of
surfactant flooding system. SPEJ: 501-10.

Nelson, R.C. and Pope, G.A., 1978. Phase relationships in chemical flooding. SPEJ, 18(5):
325-38.

Nemati, M. and Voordouw, G., 2003. Modification of porous media permeability, using
calcium carbonate produced enzymatically in situ. Journal of Enzyme and Microbial
Technology, 33: 635-642.

Neumann, A.W. and Good, R.J., 1979. Techniques of measuring contact angles. Journal of
Surface and colloid science, 11: 31-91.

Nguyen, Q.P., Thissen, M. and Zitha, P.I.J., 2002. Effect of trapped foam on gas tracer
diffusion in a visual microflow model, SPE symposium on improved oil recovery. SPE,
Tulsa, Oklahoma, USA.

Novstad, J., 1982. Surfactant retention in Berea sandstone- effect of phase behavior and
temperature. SPEJ: 962-70.

Owolabi, O.O. and Watson, R.W., 1993. Effects of rock-pore characteristics on oil recovery
at breakthrough and ultimate oil recovery in water-wet sandstones, SPE Eastern Regional
Conference. SPE, Pittsburg, PA.

Panda, T. and Gowrishankar, B.S., 2005. Production and applications of esterases. Appl
Microbiol Biotechnol, 67: 160-169.

Paul, B.K. and Moulik, S.P., 2001. Uses and applications of microemulsions. Current Science,
80(8): 990-1001.

Pavia, D.L., 2009. Introduction to spectroscopy. Brooks/Cole, Belmont, Calif., XV, 656 s.
(flere pag.) pp.

Prime, K.L. and Whitesides, G.M., 1991. Self-assembled organic monolayers: Model systems
for studying adsorption of proteins at surfaces. Science, 252(5009): 1164-1167.

- Privalov, P.L. and Gill, S.J., 1988. Stability of protein structure and hydrophobic interaction. *Advances in Protein Chemistry*, 39: 191-234.
- Puerto, M.C. and Reed, R.L., 1983. A three parameter representation of surfactant/oil/brine interaction. *SPEJ*, 23: 669-682.
- Radke, C.J., Kovscek, A.R. and Wong, H., 1992. A pore-level scenario for the development of mixed wettability in oil reservoirs, SPE Annual Technical Conference and Exhibition. SPE, Washington, USA.
- Reiner, J.M., 1969. *Behavior of Enzyme Systems*. Van Nostrand Reinhold Company, Albany, New York.
- Rosen, M.J., 2004. *Surfactants and interfacial phenomena*. Wiley-Interscience, Hoboken, N.J., xiii, 444 s. pp.
- Salathiel, R.A., 1973. Recovery by Surface Film Drainage in Mixed-Wettability Rocks. *JPT*, 255: 1216-24.
- Samuel, M. et al., 2009. Novel enzyme stabilizers for applications at extreme high temperatures, SPE Annual Technical Conference and Exhibition. SPE, New Orleans, USA.
- Savelli, G., Spredi, N. and Profio, P.D., 2000. Enzyme activity and stability control by amphiphilic self-organizing systems in aqueous solutions. *Current Opinion in Colloid & Interface Science*, 5: 111-117.
- Sayegh, S.G. and Fisher, D.B., 2008. Enhanced oil recovery by CO₂ flooding in homogenous and heterogeneous 2D micromodels, Canadian International Petroleum Conference/SPE Gas Technology Symposium 2008 Joint Conference, Calgary, Canada.
- Schroth, B.K. and Sposito, G., 1997. Surface charge properties of kaolinite. *Clays and Clay Minerals*, 45(1): 85-91.
- Seifert, W. and Teeter, R.M., 1970. Identification of polycyclic aromatic and heterocyclic crude oil carboxylic acids. *Analytical Chemistry*, 42(7): 750-758.
- Shabani Afrapoli, M., Ostvar, S., Crescente, C. and Torsaeter, O., 2009. MIOR displacement mechanisms in glass micro-model, 15th European Symposium on Improved Oil Recovery. EAGE, Paris, France.
- Shen, P., Zhu, B., Li, X.B. and Wu, Y.S., 2006. The influence of interfacial tension on water/oil two-phase relative permeability, SPE/DOE symposium on Improved Oil Recovery. SPE, Tulsa, Oklahoma, USA.
- Siddiqui, M.A. and Nasr-El-Din, H.A., 2005. Evaluation of special enzymes as a means to remove formation damage induced by drill-in fluids in horizontal gas wells in tight reservoirs. *SPE Production and Facilities*: 177-184.
- Skauge, A. and Fosse, B., 1996. A study of the adhesion, interfacial tension, and contact angle for a brine, quartz, crude oil system, 3rd International Symposium on Evaluation of Reservoir Wettability and Its Effect on Oil Recovery, Laramie, WY, USA.

Skauge, A. and Fotland, P., 1990. Effect of pressure and temperature on the phase behavior of microemulsions. SPE Reservoir Engineering: 601-8.

Skauge, A. and Ottesen, B., 2002. A summary of experimentally derived relative permeability and residual saturation on north sea reservoir cores, International Symposium of the Society of Core Analysts. SCA.

Skauge, A., Spildo, K., Høiland, L. and Vik, B., 2007. Theoretical and experimental evidence of different wettability classes. Journal of Petroleum Science and Engineering, 57: 321-333.

Skauge, A., Standal, S., Boe, S.O., Skauge, T. and Blokhus, A.M., 1999. Effects of organic acids and bases, and oil composition on wettability, SPE Annual Technical Conference and Exhibition. SPE, Houston, Texas, USA.

Skauge, A., Vik, B. and Ottesen, B., 2003. Variation of special core analysis properties for intermediate wet sandstone material, International Symposium of the Society of Core Analysts. SCA, Pau, France.

Skjæveland, S.M. and Kleppe, J., 1992. SPOR monograph: recent advances in improved oil recovery methods for NorthSea sandstone reservoirs. Norwegian Petroleum Directorate, Stavanger, XIX, 335 s. pp.

Sohrabi, M., Henderson, G.D., Tehrani, D.H. and Danesh, A., 2000. Visualization of oil recovery by Water Alternating Gas (WAG) injection - Water-wet system, SPE Annual Technical Conference and Exhibition. SPE, Dallas, TX.

Sohrabi, M., Tehrani, D.H., Danesh, A. and Henderson, G.D., 2004. Visualization of Oil Recovery by Water-Alternating-Gas Injection Using High-Pressure Micromodels. SPE Journal, 9(3): 290-301.

Somasudaran, P. and Agar, G.E., 1967. The zero point of charge of calcite. Colloid Interface Science, 24: 433.

Somerville, H.J. et al., 1987. Environmental effect of produced water from North oil operations. Marine Pollution Bulletin, 18(10).

Sorbie, K.S. and Dijke, M.I.J.V., 2005. Fundamentals of Three-Phase Flow in Porous Media of Heterogeneous Wettability.

Spildo, K., 1999. Wettability and two-phase flow in capillary systems, University of Bergen, Bergen, Norway.

Spildo, K. and Høiland, H., 1999. Interfacial properties and partitioning of 4-heptylbenzoic acid between decane and water. Journal of Colloid and Interface Science, 209: 99-108.

Standnes, D.C., Nogaret, L.A.D., Chen, H.-L. and Austad, T., 2002. An evaluation of spontaneous imbibition of water into oil-wet carbonate reservoir cores using a nonionic and a cationic surfactant. Energy & Fuels, 16: 1557-1564.

Stokes, R.J. and Evans, D.F., 1997. Fundamentals of interfacial engineering. Wiley-VCH, New York, XXVIII, 701 s. pp.

Suhy, T.E. and Harris, R.P., 1998. Application of polymer specific enzymes to clean up drill-In fluids, SPE. SPE, Pittsburgh, PA.

Tang, G.Q. and Morrow, N.R., 1997. Salinity, temperature, oil composition and oil recovery by waterflooding. SPE Reservoir Engineering, 12(4): 269-276.

Tayal, A., Kelly, R.M. and Khan, S.A., 1997. Viscosity reduction of hydraulic fracturing fluids through enzymatic hydrolysis. SPE Journal, 2: 204-.

Tie, H. and Morrow, N., 2005. Low flood rate residual saturation in carbonates rocks, International Petroleum Technology Conference, Doha, Qatar.

Treiber, L.E., Archer, D.L. and Owens, W.W., 1972. A laboratory evaluation of the wettability of fifty oil-producing reservoirs. SPEJ, 253: 531-40.

Tweheyo, M.T., Holt, T. and Torsæter, O., 1999. An experimental study of the relationship between wettability and oil production characteristics. Journal of Petroleum Science and Engineering, 24: 179-188.

Verwey, E. and Overbeek, J.T.G., 1948. Theory of the stability of lyophobic colloids. Elsevier, Amsterdam.

Vonnegut, B., 1942. Rotating bubble method for the determination of surface and interfacial tensions. Review of Scientific Instruments, 13(1): 6-9.

Weiss, H.M. et al., 2005. The Norwegian industry guide to organic geochemical analyses. Norwegian Petroleum Directorate.

Wertz, C.F. and Santore, M.M., 2002. Fibrinogen adsorption on hydrophilic and hydrophobic surfaces: Geometrical and energetic aspects of interfacial relaxations. Langmuir, 18: 706-715.

Wesson, L.L. and Harwell, J.H., 2000. Surfactant adsorption in porous media. In: L.L. Scramm (Editor), Surfactant: Fundamentals and application in the petroleum industry. Cambridge University Press.

Willhite, G.P., 1986. Waterflooding. SPE textbook series, 3, Richardson, Texas.

Wilson, P.M.D. and Brander, C.F., 1977. Aqueous surfactant solution which exhibit ultra-low tensions at the oil-water interface. Journal of Colloid and Interface Science, 60(3): 473-479.

Winsor, P.A., 1954. Solvent properties of amphiphilic compounds. Butterworths, London, IX, 207 s. pp.

Xie, X., Weiss, W.W., Tong, Z. and Morrow, N.R., 2005. Improved oil recovery from carbonate reservoirs by chemical stimulation. SPE Journal: 276-285.

Xu, W., S.C. Ayirala, and D.N. Rao, Experimental investigation of oil compositional and surfactant effects on wettability at reservoir conditions, in Society of Core Analysts. 2005, SCA: Toronto, Canada.

Yu, L., et al., Analysis of the Wettability alteration process during seawater imbibition into preferentially oil-wet chalk cores, in Society of Petroleum Engineering. 2008, SPE: Oklahoma, USA.

Zana, R., 1990. Cationic surfactants: physical chemistry. Surfactant science series, 37. Marcel Dekker Inc., New York.

Zhang, D.L., Liu, S., Puerto, M., Miller, C.A. and Hirasaki, G.J., 2006. Wettability alteration and spontaneous imbibition in oil-wet carbonate formations. *Petroleum Science and Engineering*, 52: 213-226.

Zhang, Y.P., Sayegh, S.G. and Huang, S., 2005. The role of effective interfacial tension in Alkaline/Surfactant/Polymer flooding, Canadian International Petroleum Conference. Petroleum Society of Canada, Calgary, Alberta.

Zhou, X., N. R. M. and Ma, S., 2000. Interrelationship of wettability, initial water saturation, aging time, and oil recovery by spontaneous imbibition and waterflooding. *SPEJ*, 5(2): 199-207.

Zhou, Z. and Gunter, W.D., 1992. The nature of the surface charge of kaolinite. *Clays and Clay Minerals*, 40(3): 365-368.

Zolotukhin, A.B. and Ursin, J.R., 2000. Introduction to petroleum reservoir engineering. Norwegian Academic Press, Kristiansand.